

**A STOCHASTIC TECHNO-ECONOMIC ANALYSIS OF AVIATION
BIOFUELS PRODUCTION FROM PENNYCRESS SEED OIL**

by

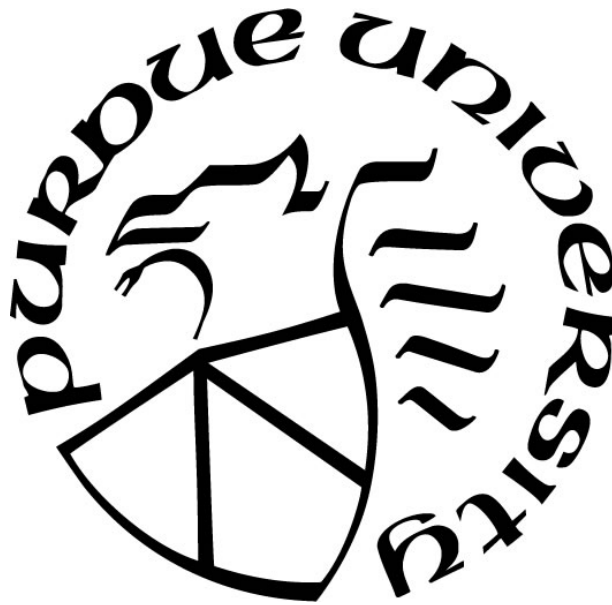
Jeremiah Stevens

A Thesis

Submitted to the Faculty of Purdue University

In Partial Fulfillment of the Requirements for the degree of

Master of Science



Department of Agricultural Economics

West Lafayette, Indiana

December 2019

THE PURDUE UNIVERSITY GRADUATE SCHOOL
STATEMENT OF COMMITTEE APPROVAL

Dr. Allan Gray, Chair

Department of Agricultural Economics

Dr. Otto Doering

Department of Agricultural Economics

Dr. Nathan Mosier

Department of Agricultural and Biological Engineering

Approved by:

Dr. Nicole J. Olynk Widmar

Head of the Graduate Program

*To the glory of the One God, Who teaches humanity all the truth that we know,
And to the memory of Dr. Wally Tyner, a caring and clear-minded teacher and friend.*

ACKNOWLEDGMENTS

This work would have been utterly impossible without the contributions of many advisors and collaborators, to all of whom I am deeply grateful for their contributions to this study. First and foremost, I am indebted to the late Dr. Wallace E. Tyner, my major professor, who taught me everything I know about benefit-cost analysis and biofuels markets, and without whose steady and kind guidance I would never have come near to completing this work. He is and will be greatly missed by many. If the following pages contain anything that proves useful to further research, policymakers, or industry participants, there can be no doubt that it is entirely thanks to his keen mind and long experience, which he freely and graciously shared with me, his student. I am sure to have learned from him imperfectly, and any mistakes or poor choices in what follows are certain to be mine, alone.

In the wake of Dr. Tyner's death, the Agricultural Economics Department at Purdue University did an admirable job ensuring that his advisees would be taken care of. I owe thanks to Dr. Nicole J. Olynk Widmar for coordinating those efforts, to Dr. Allan Gray for graciously agreeing to step in as my committee chair, and to Dr. Farzad Taheripour for taking over my research assistantship. Drs. Gray and Taheripour also provided invaluable feedback on early drafts of this paper, including their suggestion that I include alternate pricing scenarios for pennycress oil, a suggestion that greatly enhanced the results of this study.

I must thank my other committee members, Dr. Otto Doering and Dr. Nathan Mosier, for their flexibility and understanding as I attempted to bring this project to a close, and for their valuable insights and feedback. I am also grateful to Dr. Doering for the leg up his research methods course afforded me on the writing process. I thank Dr. Ken Foster for his input as I was trying to untangle the knotty price series I needed to forecast. His idea to use a price ratio as the basis for modeling the crucial relationship between soybean oil and fossil fuel prices proved invaluable. Dr. Burton English and his collaborators at the University of Tennessee, Knoxville provided invaluable assistance in modeling potential supply of pennycress oil to this study's hypothetical biofuels plants. Without their help, the analysis of breakeven prices for pennycress oil included here would have been impossible. Last but by no means least, I am forever grateful to Applied Research Associates, Inc., and to Jonathan Miller and Ed Coppola in particular, for

allowing access to their latest CH plant parameters. Without their gracious cooperation, none of the rest of this project would have been possible.

TABLE OF CONTENTS

LIST OF TABLES	x
LIST OF FIGURES	xiv
ABSTRACT	xxii
INTRODUCTION	1
Background	1
Problem Statement	2
Hypotheses	2
Methods	3
Overview	3
Key Parameters	4
Revenues	4
Costs	5
RINs Price Modeling	5
Blender Tax Credit Modeling	6
LCFS Credit Price Modeling	6
Pennycress Seed Meal Price Modeling	7
Metrics	7
Overview of the Coming Chapters	8
LITERATURE REVIEW	10
Greenhouse Gases and Aviation Biofuels	10
<i>Thlaspi arvense</i> , Field Pennycress	12
Introduction	12
Seed Oil	12
Seed Meal	13
Season and Timing	13
Yield and Inputs	14
Potential Agronomic Drawbacks	16
Weedy Habit	16
Impact on Nematode Populations	17

Potential Agronomic Benefits	18
Offseason Ground Cover	18
Pollinator Provision	18
Hydroprocessed Esters and Fatty Acids	19
Catalytic Hydrothermolysis	20
Policy	22
The United States Renewable Fuel Standard	22
California Low Carbon Fuel Standard	24
Stochastic Techno-economic Analysis	25
METHODOLOGY	31
Techno-Economic Analysis	31
Harmonizing with a Larger Pennycress Supply Chain	36
Determining the Value of Pennycress Seed Meal	37
Correlations between Price Series and “Financialization” of Commodities Markets	43
A Novel Weighted, Bounded Lag Structure for Stochastic Time Series Forecasting	46
Non-Time Series Approaches	47
The @Risk® Batch Fit Tool	48
Conventional Lag Structures	49
A Novel Approach	49
Evaluating our Stochastic Forecasts	54
Are the forecasted levels consistent with historical data and expert opinion?	54
Do the forecasts reflect any real growth trends in the data?	61
Are the autocorrelations obtained in the stochastic forecasts consistent with the data?... ..	64
Are the inter-series correlations obtained in the stochastic forecasts consistent with the data?	67
Do the shapes of the distributions of simulated prices qualitatively approximate the shapes of the distributions of historical prices?	70
Do the stochastic forecasts avoid unrealistic results?	74
Are the stochastic forecasts deliverable in an Excel workbook of reasonable size?	75
Endogenous RIN Price Modeling	76
The Market for D4 RINs	79

From Soybean Oil Prices to Biodiesel Breakeven Prices to D4 and D5 RIN prices	85
Producer Revenue from the Blender Tax Credit.....	92
Modeling the California Low Carbon Fuel Standard	95
Modeling Electricity and Natural Gas Prices	99
Modeling Fuel Yield.....	100
Modeling the N th Plant.....	100
Obtaining Breakeven Jet Fuel “Bonus”	101
Obtaining Breakeven Constant and Growing Crude Oil Prices	101
Obtaining Breakeven Prices of Pennycress Seed Oil	103
DATA	105
Consumer Price Index.....	105
CH Plant Technical and Financial Parameters	105
Learning Curves for N th Plant Cost Reductions	106
Feeding Model Nutritional Data	106
Feeding Model Price Data	107
Fossil Transportation Fuel Price Data	109
Soybean Oil and Biodiesel Price Data.....	112
Pennycress Supply and Seed Processing Data.....	114
D4 and D5 RINs Price Data.....	115
LCFS Credit Price and Quantity Data	116
Utilities Price Data.....	119
RESULTS	122
Summary.....	122
Net Present Value	122
Breakeven Jet Fuel Incentive	123
Breakeven Crude Oil Price	125
Breakeven Pennycress Seed Oil Prices	127
Ranking Scenarios and Identifying Key Variables.....	129
DISCUSSION	132
Conclusions.....	132
Price Sensitivities.....	132

Diesel Fuel vs. Jet Fuel and the BTC	134
Evaluating Hypotheses	135
Contributions of this Study	136
Practical Implications	138
Limitations	140
Suggestions for Further Research	142
APPENDIX	144
Pioneer Plant	144
BTC continues	144
Product slate contains both jet and diesel fuel	144
Maximum diesel fuel product slate	149
BTC is discontinued.....	153
Product slate contains both jet and diesel fuel	153
Maximum diesel fuel product slate	158
N th Plant	163
BTC continues	163
Product slate contains both jet and diesel fuel	163
Maximum diesel fuel product slate	168
BTC is discontinued.....	172
Product slate contains both jet and diesel fuel	172
Maximum diesel fuel product slate	177
REFERENCES	182

LIST OF TABLES

Table 2.1:	Studies of the agronomic performance of field pennycress.....	15
Table 3.1:	OLS of jet fuel price on US No. 2 diesel price.....	34
Table 3.2:	Robust OLS of gasoline price on US No. 2 diesel price.....	34
Table 3.3:	Robust OLS of pennycress seed meal shadow prices on soybean meal price.....	40
Table 3.4:	Robust OLS of pennycress seed meal shadow prices on DDGS prices.....	40
Table 3.5:	OLS of first differences of pennycress seed meal shadow prices and soybean meal prices.....	41
Table 3.6:	OLS of first differences of pennycress seed meal shadow prices and DDGS prices.....	41
Table 3.7:	Selected real DDGS, OLS-predicted pennycress meal, and feeding model-simulated pennycress meal prices.....	43
Table 3.8:	Linear correlation coefficients between monthly real prices of diesel fuel, soybean oil, and DDGS, January 2002 through December 2017.....	44
Table 3.9:	Linear correlation coefficients between yearly real prices of diesel fuel, soybean oil, and DDGS, 2002 through 2017.....	44
Table 3.10:	OLS of first differences of soybean oil to diesel price ratio on lags of soybean oil to diesel price ratio.....	51
Table 3.11:	Stochastic distribution parameters for diesel fuel, soybean oil, and DDGS price projections.....	53
Table 3.12:	Spearman rank-order correlation coefficients used between the stochastic time series for diesel fuel, soybean oil, and DDGS price projections.....	54
Table 3.13:	Robust OLS of US No. 2 diesel price on F.O.B. Brent crude oil spot price.....	59
Table 3.14:	Robust OLS of US No. 2 diesel price on F.O.B.WTI crude oil spot price.....	60
Table 3.15:	Two kinds of real annual growth rates for diesel fuel, soybean oil, and DDGS prices.....	61

Table 3.16:	Linear one-year autocorrelation coefficients for diesel fuel, soybean oil, and DDGS prices.....	65
Table 3.17:	Linear correlation coefficients between yearly real prices of diesel fuel, soybean oil, and DDGS, 2002 through 2017.....	68
Table 3.18:	Robust OLS of monthly real wet D5 RIN price on monthly real wet D4 RIN price.....	78
Table 3.19:	OLS of annual real wet D5 RIN price on annual real wet D4 RIN price.....	78
Table 3.20:	Robust OLS of monthly real biodiesel spot price on monthly real biodiesel breakeven price.....	82
Table 3.21:	First-differenced OLS of monthly real biodiesel spot price on monthly real biodiesel breakeven price.....	82
Table 3.22:	Robust OLS of monthly real “wet” D4 RIN price on monthly real biodiesel blend gap.....	83
Table 3.23:	First-differenced OLS of monthly real “wet” D4 RIN price on monthly real biodiesel blend gap.....	83
Table 3.24:	Robust OLS of monthly real biodiesel breakeven price on monthly real soybean oil price.....	85
Table 3.25:	Robust OLS of monthly nominal wet D4 RIN prices on monthly predicted nominal blend gaps if the BTC is NOT in place ex-ante.....	86
Table 3.26:	Robust OLS of monthly nominal wet D4 RIN prices on monthly predicted nominal blend gaps if the BTC IS in place ex-ante.....	86
Table 3.27:	OLS of monthly nominal wet D4 RIN prices on monthly predicted nominal blend gaps and two quarterly dummies if the BTC IS in place ex-ante.....	87
Table 3.28:	OLS of annual real biodiesel breakeven price on annual real soybean oil price.....	88
Table 3.29:	OLS of annual nominal wet D4 RIN prices on annual predicted nominal blend gaps if the BTC is NOT in place ex-ante.....	88
Table 3.30:	OLS of annual nominal wet D4 RIN prices on annual predicted nominal blend gaps if the BTC IS in place ex-ante.....	89
Table 3.31:	Robust OLS of historical annual real wet D4 RIN prices on predicted annual real wet D4 RIN prices 2011-2018.....	91

Table 3.32:	OLS of historical annual real wet D5 RIN prices on predicted annual real wet D5 RIN prices 2013-2018.....	91
Table 3.33:	Constrained OLS of monthly nominal biodiesel selling prices on monthly nominal wholesale US No. 2 diesel fuel prices, monthly nominal D4 RIN prices and a dummy variable for the BTC's being in effect ex-ante for the year in question.....	94
Table 3.34:	Constrained OLS of annual nominal biodiesel selling prices on annual nominal wholesale US No. 2 diesel fuel prices, annual nominal D4 RIN prices and a dummy variable for the BTC's being in effect ex-ante for the year in question.....	94
Table 3.35:	OLS of quarterly real LCFS credit prices on the number of deficits generated that quarter and the number of deficits generated in that quarter squared, beginning Q1 2015.....	98
Table 3.36:	Robust OLS of historical annual real wholesale crude oil prices (averages of Brent and West Texas Intermediate) on annual real wholesale jet fuel prices, 1990-2017.....	102
Table 4.1:	Descriptive statistics for price data used in simplified feed rationing model.....	109
Table 4.2:	Descriptive statistics for fossil-derived transportation fuel price data.....	112
Table 4.3:	Descriptive statistics for soybean oil and biodiesel price data.....	114
Table 4.4:	Descriptive statistics for D4 and D5 RINs data.....	116
Table 4.5:	Descriptive statistics for monthly LCFS prices and quarterly LCFS prices and deficits generated.....	119
Table 4.6:	Descriptive statistics for monthly industrial gas price data and yearly industrial electricity rate data.....	121
Table 5.1:	Net present value results for Iowa site, 2017 US \$, negative values in parentheses.....	123
Table 5.2:	Net present value results for Indiana site, 2017 US \$, negative values in parentheses.....	123
Table 5.3:	Breakeven jet fuel incentive results for Iowa site, 2017 US \$ per gallon.....	124
Table 5.4:	Breakeven jet fuel incentive results for Indiana site, 2017 US \$ per gallon.....	124
Table 5.5:	Breakeven constant crude oil price results for Iowa site, 2017 US \$ per barrel.....	126

Table 5.6:	Breakeven constant crude oil price results for Indiana site, 2017 US \$ per barrel.....	126
Table 5.7:	Breakeven starting crude oil price results with 2.25% real annual price growth for Iowa site, 2017 US \$ per barrel.....	127
Table 5.8:	Breakeven starting crude oil price results with 2.25% real annual price growth for Indiana site, 2017 US \$ per barrel.....	127
Table 5.9:	Biofuels producer's breakeven cost of pennycress oil at an Iowa site, as a percent of projected soybean oil prices.....	128
Table 5.10:	Biofuels producer's breakeven cost of pennycress oil at an Indiana site, as a percent of projected soybean oil prices.....	128
Table 5.11:	Ranking of scenarios based on probability of loss (P.O.L.), with impacts on other metrics also shown. Color gradients show ranking of scenarios based on each metric. Green is good; red is bad.....	130

LIST OF FIGURES

Figure 2.1:	A diagram of the CH process as presented in an ASTM research report	21
Figure 2.2:	A theoretical model of D4 RIN pricing.....	28
Figure 2.3:	An example of the performance of the theoretical model.....	29
Figure 3.1:	High-protein soybean meal, DDGS, and pennycress seed meal in real 2017 \$/kg.....	42
Figure 3.2:	Ratio of soybean oil price to No. 2 diesel fuel price.....	51
Figure 3.3:	Historical and stochastically forecasted US No. 2 diesel prices.....	55
Figure 3.4:	Historical and stochastically forecasted soybean oil prices.....	55
Figure 3.5:	Historical and stochastically forecasted DDGS prices.....	56
Figure 3.6:	2018 Diesel fuel price projections in 2017 \$/gal.....	57
Figure 3.7:	2018 Soybean oil price projections in 2017 \$/gal.....	58
Figure 3.8:	2018 DDGS price projections in 2017 \$/lb.....	58
Figure 3.9:	Stochastic diesel fuel projections vs EIA forecast.....	60
Figure 3.10:	Simulated annual growth rates for stochastic forecasts of diesel fuel prices.....	62
Figure 3.11:	Simulated annual growth rates for stochastic forecasts of soybean oil prices.....	63
Figure 3.12:	Simulated annual growth rates for stochastic forecasts of DDGS prices.....	64
Figure 3.13:	Simulated linear autocorrelation coefficients from stochastic forecast of diesel fuel prices.....	65
Figure 3.14:	Simulated linear autocorrelation coefficients from stochastic forecast of soybean oil prices.....	66
Figure 3.15:	Simulated linear autocorrelation coefficients from stochastic forecast of DDGS prices.....	67
Figure 3.16:	Simulated linear correlation coefficients between diesel fuel and soybean oil prices from stochastic forecast.....	68

Figure 3.17: Simulated linear correlation coefficients between diesel fuel and DDGS prices from stochastic forecast.....	69
Figure 3.18: Simulated linear correlation coefficients between soybean oil and DDGS prices from stochastic forecast.....	70
Figure 3.19: Historical price data compared to simulated results for US No. 2 diesel fuel prices from January 2003 through December 2017.....	71
Figure 3.20: Historical price data compared to simulated results for soybean oil prices from January 2003 through December 2017.....	72
Figure 3.21: Historical price data compared to simulated results for DDGS prices from January 2003 through December 2017.....	73
Figure 3.22: Percent chance of a gallon of soybean oil's being cheaper than a gallon of diesel fuel in novel weighted lag stochastic forecasts.....	75
Figure 3.23: Real wet D4 and D5 RIN monthly prices.....	77
Figure 3.24: A theoretical model of wet D4 RINs pricing with a Blender Tax Credit.....	80
Figure 3.25: An example of the performance of the theoretical model.....	81
Figure 3.26: Historical vs predicted real wet D4 RIN prices.....	90
Figure 3.27: Historical vs predicted real wet D5 RIN prices.....	90
Figure 3.28: A theoretical model of wet D4 RINs pricing with a Blender Tax Credit.....	93
Figure 3.29: ARB LCFS Credit Price, real 2017 US \$ per MT CO2 equivalent.....	97
Figure 4.1: US No. 2 yellow corn, 2017 US \$ per ton, Decatur, IL.....	107
Figure 4.2: High-protein soybean meal, 2017 US \$ per ton, Decatur, IL.....	108
Figure 4.3: Dried distiller's grains with solubles, 2017 US \$ per ton, Central IL.....	108
Figure 4.4: FOB crude oil price, 2017 US \$ per barrel.....	110
Figure 4.5: Wholesale US No. 2 diesel fuel price, 2017 US \$ per gallon.....	110
Figure 4.6: Wholesale kerosene-type jet fuel price, 2017 US \$ per gallon.....	111
Figure 4.7: Wholesale motor gasoline price, 2017 US \$ per gallon.....	111

Figure 4.8:	Soybean oil prices in Decatur, IL, 2017 US \$ per gallon.....	113
Figure 4.9:	FOB-at-plant Iowa biodiesel prices, 2017 US \$ per gallon.....	113
Figure 4.10:	Modeled breakeven biodiesel price at “typical” Iowa biodiesel plant, 2017 US \$ per gallon.....	114
Figure 4.11:	“Wet” D4 RINs price, 2017 US \$ per gallon of biomass-based diesel.....	115
Figure 4.12:	“Wet” D5 RINs price, 2017 US \$ per gallon of renewable naphtha.....	116
Figure 4.13:	Monthly LCFS credit prices, 2017 US \$ per MT CO ₂ equivalent.....	117
Figure 4.14:	Quarterly LCFS credit prices, 2017 US \$ per MT CO ₂ equivalent.....	118
Figure 4.15:	Quarterly deficits generated by obligated parties under the LCFS, MT CO ₂ equivalent.....	118
Figure 4.16:	Monthly industrial natural gas price data, 2017 US \$ per thousand cubic feet.....	120
Figure 4.17:	Yearly industrial electricity rates in Indiana and Iowa, 2017 US \$ per kilowatt-hour.....	120
Figure 5.1:	Seed processor’s breakeven selling price of pennycress oil, as a percent of projected soybean oil prices.....	129
Figure A.1:	Distribution of NPVs at pioneer Indiana site with the default product slate and a BTC.....	144
Figure A.2:	Distribution of NPVs at pioneer Iowa site with the default product slate and a BTC.....	145
Figure A.3:	Distribution of breakeven jet fuel incentives at pioneer Indiana site with the default product slate and a BTC.....	145
Figure A.4:	Distribution of breakeven jet fuel incentives at pioneer Iowa site with the default product slate and a BTC.....	146
Figure A.5:	Distribution of breakeven constant crude oil prices at pioneer Indiana site with the default product slate and a BTC.....	146
Figure A.6:	Distribution of breakeven constant crude oil prices at pioneer Iowa site with the default product slate and a BTC.....	147
Figure A.7:	Distribution of breakeven starting crude oil prices at pioneer Indiana site with 2.25% real annual price growth, the default product slate, and a BTC.....	147

Figure A.8:	Distribution of breakeven starting crude oil prices at pioneer Iowa site with 2.25% real annual price growth, the default product slate, and a BTC.....	148
Figure A.9:	Distribution of breakeven pennycress oil costs at pioneer Indiana site with the default product slate and a BTC, as a percent of soybean oil prices.....	148
Figure A.10:	Distribution of breakeven pennycress oil costs at pioneer Iowa site with the default product slate and a BTC, as a percent of soybean oil prices.....	149
Figure A.11:	Distribution of NPVs at pioneer Indiana site with a maximum diesel product slate and a BTC.....	149
Figure A.12:	Distribution of NPVs at pioneer Iowa site with a maximum diesel product slate and a BTC.....	150
Figure A.13:	Distribution of breakeven constant crude oil prices at pioneer Indiana site with a maximum diesel product slate and a BTC.....	150
Figure A.14:	Distribution of breakeven constant crude oil prices at pioneer Iowa site with a maximum diesel product slate and a BTC.....	151
Figure A.15:	Distribution of breakeven starting crude oil prices at pioneer Indiana site with 2.25% real annual price growth, a maximum diesel product slate, and a BTC.....	151
Figure A.16:	Distribution of breakeven starting crude oil prices at pioneer Iowa site with 2.25% real annual price growth, a maximum diesel product slate, and a BTC.....	152
Figure A.17:	Distribution of breakeven pennycress oil costs at pioneer Indiana site with a maximum diesel product slate and a BTC, as a percent of soybean oil prices.....	152
Figure A.18:	Distribution of breakeven pennycress oil costs at pioneer Iowa site with a maximum diesel product slate and a BTC, as a percent of soybean oil prices.....	153
Figure A.19:	Distribution of NPVs at pioneer Indiana site with the default product slate and NO BTC.....	153
Figure A.20:	Distribution of NPVs at pioneer Iowa site with the default product slate and NO BTC.....	154
Figure A.21:	Distribution of breakeven jet fuel incentives at pioneer Indiana site with the default product slate and NO BTC.....	154
Figure A.22:	Distribution of breakeven jet fuel incentives at pioneer Iowa site with the default product slate and NO BTC.....	155

Figure A.23: Distribution of breakeven constant crude oil prices at pioneer Indiana site with the default product slate and NO BTC.....	155
Figure A.24: Distribution of breakeven constant crude oil prices at pioneer Iowa site with the default product slate and NO BTC.....	156
Figure A.25: Distribution of breakeven starting crude oil prices at pioneer Indiana site with 2.25% real annual price growth, the default product slate, and NO BTC.....	156
Figure A.26: Distribution of breakeven starting crude oil prices at pioneer Iowa site with 2.25% real annual price growth, the default product slate, and NO BTC.....	157
Figure A.27: Distribution of breakeven pennycress oil costs at pioneer Indiana site with the default product slate and NO BTC, as a percent of soybean oil prices.....	157
Figure A.28: Distribution of breakeven pennycress oil costs at pioneer Iowa site with the default product slate and NO BTC, as a percent of soybean oil prices.....	158
Figure A.29: Distribution of NPVs at pioneer Indiana site with a maximum diesel product slate and NO BTC.....	158
Figure A.30: Distribution of NPVs at pioneer Iowa site with a maximum diesel product slate and NO BTC.....	159
Figure A.31: Distribution of breakeven constant crude oil prices at pioneer Indiana site with a maximum diesel product slate and NO BTC.....	159
Figure A.32: Distribution of breakeven constant crude oil prices at pioneer Iowa site with a maximum diesel product slate and NO BTC.....	160
Figure A.33: Distribution of breakeven starting crude oil prices at pioneer Indiana site with 2.25% real annual price growth, a maximum diesel product slate, and NO BTC.....	160
Figure A.34: Distribution of breakeven starting crude oil prices at pioneer Iowa site with 2.25% real annual price growth, a maximum diesel product slate, and NO BTC.....	161
Figure A.35: Distribution of breakeven pennycress oil costs at pioneer Indiana site a maximum diesel product slate and NO BTC, as a percent of soybean oil prices.....	161
Figure A.36: Distribution of breakeven pennycress oil costs at pioneer Iowa site a maximum diesel product slate and NO BTC, as a percent of soybean oil prices.....	162
Figure A.37: Distribution of NPVs at N th Indiana site with the default product slate and a BTC.....	163

Figure A.38: Distribution of NPVs at N th Iowa site with the default product slate and a BTC.....	164
Figure A.39: Distribution of breakeven jet fuel incentives at N th Indiana site with the default product slate and a BTC.....	164
Figure A.40: Distribution of breakeven jet fuel incentives at N th Iowa site with the default product slate and a BTC.....	165
Figure A.41: Distribution of breakeven constant crude oil prices at N th Indiana site with the default product slate and a BTC.....	165
Figure A.42: Distribution of breakeven constant crude oil prices at N th Iowa site with the default product slate and a BTC.....	166
Figure A.43: Distribution of breakeven starting crude oil prices at N th Indiana site with 2.25% real annual price growth, the default product slate, and a BTC.....	166
Figure A.44: Distribution of breakeven starting crude oil prices at N th Iowa site with 2.25% real annual price growth, the default product slate, and a BTC.....	167
Figure A.45: Distribution of breakeven pennycress oil costs at N th Indiana site with the default product slate and a BTC, as a percent of soybean oil prices.....	167
Figure A.46: Distribution of breakeven pennycress oil costs at N th Iowa site with the default product slate and a BTC, as a percent of soybean oil prices.....	168
Figure A.47: Distribution of NPVs at N th Indiana site with a maximum diesel product slate and a BTC.....	168
Figure A.48: Distribution of NPVs at N th Iowa site with a maximum diesel product slate and a BTC.....	169
Figure A.49: Distribution of breakeven constant crude oil prices at N th Indiana site with a maximum diesel product slate and a BTC.....	169
Figure A.50: Distribution of breakeven constant crude oil prices at N th Iowa site with a maximum diesel product slate and a BTC.....	170
Figure A.51: Distribution of breakeven starting crude oil prices at N th Indiana site with 2.25% real annual price growth, a maximum diesel product slate, and a BTC.....	170
Figure A.52: Distribution of breakeven starting crude oil prices at N th Iowa site with 2.25% real annual price growth, a maximum diesel product slate, and a BTC.....	171

Figure A.53: Distribution of breakeven pennycress oil costs at N th Indiana site with a maximum diesel product slate and a BTC, as a percent of soybean oil prices.....	171
Figure A.54: Distribution of breakeven pennycress oil costs at N th Iowa site with a maximum diesel product slate and a BTC, as a percent of soybean oil prices.....	172
Figure A.55: Distribution of NPVs at N th Indiana site with the default product slate and NO BTC.....	172
Figure A.56: Distribution of NPVs at N th Iowa site with the default product slate and NO BTC.....	173
Figure A.57: Distribution of breakeven jet fuel incentives at N th Indiana site with the default product slate and NO BTC.....	173
Figure A.58: Distribution of breakeven jet fuel incentives at N th Iowa site with the default product slate and NO BTC.....	174
Figure A.59: Distribution of breakeven constant crude oil prices at N th Indiana site with the default product slate and NO BTC.....	174
Figure A.60: Distribution of breakeven constant crude oil prices at N th Iowa site with the default product slate and NO BTC.....	175
Figure A.61: Distribution of breakeven starting crude oil prices at N th Indiana site with 2.25% real annual price growth, the default product slate, and NO BTC.....	175
Figure A.62: Distribution of breakeven starting crude oil prices at N th Iowa site with 2.25% real annual price growth, the default product slate, and NO BTC.....	176
Figure A.63: Distribution of breakeven pennycress oil costs at N th Indiana site with the default product slate and NO BTC, as a percent of soybean oil prices.....	176
Figure A.64: Distribution of breakeven pennycress oil costs at N th Iowa site with the default product slate and NO BTC, as a percent of soybean oil prices.....	177
Figure A.65: Distribution of NPVs at N th Indiana site with a maximum diesel product slate and NO BTC.....	177
Figure A.66: Distribution of NPVs at N th Iowa site with a maximum diesel product slate and NO BTC.....	178
Figure A.67: Distribution of breakeven constant crude oil prices at N th Indiana site with a maximum diesel product slate and NO BTC.....	178

Figure A.68: Distribution of breakeven constant crude oil prices at N th Iowa site with a maximum diesel product slate and NO BTC.....	179
Figure A.69: Distribution of breakeven starting crude oil prices at N th Indiana site with 2.25% real annual price growth, a maximum diesel product slate, and NO BTC.....	179
Figure A.70: Distribution of breakeven starting crude oil prices at N th Indiana site with 2.25% real annual price growth, a maximum diesel product slate, and NO BTC.....	180
Figure A.71: Distribution of breakeven pennycress oil costs at N th Indiana site with a maximum diesel product slate and NO BTC, as a percent of soybean oil prices.....	180
Figure A.72: Distribution of breakeven pennycress oil costs at N th Iowa site with a maximum diesel product slate and NO BTC, as a percent of soybean oil prices.....	181

ABSTRACT

Much of current interest in aviation biofuels centers on trying to curb emissions of carbon dioxide and other greenhouse gases (GHGs) [1]. The problem is that the alternative aviation fuels which have been developed so far are not economically viable without policy supports and are underwhelming in regards to their environmental sustainability. The objective of this research is to identify biofuel pathways that perform better economically and environmentally than those which have been developed thus far. This paper will pursue this objective by examining the economic performance of a CH pathway fed by field pennycress under a number of possible scenarios.

We conduct a stochastic discounted cash flow techno-economic analysis (TEA) of a plant designed to use catalytic hydrothermolysis (CH) technology to produce renewable diesel fuel, renewable jet fuel, and renewable naphtha from pennycress seed oil on a “greenfield” site under sixteen different scenarios defined by plant location, stage of commercialization, choice of fuel product slate, and policy environment. We combine process parameters such as conversion efficiencies, heat and water requirements, and capital costs for our model plant with stochastic projections of key input and output prices in order to model the distribution of possible financial outcomes for the plant over a twenty-year productive life. Our work follows McGarvey and Tynner (2018) in many respects, but uses updated process parameters from Applied Research Associates, Inc. (ARA), connects with economic analyses of the potential pennycress oil supply chain, and includes novel approaches to modeling key policies (US Renewable Fuel Standard, California Low Carbon Fuel Standard, and US Biodiesel Blender Tax Credit) and price series (US No. 2 diesel fuel, soybean oil, and dried distiller’s grains with solubles) [2]. Our output metrics include distributions of Net Present Values (NPVs), Probabilities of Loss (POLs), and distributions of Breakeven Prices (BEPs) for key inputs and outputs.

Our results show that aviation biofuels production at a greenfield CH plant fed by pennycress seed oil is not economic under current market and policy conditions. Our breakeven metrics for a renewable jet fuel policy incentive, crude oil prices, and the input cost of pennycress oil indicate this could change if one of the following were to occur:

- A crude oil price increase of at least 31-52%
- A jet fuel price increase of at least 11-26%

- A pennycress oil price discount of 2-6% from soybean oil prices
- Some combination of the above

These findings are heavily influenced by current policy design.

INTRODUCTION

Background

The air transport sector currently accounts for around 2% of global emissions of greenhouse gases (GHGs), and that figure could grow to up to 3% by 2050 in the absence of an effective mitigation effort [3, 4]. Due to the technical requirements of commercial flight, the use of alternative liquid fuels that conform to aviation's stringent fuel quality standards will be a necessary element of any such effort [1, 5]. These quality standards restrict the use of "run-of-the-mill" biofuels, such as widely available fatty acid methyl ester products, and increases the pressure to find high-quality alternatives, especially so-called "drop-in" fuels, which are one-to-one functional substitutes for existing fossil fuels approved for blending at up to 100% of final product volume [6]. Government and industry organizations such as the United States Federal Aviation Administration and the International Civil Aviation Organization are actively encouraging the development of such alternatives [7-12].

Though life cycle emissions reductions from hydrotreated fuels made from vegetable oils are often estimated at around 50% compared to traditional petroleum-based fuels [13], there are still important concerns about their overall sustainability. Two important such concerns are competition with food production and the environmental impacts of induced land use change (ILUC) [1, 14, 15]. Field pennycress (*Thlaspi arvense*) is a not-yet-commercialized oilseed crop that has been the subject of recent interest for use as a biofuel feedstock due to its high yields with low inputs and the possibility of growing it on land that would ordinarily be left fallow as a "cash cover crop", thus reducing land use change impacts and competition with food production to a minimum [1, 14, 16-19].

The economic environment surrounding biofuels is incredibly complex, and is decisively shaped by the design of numerous government policies designed to promote their production and use. In the United States alone, these include the United States Renewable Fuel Standard (RFS), California Low-Carbon Fuel Standard (LCFS), and Biodiesel Blender Tax Credit (BTC). The complexities of these policies, their interactions, and their links to other markets place difficult demands upon techno-economic analyses (TEAs) of biofuels production, such as this one. Our guiding principle in analyzing this complex economic environment is to seek to model each of

these policies' impacts in ways that are realistic and in harmony with our other assumptions and modeling choices.

Commercial production of biofuels from triglyceride feedstocks such as vegetable oils is currently dominated by the hydroprocessed esters and fatty acids (HEFA) conversion technology [6]. Catalytic hydrothermolysis (CH) is a similar, relatively new triglyceride-to-biofuel process that was jointly developed by Applied Research Associates, Incorporated (ARA) and Chevron Lummus Global [6, 20]. Though the literature strongly suggests that neither process is financially viable without policy supports [2, 21-26], CH boasts of technical advantages that may make it more economic than HEFA [27, 28]. There are currently no stochastic TEAs examining CH's application in a pennycress-to-renewable jet fuel pathway, but one recent paper by Elspeth McGarvey and Dr. Wallace Tyner (2018) does examine the closely-related case of CH conversion of *Brassica carinata* oil into aviation biofuel [2]. That study used now-outdated CH process parameters, did not make explicit connections to a supply chain for its novel oilseed feedstock, and modeled the values of credits generated under policies such as the RFS as simple, static point-estimates.

Problem Statement

The problem is that the alternative aviation fuels which have been developed so far are not economically viable without policy supports and are underwhelming in regards to their environmental sustainability. The objective of this research is to identify biofuel pathways that perform better economically and environmentally than those which have been developed thus far. This paper will pursue this objective by examining the economic performance of a CH pathway fed by field pennycress under a number of possible scenarios.

Hypotheses

We have two hypotheses. First, we expect that “greenfield” CH aviation biofuels facilities (facilities built on a site with no pre-existing industrial infrastructure) using pennycress seed oil as a feedstock would not be economically viable at projected prices, even with policy supports such as the RFS and the California Low Carbon Fuel Standard (LCFS) in effect. We test this hypothesis by realistically modeling the prices of the credits these policies generate and including these credits as sources of revenue in a discounted cash flow model, from which we estimate multiple measures

of such a facility's financial performance over a twenty-year project life. Second, we expect that the US biodiesel Blender Tax Credit (BTC) would be unimportant to such a plant's financial performance, now that the RFS is in effect [29]. We test this hypothesis by comparing the results from scenarios in which the BTC continues its recent behavior throughout the model facility's productive life with results from scenarios in which the BTC is discontinued completely for the duration of the project.

Methods

Overview

We conduct a stochastic discounted cash flow TEA of a plant designed to use CH technology to produce renewable diesel fuel, renewable jet fuel, and renewable naphtha from pennycress seed oil on a "greenfield" site. We combine process parameters such as conversion efficiencies, heat and water requirements, and capital costs for our model plant with stochastic projections of key input and output prices in order to model the distribution of possible financial outcomes for the plant over a twenty-year productive life. Our work follows McGarvey and Tyner (2018) in many respects, but uses updated process parameters from Applied Research Associates, Inc. (ARA), connects with economic analyses of the potential pennycress oil supply chain, and includes novel approaches to modeling key policies (RFS, LCFS, and BTC) and price series (US No. 2 diesel fuel, soybean oil, and dried distiller's grains with solubles) [2]. Our output metrics include distributions of Net Present Values (NPVs), Probabilities of Loss (POLs), and distributions of Breakeven Prices (BEPs) for key inputs and outputs.

Our analysis considers a total of sixteen scenarios. These are defined by two choices of states in which to locate the facility (Iowa vs. Indiana), two degrees of commercialization of the required technology (pioneer vs. "nth"), two states of the world for the BTC (continuing to exhibit similar behavior as in the period from 2011 to 2018 for the entire project life vs. being discontinued completely for the entire project life), and two potential product slates (one containing both renewable diesel and renewable jet vs. one producing only renewable diesel and renewable naphtha).

This is a stochastic analysis, and so we define a number of parameters which are subject to practically significant uncertainty as distributions, instead of fixed point-estimates. Using Monte

Carlo simulation, values for these parameters are drawn randomly from the specified distributions, the workbook is calculated and the results stored, and then the process is repeated many, many times (5000 in our case), yielding result distributions for each metric that explicitly account for the variability that is anticipated in parameter values. Thus, all of our output metrics take the form of distributions, rather than single numbers. We use @Risk™ Excel add-in software from the Palisade Corporation® to perform this procedure.

In our stochastic price forecasts, we aim to prevent unrealistic “runaway” predictions, such as can result from unbounded lag structures like Brownian Motion, as well as the “piles” of observations that can occur at the bounds of bounded lag structures, while still maintaining the highly persistent nature of these series. This is especially important for the prices of diesel fuel, soybean oil, and dried distiller’s grains with solubles (DDGS). For these prices, we also aim to account for historical correlations between them, and to harmonize our predicted diesel fuel price levels with the range of crude oil price projections available from the Energy Information Administration (EIA). We developed a novel weighted, bounded lag structure for developing stochastic forecasts of key price series that allowed us to meet these objectives. Conceptually, this structure defines the price for each commodity in each period as a weighted average between the price in the previous period and a stochastic element drawn from a bounded distribution whose minima and maxima are based on historical price data and whose mode is based on the previous random draw. These stochastic distributions are correlated to each other using a correlation matrix in @Risk®.

Key Parameters

Revenues

The kind of plant modeled here is designed to produce a product slate consisting of renewable diesel fuel, renewable jet fuel, and renewable naphtha (gasoline). Plant revenues are from sale of these three fuel products, which we assume to be of drop-in quality [6], with base prices equal to the wholesale prices of the equivalent petroleum fuels. In addition to these base prices, we assume that renewable diesel receives full pass-through of D4 Renewable Identification Number (RIN) value, partial pass-through of BTC value, if applicable, and full pass-through of LCFS credit value. The total effective unit price received by the producer we model is thus the

sum of all of these values. Equivalently, renewable jet fuel receives an effective price equal to the petroleum jet fuel wholesale price plus value from the D4 RIN price and the price of LCFS credits, and renewable naphtha receives an effective price equal to the motor gasoline wholesale price plus value from D5 RINs and LCFS credits.

Costs

Most of the cost parameters for the type of plant modeled here were provided by engineers from ARA, Inc. Among others, these include total capital costs, labor costs, and the amounts of pennycress seed oil, water, electricity, and natural gas needed each year. These last four are then combined with projections of those prices based on historical data to yield annual cost flows, with soybean oil prices used as a proxy for the price of pennycress oil. Financial assumptions, such as a real annual discount rate of 10%, a nominal annual interest rate on debt of 8%, a ten-year loan repayment period, and the timing of capital outlays and depreciation were also supplied by ARA. The most important fixed cost flows, then, are related to capital and labor, while the most important variable cost flows are from purchase of pennycress seed oil and natural gas.

RINs Price Modeling

In order to model revenues from RINs effectively, we assume that the RFS will continue in its current form for the next twenty to thirty years, that the market for D4 and D5 RINs is competitive, and that the demand in that market is perfectly inelastic at the level determined by the policy's mandate. Thus, we assume close-to-unit pass-through of D4 and D5 RINs values to producers at the time of sale, and that the values of those RINs credits are determined by the marginal production cost for RINs in that "bucket" of the RFS mandates. For D4 RINs, this marginal gallon is taken as a gallon of US soybean oil biodiesel [30-33]. In order to model the marginal costs of US biodiesel production into the future, we assume that the level of the RFS mandates stay in roughly constant proportion to the US biodiesel production capacity, such that per-unit fixed costs stay constant. Thus, we rely on a Biodiesel Profitability Model developed by researchers at Iowa State University [34] to model the costs of production of US biodiesel based on the cost of its primary input (soybean oil). We then model the price of D4 RINs in each period based on the "blend gap" between the cost of producing biodiesel in that period and the wholesale

price of diesel fuel in that period [30-33], and use linear regression to estimate the price of D5 RINs from the D4 RINs price.

Our RINs price modeling is complicated slightly by the biodiesel Blender Tax Credit (BTC), which is thought to reduce the value of RINs relative to the biodiesel blend gap in years in which it is in effect ex-ante [29, 32, 33]. In years in which it is reinstated retroactively, value from the BTC is thought to be shared between producers and blenders without affecting RINs prices [29, 32, 33]. We assume retroactively reinstated BTC value to be split roughly evenly between blenders and producers [29].

Blender Tax Credit Modeling

The BTC is a US policy that grants a nominal \$1.00 per gallon tax credit to blenders of transportation fuels for every gallon of biodiesel or renewable diesel that they blend into their final product. This policy is put into effect one year at a time, and must be either renewed or allowed to expire each calendar year. It has often been reinstated retroactively for years in which it was previously allowed to expire. The biodiesel portion of the RFS began normal operations in 2011, after allowing compliance for 2009 and 2010 to be demonstrated jointly by the end of February 2011 [35]. Since that time, the BTC has been in effect ex-ante in 2011, 2013, and 2016, and reinstated retroactively in 2012, 2014, 2015, and 2017. Based on this 2011-2018 sample period, we model the BTC as an annual, random binary variable which takes value “1” if the BTC is in effect ex-ante, and value “0” if it is not. If the BTC is not in place ex-ante, a secondary binary random variable defining the probability of its being reinstated retroactively then takes effect. Both of these variables are set to zero in all years in the scenarios that assume that the BTC is discontinued.

LCFS Credit Price Modeling

For our stochastic forecasts of the values of LCFS credits, we assume that the policy will remain in effect as currently conceived for the next twenty to thirty years, and that pass-through of credit prices from blenders to producers is equal to or close to 100%. We further assume a price cap based on the statute and a growth rate and price floor based on data since a significant climb in credit prices began in mid-2018, and that the biofuel plant considered would sell all of its output in the state of California to take advantage of the LCFS. The LCFS credit price in each period is

drawn from a bounded distribution with an upper bound equal to the statutory limit of \$200 per MT CO₂ equivalent (2016 US dollars) [36], a mode equal to the previous period's price times a growth rate drawn from the data since a significant climb in credit prices began in mid-2018, and a lower bound based on the same data.

Pennycress Seed Meal Price Modeling

In order to understand the cost and revenue structures faced by pennycress seed processors, we have to make an assumption about the market price of the seed meal co-product, which we assume is sold domestically as a component in animal feed. We approach this by assuming that its market value would be driven by its nutritional content and by the prices of other common ingredients in animal feed in the US. This allows us to simplistically model potential demand for pennycress seed meal as an ingredient in animal feed by using a monthly feed cost minimization linear program based on the nutritional needs of some major US livestock species [37]. The model minimizes the feed cost for each species in each month individually. Monthly price data for corn, soybean meal, and DDGS are taken from the USDA, and the “price” of pennycress seed meal in each month is set to zero. We force pennycress seed meal into each ration at an 8.5% inclusion rate, a rate that appears safe based on previous studies [38, 39], and use the largest shadow prices in each month as the marginal “bid” in the market for pennycress meal in that month. In doing so, we ignore the potential effects of changes in technology over time, market power, transaction costs, general equilibrium effects, and international trade. We then use OLS on the levels and first differences of our real and simulated “prices” to identify the DDGS price as a reasonable proxy for the potential market value of pennycress meal. Once DDGS prices were identified as a suitable proxy for pennycress seed meal prices, we were able to link our work to pennycress supply chain analyses produced by researchers at the University of Tennessee, Knoxville. We draw on their work to give context to our input BEPs for pennycress seed oil.

Metrics

The foundation of all of our metrics of financial performance is the NPV, which is found by discounting the total net cash flow for each year, and then summing these discounted net flows over the life of the investment. A positive NPV indicates that the investment earns returns at an annual rate that is at least as great as the discount rate, or “hurdle rate”. We use 2017 as a base

year for all our prices, and as the year in which plant construction is assumed to begin. A scenario's POL is the probability that the project fails to earn returns at least as great as the specified hurdle rate. This is equal to the percent of that scenario's NPV distribution that is less than zero.

From the NPV, we calculate BEPs. A BEP is the price of an input or output that drives the NPV to zero. A project with an output BEP lower than the actual price of that output would earn annual returns at least as great as the discount rate, barring changes in that key price. Conversely, an input BEP higher than current or likely prices for that input indicates a favorable project. We do this on the output side for the price of crude oil, which drives the prices received for all of our fuel products, and on the input side for the price of pennycress seed oil, expressed as a percent of the soybean oil price. There are two versions of the crude oil BEP, one which assumes that the crude oil price is constant in real terms (the “constant crude oil BEP” below), and another which assumes that its real price grows at 2.25% per year over the life of the plant, which we call a “starting crude oil BEP”.

We also calculate a breakeven per-gallon “bonus” for renewable jet fuel, which is the amount of additional revenue (above projected jet fuel prices) the producer would need to receive per gallon of jet fuel in order to breakeven, leaving all price projections unchanged. Finally, we draw on the work of Markel et al., 2018 and Trejo-Pech et al., 2019 [40, 41] to calculate an output BEP for pennycress seed oil from the perspective of the seed crusher, not the biofuels producer. This is also expressed as a percent of the soybean oil price. If this output BEP for pennycress oil is lower than the input BEP for pennycress oil from the side of the biofuels producer, then the pathway would have sufficient margin at each stage of the supply chain to function, barring outside influences. It should be noted that these analyses focus on the crusher, but also examine the cost structures of farmers, and set the price of pennycress seed at a level that reliably pays them the necessary margin over their production costs [40, 41]. Thus, though we only discuss the pennycress oil output BEP from the crusher's perspective, the analysis comes with farmers' interests “baked in”.

Overview of the Coming Chapters

The remainder of this paper is organized into five chapters: a literature review, a detailed methodology, a chapter presenting the data we use, a presentation of our results, and a discussion chapter. Our literature review gives more detail on the background of this research, including an

extensive review of those features of field pennycress relevant to its commercialization as an energy crop, and then compares and contrasts our work with related analyses of oilseed-to-aviation-biofuels pathways already available in the academic literature. In the methodology chapter, we present the details of our approaches for modeling key parameters and how we combine those parameters to produce our result metrics. Special emphasis is given to our methods for modeling correlated stochastic price series and dynamic, endogenous RINs values. The data chapter presents the data we use, explains where we obtain them and how we use them, and provides tables of their summary statistics, where applicable. In our results chapter, we present graphical summaries for each of our results and call out their most meaningful features. We then demonstrate how our result metrics allow us to compare and rank our sixteen scenarios and identify those environmental variables that are especially important to the financial success of our model plant. This leads into the discussion chapter, where we draw conclusions from our results, discuss their relevance to our hypotheses and the existing literature, highlight some practical implications of our work, acknowledge the limitations imposed on our results by our assumptions and methodological choices, and then offer suggestions for future research.

LITERATURE REVIEW

Greenhouse Gases and Aviation Biofuels

Much of current interest in aviation biofuels centers on trying to curb emissions of carbon dioxide and other greenhouse gases (GHGs) [1]. Lifecycle analyses of GHG emissions due to the production, transportation, and consumption of aviation biofuels have indicated 33-89% reductions compared to equivalent amounts of conventional, fossil-derived fuels [7, 13]. Alternative fuels for aviation are already in the early stages of adoption by several important consumers of jet fuel. Los Angeles International Airport, Oslo Airport, Stockholm Arlanda, and Bergen airport have all begun making regular use of alternative fuels [8]. A number of airlines have also introduced their use for certain flights or on a time-limited basis [6]. The United States Navy and Air Force have also begun performing on ambitious plans to replace up to 50% of their traditional fuel consumption with more sustainable alternatives [7]. Governments and industry organizations are likewise encouraging the interest in alternative fuels for aviation. The United States Federal Aviation Administration has set a goal of using 1 billion gallons of alternative fuels in US aviation by 2018, while the European Advanced Biofuels Flightpath targets the use of 2 million metric tons (roughly 650 million US gallons) of aviation biofuels by the year 2020 [7, 42]. The International Civil Aviation Organization (ICAO) has also taken an active role in encouraging and disseminating research on the topic, and is working on incorporating a formal definition of a Sustainable Aviation Fuel (SAF) into its Carbon Offsetting and Reduction Scheme for International Aviation (CORSIA) [9, 10]. This market-based measure (MBM) employs a cap-and-trade structure to push for carbon-neutral growth in the international civil aviation industry past the year 2020. Seventy-two states are currently participating voluntarily, representing 87.7% of international air traffic, and participation will become mandatory for almost all member states starting in 2027 [11, 12].

For all the potential that aviation biofuels seem to hold, quantifying the actual environmental impact of their production and use is difficult. Induced land use change (iLUC), as well as specific decisions made at the level of individual producers, play a large role in shaping a given biofuel pathway's GHG emissions impact, and both are very hard to quantify with reliable data [1, 13]. There is intuitive reason to believe that land use change may be especially important

for pathways which depend on crops grown at dedicated biofuel feedstocks, as is the case with oilseed-based pathways. However, most life cycle assessments (LCAs) examining such pathways do not include land use change in their estimates, so the iLUC effects of these pathways are not as well understood as they are for other pathways, such as those based on corn stover [13-15]. Another factor which leads to a high degree of variability in LCAs of biofuel pathways is the question of how to treat co-products, such as seed meal. How much of the pathway's GHG emissions get assigned to the co-product streams, versus the primary product stream, can have a very large impact on the outcome of the analysis [14]. Further complicating matters, there are numerous dimensions to sustainability other than GHG emissions, such as impacts on farmer livelihoods and the social structures of rural communities and potential losses of biodiversity and ecosystem services, which are even more difficult to measure [1]. Despite these limitations, LCAs are still the standard method for assessing a pathway's potential environmental impacts, and are used as official measures in important policies, including the US Renewable Fuel Standard (RFS) [14].

The only LCA in the literature for pennycress oil as a hydroprocessed jet fuel feedstock found that the pathway led to roughly 50% lower GHG emissions than an equivalent amount of petroleum fuel production, which is in line with estimates for other hydrotreated vegetable oil products [13, 16]. This study did not consider iLUC, but intensifications of existing production systems through the addition of an offseason cover crop, like the proposed pennycress pathway, are generally considered as having negligible iLUC impacts and to be fairly "safe bets" in regards to other aspects of sustainability which may be difficult to quantify [1, 14, 16]. This, taken with the consistency of the results with those from studies of similar pathways, indicates that the current LCA of the pennycress pathway may be treated as reliable, and that products of this process would qualify as advanced biofuels under the US Renewable Fuel Standard [16].

Two LCAs examining Italian *Brassica carinata*-to-biodiesel pathways using transesterification technology have reached differing conclusions about their environmental impacts [43, 44]. The two studies considered different co-product slates, assumed different iLUC impacts, and used different approaches for considering the sustainability impacts of co-product streams. The consistent result between the two is that the co-product slate considered has a large impact on the overall sustainability of the pathway. For the purposes of this study, which will consider a substantially different conversion technology and agronomic setting, the importance of

co-product streams on overall pathway performance is likely the most relevant result of these two LCAs.

***Thlaspi arvense*, Field Pennycress**

Introduction

Thlaspi arvense, or field pennycress, is a relatively short-season winter annual in the Brassica family that is the subject of significant interest as a biofuel crop [18, 45]. It has an extensive range, being found in temperate zones on every continent, with its North American range stretching from Alaska to Missouri, where it is normally considered as a weed, due in part to its prolific seed production [46-48]. Its short growing season and high yield under low inputs make it attractive for inclusion as a winter-season “cash cover crop” in the US Corn Belt [18, 45]. Under those conditions, grown on land that would otherwise normally be fallow, the use of field pennycress as a biofuel crop is not expected to have significant induced land use change (iLUC) impacts. Without iLUC, jet and diesel products derived from pennycress seed oil could have up to 50% lower lifecycle GHG emissions than petroleum-based equivalents, and would qualify for significant support from government policies such as the California Low-Carbon Fuel Standard (LCFS) and the US Renewable Fuel Standard (RFS) [16, 18, 45, 49]. This section of the lit review will focus first on the value of field pennycress as an energy crop and potential livestock feed source before considering other key agronomic factors related to commercial pennycress production.

Seed Oil

Pennycress seed has a high oil content, ranging from 29% to 36% by weight on a dry basis [50-52]. Pennycress seed oil has been found to be upwards of 90% unsaturated, and mostly composed of erucic (22:1) and linoleic (18:1) acids, which make up 32.8% and 22.4% of the oil by weight, respectively [53]. Its high levels of erucic acid and glucosinolates make it unsuitable for human consumption, but it is a very promising feedstock for the production of middle-distillate fuels, such as jet and diesel [27, 51, 53, 54]. Its high degree of unsaturation, especially polyunsaturation (38.3% by weight), is desirable for producing biofuels of particularly high quality [27, 28, 50].

Seed Meal

Also of interest to this paper is the potential value of pennycress seed meal as a co-product of pennycress oil extraction. The ability to sell seed meal as a co-product has been previously shown to be a key factor in the economic feasibility of biofuel production from oilseed crops [21, 55]. Most of the interest in valorizing pennycress seed meal is for its potential as a livestock feed. Estimates for the protein content of pennycress seed meal range from 26% to 35% [56-58], and the amino acid profile of this protein fraction has been shown to compare favorably with soybean and rapeseed meal, in terms of nutritional value [57]. However, pennycress seed meal also has high levels of glucosinolates, notably sinigrin, which is what gives horseradish its distinctive taste and smell [45]. These compounds and their decomposition products, isothiocyanate and allyl isothiocyanate, are at least unpalatable, and can be harmful if consumed in sufficient quantities [18, 38, 45]. Treatments do exist, however, which can substantially reduce the levels of these anti-nutritional elements in the meal. These include mild heat-treating (90°-120°C for 30 minutes) [51] or soaking the meal in water for 24 hours [59]. The literature does not contain an analysis of the effectiveness of this soaking treatment for pennycress seed meal, specifically, but its effectiveness has been demonstrated for the seed meals of other closely-related plants in the *Brassicaceae* family [59, 60]. Even untreated, however, pennycress seed has recently been shown to be safe for inclusion in broiler diets at up to 8.5% of the ration [38]. A previous study showed that it could be fed in dairy rations at up to 10% without decreasing production or introducing off flavors or odors into the milk [39]. These results are consistent with the 10% guideline used for other mustard family seed meals [18, 61].

Season and Timing

As stated above, pennycress's relatively short season enables its use preceding soybeans in existing corn-soybean and continuous soybean production systems in the US Corn Belt [17, 45]. Even with pennycress's short growing season, however, relay cropping may be an important management practice for growing it successfully [18]. Pennycress has been shown to produce its best oil yields when planted in late August to early September, leading Dose et al. [52] to recommend relaying it into late-season corn, as do Sindelar et al. [18]. Pennycress is typically harvested in early- to mid-May, which would allow farmers at some latitudes to harvest pennycress

and then still plant their soybeans by late May [17]. Phippen and Phippen found that full-season soybeans could still get optimal yields under these conditions in research trials in Macomb, Illinois [17]. Further north in Minnesota, however, sequential cropping of pennycress and soybeans did significantly delay soybean planting, thereby reducing soybean yields [62]. In this case, the authors noted that the overall seed yield of the pennycress-soybean system was still higher than the yield from soybeans alone. By comparison with work done on using the related, longer-season plant *Camelina sativa* as a “cash cover crop”, it has been suggested that this decrease in soybean yield due to delayed planting could be avoided by relaying the soybean crop into late-season pennycress [18, 63].

Yield and Inputs

Predictions of seed yield for commercial pennycress stands vary significantly based on the setting of the study in question. In general, field trials [17, 52, 62] have found lower seed yields than studies of pennycress as a weed [47, 48] or studies conducted in more controlled research settings [19, 64, 65]. Estimated seed yields as low as 672 kg/ha [17] and as high as 2242 kg/ha [16] are available in the literature, with most estimates coming between 1300 and 1500 kg/ha. These studies also give quite different estimates of the chemical inputs, such as fertilizers and herbicides, which might be required for commercial pennycress production [16, 17]. These results are summarized in Table 2.1 on the following page.

Table 2.1: Studies of the agronomic performance of field pennycress

Year	Author(s)	Setting	Inputs	Seed Yield
2012	Phippen & Phippen	field trial	none used	672-896 kg/ha
2017	Agricultural Marketing Research Center	farm conditions	56.0-22.4-22.4 kg N-P-K per ha	785- 1009 kg/ha
2015	Johnson, Kantar, Betts, & Wyse	field trial	used burn-down herbicide after pennycress harvest, fertilizer not reported	1000- 1400 kg/ha
2017	Dose, Eberle, Forcella, & Gesch	field trial	90-34-34 kg N-P-K per ha	1000- 1400 kg/ha
1944	Clopton & Triebold	research	irrigation	1338 kg/ha
1975	Best & McIntyre	weed	not reported	1500 kg/ha
1993	Carr	research	not reported	1500 kg/ha
2002	Warwick, Francis, & Susko	weed	not reported	1500 kg/ha
2015	Carvalho Carli & Phippen	laboratory	140 kg N per ha	2090 kg/ha
2013	Fan, Shonnard, Kalnes, Johnsen, & Rao	cited from industry, literature	85.2-42.6-31.4 kg N-P-K per ha	2242 kg/ha

[16, 17, 19, 47, 48, 52, 62, 64-66]

Perhaps more helpful than the variable reports of the inputs used in these studies are estimates of the amounts of the plant macronutrients nitrogen (N), phosphate (P), and potassium (K) present in a kilogram of pennycress seed. When multiplied by expected yield, these numbers

will approximate the nutrient offtake that would result from growing and harvesting a pennycress crop. Two of these estimates were found in the literature. Fan et al. cite an industry-supplied nutrient removal rate of 0.038-0.019-0.014 kg N-P-K per kg of seed [16]. The Agricultural Marketing Research Center (AGMRC) at Iowa State University estimates a nutrient removal rate between 0.056-0.022-0.022 kg N-P-K per kg of seed and 0.071-0.029-0.029 kg N-P-K per kg of seed [66].

It seems likely that the optimal balance of fertilizer inputs and seed yield would depend on a farmer's objectives. Since part of the goal of using a cover crop is to scavenge nutrients left over in the field from the primary crop, thus using fertilizer more efficiently and yielding environmental benefits from reduced waterway nutrient loading [67], it may well be worth it for some farmers to accept lower seed yields and not use additional fertilizer in pennycress production. The tradeoffs in this area of pennycress management require further research.

Potential Agronomic Drawbacks

Weedy Habit

Perhaps one of the largest challenges facing commercial pennycress production is that wild pennycress is commonly thought of as a weed, especially in the Northern Corn Belt and the Canadian Prairie Provinces, where it can compete with canola, wheat, and safflower for scarce soil moisture [47, 48]. The first descriptions of it as a weed in North America dates to 1818, when it was observed in the Detroit area by naturalist Thomas Nuttall [68]. The wild plant has exceptional cold tolerance, and is a prolific producer of high-dormancy, very persistent seeds [47, 48, 68]. In addition to yield losses, contamination of stands of alfalfa or canola with pennycress can lead to significant losses in quality, due to its high erucic acid and glucosinolate contents [47, 68, 69]. If present in sufficient quantities in hay crops or pasture, it can cause livestock to become seriously and sometimes fatally ill [47, 48, 68].

The good news on this front is two-fold: First, pennycress is susceptible to a wide range of common herbicidal chemistries [45, 47, 48, 62]. Second, commercially-selected cultivars have been demonstrated to lack the weedy habits of their wild neighbors due to their loss of seed dormancy, variable flowering, and pod shatter and the retention of the vernalization requirement of wild "winter type" pennycress [45, 70]. Variable flowering time and seed pods that shatter

easily are unattractive traits in cultivated varieties for a number of reasons. As it relates to “weediness,” they result in a higher number of the crop’s seeds having already been dropped to the ground by the time it is harvested. Commercially available pennycress varieties exhibit synchronized flowering and much lower rates of pod shatter than their wild relatives [45, 70], and should therefore leave much less seed in the field post-harvest than wild pennycress would do.

The impact of this reduced quantity of escaped seed is further reduced by the combination of low dormancy, a vernalization requirement for flowering, and heat intolerance. Seed dormancy is a noted characteristic of wild pennycress, contributing to the establishment of a highly persistent seed bank [47, 48, 68]. New commercially developed pennycress varieties are highly non-dormant, with immediate germination rates upwards of 90%, even in the dark [70, 71]. This means that only a very small proportion of seed left in the field after pennycress harvest is likely to persist past the next growing season, which simplifies the control of “volunteer” pennycress in subsequent crops. Reduced seed dormancy is paired in these new commercial varieties with retention of vernalization requirement of wild “winter type” pennycress, meaning that they will not flower without prolonged exposure to low temperatures [70]. Both wild and commercial pennycress are easily heat-stressed [45, 65]. Thus, of the escaped pennycress seeds left in the field after pennycress harvest, the vast majority are likely to germinate immediately, but be unable to flower or set seed over the course of the subsequent soybean growing season [70]. Instead, heat-intolerant volunteer pennycress would likely succumb to the high temperatures of summer and die under the canopy of the subsequent soybean crop [70]. Whether a “burn-down” herbicide treatment would still be desirable following pennycress harvest is unclear. Some trials report using one [62] while others do not [17].

Impact on Nematode Populations

Another potential drawback to the use of pennycress in systems that include soybeans is that pennycress has been identified as a host for soybean cyst nematode [72]. However, it has also been shown that the use of *Brassica* cover crops can substantially reduce the populations of other nematode species which are harmful to soybeans [73]. The net effect growing pennycress would have on the nematode pressure faced by subsequent soybean crops is therefore somewhat unclear, and an important topic for further research.

Potential Agronomic Benefits

Offseason Ground Cover

The use of cover crops has long been found to yield soil health, productivity, and environmental benefits [74]. Much of the literature focuses on the effects of using cool-season grasses, especially cereal rye [67, 74-80], legumes such as crimson clover or hairy vetch [74, 76, 81], or some combination of these two groups [75, 78, 81, 82]. Benefits from using a cover crop may include higher yield from the primary crop [74, 75, 82], increase soil organic carbon levels [78-81], reduced soil erosion [77, 79], reduced runoff and nitrogen leaching [67, 77, 81], and reduced weed pressure [76]. As noted, these studies primarily concern the benefits of using either cool-season grasses, legumes, or both as cover crops. Pennycress is neither a cool-season grass nor a legume, so it is uncertain whether all or any of these results would also apply to the use of pennycress as a cover crop. Only one study was found in the literature which included findings directly related to pennycress's value as a cover crop. Johnson et al. (2015) found that including pennycress as a cover crop preceding soybeans led to a reduction of weed biomass in the production system of more than 80% compared to letting the land lie fallow in the winter [62]. This effect was found to not be strongly influenced by the amount of cover crop biomass generated, leading the authors to suspect allelopathic activity from pennycress's production of glucosinolates to be at least part of the cause. This is supported by other studies that found glucosinolate-containing seed meals to have a strong pre-emergent herbicidal effect [62, 83-86]. While the applicability of other claimed benefits from cover-cropping to pennycress production is unclear, it does seem reasonable to expect the practice to yield at least some weed control benefits.

Pollinator Provision

A final agronomic benefit to consider which may result from producing pennycress as a cash cover crop is increased offseason and early-season food provision for important pollinators [87]. Extensive "landscape scale" planting of mass-flowering oilseed crops such as pennycress has been shown to have positive impacts on pollinator populations [88], and these impacts have been shown to continue through the growing seasons of the subsequent crop, a "temporal spillover" effect [89]. Maintaining healthy pollinator populations can often sound like a soft, vague idea, and the direct impacts on the performance of agronomic crops can be difficult to quantify.

However, pennycress attracts significant numbers of Syrphid flies, whose larval stages prey on soybean aphids [90-92], giving some producers a tangible reason to take pennycress's value as an early-season pollinator food source into account.

Hydroprocessed Esters and Fatty Acids

Currently, the oilseed-to-biofuels pathway is dominated, both in the industry and in the literature, by Hydroprocessed Esters and Fatty Acids (HEFA) production systems [6, 21, 25, 26]. HEFA fuels were approved by ASTM for blending with conventional fuels at up to 50% in 2011, and are considered of “drop-in” quality [6, 24]. A significant number of commercial HEFA plants are currently operational, both in the US and in Europe [6, 93]. The generic process converts triglyceride feedstocks into hydrocarbon fuels via some combination of the following reactions. First is hydrogenation, in which unsaturated fatty acids are converted to higher-energy saturated fatty acids, replacing C=C double bonds with C-C single bonds through the introduction of hydrogen at one of the two carbon atoms involved. Next is the freeing of fatty acids from the glycerol “backbone” of the triglyceride molecule either through thermolytic processes or through “propane cleaving,” in which free hydrogen replaces the fatty acids bound to glycerol, which is thereby converted into propane, and free fatty acids. The next step is a reaction designed to remove oxygen from the free fatty acids either through decarboxylation or through hydrodeoxygenation. Finally, the saturated, deoxygenated free fatty acids are treated with hydrogen to “crack” the fatty acid chains into smaller-length hydrocarbon chains that fall in the target range for the product distribution and to isomerize the resultant products, modifying the mix of straight-chain vs. aromatic compounds to meet target specifications. The final product stream is then fractionated into naphtha, jet, and diesel portions via distillation [94].

Numerous techno-economic analyses (TEAs) of HEFA production technologies have been performed [21-23, 95]. They have all found the HEFA conversion pathway to be uneconomic without policy supports, such as the US Renewable Fuel Standard (RFS), at current petroleum jet fuel prices [21-24]. Exploring new pathways, such as catalytic hydrothermolysis (CH), is therefore justified. Given some of the similarities between the two technologies, however, there are some conclusions from HEFA TEAs that can be helpful in guiding analyses of CH's financial feasibility. First, it has been shown that the cost of the triglyceride feedstock plays a major role in determining a HEFA plant's profitability, especially when compared to other pathways, which make use of

lower-value, often cellulosic, feedstocks [23, 55, 95-98]. Thus, the projected prices of pennycress and *B. carinata* seed will be an important factor in this paper. A second important factor in the profitability of oilseed-to-biofuel projects is often the ability to sell non-fuel co-products, such as extracted seed meal [22, 55]. Any demonstrated valuable application for either pennycress meal or *B. carinata* meal, or both, will be an important factor in this analysis. A third important factor is selecting the right plant capacity. On the one hand, economies of scale have been demonstrated for these sorts of plants [23]. On the other hand, Pearlson et al., (2013) showed that a very important factor in paying down initial capital investment was avoiding idle capacity, suggesting that it may be better make a conservative capacity choice, based on feedstock availability.

Catalytic Hydrothermolysis

Catalytic Hydrothermolysis (CH) is a hydrothermal technology optimized for converting triglyceride feedstocks, preferably those with > 30% polyunsaturated fatty acid content, into non-ester middle distillate fuels, especially jet fuel [27, 28]. The stated advantages of this process design over other triglyceride-to-jet technologies are reduced degradation of feedstock to char/coke, reduced formation of low-value gaseous byproducts, improved distribution of C-chain length in the product stream, and higher output content of high-density cycloparaffins and aromatics [27, 28, 99]. These advantages suggest that CH has the potential to be more economic than either of the more established pathways Hydroprocessed Esters and Fatty Acids (HEFA) and Hydrothermal Liquefaction (HTL) [6, 27, 28, 100].

The CH technology shares points of contact with both HEFA and HTL processes [94, 100]. Its notable similarities to HEFA technologies include its use of triglyceride feedstocks and the same basic categories of reactions, including hydrogenation, splitting of triglycerides to free fatty acids, decarboxylation and/or hydrodeoxygenation, and cracking of fatty acid chains [94]. HEFA-based processes tend to split these reactions into multiple process steps, whereas CH technology allows for direct conversion to high-quality output molecules in a single step [94, 99]. Further, while most HEFA technologies operate at high temperatures and atmospheric pressure, CH uses slightly lower temperatures but much higher pressures to make use of the unique properties of super-critical water as a solvent, reactant, and catalyst [27, 28]. The water-based nature of CH-based systems allows them to hydrolyze fatty acids directly to the cycloparaffins and aromatic molecules, which contribute to CH's higher product quality, compared to HEFA [6, 99]. This use

of high-pressure water is the most notable similarity between CH and HTL technologies, which have been explored since at least the 1970s, and many of which are designed to make use of solid-phase biomass feedstocks, hence the name “liquefaction” [25, 94, 100]. A flow chart of the process is reproduced from Coppola, 2019, in Figure 2.1 below.

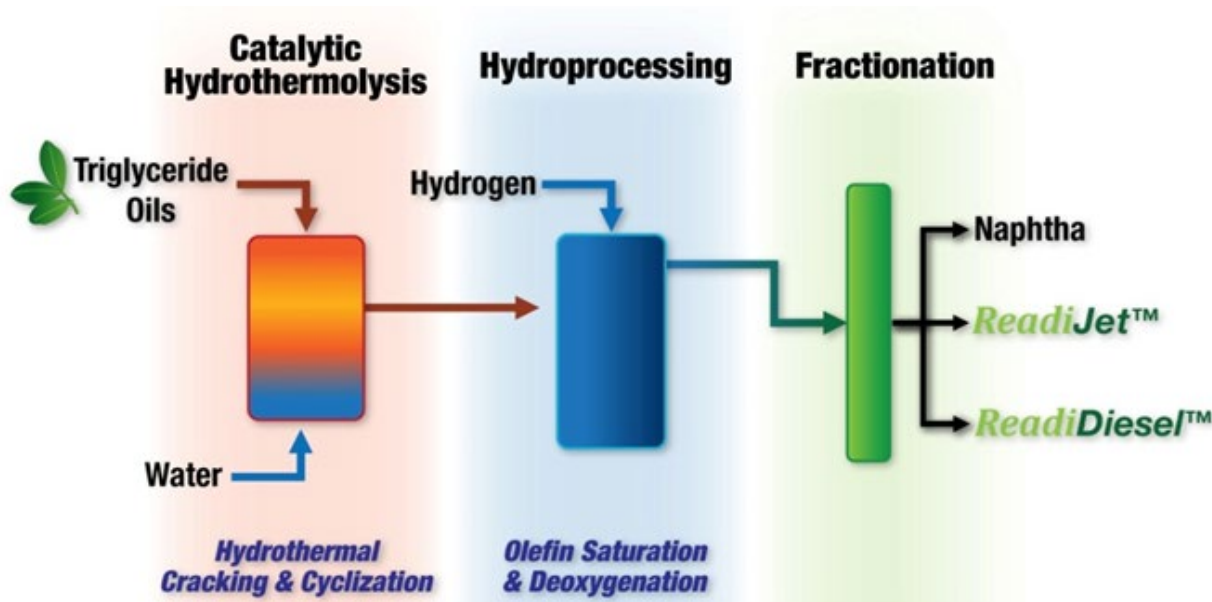


Figure 2.1: A diagram of the CH process as presented in an ASTM research report, from Coppola, 2019

Per Mawhood et al., 2016, CH currently has a Fuel Readiness Level (FRL) of 6 out of 9, corresponding to the early stages of the certification process [6]. The CH process was jointly developed by Applied Research Associates, Incorporated (ARA) and Chevron Lummus Global (CLG). It is under patent protection, and is not currently commercialized on the same scale as HEFA technologies. The fuels produced from the CH process are of higher quality than those from HEFA processes and appear likely to qualify as 100% drop-in fuels. An ASTM team has been assembled to verify this claim, and final certification is still pending [6]. However, ARA and CLG have already performed on a 2015-2016 contract to provide drop-in bio jet fuel to the US Navy out of their demonstration ISOCONVERSION facility in St. Joseph, Missouri [6, 20]. CH’s technical potential and its closeness to full certification and commercialization [6] warrant serious examination of its financial feasibility.

The literature contains one techno-economic analysis (TEA) of the CH process, performed by Elspeth McGarvey and Dr. Wallace Tyner [2]. In this paper, the authors stochastically modeled

the economic performance of “pioneer” and “nth” CH plants on “greenfield” sites with no industrial infrastructure in place) and “brownfield” sites, which already have industrial infrastructure, for each of three different feedstocks (brown grease, yellow grease, and *B. carinata* seed oil), yielding a total of twelve possible scenarios [2]. Their analysis found that the CH pathways modeled performed similarly, on the whole, to HEFA pathways previously studied by such authors as Pearlson and de Jong [2, 21, 24, 25]. As in those previous studies, policy supports and low-cost feedstocks were found to be critical to the pathway’s viability [2]. As modeled, *B. carinata* seed oil was too expensive a feedstock for that scenario to yield favorable results [2].

In many respects, the CH pathway we consider here is similar to McGarvey and Tyner’s *B. carinata* pathway. There are some significant differences, however. One is that we model two versions of a CH facility, one which produces roughly equal amounts of renewable diesel fuel and renewable jet fuel, and another that foregoes the production of renewable jet fuel entirely in order to maximize renewable diesel production. Another difference is that we use updated plant parameters from ARA, Inc., including a much higher estimate of the required initial capital investment.

Policy

Two government policies will significantly impact this analysis: The US Renewable Fuel Standard (RFS) and the California Low-Carbon Fuel Standard (LCFS). Both policies are “market-based measures” (MBMs), most often called “cap-and-trade” systems, in which emissions reductions from such activities as the production of biofuels generate credits which can be sold to “obligated parties,” who can use them to satisfy the emissions reductions targets the two policies set for their own activities. A single gallon of renewable fuels is eligible to produce a credit under both programs, if it meets both sets of criteria [101]. Additional revenue from the sale of these credits can have a significant impact on biofuels’ ability to compete with petroleum-based fuels [2, 22, 24], and will be considered in this analysis for the case of CH-derived fuels made from field pennycress seed oil.

The United States Renewable Fuel Standard

The 2005 Energy Policy Act created the RFS, which is implemented by the Environmental Protection Agency, with the US Departments of Agriculture and Energy in consulting roles [102].

Obligated parties under the RFS are refiners and importers of gasoline and diesel fuel in the United States [102]. Each obligated party has an annual mandate from the EPA to meet a Renewable Volume Obligation (RVO), which is essentially a percentage of its fossil diesel and gasoline fuel output plus any deficit remaining from a previous year [103]. The EPA sets these percentages by comparing a target volume of renewable fuel production for a given year to the projected total diesel and gasoline production in that year [102]. The Standard requires obligated parties to “retire” enough credits each year in order to be in compliance with their RVO [102]. These credits, in the form of Renewable Identification Numbers (RINs), are generated by the production of certain categories of renewable fuels, including renewable analogs for gasoline, diesel fuel, jet fuel, and heating oil. RINs remain associated with a specific batch of fuel until that batch is blended into a final fuel product, at which point the RINs may either be retired by the blender for compliance or traded to an obligated party. These trades are carried out through the EPA-Moderated Transaction System (EMTS), a database which serves to clear RIN transactions and keep records of the credit balances of all RFS participants [104].

RINs fall into one of a number of categories, identified by a D-code. The categories are “conventional” (at least 20% GHG reduction per petroleum equivalent, code D6), “advanced” (at least 50% reduction in GHGs against petroleum equivalent, code D5), “biomass-based diesel” (at least 50% reduction in GHGs against petroleum equivalent, code D4), and “cellulosic” (at least 60% GHG reduction compared to petroleum equivalent, code D3). A D3 code or a D4 code can be used to meet a D5 requirement, and a credit that meets the D5 criterion can also be used to satisfy a D6 requirement [105]. Each category is subject to certain minimum requirements set by the EPA. Total “advanced” (D5) requirement rises from 11 billion gallons to 21 billion gallons from 2018 to 2022. Within that, the “cellulosic” (D3) requirement rises from 7 billion gallons to 16 billion gallons from 2018 to 2022. Obligated parties can also purchase “cellulosic waiver credits” from the EPA, and retire them along with a non-cellulosic “advanced” RIN to meet the cellulosic requirement [102]. This can be done only in years in which EPA waives any part of the cellulosic (D3) mandate, which has been and will continue to be the case every year [102, 105].

Under RFS, estimates of GHG reductions for a specified renewable fuel product are based on “well-to-wheel” LCAs which take into account both direct and indirect emissions, including the net impacts of any co-products, which are assessed by looking at “the emissions impacts of their most likely uses and the products they replace in the market” [106]. The methodology of

considering the emissions differentials between process co-products and their substitutes as an important impact of the LCA is often called a “displacement” or “system expansion” method, and has been shown to result in higher emissions reductions estimates for pathways similar to the ones examined in this paper than the more conservative “allocation” methods [14, 16, 44]. A further positive for the pathways considered here is that the RFS has already approved a category of fuel products based on transesterification or hydrotreating of oilcrop feedstocks, including oil from annual cover crops such as *Camelina sativa*, to produce biodiesel, renewable diesel, and jet fuel, stating that fuels in this category generate a D4 advanced RIN [107]. Under the RFS system, biofuels that meet the threshold for emissions reductions and other criteria established by EPA get 1 RIN per ethanol equivalent gallon regardless of the actual level of emissions reductions. A gallon of biodiesel contains about 1.5 times the energy of ethanol, so it generates 1.5 RINs [108].

California Low Carbon Fuel Standard

LCFS, administered by California’s Air Resources Board (ARB), began implementation in 2011 as part of the state’s goal to reduce its GHG emissions to 1990 levels by the year 2020 [109]. To that end, the operational goal of the LCFS is to reduce GHG emissions from the state’s transportation sector to no more than 80% of 2011 levels by the year 2030 [49]. While fuels produced outside California can generate LCFS credits if they are sold in the state, the LCFS obligated parties are limited to providers of certain transport fuels in California, though Oregon, Washington state, and the Canadian province of British Columbia have adopted or are adopting similar programs as part of the Pacific Coast Collaborative (PCC) [49]. While suppliers of aviation fuels are not obligated parties under the LCFS, there is a plan to include alternative jet fuels as “opt-in” fuels which could generate credits even though their petroleum analogs do not generate deficits [110]. Providers of gasoline and diesel fuels generally are obligated parties, and renewable diesel and naphtha products do generate LCFS credits [49].

LCFS credits are not categorized by fuel type, like RINS are. They are based on a pathway’s “carbon intensity score” (CI), which measures the mass of CO₂ equivalent per MJ of petroleum equivalent. Fuels whose CI is below the annual target level set by the ARB generate a credit, while fuels with a higher CI score generate a deficit [36, 49, 109]. This CI score is determined by an LCA methodology which considers both direct and indirect impacts, much like the methodology employed for RINs under the RFS [109]. This LCA must be based on two years

of commercial production data [101]. Another significant difference between the policies is that while the RFS specifies a displacement-based approach to co-products, the LCFS requires that CI scores be based on whatever co-product accounting method yields the highest CI score [101]. The LCFS requires this specific accounting of lifecycle emissions for a fuel because the credit a fuel receives is based on how much lower its CI score is than that year's target, so that fuels with lower CI scores earn more credits [36, 49, 101]. This is unlike the RFS. Under the RFS, as long as a fuel meets the minimum lifecycle emissions reductions threshold and other requirements for a given RIN category, it generates that category of RIN [104].

Stochastic Techno-economic Analysis

Techno-economic analyses (TEAs) are well-established in the literature as tools for evaluating potential investments in the biofuels sector [21, 22, 24, 95, 111, 112]. TEAs are normally based on spreadsheets that contain the values of all predicted cash flows over the life of the project. These cash flows are then discounted and analyzed to obtain measures of the project's worth or financial viability. This is often referred to in the literature as "discounted cash flow rate of return" (DCFROR) modeling. The three traditional metrics of DCFROR analyses are net present value (NPV), benefit-cost ratio (B/C), and internal rate of return (IRR), though break-even prices (BEPs) for key outputs or inputs are increasingly common. The NPV of a project is simply the discounted sum of all positive and negative financial flows over the course of the project's life, given a certain price forecast and discount rate. Attractive projects have an NPV greater than zero. A project's B/C is the ratio between the NPV of its benefit flows and the NPV of its cost flows for a given forecast of prices, in which both these sums are given a positive sign. Attractive projects have a B/C greater than one. A project's IRR is the discount rate which drives its NPV to zero for a given forecast of prices. Attractive projects have IRR's greater than or equal to the decision-maker's specified "hurdle rate," which represents the minimum rate of return the decision-maker demands for such a project. A BEP is the input and / or output price which drives the NPV to zero for a given discount rate (the "hurdle rate" mentioned above). Attractive projects have output BEPs which are below the forecasted output price(s) and input BEPs that are above the forecasted input price(s), but these forecasted prices are not included in the model in BEP analysis. They are used ex-post for comparison purposes [111, 112].

Stochastic techno-economic analysis is a modeling technique that treats risk and uncertainty explicitly, normally by using computer-based Monte Carlo simulation. Instead of inputting point estimates based on long-term averages for model parameters, such as input and output prices, probability density functions for these values are constructed from historical data, expert opinion, or other sources. In Monte Carlo simulation, a computer program will randomly sample these distributions to obtain parameter values for each of the thousands of iterations of the model, storing the results from each iteration. The results are then compiled into probability distributions for the desired metrics of project worth which can better capture the uncertainty involved in a potential investment, and allow project stakeholders to make better-informed decisions in the face of uncertainty [24, 112, 113].

The value in this modeling technique lies in its ability to capture the well-attested stochastic nature of prices and other process parameters [113]. Deterministic analyses often list variability or uncertainty in these parameters as important research limitations [23, 25]. The standard way of addressing this uncertainty is through sensitivity analysis, which, though sometimes valuable, only allows for one parameter to be changed at a time. If multiple parameters are uncertain, and hence likely to change simultaneously, then sampling a probability distribution may better capture the aggregate effects of uncertainty on the results. Further, as project stakeholders are likely to be risk-averse, a deterministic BEP, where there is a 50% probability of making less than the stipulated rate of return, is not a highly useful decision-making aid [112, 113]. A drawback to this modeling decision is that it requires a more thorough knowledge of how key parameters likely would vary in the future, which is often scarce for new industrial processes [112].

This paper will perform stochastic TEAs of two pennycress-fed catalytic hydrothermolysis (CH) biofuels pathways, one that produces renewable jet fuel and one that does not. There is only one stochastic TEA available in the literature for the CH technology, the recently published article by McGarvey and Tyner [2]. The authors of this paper modeled CH aviation biofuels pathways that used brown grease, yellow grease, and *B. carinata* oil as feedstocks [2]. The close similarities between pennycress and *B. carinata*, both of which are mustard-family oilseeds that produce oil high in erucic acid [114-117], will allow this paper to draw on the work done by McGarvey and Tyner in significant ways. Most notable is the author's use of "progress curves" to move from the expected performance of a "pioneer" plant to the expected performance of an "nth" plant [2]. A "pioneer" plant is one built early in the commercialization process for a given pathway, while an

“ n^{th} ” plant is one built when the pathway is more mature. N^{th} plants benefit from the trial-and-error refinement process involved in commercializing a new technology, and therefore usually perform better than pioneer plants. Many TEAs of biofuel production processes available in the literature claim to analyze the expected performance of a future n^{th} plant for a pathway that is not yet commercialized, but they do not clearly state how data from trial or demonstration plants are modified to arrive at the data that are used to model the n^{th} plant [23, 24, 118]. One paper used data from n^{th} plant studies available in the literature as its starting point, and then worked backwards to the “pioneer” plant [25]. Prior to the publication of McGarvey and Tyner’s paper, the literature lacked a transparent, consistent approach to n^{th} vs. pioneer estimation.

The approach to this issue taken by McGarvey and Tyner was to use “progress curves” from similar industries to explicitly estimate the improvements that were expected between the pioneer data obtained from trials and demonstration plants and an n^{th} plant built ten years into the future [2]. Progress curves are essentially empirical estimates of the cost decreases expected in an industry as its output-to-date doubles [2, 119]. Selecting progress curves from industries that are as closely analogous as possible to the pathway being modeled is very important, and the authors seem to have largely succeeded on this count. For their *B. carinata* pathway, McGarvey and Tyner used a progress curve from the commercialization of rapeseed production in Germany to approximate the efficiency gains in the production and marketing of *B. carinata* seed oil [2]. Decreases in capital costs between pioneer and n^{th} plants were modeled using estimates that the U.S. Energy Information Administration uses for all biofuel pathways [2]. Decreases in operating costs were estimated based on the efficiency gains made in the Brazilian sugarcane ethanol industry [2]. Each of these progress curves predicted a ten- to twenty-percent cost decrease as output-to-date doubled [2].

McGarvey and Tyner’s analysis is still quite recent and their *B. carinata* pathway ought to be quite similar to the pennycress-based pathway considered here, and so we also make use of their operating cost progress curve based on Brazilian ethanol production. We take issue, however, with their application of a progress curve to the cost of *B. carinata* oil, since their base assumption for its price is that it would be equal to the price of soybean oil, which is a commodity that is already reached mature commercialization. This pricing assumption is based on opportunity cost, not production cost, and treats *B. carinata* oil as a perfect substitute for soybean oil in the biofuel feedstock market. Their base assumption, then, is not consistent with their use of a learning curve,

which would imply that future prices of *B. carinata* oil would fall to reflect decreasing costs of production, whereas their beginning prices are based on comparison to an already-mature commodity, and reflect opportunity costs, not production costs. For this reason, we do not follow their approach in applying a progress curve to the feedstock costs of n^{th} plants.

One important area in which existing stochastic TEAs of biofuel production pathways, including the one performed by McGarvey and Tyner, may be improved is the modelling of RIN prices. The prices of D-4 RINs have been shown to be important factors in the economic viability of biofuel production pathways similar to the one under consideration in this paper [22], and these prices have demonstrated considerable variability over the life of the RFS [120]. Further, there is a significant body of work that suggests that D-4 RIN prices may vary systematically based on the “blending margin”, or the difference between the fossil diesel price and the biodiesel price in a given period [29-33, 121, 122]. Figure 2.2 below, from Irwin and Good’s *farmdoc daily* article of 23 August, 2017, illustrates the concept.

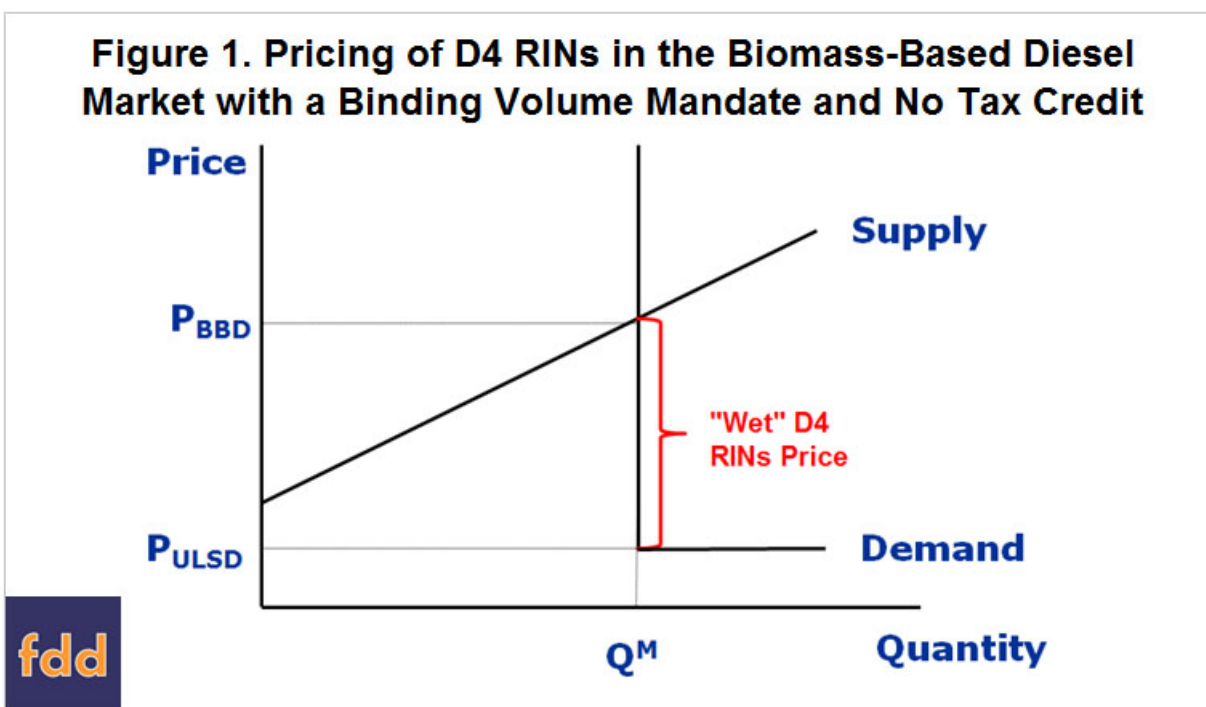


Figure 2.2: A theoretical model of D4 RIN pricing, from Irwin, S. and Good, D., 2017

The reasoning that supports this idea is simple. Since the RFS forces a higher quantity of D-4-generating fuels to be produced and bought than would be the case without the policy, the D-

4 RIN price becomes the additional payment beyond the cost of fossil-based diesel which blenders must pay to producers in order to incentivize producers to supply the quantities of these biofuels that blenders need in order to meet their RVO mandates [121]. This conceptual framework has been shown to perform quite well as a predictor of D-4 RIN prices [30], as shown in Figure 2.3 below, also from Irwin and Good, 2017.

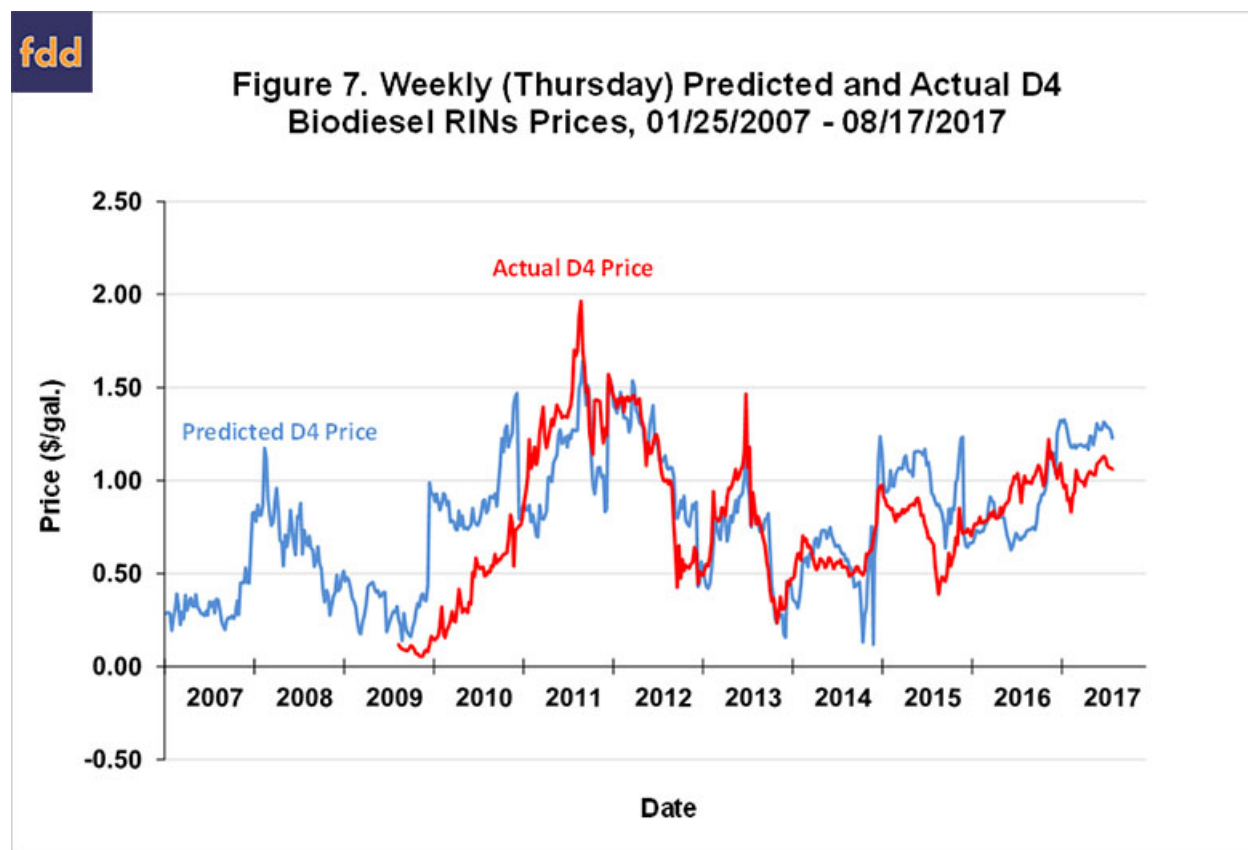


Figure 2.3: An example of the performance of the theoretical model, from Irwin, S. and Good, D., 2017

Despite this evidence of systematic variability in RIN prices, they are usually modeled as either static [2] or random [22, 24, 113] in existing biofuel production TEAs. By modelling RIN prices dynamically based on forecasted biodiesel prices (or a close proxy, such as soybean oil price) and forecasted fossil diesel prices, it may be possible to generate a much more accurate estimate of a pathway's economic viability.

Another way in which we seek to improve on the work of McGarvey and Tyner is by explicitly linking our analysis to ongoing research into the economics of stages further upstream

from ours in a potential pennycress-to-fuel value chain, something that McGarvey and Tyner could hardly do for *B. carinata*, since they had to handle two other feedstock choices, as well. Since field pennycress is not yet commercialized, this additional step increases the value of our work to future research into this pathway. We also make use of improved stochastic forecasting techniques for key prices, such as soybean oil and diesel fuel, examine the impacts of the US biodiesel Blender Tax Credit policy, employ a more-rigorous method for modeling the value of LCFS credits, and avoid specifying the savings of using a generic “brownfield” site, preferring to let those opportunities be handled on a case-by-case basis.

METHODOLOGY

Techno-Economic Analysis

As has been presented in the Literature Review section entitled “Stochastic Techno-economic Analysis”, TEAs are a standard approach for evaluating a proposed biofuels project’s attractiveness as an investment. We conduct a stochastic TEA with the goal of producing seven output metrics for the biofuel production step of a proposed pennycress seed oil-fed CH fuel production facility. These outputs are: a distribution of NPVs, a probability-of-loss (POL) estimate, and a suite of breakeven prices (BEPs). Our BEP metrics are: a distribution of breakeven jet fuel bonuses / incentives, a distribution of breakeven constant crude oil prices, assuming that the prices of diesel fuel, jet fuel, and gasoline vary accordingly, a distribution of breakeven starting crude oil prices, assuming 2.25% yearly real price growth, and assuming that the prices of diesel fuel, jet fuel, and gasoline again vary accordingly, a distribution of breakeven costs of pennycress seed oil from the perspective of the biofuels producer, as a percent of the soybean oil price, and a distribution of breakeven selling prices of pennycress oil from the perspective of the seed processor, again measured as a percent of the soybean oil price.

This TEA is conducted from the perspective of the proprietors of the proposed biofuel production facility. Accordingly, their costs are the costs of building, maintaining, and running the biofuels production facility, and their benefits are equal to their revenues. These revenues come from sales of drop-in quality diesel fuel, jet fuel, and gasoline substitutes, and from the “sale” of credits generated under three policies: The US Renewable Fuel Standard (RFS), the biodiesel Blender Tax Credit (BTC), and the California Low Carbon Fuel Standard (LCFS). We put “sale” in quotation marks because these policies are structured such that it is not producers of biofuels, but blenders, who can directly reap the benefits of these credits. However, current monetary values of these credits are easy to discover, either through officially-sanctioned electronic transaction systems, such as exist for the RFS’s RINS and LCFS credits, or through public statute (the BTC is always worth one nominal dollar per gallon). Further, the RFS and LCFS are cap-and-trade policies that present biofuel blenders with an inflexible mandate either for biofuels directly (the RFS), or for carbon-intensity reductions (the LCFS). If the constraints imposed by the policies bind, as positive prices for the relevant credits imply that they do, then blenders’ aggregate demand

for RINs and LCFS credits ought to be relatively inelastic [32, 123], increasing the bargaining power of biofuel producers relative to blenders. Therefore, we assume full or nearly full pass-through of the monetary values of RINs and LCFS credits from blenders to producers, and half-and-half split of the value of the BTC. We test these assumptions for RINs and the BTC later in this chapter. In the case of LCFS credits, a lack of pertinent cost and price data forces us to rely on the structural similarities between that policy and the RFS as support for our assumption. In making these assumptions, we follow much of the available biofuels TEA literature [2, 22, 24, 113].

As fuels generated by the CH process are of “drop-in” quality [6], we assume that the producer receives payment for the value of each physical fuel product that is equal to the price of the fossil-derived fuel for which it is a substitute (diesel fuel, jet fuel, or gasoline). Thus, the total unit payment for each biofuel produced is taken to be equal to the sum of the corresponding fossil fuel price and the per-unit value of any relevant policy incentives. An alternative approach would be to attempt to model the market prices of our three biofuel products directly, which would be exceedingly difficult to do with existing data. Price data for ethanol and soy biodiesel are available, but these price series do not have as much history as do data for fossil fuel prices, and those products are poor analogs for ours, as neither one is a drop-in fuel, like the products of a CH biofuels facility would be. We are ignorant of any existing source of data on the market price for bio-jet fuel. Since the prices of our three fossil fuels are intimately related with each other, we can stochastically forecast a single price series, and base the prices of the other two off of that result. We use diesel fuel prices for this purpose.

Successful implementation of a TEA requires capturing the correct timing of all cash flows, including not only revenue and input cost flows, but also debt, taxes, and working capital. This means that the analysis has to be done in both nominal and real terms, with some flow categories, like debt, calculated in nominal terms and then converted to real, and others, like working capital, calculated in real terms and converted to nominal. If done correctly, both approaches yield identical results, functioning as a check on possible mistakes. For the purposes of this analysis, conversion between real and nominal terms was performed using an assumed annual inflation rate of 2%.

NPVs are found by summing all positive and negative cash flows for each year, discounting these yearly net revenue flows, and then summing them over the project life. We implement this

procedure with the help of Microsoft Excel's NPV function. This is a stochastic TEA, so key uncertain parameters are described using distributions instead of point-estimates, and output distributions are obtained through Monte Carlo simulation using the @Risk[®] Excel add-in from Palisade Corporation[™]. Each parameter distribution is sampled once for each of 5000 runs of the workbook, and the NPV and breakeven estimates for each run are stored in the appropriate output cells, yielding output distributions instead of deterministic estimates of project worth. Breakeven parameter values for each iteration of the model are found by using Excel's Goal Seek function to drive the NPV to zero by changing the parameter of interest. Probabilities of loss are estimated from the NPV distributions as the percent of the 5000 iterations which had negative NPVs.

We explore a total of sixteen mini-scenarios in this analysis. We follow McGarvey and Tyner, 2018, in using learning curves to estimate expected improvements in process performance between pioneer-plant scenarios and n^{th} -plant scenarios [2]. Further, two plant locations were considered based on input from ARA, Inc., one in Iowa and one in Indiana. Unfortunately, detailed estimates of the differences in capital expenditure required between the two sites were unavailable, so different industrial electricity rates for the two states represent the sole differentiating factor in the analysis of these two locations. The default composition of our product slate contains roughly equal shares of diesel fuel and jet fuel. Due to diesel fuel's higher unit price, we explore the implications of "max diesel" scenarios, in which only renewable diesel and renewable naphtha are produced. Finally, we examine the effects of permanently removing the BTC, which some believe to be a redundant policy now that the RFS is in place [29]. All told, a pioneer and n^{th} plant scenario for each of two potential locations with two potential product slates and two potential policy environments yielded sixteen scenarios for consideration in this study.

Three input distributions used in this analysis are of particular note for the role that decisions made about them had in shaping this methodology. First is the price of ultra-low-sulfur diesel fuel, from which the prices of jet fuel and gasoline are predicted using a linear regression, as shown in Tables 3.1 and 3.2 below. Since the fuel outputs of the CH process are of "drop-in" quality [6], these fossil fuel prices were taken as fair estimates of the market value of the renewable diesel, jet, and gasoline produced by the proposed plants. Second is the price of soybean oil, which serves as a proxy for the market value of the pennycress seed oil input due to its close substitutability with other vegetable oils in common industrial biofuels production processes [54, 124, 125]. Third is the price of dried distiller's grains with solubles (DDGS), which will be shown

to be a close proxy for the market value of pennycress seed meal as an animal feed source. The particular attention given to these three input distributions is due mostly to the fact that the underlying price series demonstrate a troublesome degree of correlation with each other, which makes them particularly difficult to model effectively.

Table 3.1: OLS of jet fuel price on US No. 2 diesel price

	Jet fuel, 2017 \$/gal
US No. 2 diesel, 2017 \$/gal	0.994*** (0.0108)
Constant	-0.0537** (0.0209)
Observations	28
R-squared	0.997

Standard errors in parentheses
*** p<0.01, ** p<0.05, * p<0.1

Table 3.2: Robust OLS of gasoline price on US No. 2 diesel price

	Gasoline, 2017 \$/gal
US No. 2 diesel, 2017 \$/gal	0.838*** (0.0197)
Constant	0.319*** (0.0285)
Observations	35
R-squared	0.990

Robust standard errors in parentheses
*** p<0.01, ** p<0.05, * p<0.1

Before moving on, it is worthwhile to address the question of whether the price of soybean oil is a legitimate proxy for the value of pennycress oil (or the value of other “novel” vegetable oils). Pennycress oil is not edible due to its high concentration of very-long-chain fatty acids [45, 50]. Thus it would face only the fraction of vegetable oil demand that comes from non-food uses, mostly represented by demand from biofuel producers. Even so, we believe that it is fully appropriate to take for our base assumption that pennycress oil would be valued at the price of soybean oil, at least during the early stages of commercial production. The reasoning for this is

straightforward; between 1.5 and 2 billion gallons of transesterified biodiesel are produced in the United States annually, with 55-60% of this being produced from soybean oil [126, 127], making soybean oil the “marginal feedstock” for biodiesel production. Even in cases in which other feedstocks are used, the prices of commodity oils and greases are highly correlated with each other, as one would expect of substitute goods [128]. Unless and until pennycress production expands to a sufficient scale to make up a significant segment of the aggregate supply of biomass-based diesel feedstocks, it will not impact the “going rate” for those feedstocks, currently set by the prices of vegetable oils such as soybean and canola oils. A rational actor in such a market would not sell pennycress oil for less than the prices of the available substitutes, unless forced to do so by high transaction costs, adverse market power from buyers, or a technical limitation imposed by the physical and chemical properties of the oil, itself, that made it less useful for biofuel production. This last case has been shown to be unlikely [53, 54, 124, 125, 129].

Of course, one way that a pennycress oil’s inedible nature could cause a gap to open between its price and the price of soybean oil would be for pennycress production to expand to sufficient levels to cause a significant shift in the balance of supply and demand in the market for vegetable oil inputs to biofuel production. 1600 lbs. of seed per acre is a currently-accepted estimate of potential commercial pennycress yield [41]. At an oil content of 38% by weight and an oil density of 7.68 lbs. per gallon (the approximate density of most vegetable oils), this equates to roughly 79 gallons of pennycress oil per acre. To supply even 25% of the overall US biodiesel input supply market from pennycress, then, would require harvesting more than 6.3 million acres of pennycress each year. Put differently, this would be enough pennycress to supply the feed oil needs of seven plants of the size of the facility modeled here. Given that commercial pennycress production is currently non-existent, and that the biomass-based diesel market appears likely to keep growing due to policies such as the RFS and the LCFS, it seems safe to assume that the price of soybean oil would serve as a fair proxy for the price of pennycress oil for the foreseeable future.

Even with this support, our base assumption of perfect parity between the soybean oil price and the price of pennycress oil is a strong assumption that would only reflect reality under a certain set of market conditions. Further, this kind of approach papers over the distinctive properties of a novel oilseed crop by focusing solely on the “demand side” of the equation, with no reference to the costs of production that would shape its supply. These costs of production can often be estimated from the results of agronomic field trials, and they form the basis of a modeling approach

based on the cost of production that seeks to identify a novel feedstock's minimum selling price (MSP). This approach is common in the literature [22, 93].

With this in mind, we lean on the efforts of other researchers [40, 41] to generate a distribution of BEPs/MSPs for pennycress oil as a percent of the price of soybean oil from the perspective of a pennycress seed processor, using harmonized financial assumptions and the same price projections as in the rest of our analysis. We could build another scenario taking these processor-perspective BEPs as the cost of pennycress oil at our biofuels facility and compare the results to those under our base assumption. There would be some value in this approach, but it would fail to truly “bridge the gap” between these alternate assumptions, in terms of understanding the distance between them and how far one has to move across that gap to cross over from profitability to unprofitability, or vice-versa. We accomplish this goal by calculating another distribution of BEPs for pennycress oil, also measured as a percent of the soybean oil price, this time from the perspective of the biofuels producer. Comparing our two BEP distributions for the price of pennycress oil to each other, we can assess whether the supply chain, as a whole, generates enough margin for each stage to cover its costs, as is typical of the MSP approach. Measuring both BEPs as a percent of the soybean oil price allows for instructive comparisons with our base assumption for pennycress pricing.

Harmonizing with a Larger Pennycress Supply Chain

As pennycress is not yet grown, processed, or traded at a commercial scale, a TEA of a plant designed to produce biofuels from its seed oil would have little meaning apart from a larger analysis of whether each of the other stages in a proposed pennycress-to-biofuels value chain would also be economically viable. Such a full-chain analysis is beyond the scope of this paper, but the analysis performed here includes conscious efforts to connect with and contribute to work being done on this broader question by a team of researchers led by Dr. Burton English at the University of Tennessee, Knoxville, who are modeling the economics of commercial pennycress seed production and processing. We collaborate with them to form our assumptions about the value of pennycress seed meal and which players in the chain would capture that value, and we rely on their TEAs of pennycress seed production and processing to develop our input and output BEPs for pennycress seed oil.

Based on their research, they have set the model capacity for a pennycress seed crushing facility at 263,200 tons of seed per year, insufficient to supply the needs of the commercial-size 5000 barrel per day biofuels facility considered here. Therefore, the plant examined in this study was assumed to have no on-site crushing capacity. Instead, the plant would buy pennycress seed oil from a number of off-site crushing facilities. Under our base assumption, the biofuels plant would purchase extracted pennycress oil at the price of soybean oil, the most widely available substitute input. Further, the seed meal co-product was assumed to be owned and sold by the extraction facilities, so that, unlike in some other studies [22, 130], there was no discount applied to the input cost of the biofuels plant due to a “credit” from sale of solvent-extracted seed meal as a co-product.

Thus, the soybean oil price was assumed as an output price for Dr. English and his team and was assumed as an input price for the purposes of this analysis. For this reason, a common set of stochastic soybean oil price projections was necessary as a starting point for both research projects. In addition, the “upstream” portions of the pennycress supply chain needed an assumed pennycress meal value from which to work, and the “downstream” portion (the biofuels facility modeled here) needed stochastic projections for a number of other prices, most notably the price of ultra-low-sulfur diesel fuel, which was used to determine the value of the fuel product slate. In fact, a common set of assumptions between these two research projects proved necessary for all three of these prices due to the correlations between them exhibited in the historical data.

Determining the Value of Pennycress Seed Meal

The price that the pennycress seed meal co-product would fetch in the animal feed market ought to vary with its nutritional value as a livestock feed and with the prices of substitute goods, such as soybean meal and DDGS. Both are high-volume feedstuffs in the United States for which ample price data are available [131-134]. Estimating a robust statistical relationship between the nutritional, practical value of pennycress seed meal for livestock producers and the prices of these substitute goods would allow a pennycress seed meal “price” to be simulated based on available price series data. Following Hubbs, Bista, Preckel, and Richert (2009), these relationships were estimated by running simplified cost-minimizing linear programs for feeding five major categories of livestock: dairy cows, beef cattle, swine, laying hens, and broilers [37]. In each case, the nutritional requirements used were based primarily on the most-recently updated National

Research Council (NRC) nutrition guidelines [135-138]. In the case of broilers and laying hens, the lysine requirement was adjusted upward based on values in the literature in order to reflect changes in feeding recommendations since the last NRC update for these species, which was released in 1994 [139]. Four feed ingredients were included as options in this linear program: maize, soybean meal, DDGS, and defatted pennycress seed meal. Information on the nutritional values of these feedstuffs was obtained from the routinely updated INRA, CIRAD, AFZ, and FAO information platform “Feedipedia” in the case of maize, soybean meal, and DDGS [140-142]. Pennycress seed meal, like soybean meal or DDGS, enters feed rations primarily as a source of protein. Consistent estimates of the crude protein percentage and amino acid profile of pennycress seed meal were found in the academic literature [38, 56, 57]. Where information about pennycress seed meal’s level of another nutrient was unavailable in the literature, the values for three kinds of rapeseed meal and *Camelina sativa* meal available on Feedipedia were averaged and used as a proxy [143, 144]. These are closely-related plants to field pennycress [18, 45], and so this approximation method should serve the purposes of this very simplified feeding model.

In this model, the feeding costs for each livestock category are minimized (Equation 3.1) subject to the constraints that the minimum nutrient requirements of each species are met (Equation 3.2) and that the rate of pennycress seed meal inclusion is equal to 8.5% (Equation 3.3) [38]. The price data for this model are monthly data from January 2001 to October 2018 obtained from the USDA Agricultural Marketing Service, deflated into real terms via the Consumer Price Index with 2017 serving as the base year [133, 134, 145]. The pennycress price was set to zero in all months, and the model was solved for each month’s price data. A monthly model was used for three reasons. First, more observations in the dataset should increase the raw statistical power of inference performed on the results. Second, this method also allows for the results to be analyzed in a first-differenced model. As will be presented below in Tables 3.3 to 3.6, this step greatly clarifies the choice of which historical variable to use as a predictor of pennycress meal price. Third, it was simple to implement: historical data from the USDA was loaded into an Excel spreadsheet, and the GAMS program used to solve the model was instructed to iterate over each line in that Excel spreadsheet, storing the desired results each time. This amounted to only six lines of code. In this way, the negatives of the shadow prices on the pennycress inclusion constraints for each variety of livestock in each month represent the maximum price that a feeder of that livestock variety would be willing to pay for pennycress seed meal, given the prices of

maize, soybean meal, and DDGS, in real 2017 dollars per kilogram. Selecting the highest “price” for pennycress seed meal in each month yielded a time series of “prices” for pennycress seed meal.

The feeding cost minimization model was formulated as follows:

$$\text{Minimize } C_s = \sum_f p_f x_{fs} \quad (\text{Equation 3.1})$$

$$\text{subject to: } \sum_f v_{nf} x_{fs} \geq M_{ns} \quad (\text{Equation 3.2})$$

$$x_{\text{"pennycress meal"}s} = 0.085 \quad (\text{Equation 3.3})$$

$$x_{fs} \geq 0 \quad (\text{Equation 3.4})$$

s = livestock species

f = feed ingredient

n = nutrient

C_s = total cost of the diet for species s in real 2017 \$ per kilogram

p_f = price of feed ingredient f in real 2017 \$ per kilogram

x_{fs} = kg of feed ingredient f in one kg of feed for livestock species s

v_{nf} = amount of nutrient n in one kg of feed ingredient f

M_{ns} = minimum level of nutrient n needed in one kg of feed for livestock species s

Regression methods were used to relate this time series of simulated pennycress seed meal prices to the real data for soybean meal and DDGS prices. Binary ordinary least squares (OLS) regression with heteroskedasticity-robust standard errors was used to estimate these relationships. First-differenced models were used to check that observed correlations were not simply due to levels effects in the data. The regression tables are presented below, along with a graph of the simulated prices of pennycress meal and the price data for soybean meal and DDGS.

Table 3.3: Robust OLS of pennycress seed meal shadow prices on soybean meal prices

	Pennycress seed meal, 2017 \$/kg
Soybean meal, 2017 \$/kg	0.577*** (0.0324)
Constant	-0.000651 (0.0109)
Observations	214
R-squared	0.679
Robust standard errors in parentheses *** p<0.01, ** p<0.05, * p<0.1	

Table 3.4: Robust OLS of pennycress seed meal shadow prices on DDGS prices

	Pennycress seed meal, 2017 \$/kg
DDGS, 2017 \$/kg	1.106*** (0.0411)
Constant	0.0262*** (0.00567)
Observations	214
R-squared	0.814
Robust standard errors in parentheses *** p<0.01, ** p<0.05, * p<0.1	

Table 3.5: OLS of first differences of pennycress seed meal shadow prices and soybean meal prices

	D.Pennycress seed meal, 2017 \$/kg
D.soybean meal, 2017 \$/kg	0.345*** (0.0447)
Constant	-0.000108 (0.00143)
Observations	213
R-squared	0.221
Standard errors in parentheses *** p<0.01, ** p<0.05, * p<0.1	

Table 3.6: OLS of first differences of pennycress seed meal shadow prices and DDGS prices

	D.Pennycress seed meal, 2017 \$/kg
D.DDGS, 2017 \$/kg	1.379*** (0.0526)
Constant	2.62e-05 (0.000784)
Observations	213
R-squared	0.765
Standard errors in parentheses *** p<0.01, ** p<0.05, * p<0.1	

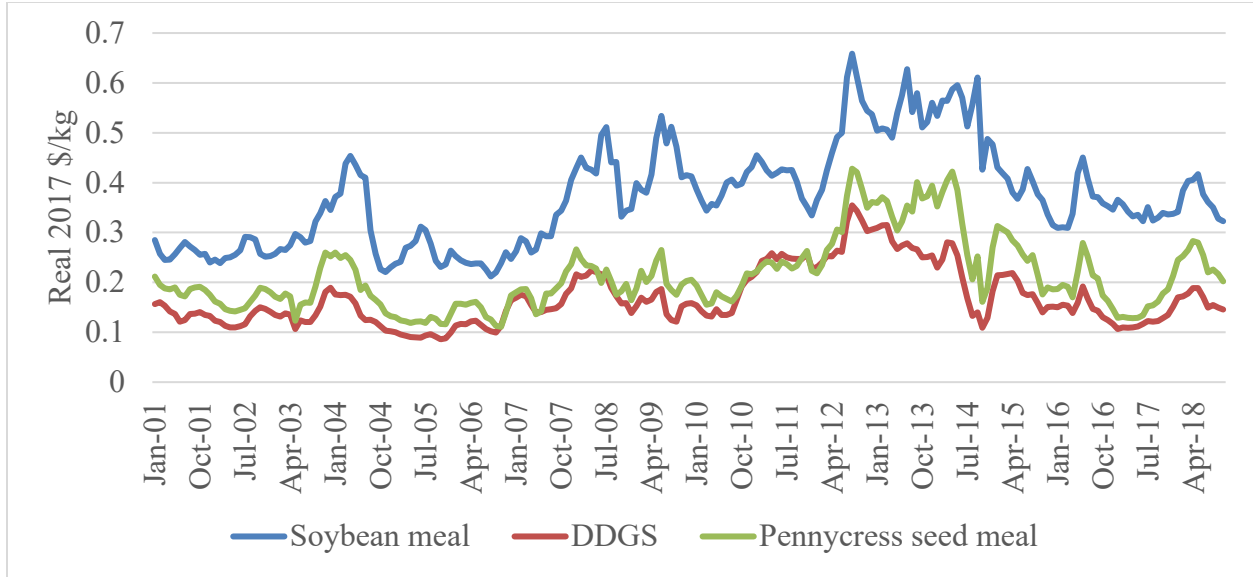


Figure 3.1: High-protein soybean meal, DDGS, and pennycress seed meal in real 2017 \$/kg

As Figure 3.1 and Tables 3.3 to 3.6 show, there are significant correlations between both soybean meal and DDGS prices and the simulated prices for pennycress seed meal. These relationships hold up in the first-differenced data as well as in the levels, pointing further towards a real explanatory relationship. The relationship is remarkably strong in the case of DDGS, for which pennycress seed meal appears to be a close substitute, with an R^2 value of 0.765 in the first-differenced model. This is easily explained by examining the crude protein percentages of these three feedstuffs. The value for high-protein soybean meal given by Feedipedia comes to 47.1% on an as-fed basis, while DDGS's crude protein level is only 26.3% as-fed [140, 142]. Solvent-extracted pennycress seed meal comes in much closer to DDGS, with values in the literature ranging from 31-33% as-fed [38, 57]. So, the market value of pennycress seed meal in any given period can be closely approximated as a linear function of the DDGS price in that period (Equation 3.5).

$$\begin{aligned} \widehat{\text{pennycress seed meal price}_t} (\$ \text{ per kg}) \\ = \$0.0262 \text{ per kg} + (1.106 * \text{DDGS price}_t (\$ \text{ per kg})) \end{aligned} \quad (\text{Equation 3.5})$$

Historical price data for DDGS are readily available from the USDA [134], making this approach to valuation of pennycress seed meal for use in animal feed both practical and powerful for a wide range of values, as demonstrated by Table 3.7.

Table 3.7: Selected real DDGS, OLS-predicted pennycress meal, and feeding model-simulated pennycress meal prices

DDGS price, 2017 \$/kg	OLS pennycress meal price, 2017 \$/kg	Feeding model pennycress meal price, 2017 \$/kg
0.086	0.12	0.12
0.12	0.16	0.16
0.15	0.19	0.20
0.21	0.26	0.25
0.35	0.42	0.43

Correlations between Price Series and “Financialization” of Commodities Markets

Having established that the price of DDGS may be used as a proxy for pennycress seed meal, we turn to address the correlations that exist between the historical prices of DDGS, soybean oil, and diesel fuel. Table 3.8 below presents the linear correlation coefficients between monthly prices for these commodities from January 2002 to December 2017, while Table 3.9 contains linear correlations between yearly average prices over the same period. The correlations between these price series are clearly significant. Even so, they also appear to be loose enough that deterministically predicting any of these prices based on the others would be inappropriate unless compelling evidence could be presented for a real causal mechanism underlying the observed correlations. The phenomenon of apparent co-movement between the prices of dubiously related commodities is one that has garnered significant attention in the literature.

Table 3.8: Linear correlation coefficients between monthly real prices of diesel fuel, soybean oil, and DDGS, January 2002 through December 2017

	US No. 2 diesel, 2017 \$/gal, monthly	Soybean oil, 2017 \$/gal, monthly	DDGS, 2017 \$/lb, monthly
US No. 2 diesel, 2017 \$/gal, monthly	1.000		
Soybean oil, 2017 \$/gal, monthly	0.8042	1.000	
DDGS, 2017 \$/lb, monthly	0.6522	0.7511	1.000

Table 3.9: Linear correlation coefficients between yearly real prices of diesel fuel, soybean oil, and DDGS, 2002 through 2017

	US No. 2 diesel, 2017 \$/gal, yearly	Soybean oil, 2017 \$/gal, yearly	DDGS, 2017 \$/lb, yearly
US No. 2 diesel, 2017 \$/gal, yearly	1.000		
Soybean oil, 2017 \$/gal, yearly	0.8444	1.000	
DDGS, 2017 \$/lb, yearly	0.7231	0.7987	1.000

Beginning near the start of the new millennium, multiple observers of physical commodities markets noticed a set of difficult-to-explain changes in the behavior of these markets. Commodities that lacked a clear technical or economic relation to each other began to move together more closely than they had in the 1990s, the levels of many commodity prices began to increase quickly, particularly in the years 2006 to 2008, and there was a perceived increase in commodity price volatility. The common shorthand for these changes is “financialization”, referring to a set of hypotheses positing that these changes were in some way or another the result of increased investment in these markets from “financial” investors, such as investment banks and mutual funds. Especially for agricultural and energy commodities, such as those that are of interest

to this analysis, it can be hard to neatly divide the topic of financialization from the questions of the “food vs. fuel” debates of the early 2000s, concerned with linkages between energy and agricultural prices due to biofuels policies. These two streams of research often appear together in the literature, and it will serve our purposes well to consider them jointly.

Academic research in this area has focused its attention on six questions. First, has there been a real change in the degree of co-movement between the prices either of a subset of commodities, or of commodities, in general? Second, if there has been a real increase in commodity price co-movement, what are its causes? Third, have commodity prices since the turn of the millennium risen beyond levels that can be explained through normal mechanisms of supply and demand? Fourth, if such “bubble” behavior has occurred, what are its causes? Fifth, have commodity prices become significantly more volatile? Sixth, if so, what has caused the increased volatility? The literature is divided on every one of these questions. Some papers tend to suggest that there has been a real increase in commodity price co-movement [146-152], some suggest otherwise [128, 153-155], and still others essentially say “it depends” [123, 156]. If there has been an increase in the correlations between certain commodity prices, then it might be due to biofuels policy [146], the trading activity of investors from the financial sector [151, 152, 157], or a complex combination of these and other factors, including exchange rates, global macroeconomic trends, monetary policy, and exceptional events like the 2008 financial crisis [123, 147, 148, 150, 158, 159]. Some studies have even found that biofuels policies would tend to buffer the prices of agricultural commodities from shocks to energy prices within certain relative price ranges [155, 156]. The literature is similarly inconclusive on the questions pertaining to price bubbles [147, 151-154, 157, 158] and volatility [123, 151, 152, 154].

If there is one conclusion that can be drawn from this literature, it is that the system of influences driving the behavior of commodity prices is complicated. The relationships between the three commodity prices of particular interest here are likely to shift as their relative prices and stocks-to-use ratios move [147, 156], macroeconomic conditions and exchange rates change [158, 159], and policy constraints bind and unbind [123]. All of these factors could, perhaps, be appropriately taken into account if we were only tasked with developing reasonable expected levels for these prices one or two months or years into the future. However, in order to perform a TEA of a proposed biofuels production facility with a 20-year productive life, we needed to develop reasonable price distributions for these commodities far into the future. Ignoring the

correlations between these prices shown by over fifteen years of data would be unwise. Explicitly modeling all of the factors likely to influence these relationships over the next two decades would be infeasible. Instead, we decided to model these prices so that they would generally follow each other about as closely as they had in the sample period, especially on longer time scales, while allowing them enough independence from each other that knowing one price would not allow one to pinpoint the levels of the other prices in that period.

A Novel Weighted, Bounded Lag Structure for Stochastic Time Series Forecasting

After investigating the relationships between the prices of US No. 2 diesel fuel, soybean oil, and DDGS, we wanted the stochastic forecasts to approximate the behaviors these prices show in the sample, without specifying any overly precise mathematical relationships between them. This decision ruled out such methods as vector autoregression (VAR) or vector error correction models (VECMs). These are powerful approaches for investigating the relationships between time series, but the very precision that makes them useful for this purpose also makes them strongly susceptible to structural changes, which are quite common in commodity price series [159]. Indeed, many studies of the relationships between commodity prices have used these approaches, but the results tend to be quite sensitive to the choice of sample period [146, 148, 149]. To use these approaches to forecast prices over a twenty-year time horizon would require an assumption that no meaningful structural changes would be likely to occur during the forecast period. That is an assumption we was not willing to make.

Having ruled out VAR and VECM modeling, we decided to use seven objectives to guide our choice of forecasting method. First, the price levels yielded by the forecast should be consistent both with the levels of real prices during the sample period and with any publicly available forecasts for those prices developed by experts in that field. In practice, this meant that the diesel forecast should be consistent with the range of Energy Information Administration (EIA) forecasts of crude oil price. Second, the forecasts should reflect the real growth rates observed in the sample data, if any. Third, the year-to-year autocorrelations for each price series over the 22-year forecast period should be similar to those observed in the data over the 16-year sample period. Fourth, the pairwise correlations between the price series over the forecast period should be similar to those observed over the sample period. Fifth, the shapes of the distributions of forecasted prices should be qualitatively similar to the shapes of the price distributions in the sample data. Sixth,

the forecast should not yield highly unrealistic results, such as predicting negative prices or forecasting that soybean oil will become consistently cheaper than diesel fuel. This last state of affairs is one that some methods proved highly likely to predict, yet soybean oil has only been cheaper than diesel fuel in 21 out of the 192 months of the monthly sample data. In the yearly averages of the sample data, soybean oil has been less expensive than diesel fuel in one out of 16 years. This makes intuitive sense, since if soybean oil were to be cheaper than diesel fuel for a significant length of time, one would expect that producers of biodiesel would bid up the price of soybean oil to roughly match that of diesel fuel, unless they faced binding capacity constraints, which could be removed over the long run. In all but the most-extreme iterations of the model, then, diesel fuel should be less expensive than soybean oil on a per-gallon basis. Seventh, annual forecasts should be deliverable in an Excel workbook of reasonable size.

Non-Time Series Approaches

One simple approach to modeling these variables would be to fit distributions to the historical price data for each variable, use a correlation matrix to define the correlations between them, and then draw from this distribution once for each iteration of the model. This would assign a constant price level for each simulated 23-year project life. The appeal of this approach is its simplicity, but it is not very realistic. The historical price data exhibit non-zero growth trends in real terms, along with considerable year-to-year variability. Assigning constant levels to these prices over the entire project life thus fails to accurately simulate the behavior we would expect out of these prices. This approach would tend to make the outcome distributions “wider,” unrealistically inflating the variances of our financial performance measures. This is because each price would only be drawn once per iteration, effectively resulting in a “sample size” one-twentieth as large as what would result if prices were drawn in each year. Variance increases as sample size decreases. In reality, an extremely high price in one year is likely to be offset by lower prices in later years, due to year-to-year variation in price levels. This does not happen in the approach described above.

At the opposite end of the spectrum, price distributions could be defined independently for each year of the model, and a correlation matrix could be used to define the relationships between them in each year. This approach would result in unrealistically low variances in the bottom-line measures, as extremely high or low prices in any given year would have no effect on prices in

subsequent years, belying the highly persistent nature of these prices. It would also be difficult to introduce the real growth trends observed in the data into the projections using this approach. Both of these two approaches ignore key aspects of the data in ways that would reduce the model's accuracy in assessing the variances of our project worth measures, making it a less effective tool for assessing the riskiness of the investments in question.

The @Risk® Batch Fit Tool

Another approach to this issue would be to make use of the @Risk® time series tool called Batch Fit. This tool fits each time series in a “batch” to one of eleven different time series modeling techniques, such as Brownian motion, GARCH, ARMA, and others, making them stochastic through a random error term and correlating them to each other with a correlation matrix. There were a few practical problems with this approach, however. First, the use of absolute references and array formulas in the output made it difficult to transfer the results into another workbook. Second, the correlations between output distributions that this tool yields were consistently much lower than those observed in the sample data, meaning that the correlation matrix would have to be adjusted manually. Since the correlation matrix applies to the data after Batch Fit has transformed them for stationarity and / or non-negativity, it can be difficult to conceptualize what one is doing when one attempts to adjust this matrix manually.

In addition to these practical concerns, this approach failed to satisfy the objectives outlined above. First, the forecasting methods used by the Batch Fit tool often failed to produce forecasts of the price of diesel fuel whose distributions were consistent with the range of crude oil forecasts published by the EIA. Second, Batch Fit forecasts consistently overestimated the probability of soybean oil's being less expensive than diesel fuel. Most of the time, Batch Fit forecasts predicted that a gallon of soybean oil would almost always cost less than a gallon of diesel fuel starting ten years in the future. As previously discussed, this seems like an unrealistic result. Third, the automated nature of Batch Fit predictions means that monthly data can only yield monthly forecasts, while annual forecasts can only be made based on annual data. The only way to use Batch Fit and yet avoid building a workbook with 240 distinct stochastic entries for each time series would be to base the forecasts on only the 16 data points of annual data. This was an unacceptable trade-off between file size and analytical rigor.

Conventional Lag Structures

Lag structures make the price in each period equal to the price in the previous period plus a random change or multiplied by a random percent change plus one. This approach is easy to implement, preserves the highly persistent nature of the price series modeled, allows growth trends to be taken into account, and would permit correlations to be specified between the random change elements of the three series of interest in each period. For all their benefits, conventional lag structures would fail to meet our objectives for forecasting diesel fuel, soybean oil, and DDGS prices. First, though the random element in the structure can easily be specified with a bounded distribution, this limit to the size of period-over-period changes does not prevent the simulated price levels themselves from taking unrealistic values. Unless bounds are imposed on the levels, there is nothing to stop “runaway” iterations of the model from predicting unrealistic or even impossible results, such as negative prices or absurdly high prices, like \$20 per gallon for diesel fuel. Thus, it is usually necessary to impose bounds on lagged price levels by using nested minimum and maximum statements. While this is a viable method, it comes with the undesirable effect of yielding price distributions that do not qualitatively resemble the data on which they are based. The historical data for many price series, including those of interest here, are distributed in a more or less bell-shaped fashion, with most observations falling in the center of the range. By contrast, bounded lag structures tend to result in distributions that are shaped more like a capital “U” or a capital “W”. These are very wide, uniform distributions of observations between the bounds with unrealistic “piles” of observations at the bounds. Another difficulty presented by this method is that it again presents the difficulty of choosing to model the random change term based either on the monthly data, resulting in a monthly forecast of unwieldy size, or on the annual data, which in this case would result in a fit based on only 16 observations.

A Novel Approach

In this analysis, a novel bounded lag structure was developed for stochastic forecasting of the prices of ultra-low sulfur diesel fuel, soybean oil, and DDGS. Conceptually, this structure defines the price for each commodity in each period as a weighted average between the price in the previous period and a stochastic element drawn from a bounded distribution whose minima

and maxima were based on historical price data and whose mode was based on the previous random draw. The details of the structure used for diesel fuel is presented in Equation 3.6 below.

$$\begin{aligned}
 & Diesel_t \\
 &= 0.7 * Diesel_{t-1} + 0.3 \\
 &* RiskTriang(lower\ bound_{diesel}, \min(growth_{diesel} \\
 &* diesel\ random\ element_{t-1}, upper\ bound_{diesel}), upper\ bound_{diesel}) \quad (Equation\ 3.6)
 \end{aligned}$$

As Equation 3.6 shows, the diesel price in the previous period received a weight of 0.7, while the current period's random element received a weight of 0.3. This random element is drawn from a triangular distribution. The lower bound of this distribution was defined as 0.75 times the lowest real price observed in the monthly data, which run from January 1983 to December 2017, and were converted into real 2017 dollars per gallon using the Consumer Price Index. The upper bound of the distribution was defined as 1.25 times the highest observed real price in the same dataset. The mode was defined either as the previous random draw times a growth factor or as the upper bound of the distribution, whichever is lower. This structure prevents errors resulting from the distribution's having a mode outside its allowed range. The growth factor used was defined as one plus the median monthly percent change in the data, raised to the twelfth power. For the values of these parameters alongside those for soybean oil and DDGS, see Table 3.11.

For soybean oil, a slightly different approach was used. While investigating the data, it was found that the ratio between the prices of soybean oil and diesel fuel exhibited mean-reverting behavior. This can be seen in Figure 3.2 and Table 3.10 below, which present a graph of the ratio over time and a regression of its first differences on its lagged levels. In Figure 3.2, we see that the ratio of these prices tends to oscillate around a mean of roughly 1 to 1.5. In Table 3.10, we see that the relationship between the lagged levels of the ratio and its first differences is negative, implying that once the ratio reaches a certain threshold level, it is likely to fall in the following period. Based on this regression, that threshold level can be calculated as approximately 1.36, in line with the visual evidence presented in Figure 3.2.

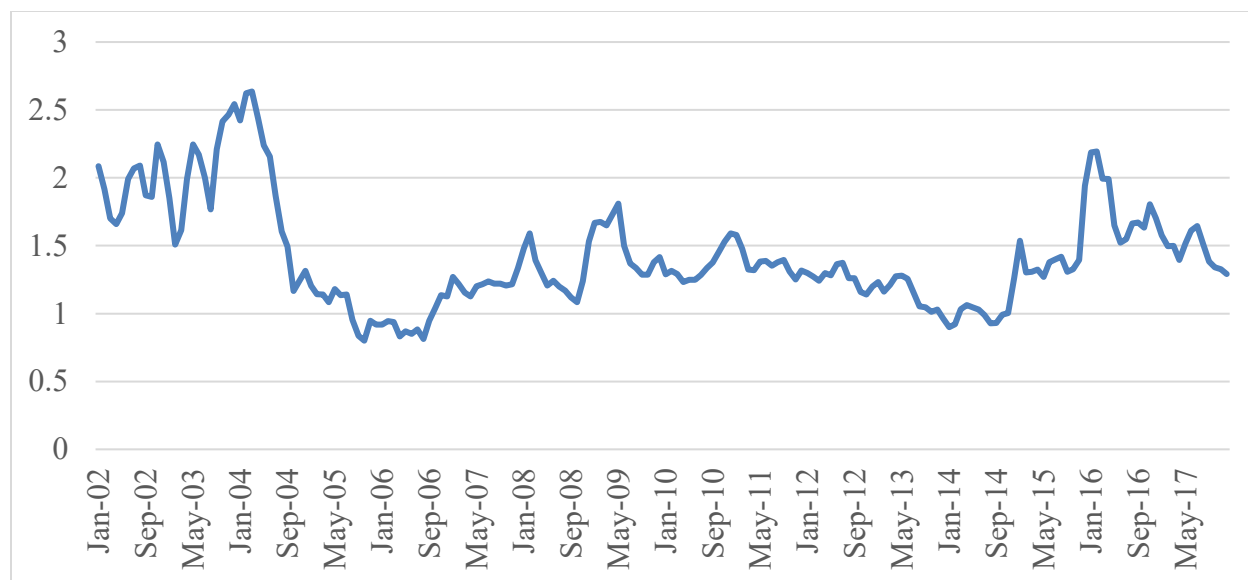


Figure 3.2: Ratio of soybean oil price to No. 2 diesel fuel price

Table 3.10: OLS of first differences of soybean oil to diesel price ratio on lags of soybean oil to diesel price ratio

	D.Soybean oil to diesel price ratio
L.Soybean oil to diesel price ratio	-0.0618** (0.0236)
Constant	0.0838** (0.0349)
Observations	191
R-squared	0.0350

Standard errors in parentheses

*** p<0.01, ** p<0.05, * p<0.1

The relationship between soybean oil and diesel fuel prices defines the margin between a pennycress oil CH plant's primary raw material cost and the prices of its outputs. It also was used in this analysis to model the value of the RIN credits it would generate. Therefore, the relationship between these two prices was of the utmost importance. For this reason, the random element in the stochastic forecasts for soybean oil prices was defined based on the ratio between soybean oil and diesel fuel prices in the data. The details of this structure are presented below in Equation 3.7.

$$\begin{aligned}
& \text{Soybean oil}_t \\
& = 0.25 * \text{Soybean oil}_{t-1} + 0.75 \\
& * (\text{diesel random element}_t \\
& * \text{RiskPert}(0.91479, 1.118, 2.9781))
\end{aligned}
\tag{Equation 3.7}$$

As Equation 3.7 shows, the previous soybean oil price received a weight of 0.25, while the random soybean oil element for that period received a weight of 0.75. The ratio between soybean oil and diesel fuel prices was modeled with a Pert distribution based on annual average real prices from 2002 to 2017. As previously stated, a point of concern for these forecasts was to limit the number of years in which the soybean oil price was predicted to be lower than the diesel fuel price. This concern drove the decision to use annual data when defining the soybean oil to diesel fuel price ratio. A Pert distribution fit to the monthly price ratio had a minimum of 0.79101, a mode of 1.1634, and a maximum of 3.1453. Using the narrower ratio distribution based on yearly averages seemed better suited to the purposes of this analysis. Concerns about predicting an unrealistically narrow range of soybean oil prices were allayed by the fact that the distribution of price ratios was multiplied by the diesel fuel random element for each period to yield the random element for soybean oil. The diesel fuel random element, which was based on monthly data, introduced sufficient variation into the soybean oil price projections to reasonably replicate the variation observed in the data.

DDGS prices were modeled similarly to diesel fuel prices, with the exception that a small weight was assigned to an additional component based on a regression of DDGS prices on diesel fuel prices, constrained through the origin. Without this additional term, it proved difficult to obtain predictions for DDGS prices that exhibited the desired degree of correlation to diesel fuel prices. This may be due to the relative magnitudes of these two series. Since DDGS prices were measured in dollars per pound, while diesel fuel and soybean oil were priced in dollars per gallon, the DDGS prices were significantly smaller. With the additional constrained regression term, the desired levels of correlation were obtained. This structure is presented below in Equation 3.8.

$$\begin{aligned}
& DDGS_t \\
& = 0.1 * (0.033131 * \text{diesel random element}_t) + 0.9 \\
& * (0.6 * DDGS_{t-1} + 0.4 \\
& * RiskTriang(\text{lower bound}_{DDGS}, \min(\text{growth}_{DDGS} \\
& * DDGS \text{ random element}_{t-1}, \text{upper bound}_{DDGS}), \text{upper bound}_{DDGS})) \quad (\text{Equation 3.8})
\end{aligned}$$

As in the equation for diesel fuel, the random element was defined as a triangular distribution with a minimum defined as 0.75 times the lowest real monthly price in the data and a maximum defined as 1.25 times the highest real monthly price in the data. The mode of the triangular distribution was defined either as the previous random element times a growth factor defined by the monthly data or as the upper bound of the distribution, whichever was lower. The growth rate was defined as one plus the median monthly percent change in the data, raised to the twelfth power. All of this follows the structure used to project diesel fuel prices. The difference is found in the two levels of weights used in this equation. In the outer level, a prediction of the DDGS price based on a constrained regression on the diesel fuel price received a weight of 0.1, while the part of the equation that mirrors the equation used for diesel fuel received a weight of 0.9. In the inner level, the previous DDGS price received a weight of 0.6, while a weight of 0.4 was assigned to the random DDGS element for that period. The parameter values used in the random elements of the equations for diesel fuel, soybean oil, and DDGS can be found in Table 3.11 below.

Table 3.11: Stochastic distribution parameters for diesel fuel, soybean oil, and DDGS price projections

	US No. 2 Diesel fuel, 2017 \$/gal	Soybean oil to diesel fuel price ratio	DDGS, 2017 \$/lb
Distribution	triangular	Pert	triangular
Minimum	0.3918	0.9148	0.02926
Mode	See Equation 6	1.118	See Equation 8
Annual Real Growth Rate	3.353%	NA	1.370%
Maximum	5.438	2.978	0.2010

An @Risk correlation matrix containing Spearman rank-order correlation coefficients was used to correlate the stochastic series for diesel fuel, soybean oil, and DDGS prices defined by Equations 2.6 to 2.8. This correlation matrix is reproduced in Table 3.12 below. Like the weights on previous values and current random elements used in Equations 3.6 to 3.8, the coefficients in this matrix were selected to cause the stochastic projections to exhibit similar correlative behaviors to the historical price series on which they are based. Therefore, they do not have much real meaning beyond that these are the values that were found to “work”.

Table 3.12: Spearman rank-order correlation coefficients used between the stochastic time series for diesel fuel, soybean oil, and DDGS price projections

	US No. 2 Diesel fuel, 2017 \$/gal	Soybean oil to diesel fuel price ratio	DDGS, 2017 US \$/lb
US No. 2 Diesel fuel, 2017 \$/gal	1.0		
Soybean oil to diesel fuel price ratio	-0.90	1.0	
DDGS, 2017 US \$/lb	0.55	-0.20	1.0

Evaluating our Stochastic Forecasts

Are the forecasted levels consistent with historical data and expert opinion?

The first criterion for our forecasts was that the levels of all our projected prices should be consistent with the historical data and that our projections of diesel fuel price should be consistent with the EIA forecasts of crude oil prices. Since the minimum and maximum values for the random elements in our projections were drawn from the data, we would expect them to be quite consistent with historical prices. Figures 3.3 through 3.5 on the next page compare historical diesel fuel, soybean oil, and DDGS annual prices from 2002 to 2017 with five sample iterations of stochastic forecasts for the same period produced using the method outlined above.

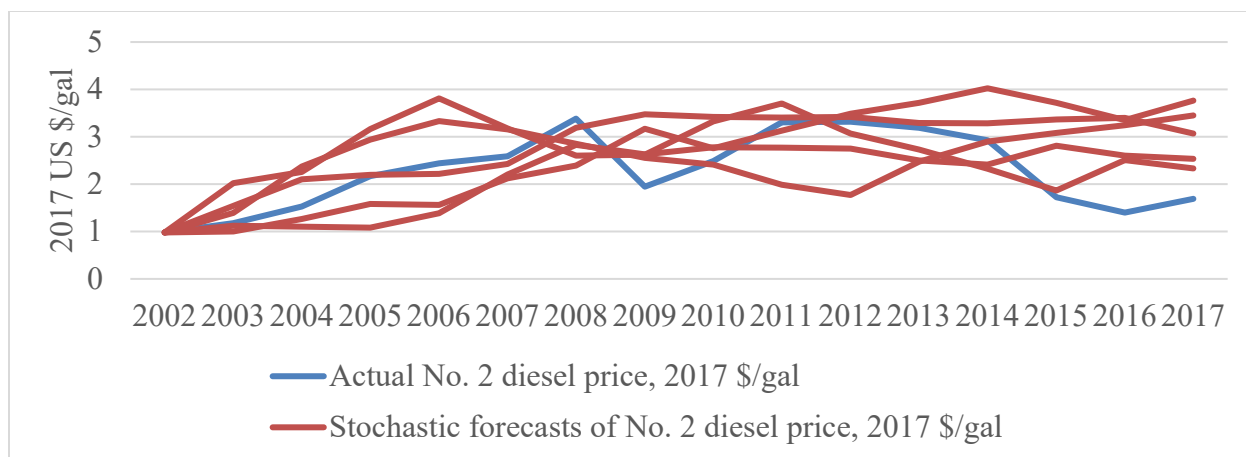


Figure 3.3: Historical and stochastically forecasted US No. 2 diesel prices

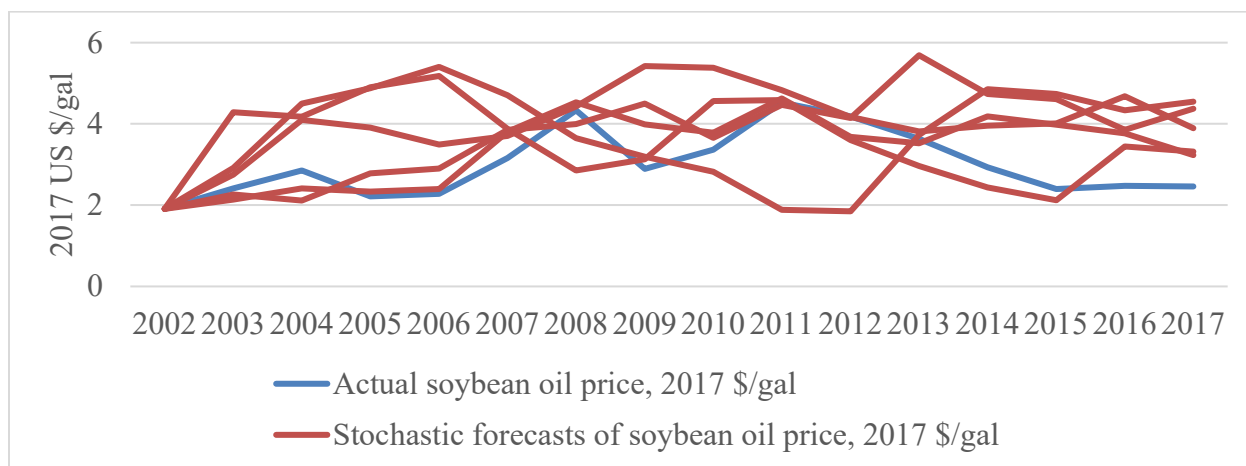


Figure 3.4: Historical and stochastically forecasted soybean oil prices

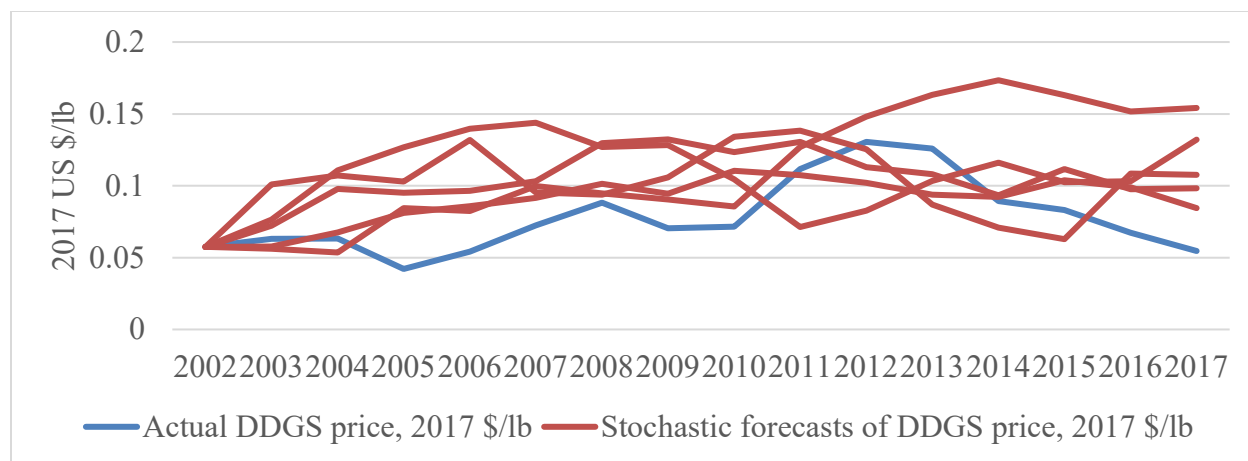


Figure 3.5: Historical and stochastically forecasted DDGS prices

As the preceding figures show, the stochastic forecasting method employed here does a good job of simulating the past for diesel fuel, a credible job for soybean oil, and a passable job for DDGS. The predictions tend to skew positive when applied to the past, especially for soybean oil and DDGS, though they do appear to be “in the ballpark”. We are willing to accept this performance because the parameter values in this forecasting system were not optimized for the goal of predicting the past, but for the goal of producing credible ranges of predicted values far into the future. This is especially true of the growth factors we used. There are two benchmarks we can employ to check the model’s forward-looking performance. First, since 2017 was taken as the base year for this study, real price data are already available for the first forecasted year, which was 2018. Our method’s performance for 2018 is presented below. The second forward-looking benchmark we can use to evaluate our forecasts is the EIA’s set of long-range predictions for crude oil prices.

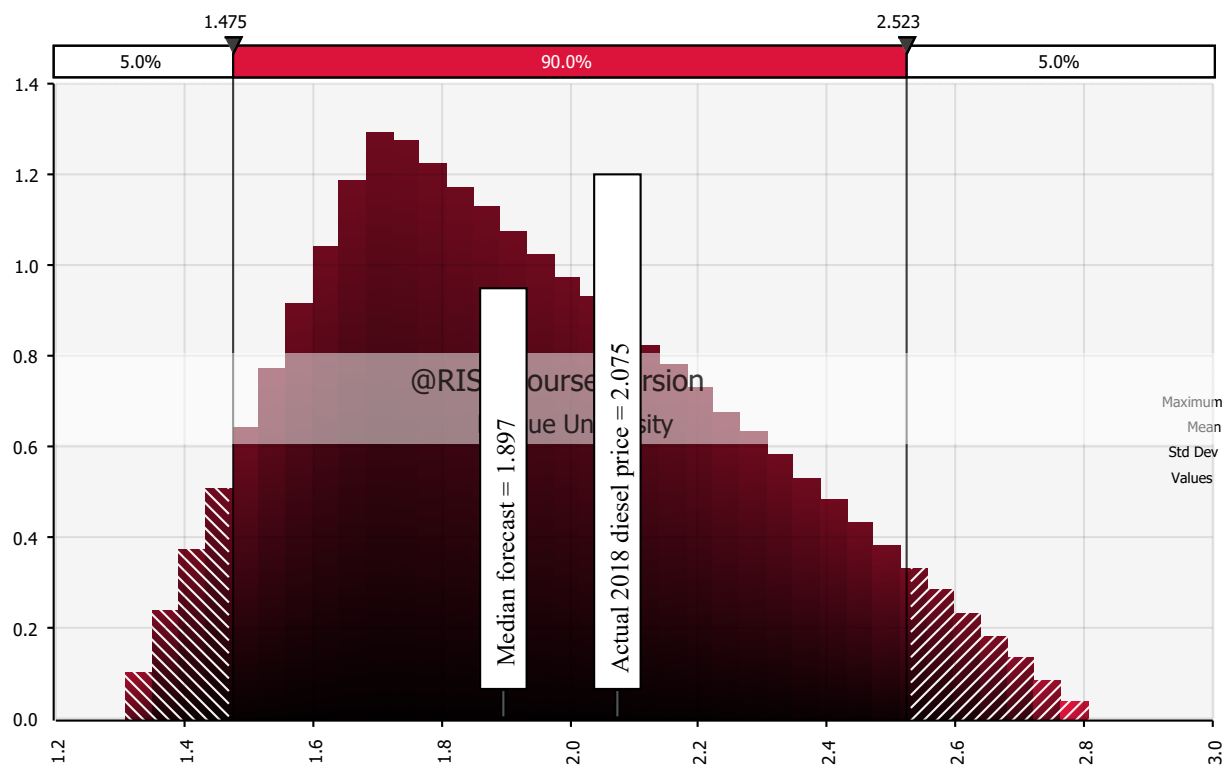


Figure 3.6: 2018 Diesel fuel price projections in 2017 \$/gal

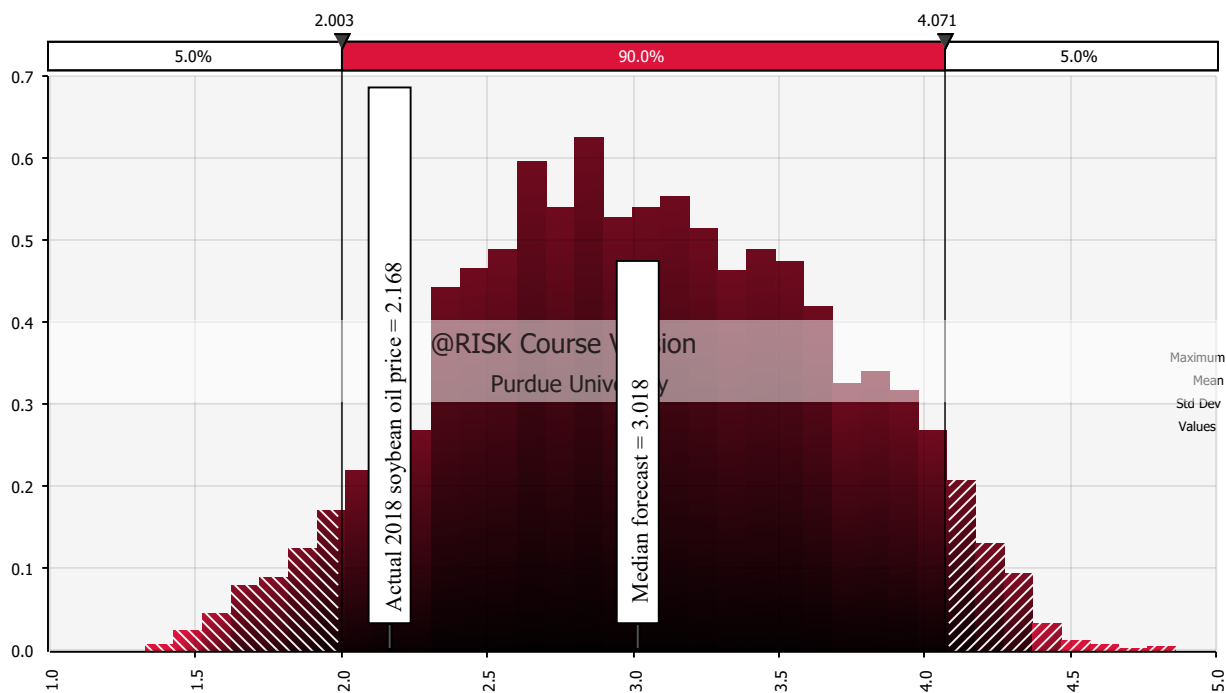


Figure 3.7: 2018 Soybean oil price projections in 2017 \$/gal

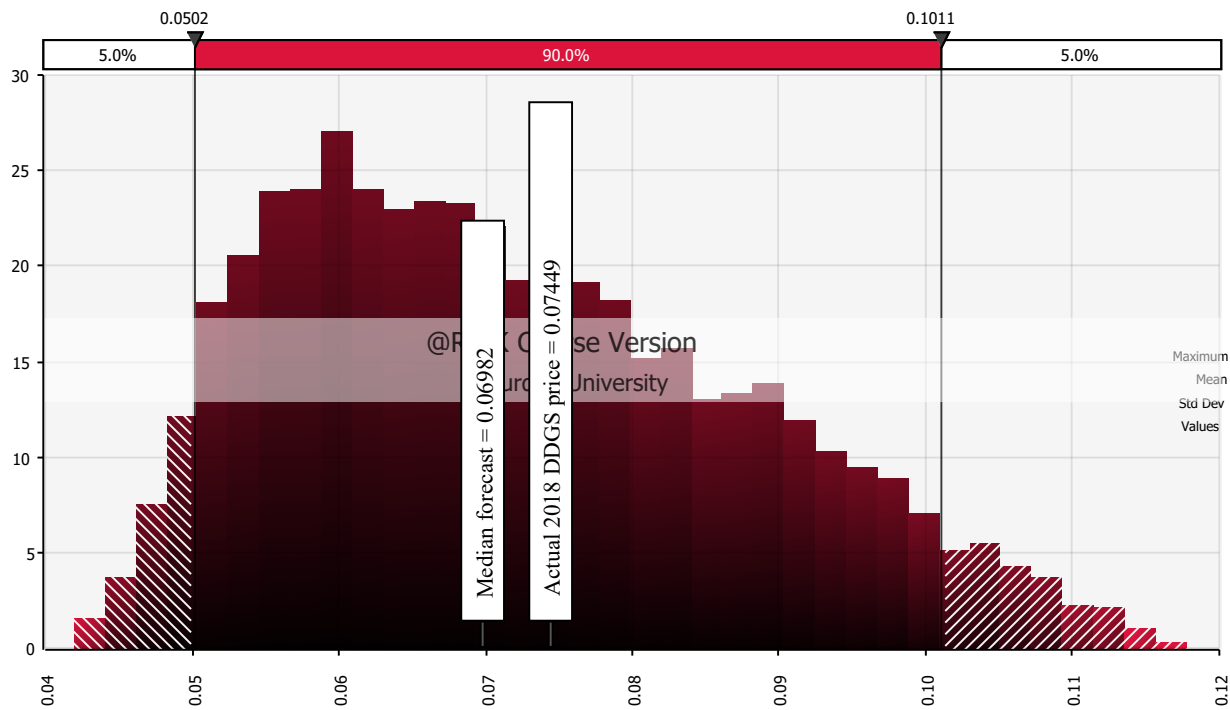


Figure 3.8: 2018 DDGS price projections in 2017 \$/lb

As Figures 3.6 to 3.8 show, our method for stochastic forecasting performed reasonably well for all three commodities of interest in 2018, with the actual 2018 price comfortably within the 90% confidence interval in all three cases. For diesel fuel and DDGS, the model performed even better. The actual 2018 price for diesel fuel is quite close to the central bulk of the results distribution, ranking in the 67.5th percentile with a z-score of 0.424. For DDGS, the actual 2018 price is even closer to the center of the distribution, marking the 59.7th percentile, and having a z-score of 0.152. Our forecast did not perform as well for soybeans, significantly overshooting the actual value, which scored in the 8.72th percentile of the results distribution. Some of this may be due to downward pressure exerted on US soybean prices by ongoing trade disputes between the US and China, as found by Taheripour and Tyner [160]. Even correcting for the 4-5% reduction in US soybean prices due to Chinese tariffs those authors found, and assuming unit pass-through of that price reduction to soybean oil, the actual price would only attain to the 11.9th percentile, with a z-score of -1.21. On the whole, our forecast appeared to do a serviceable job of forecasting price levels for 2018.

The EIA provides long-range forecasts of Brent and West Texas Intermediate (WTI) crude oil prices under eight different scenarios, along with historical prices for both. Using monthly price data for the wholesale price of US No. 2 diesel fuel, also from the EIA, we regressed the diesel fuel price on both crude prices to establish relationships between them that would allow us to turn the long-range crude oil price forecasts into long-range diesel fuel price forecasts. The regression results are below.

Table 3.13: Robust OLS of US No. 2 diesel price on F.O.B. Brent crude oil spot price

	US No. 2 diesel, 2017 \$/gal
F.O.B. Brent crude, 2017 \$/barrel	0.0271*** (0.000215)
Constant	0.158*** (0.00998)
Observations	380
R-squared	0.983

Robust standard errors in parentheses

*** p<0.01, ** p<0.05, * p<0.1

Table 3.14: Robust OLS of US No. 2 diesel price on F.O.B.WTI crude oil spot price

US No. 2 diesel, 2017 \$/gal	
F.O.B. WTI crude, 2017 \$/barrel	0.0306*** (0.000315)
Constant	-0.0198 (0.0139)
Observations	396
R-squared	0.971

Robust standard errors in parentheses
*** p<0.01, ** p<0.05, * p<0.1

Using these regression results, 16 long-range forecasts of US No. 2 diesel fuel prices were developed from the EIA crude oil forecasts. Figure 3.9 below presents an overlay of the simulated results of our stochastic forecasts of the diesel fuel price with these 16 EIA forecasts in two-year intervals from 2018 to 2040, covering the entire productive lives of the pioneer CH plants considered here. Clearly, the method we used to forecast diesel fuel prices produces results that are consistent with expert expectations.

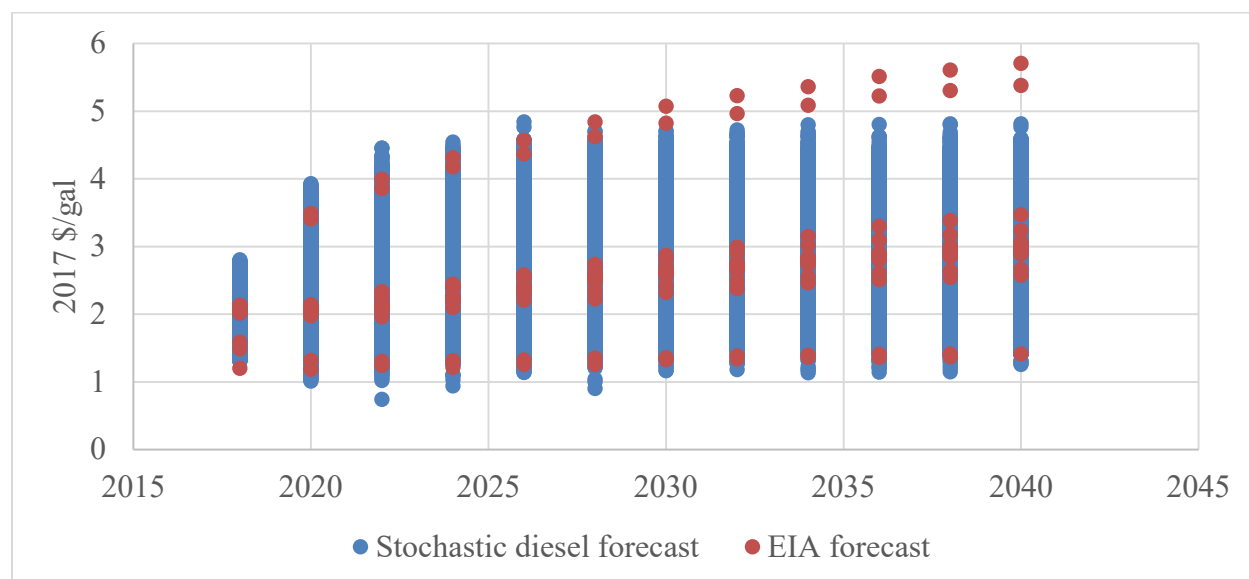


Figure 3.9: Stochastic diesel fuel projections vs EIA forecast

Do the forecasts reflect any real growth trends in the data?

All three of the price series of interest here show evidence of a real annual growth trend. There are several ways to calculate such trends. We will consider two here. The first method is to employ a simple “final divided by initial” formula for the compound annual growth rate, or CAGR (Equation 3.9). The other method is to regress the natural logarithms of the variable of interest on a variable for the year (Equation 3.10), and then exponentiate the coefficient on the year variable (Equation 3.11).

$$CAGR = (final\ observation / initial\ observation)^{1/number\ of\ periods} - 1 \quad (\text{Equation 3.9})$$

$$\ln(variable\ of\ interest) = \beta_0 + \beta_1 year + error \quad (\text{Equation 3.10})$$

$$Semi - logarithm\ regression\ growth\ rate = e^{\beta_1} - 1 \quad (\text{Equation 3.11})$$

These two approaches will often give different results because the CAGR depends only on the first and last observations, whereas the regression-based growth rate contains information from the entire sample. Results of these two methods for our data are presented in Table 3.15 below.

Table 3.15: Two kinds of real annual growth rates for diesel fuel, soybean oil, and DDGS prices

	CAGR	Semi-log OLS growth rate
US No. 2 diesel fuel	3.45%	2.64%
Soybean oil	1.60%	1.44%
DDGS	-0.317%	2.89%

The negative CAGR result for DDGS demonstrates the influence of the final observation. Only two years in our DDGS data had average real prices lower than the 2002 starting price: 2006 and 2017, which was our final observation. Ending the sample in any of the other 13 years would have given a positive CAGR, more in line with the regression-based result.

Having established that our data display evidence of real growth trends, we will now attempt to evaluate how well our simulations reflect these growth trends. The following figures present the distributions of regression-based annual growth trends obtained from one simulation of our stochastic forecasts for the pioneer productive life period (2018-2039).

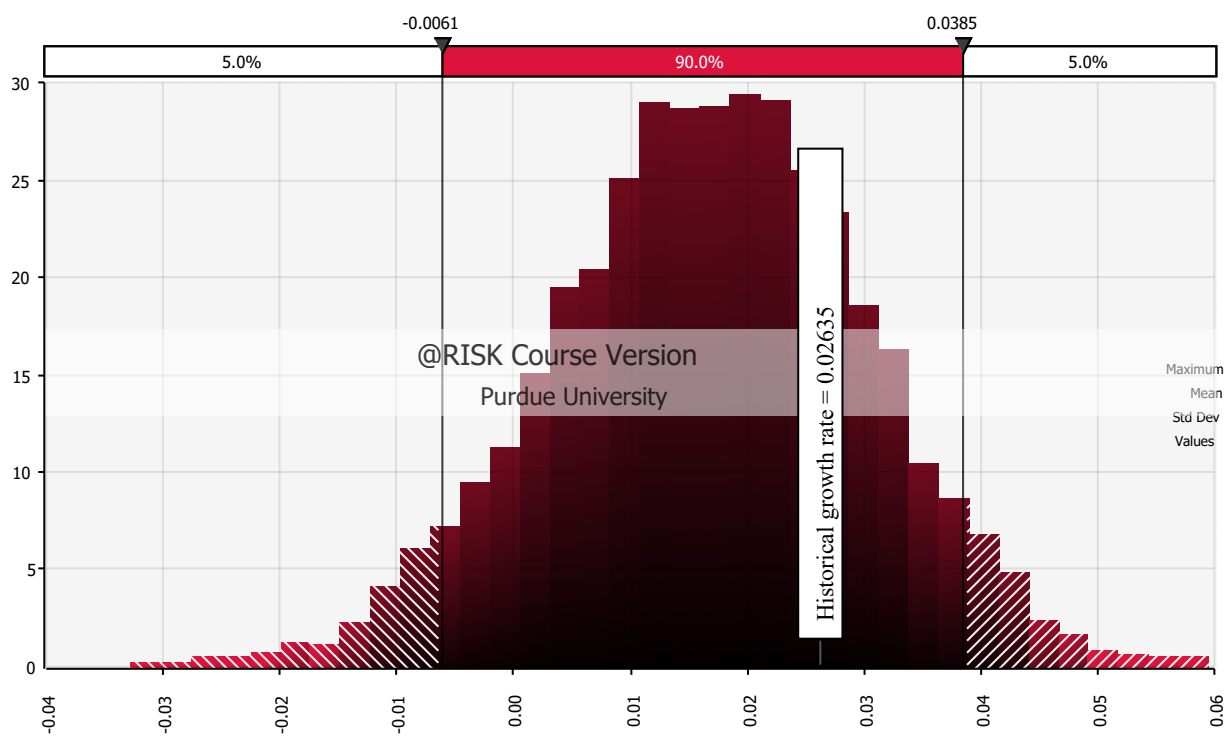


Figure 3.10: Simulated annual growth rates for stochastic forecasts of diesel fuel prices

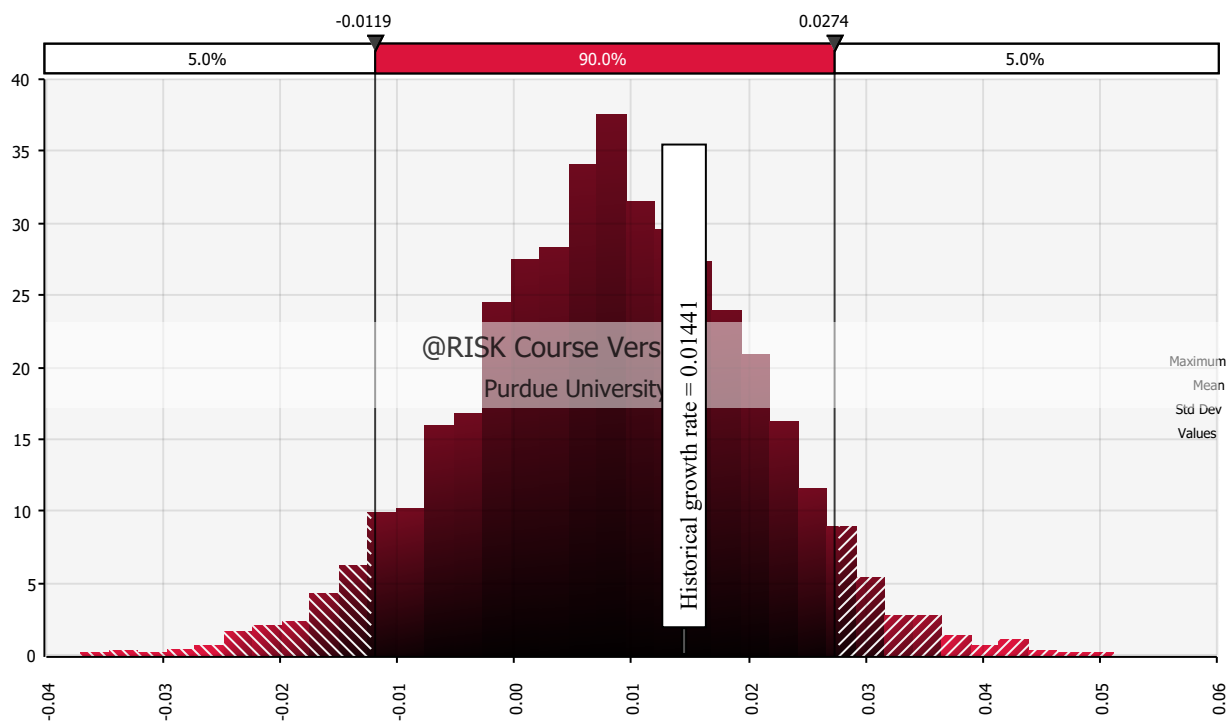


Figure 3.11: Simulated annual growth rates for stochastic forecasts of soybean oil prices

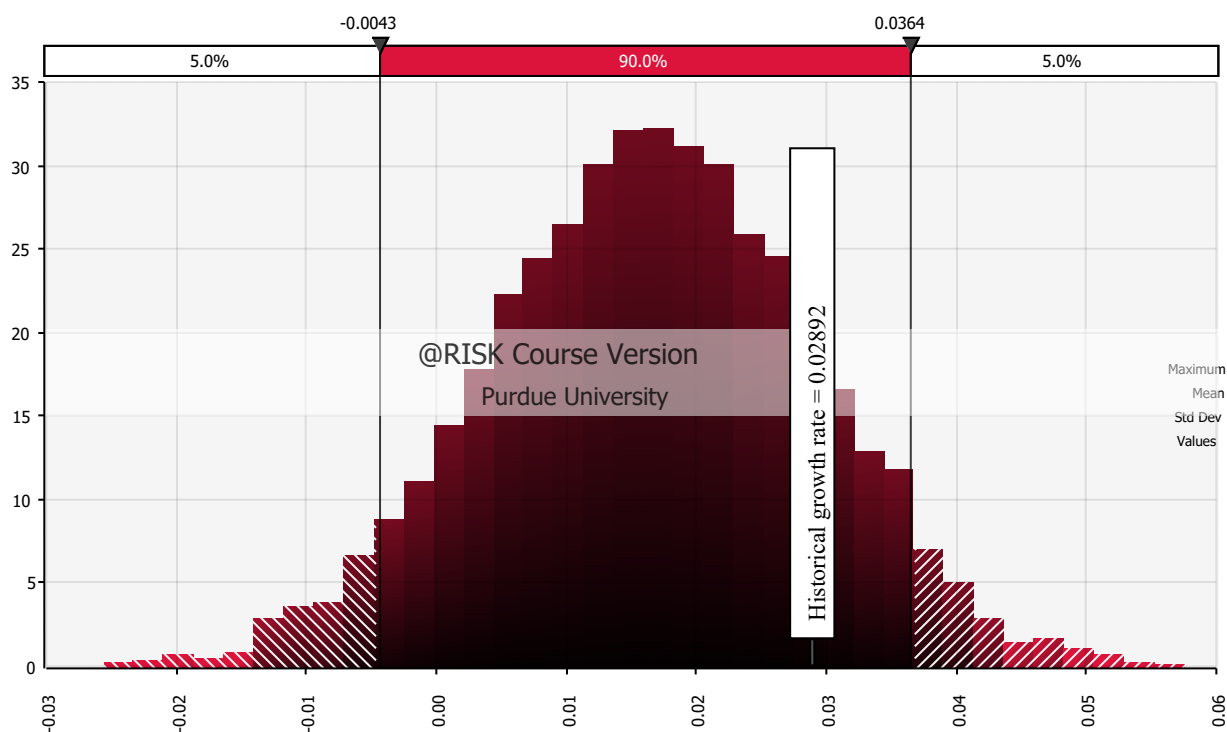


Figure 3.12: Simulated annual growth rates for stochastic forecasts of DDGS prices

Since the growth factors used in our stochastic projection method were drawn from historical price data, and since they produce simulation results whose growth rates are similar to the annual real growth rates observed in the data, we concluded that the stochastic forecasting method used here satisfies our second criterion.

Are the autocorrelations obtained in the stochastic forecasts consistent with the data?

The three price series of interest here all exhibit significant degrees of year-over-year autocorrelations, as do many price series data. Table 3.16 contains their year-over-year linear autocorrelation coefficients, and Figures 3.13 through 3.15 show the distributions of year-over-year autocorrelations obtained in one simulation of the stochastic forecasts of each price, with markers calling out the level of autocorrelation observed in the data. These figures present a compelling case that our stochastic forecasting method has accurately captured the persistence of these series. This was the purpose played by the weights placed on previous values in the formulae for each period's diesel fuel and DDGS price. These weights allowed the forecasts to be “tuned”

to match each series' level of persistence, with higher weights typically leading to higher degrees of autocorrelation.

Table 3.16: Linear one-year autocorrelation coefficients for diesel fuel, soybean oil, and DDGS prices

	US No. 2 Diesel fuel, 2017 \$/gal	Soybean oil, 2017 \$/gal	DDGS, 2017 \$/lb
Linear one-year autocorrelation coefficient	0.8438	0.5620	0.7187

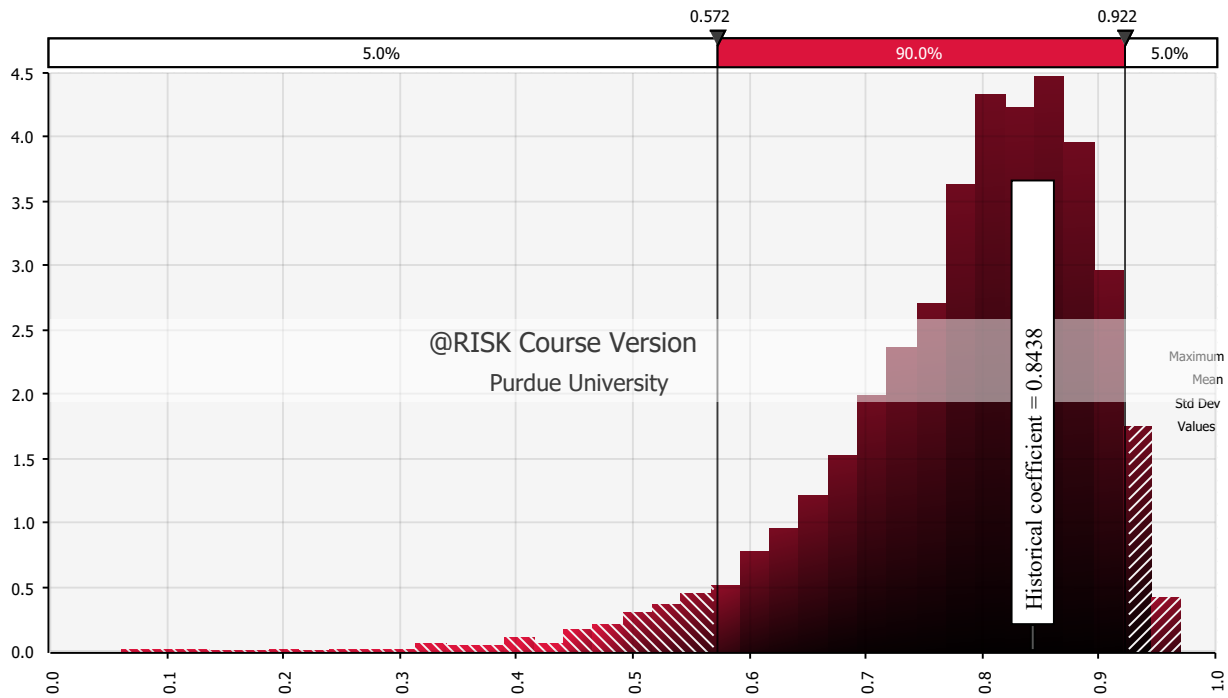


Figure 3.13: Simulated linear autocorrelation coefficients from stochastic forecast of diesel fuel prices

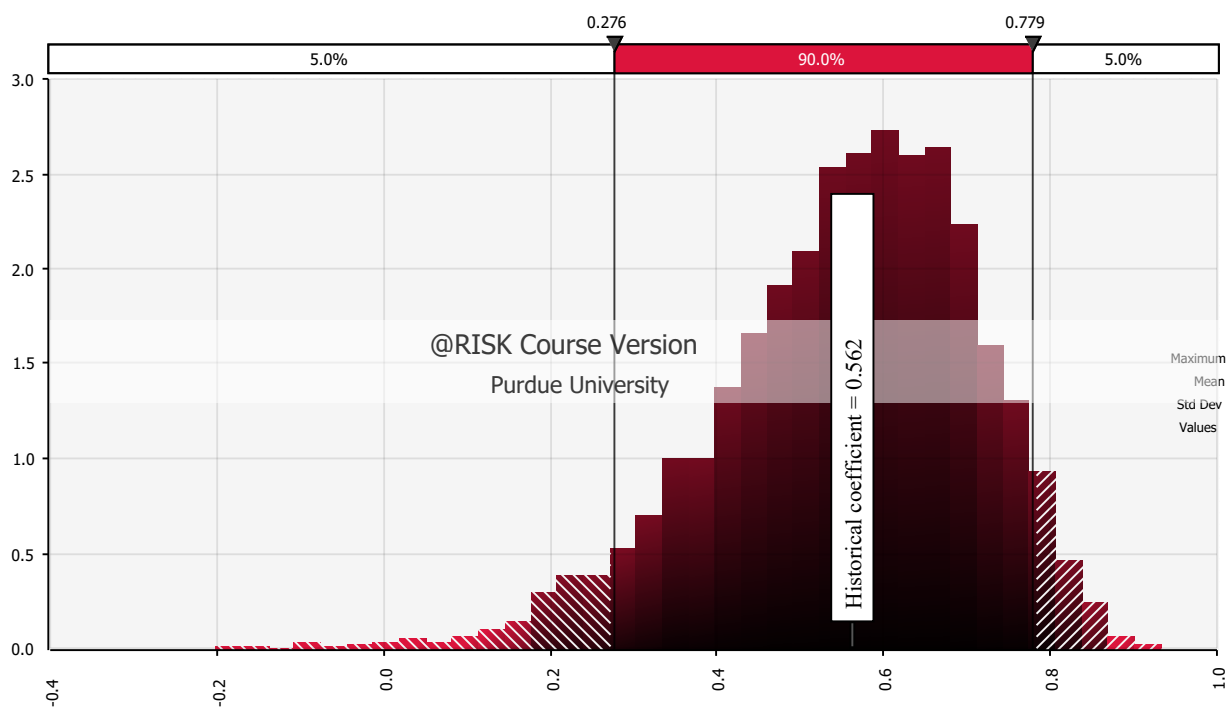


Figure 3.14: Simulated linear autocorrelation coefficients from stochastic forecast of soybean oil prices

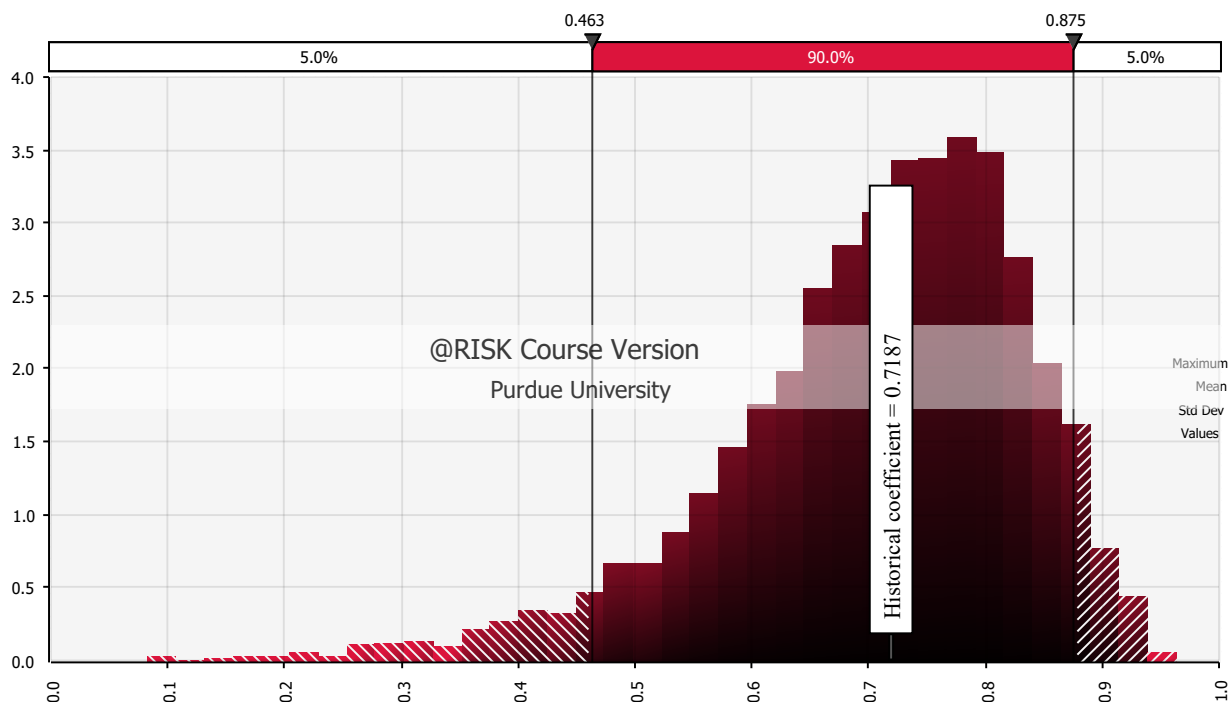


Figure 3.15: Simulated linear autocorrelation coefficients from stochastic forecast of DDGS prices

Are the inter-series correlations obtained in the stochastic forecasts consistent with the data?

Our primary motivation in developing the stochastic time series forecasting method employed here was to adequately capture the correlations between diesel fuel, soybean oil, and DDGS prices. These correlations have been presented previously in Table 3.9, but are reproduced here for convenient reference. The Spearman rank-order correlation matrix in Excel allowed the linear correlations between our stochastic projections to be “tuned” to match the linear correlations observed in the data, like the weighting system allowed the degree of autocorrelation to be adjusted for each series. The distributions of inter-series correlations obtained in one simulation of our stochastic forecasts are presented in Figures 3.16 to 3.18 below, with markers indicating the level of linear correlation observed for that relationship in the annualized price data. Like the autocorrelations, the inter-series correlations in the data appear to be well reflected by our stochastic forecasts.

Table 3.17: Linear correlation coefficients between yearly real prices of diesel fuel, soybean oil, and DDGS, 2002 through 2017

	US No. 2 diesel, 2017 \$/gal, yearly	Soybean oil, 2017 \$/gal, yearly	DDGS, 2017 \$/lb, yearly
US No. 2 diesel, 2017 \$/gal, yearly	1.000		
Soybean oil, 2017 \$/gal, yearly	0.8444	1.000	
DDGS, 2017 \$/lb, yearly	0.7231	0.7987	1.000

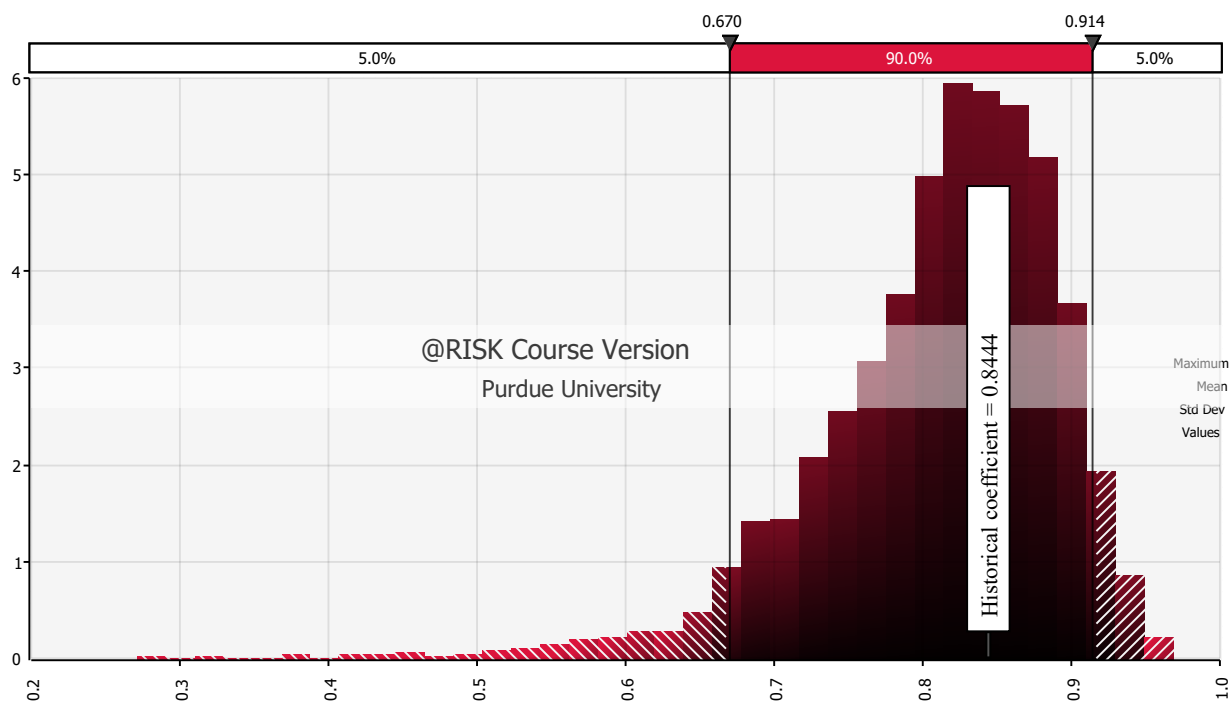


Figure 3.16: Simulated linear correlation coefficients between diesel fuel and soybean oil prices from stochastic forecast

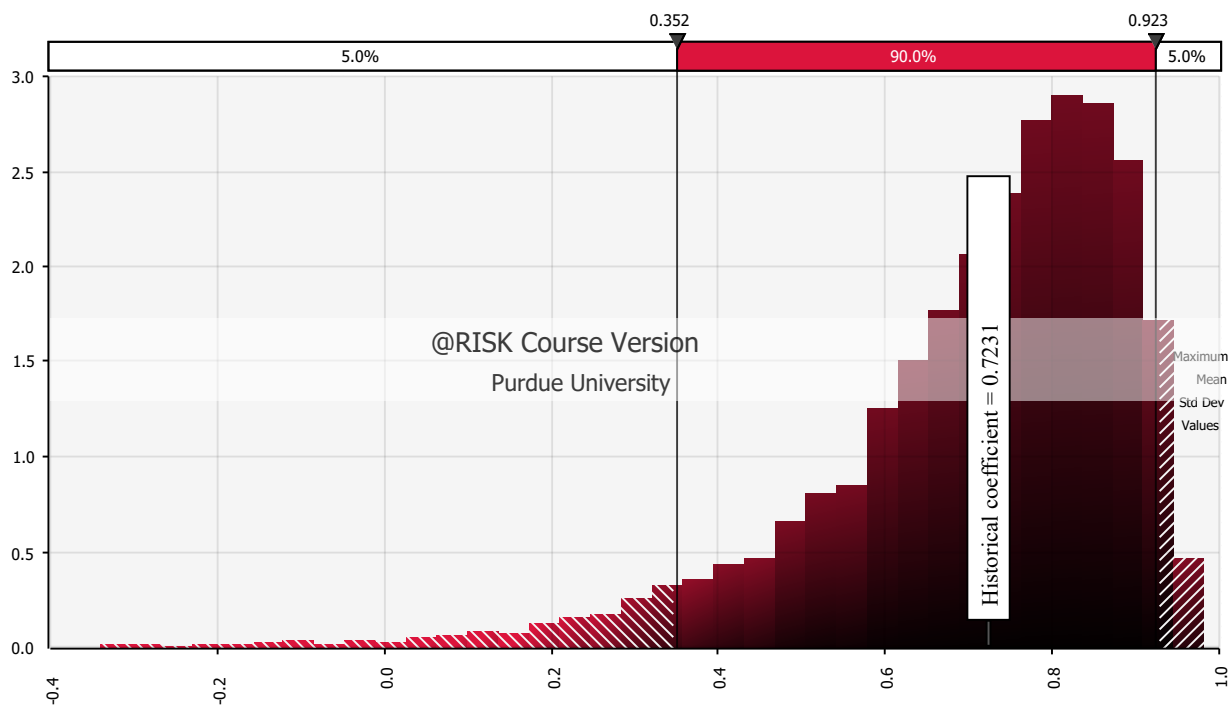


Figure 3.17: Simulated linear correlation coefficients between diesel fuel and DDGS prices from stochastic forecast

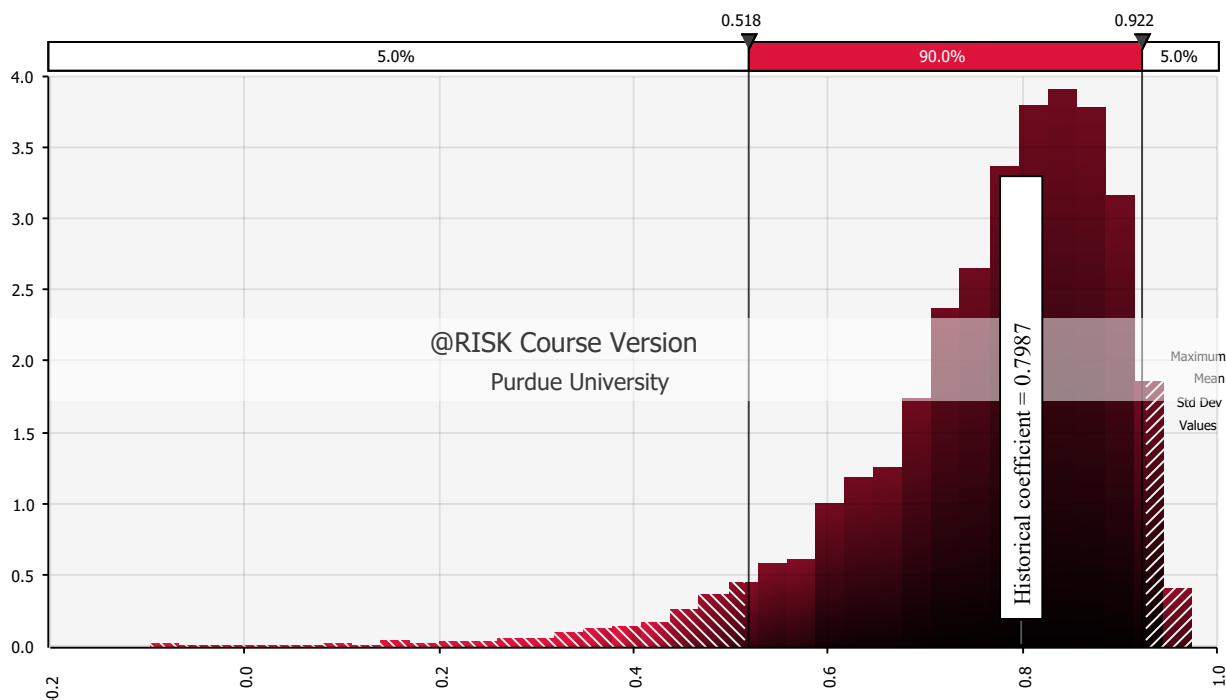


Figure 3.18: Simulated linear correlation coefficients between soybean oil and DDGS prices from stochastic forecast

Do the shapes of the distributions of simulated prices qualitatively approximate the shapes of the distributions of historical prices?

One criticism of conventional bounded lag structures is that they tend to result in “U-shaped” distributions, with lots of observations occurring at the upper and lower bounds and a somewhat flattened central range in between. If such a shape were common for distributions of historical prices, then this would not be a problem. In fact, however, most distributions of historical prices have significantly higher observation frequencies towards the center of their ranges than near the extremes. The result is typically a variation on either the classic bell-shaped curve or a flatter triangular distribution. Diesel fuel, soybean oil, and DDGS prices all exhibit this pattern. Figures 3.19 through 3.21 present histograms of the historical monthly prices (January 2003 through December 2017) for these three series interposed with histograms of simulated results from our novel forecasting method for the same period. Monthly data were used in order to have enough observations to discern the shapes of the distributions.

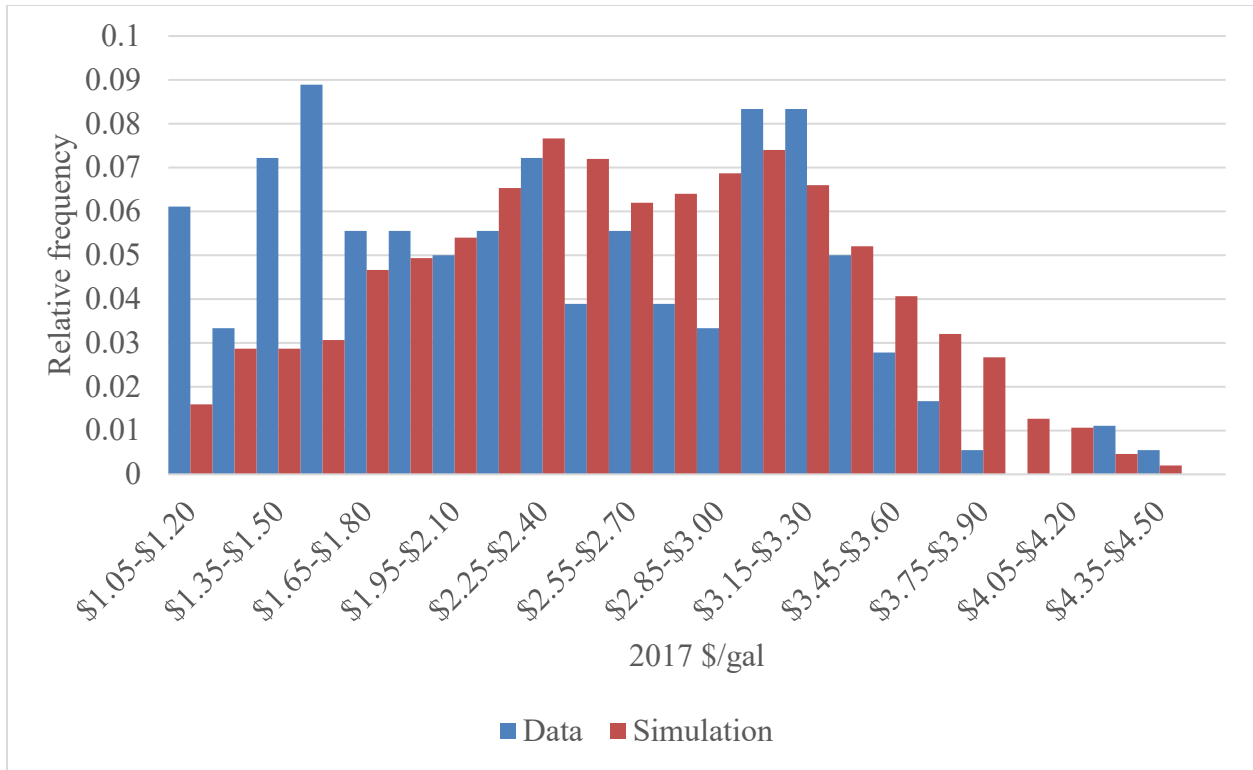


Figure 3.19: Historical price data compared to simulated results for US No. 2 diesel fuel prices from January 2003 through December 2017

In Figure 3.19 above, we see that the actual prices of diesel fuel for the 2003-2017 period form a right-skewed distribution that may be bimodal, with a large spike in observation frequency in the range of \$1.00 to \$1.80 per gallon and a less-pronounced “hump” between \$2.00 and \$3.50 per gallon. The distribution of simulated results matches this shape quite well, except for the large number of prices occurring near the low end of the range, a feature of the data which is absent from the simulated result. Neither the data nor the simulation not show a similar spike on the high end of their range, such as would likely result from the use of a conventional bounded lag structure.

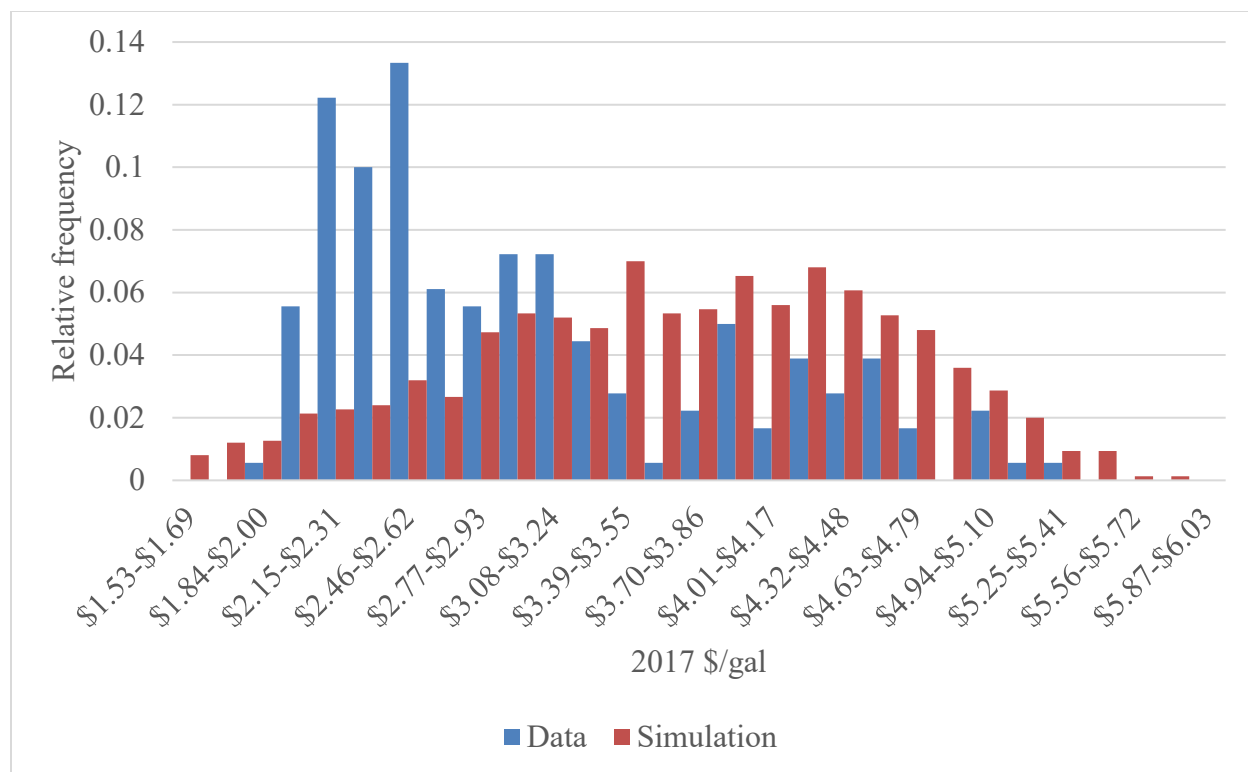


Figure 3.20: Historical price data compared to simulated results for soybean oil prices from January 2003 through December 2017

Figure 3.20 compares the actual price data for soybean oil with simulated results from our model. Both distributions have a single mode, with the relative frequency of observations tapering off to either side. Like in the diesel fuel comparison, however, the stochastic simulation results do not match the heavy concentration of observations near the lower end of the range, as we see in the data. The data are strongly right-skewed, with the bulk of observations' being on the low end, while a long tail stretches toward higher prices. The simulation results appear to be slightly left-skewed, and their mode is much less pronounced than that we see in the data.

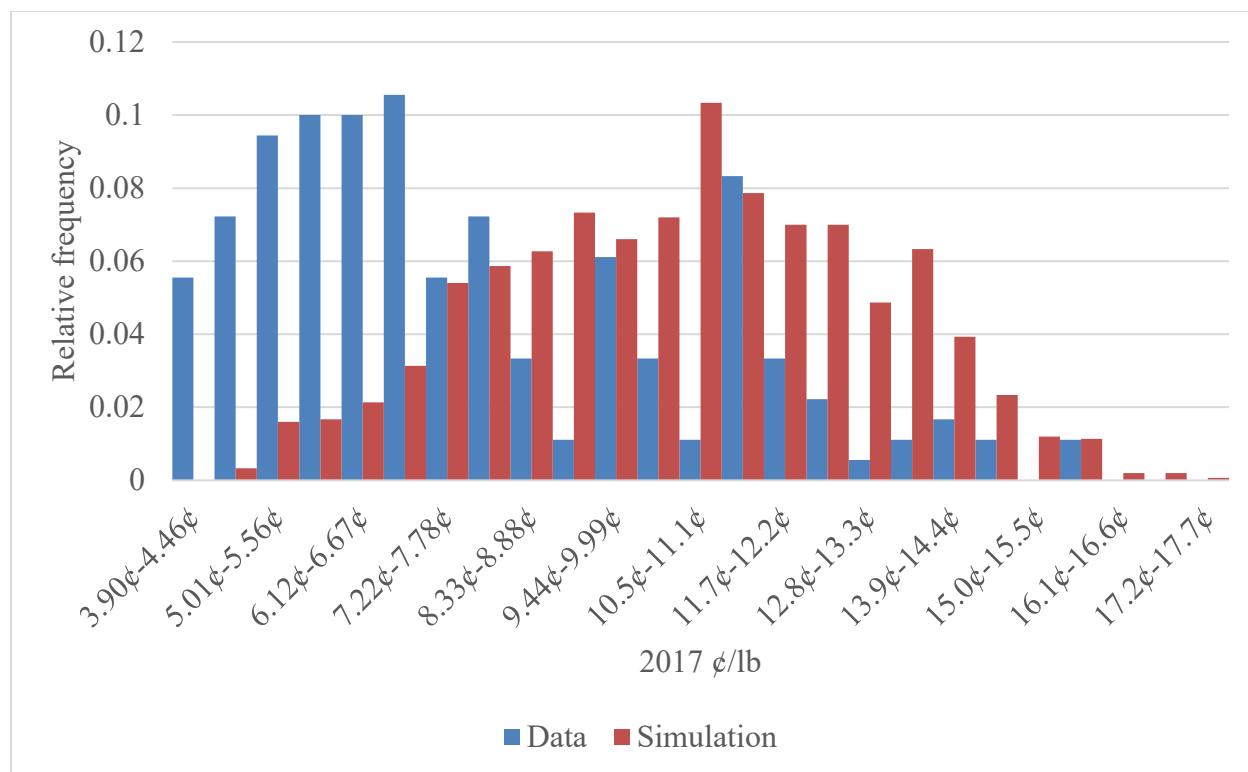


Figure 3.21: Historical price data compared to simulated results for DDGS prices from January 2003 through December 2017

When we come to the comparison for DDGS prices, we see a story very similar to what we saw for soybean oil prices. The bulk of the observations in the data occur towards the low end of their range, whereas the simulation results are much more evenly distributed. Both distributions have a single mode, with relative frequency of observations falling off on either side.

The stochastic forecasting method used here did not perform particularly well on the “shape-matching” criterion. Our results lacked the strong right skew seen in the data, and tended to have centers of mass located roughly in the middle of their ranges, whereas the bulk of observations in the data occurred toward the lower ends of their ranges. While there is clearly room to improve on our novel weighted lag method, we still considered that these results were preferable to the sort of U-shaped curves commonly produced by conventional bounded lag structures, since the extremes of the distributions of historical prices had lower observation densities than their more central regions for all three price series of interest.

Do the stochastic forecasts avoid unrealistic results?

Two problematic results were common among the other techniques we tried while developing our novel weighted lag structure. First, some of @Risk's time series techniques required a logarithmic or square root transform of the data in order to avoid predicting negative prices, and these transforms could impact their models' goodness-of-fit to the untransformed data. Negative prices can also be predicted by conventional unbounded lag structures. Second, many forecasting methods called for soybean oil prices to be lower than diesel fuel prices on a consistent basis starting around the tenth forecast year. Soybean oil prices do exhibit lower real growth rates than diesel during our sample period (Table 3.15). Even so, for soybean oil to be consistently less expensive than diesel fuel would be a reversal of decades of history in which the opposite has generally been true, with only rare exceptions. Our forecasts automatically meet our objective of avoiding negative price predictions. Because our method boils down to averaging the last prices in the sample period (all of which are, of course, positive numbers) with random draws from distributions with lower bounds greater than zero, it is not possible for it to predict negative prices. Our model also does an admirable job of not letting soybean oil prices' lower growth rates drive us to improbably conclusions. As has been stated previously, the proportion of periods in the sample data in which soybean oil has been cheaper than diesel is roughly 11% for the monthly data and roughly 3% for annual average prices. Figure 3.22 presents a distribution of the percentage of iterations of our model in which this unlikely result attains. As Figure 3.22 shows, our model matches the sample data quite well in this regard.

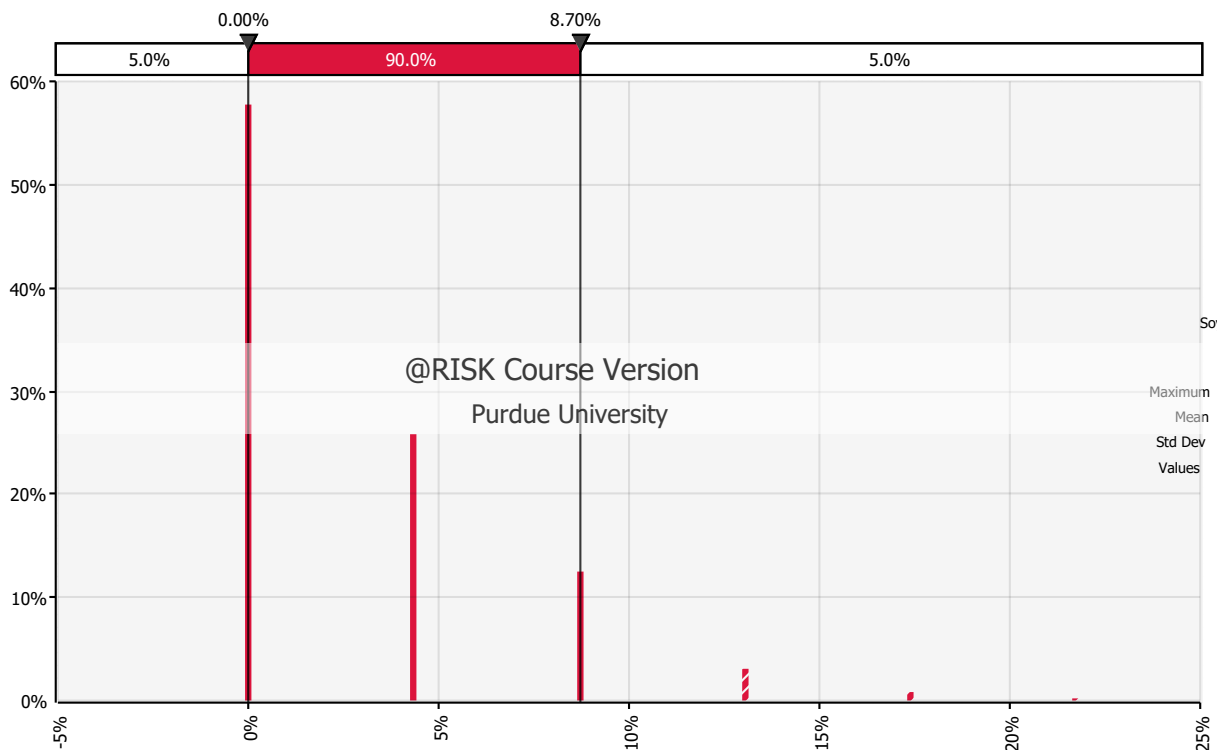


Figure 3.22: Percent chance of a gallon of soybean oil's being cheaper than a gallon of diesel fuel in novel weighted lag stochastic forecasts

Are the stochastic forecasts deliverable in an Excel workbook of reasonable size?

There are drawbacks to both annual and monthly forecasting methods. Annual stochastic forecasts, by their nature, must fit distributions to annual data, effectively dividing the potential sample size by twelve. Monthly stochastic forecasts benefit from the opportunity to fit distributions to a much larger sample, but they then yield monthly output distributions, greatly increasing the number of stochastic elements in the analysis. Our novel approach to time series forecasting bridges the gap between monthly and annual forecasts, drawing insights such as growth rates and upper and lower bounds from the monthly data in order to be working from a larger sample size, while still only using one distribution per price for each year of the forecast period. As has been shown, this method produces forecasts that line up quite well with key features of the data. To further check whether our forecasts lost some of their power for being annual in nature, we checked their performance against monthly forecasts that were equivalent in structure, except that they used one output distribution per month in the forecast period, and then averaged these

results by year. The check was performed by building a workbook that included both versions of the forecasts, defining a range of cells as the differences between the yearly prices predicted by the two methods, running a 5000-iteration simulation of that workbook, and then looking at the distributions of these differences. The two methods were deemed to be statistically equivalent if zero fell within the middle 90% intervals of these distributions of differences. This was the case for all prices in all years. Our forecasts draw on the information available in monthly data while delivering results in a convenient, annual format.

Endogenous RIN Price Modeling

That RIN prices should be important variables for the economic viability of a biofuels production pathway is hardly surprising. One of the primary purposes of the RFS, the policy that created RIN credits, is to force more biofuels into production by leveling the playing field with fossil fuels. The RFS accomplishes this through volume mandates called RVOs that are set each year by the EPA. Blenders of transportation fuels have to meet these biofuel volume mandates, which means that they have to pay producers of biofuels whatever it takes to get the volumes they need. Producers of biofuels are not substantially consolidated [161], and so the prices they demand from blenders are essentially determined by the marginal costs of production, as predicted by the theory of perfect competition. In this section, we use regression methods to investigate the implications of this theory for modeling RIN values. One difficulty we face in relying on this method is that the RFS has only been in operation in its present form since 2009, which means that attempts at statistical inference from the annual data faced severe sample size limitations. To overcome this obstacle, we performed regressions using the monthly data to establish which variables were statistically significant and to establish ballpark values for their coefficients, and then performed regressions with the chosen variables in the annual data to find the coefficient values for an annual RIN pricing model.

The pathway considered here uses vegetable oil (in this case, pennycress seed oil) to produce renewable diesel and renewable jet, which qualify for a D4 RIN, and renewable naphtha, which qualifies for a D5 RIN [107]. D4- and D5-qualifying products are often produced by the same or similar processes [107], and they are essentially interchangeable for compliance purposes, both falling under the “Advanced Biofuels” portion of the mandate [105]. For these reasons, it would not be surprising to find that D4 and D5 RINs tend to be similarly priced. On investigation

of the data, that is exactly what we find. Table 3.18 reports the results of regressing monthly real “wet” D5 RIN prices on monthly real “wet” D4 RIN prices from January 2013 through December 2018. Here and elsewhere, we use a sample start date of January 2013 for any analysis directly involving D5 RINs. This is because in 2013 D5 RINs begin to follow D4 RINs much more closely than they had previously, as Figure 3.23 shows. This may be due to changes in how cellulosic RVOs were handled under the RFS dating to that time. Cellulosic D3 and D7 RINs can be substituted for D4 RINs to fill the D5 “Advanced Biofuels” category under the RFS’s nested compliance structure. From 2011 to 2013, legal challenges to the cellulosic component of the RFS resulted in much lower cellulosic RVOs than the policy had originally called for. This may have resulted in a significant number of “extra” cellulosic RINs’ being used for compliance with the broader “Advanced Biofuels” mandate. Starting from 2013, cellulosic RVOs have been high enough to force all available cellulosic RINs to be used for compliance with that specific subsection of the standard [105, 162]. Thus, D4 RINs became the dominant means for compliance with broader D5 “Advanced” requirements. RINs are officially counted and traded based on the volume of fuel that has the same energy content as a gallon of ethanol. “Wet” RIN prices are the RIN values per actual gallon of a specific biofuel.

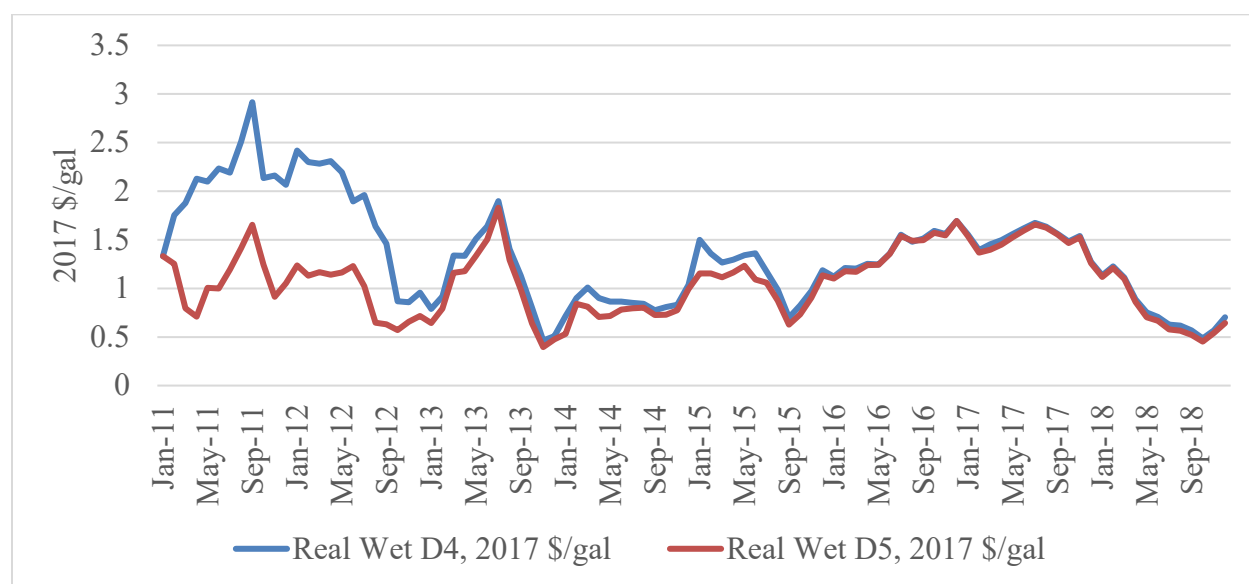


Figure 3.23: Real wet D4 and D5 RIN monthly prices

Table 3.18: Robust OLS of monthly real wet D5 RIN price on monthly real wet D4 RIN price

	Wet D5 RIN, 2017 \$/gal renewable naphtha
Wet D4 RIN, 2017 \$/gal renewable biomass-based diesel	1.01*** (0.0205)
Constant	-0.0888*** (0.0213)
Observations	72
R-squared	0.965

Robust standard errors in parentheses

*** p<0.01, ** p<0.05, * p<0.1

As expected, D5 RINs and D4 RINs are strongly related. Using this result as a guide, we performed a regression on the annual data, the results of which are reported in Table 3.19. Again, since the monthly data gave strong evidence of the significance of this relationship, we took the coefficients from the annual regression as valid, provided that they were similar to those obtained from the monthly data.

Table 3.19: OLS of annual real wet D5 RIN price on annual real wet D4 RIN price

	Wet D5 RIN, 2017 \$/gal renewable naphtha
Wet D4 RIN, 2017 \$/gal renewable biomass-based diesel	1.06*** (0.0920)
Constant	-0.146 (0.108)
Observations	6
R-squared	0.971

Standard errors in parentheses

*** p<0.01, ** p<0.05, * p<0.1

That the coefficient on the wet D4 RIN price was still significant at the 1% level with only 6 observations is striking, though it would still be difficult to give much credence to the results without the monthly regression as a point of reference. Based on these results, we concluded that

if we could understand the cost structure for either D5 or D4 RINs well enough, then we also ought to be able to predict the other price.

The Market for D4 RINs

In our literature review, we introduced a theory of D4 RIN pricing used by several close observers of the US RIN market, perhaps most notably by Scott Irwin and Darryl Good of the University of Illinois at Urbana-Champaign in a series of *farmdoc daily* articles appearing from 2013 to 2017. To our knowledge, this theory has yet to be relied upon for RIN price modeling in a published biofuels TEA, but it appears fundamentally sound, and the results Irwin and Good have obtained using it are striking. We reproduce graphics from their articles again here for reference. The theory states that since transesterified soybean oil biodiesel is responsible for the majority of D4 RIN generation [105, 126, 127], that biodiesel represents the “marginal gallon” for that section of the RFS mandates. (In fact, transesterified soybean oil biodiesel is such a large percentage of the biomass-based diesel produced in the United States that some authors, including Irwin and Good, use “biodiesel” to refer to the entire biomass-based diesel category.) Therefore, the market value of the D4 RIN is determined by the difference between the cost of producing biodiesel and biodiesel’s value to fuel blenders in the absence of the RFS. Since relatively small volumes of biodiesel are blended with fossil diesel to be sold to the end user, the functional differences between the two products are insignificant. To blenders, biodiesel is just a substitute for fossil diesel fuel, and so the market price of fossil diesel fuel would determine its value in the absence of the RFS. The RFS aims to bridge the gap created by the fact that a gallon of biodiesel is more expensive to produce than a gallon of fossil diesel, and the mechanism that closes that gap is the D4 RIN.

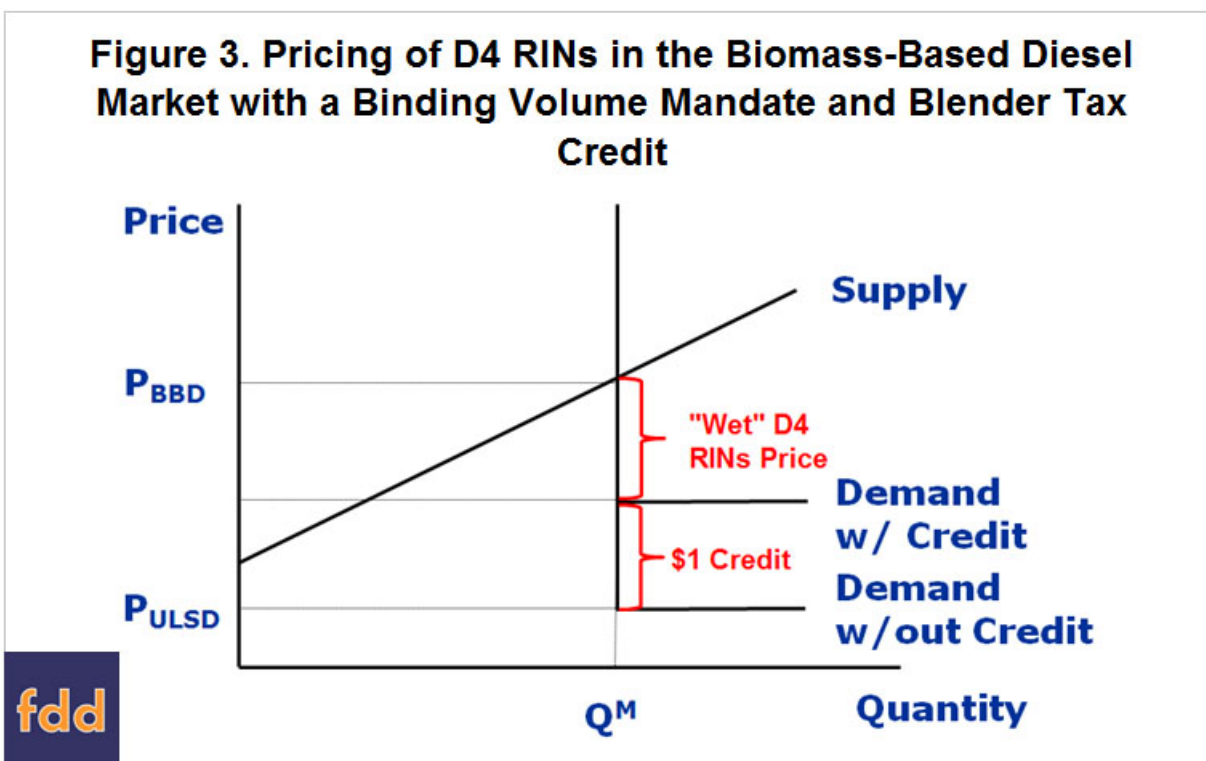


Figure 3.24: A theoretical model of wet D4 RINs pricing with a Blender Tax Credit, from Irwin, S. and Good, D., 2017

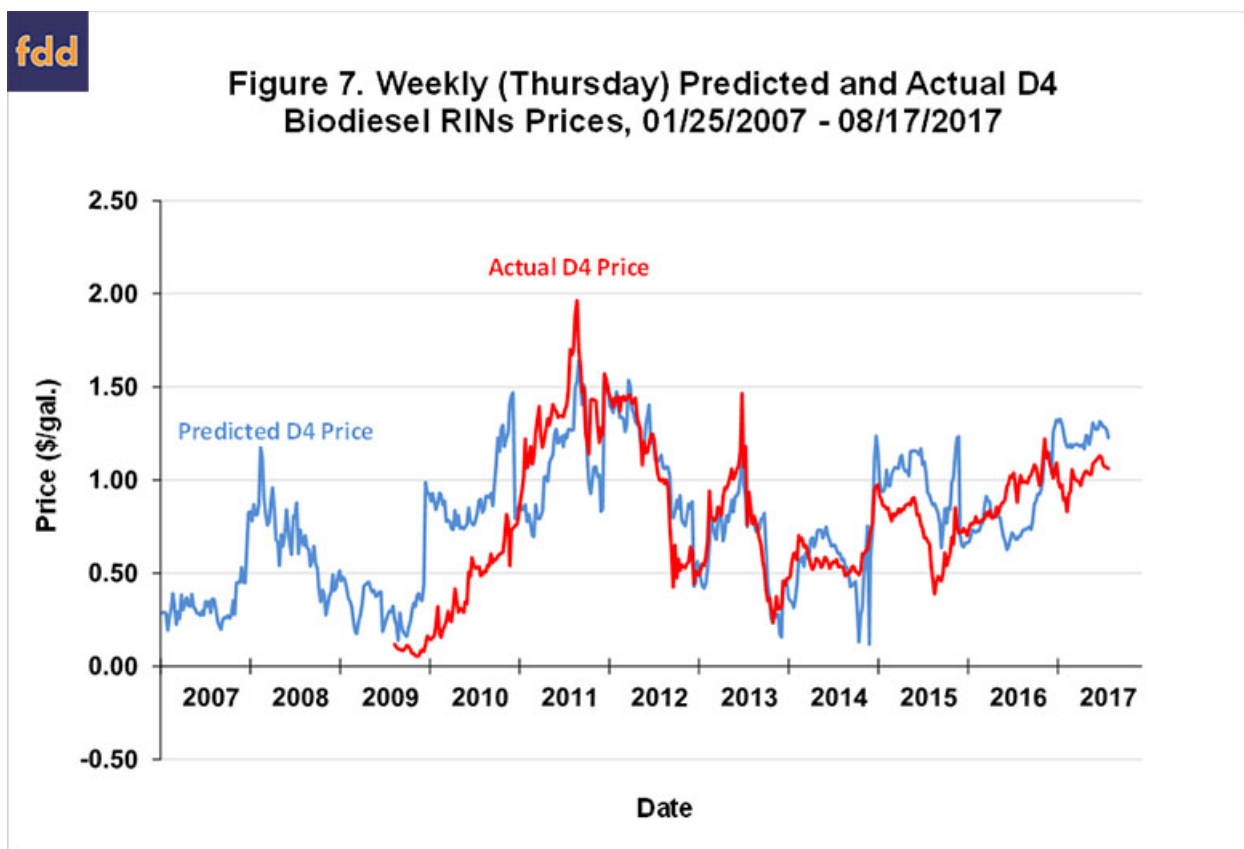


Figure 3.25: An example of the performance of the theoretical model, from Irwin, S. and Good, D., 2017

We tested the validity of this theoretical model of D4 RIN price determination in two ways. First, the model depends on the assumption that since rational producers of biomass-based diesel will not produce if they must sell their product for less than their breakeven price, the average breakeven price of all active biodiesel producers will be a powerful estimator of the actual biodiesel selling price. Biomass-based diesel fuel bought from a producer is a bundle of two products: the physical fuel product, and the attached D4 RIN, which cannot be separated from the physical product until that fuel is purchased by a blender. If the assumption above holds, then the sum payments for these two products (the actual biodiesel selling price) will equal the breakeven price of biodiesel production. Data on the breakeven price of biodiesel production and FOB-at-the-plant biodiesel spot prices were taken from the Iowa Biodiesel Producer Profitability Model developed and published by the Iowa State University Agricultural Marketing Resource Center [34], which models the breakeven selling price of biodiesel for a “typical” Iowa biodiesel plant, taking into account the prices of inputs such as soybean oil, methanol, and natural gas. As Tables

3.20 and 3.21 below show, there is a strong predictive relationship between the modeled biodiesel breakeven price and the actual biodiesel spot price.

Table 3.20: Robust OLS of monthly real biodiesel spot price on monthly real biodiesel breakeven price

	Biodiesel spot price, 2017 \$/gal
Biodiesel breakeven price, 2017 \$/gal	1.10*** (0.0394)
Constant	-0.217* (0.130)
Observations	96
R-squared	0.905
Robust standard errors in parentheses *** p<0.01, ** p<0.05, * p<0.1	

Table 3.21: First-differenced OLS of monthly real biodiesel spot price on monthly real biodiesel breakeven price

	d.Biodiesel spot price, 2017 \$/gal
d.Biodiesel breakeven price, 2017 \$/gal	0.830*** (0.120)
Constant	-0.00247 (0.0155)
Observations	95
R-squared	0.338
Standard errors in parentheses *** p<0.01, ** p<0.05, * p<0.1	

Second, we test the validity of the assumption that the portion of the biodiesel selling price that exceeds the price of fossil diesel fuel may be attributed to the value of the attached D4 RIN, plus any value from the biodiesel Blender Tax Credit (BTC), a nominal tax credit of \$1 per gallon of biomass-based diesel fuel a blender purchased in that year. If this assumption holds, then the gap between the biodiesel selling price and the wholesale price of fossil diesel fuel should equal

the value of the D4 RIN, plus any shared value from the BTC. This gap, which we refer to henceforward as the “blend gap”, is the negative of what is commonly referred to as the “blending margin”. We address the BTC in greater detail later on; for now, we will constrain our attention to years in which the BTC was not known to be in effect ex-ante (2012, 2014, 2015, 2017, and 2018).

Table 3.22: Robust OLS of monthly real “wet” D4 RIN price on monthly real biodiesel blend gap

	Wet D4 RIN price, 2017 \$/gal
Biodiesel blend gap, 2017 \$/gal	1.09*** (0.116)
Constant	-0.0298 (0.132)
Observations	60
R-squared	0.732
Robust standard errors in parentheses *** p<0.01, ** p<0.05, * p<0.1	

Table 3.23: First-differenced OLS of monthly real “wet” D4 RIN price on monthly real biodiesel blend gap

	d.Wet D4 RIN price, 2017 \$/gal
d.Biodiesel blend gap, 2017 \$/gal	0.357*** (0.105)
Constant	-0.0154 (0.0200)
Observations	60
R-squared	0.165
Standard errors in parentheses *** p<0.01, ** p<0.05, * p<0.1	

As Tables 3.22 and 3.23 show, there is a strong predictive relationship between the gap between biodiesel and fossil diesel prices and the price of the D4 RIN, supporting the idea that

RINs prices are determined in the way that our theoretical model indicates, and that producers of biomass-based diesel fuel receive the full value of the “attached” RINs they sell along with their physical product. Though the R-squared is much lower, this relationship holds up in the first-differenced data, indicating that the strong correlations observed are not merely due to unit-root levels effects. Further, the robust regression in the levels data indicates that the blend gap is an unbiased estimator of the D4 RIN price, since the constant in that regression is not significant, and the coefficient on the blend gap is not statistically different from 1. Testing whether the coefficient on the blend gap is equal to one yields an $F(1,58)$ statistic of 0.650, corresponding to a p-value of 0.424. Our theoretical model relating D4 RINs prices to the gap between biodiesel and fossil diesel prices appears justified.

Irwin and Good have tested this model using historical biodiesel and fossil diesel spot prices, with impressive results, as Figure 3.25 shows. Our task was slightly more difficult, since we intended to make a forward-looking model, and therefore needed to predict the cost of producing biodiesel, instead of relying directly on historical price data. Fortunately, the cost of producing biodiesel is driven almost entirely by the price of soybean oil, the primary feedstock for the process [155]. We developed methods for simulating diesel fuel and soybean oil prices. All that remained in order to model RIN values that were consistent with our projections of those prices was to establish a relationship between the soybean oil price and the breakeven price of biodiesel, subtract off our estimates of fossil diesel prices to get the gap that the D4 RINs must close, and then establish a relationship between this gap and realized D4 RIN prices.

There is one more complication to this model that must be taken into account. A nominal one-dollar-per-gallon tax credit has sometimes been given to diesel fuel blenders for every gallon of biomass-based diesel that they buy. This further incentive is called the Blender Tax Credit (BTC), and it has two effects on the biodiesel market, and thus the market for D4 RINs. First, in years for which the credit is known in advance to be in effect, it makes biodiesel roughly \$1 per gallon more valuable to blenders than its substitute, fossil diesel. The result is that the RIN credit has a smaller gap to close than in other years, as shown in Figure 3.24, reproduced from Irwin and Good, 2017. The other effect that the BTC has had on the market for biodiesel depends on the fact that it is an annual policy, and it has been allowed to expire at the end of the year multiple times since it was enacted. Therefore, in years when market participants know that the BTC is set to expire, blenders rush to buy as much biodiesel as they can before the year ends, in order to take

advantage of the tax credit. Given these effects, we chose to model RIN prices in years for which the BTC is in place ex-ante differently from RIN prices in years in which it is in place ex-post or not at all. Once those relationships were established, we modeled our “predictions” of the BTC’s status as a random binary variable for each year, setting the probability of the BTC’s being in place in any given year based on the recent history of the policy.

From Soybean Oil Prices to Biodiesel Breakeven Prices to D4 and D5 RIN prices

In order to establish a relationship between soybean oil prices and biodiesel production costs, we used a biodiesel plant profitability model developed by Iowa State University’s Ag Marketing Resource Center [34]. They use monthly USDA data on soybean oil prices along with monthly data on the prices of methanol and natural gas along with a set of financial assumptions meant to be representative of a typical Iowa biodiesel facility to estimate a breakeven price for biodiesel. These nominal breakeven prices were converted into real terms using the CPI and regressed on the real soybean oil prices used in the rest of this analysis. The results for years 2011 through 2018 are presented in Table 3.24.

Table 3.24: Robust OLS of monthly real biodiesel breakeven price on monthly real soybean oil price

	Biodiesel breakeven price, 2017 \$/gal
Soybean oil price, 2017 \$/gal	0.997*** (0.00421)
Constant	0.667*** (0.0151)
Observations	96
R-squared	0.997

Robust standard errors in parentheses

*** p<0.01, ** p<0.05, * p<0.1

The breakeven price of biodiesel appears to be roughly equal to the soybean oil price plus \$0.67 per gallon. By subtracting the real wholesale price of diesel fuel in each period from these fitted values for the biodiesel breakeven price, we can estimate the “blend gap” between biodiesel and fossil diesel prices. According to theory, the D4 RIN value should be roughly equal to this

gap for years without the BTC in place. For years with the BTC in place, the amount of the BTC plus the amount of the D4 RIN should sum to cover the blend gap. We proceeded by creating a series of estimated real blend gap values, converting them to nominal terms, and regressing nominal D4 RIN prices on these nominal blend gap fitted values, with separate regressions for years in which the BTC was in place ex-ante and years in which it was not. The conversion to nominal terms was performed in order to better capture the impact of the BTC, which is a nominal \$1 per gallon tax credit. The results of these regressions are reported in Tables 3.25 and 3.26.

Table 3.25: Robust OLS of monthly nominal wet D4 RIN prices on monthly predicted nominal blend gaps if the BTC is NOT in place ex-ante

	Wet D4 RIN price, \$/gal
Blend gap, \$/gal	0.931*** (0.0901)
Constant	0.151* (0.0876)
Observations	60
R-squared	0.643
Robust standard errors in parentheses *** p<0.01, ** p<0.05, * p<0.1	

Table 3.26: Robust OLS of monthly nominal wet D4 RIN prices on monthly predicted nominal blend gaps if the BTC IS in place ex-ante

	Wet D4 RIN price, \$/gal
Blend gap, \$/gal	0.660*** (0.184)
Constant	0.486* (0.264)
Observations	36
R-squared	0.280
Robust standard errors in parentheses *** p<0.01, ** p<0.05, * p<0.1	

These results indicate that the blend gap predicted by the relationship between the biodiesel breakeven price and the price of soybean oil is a significant variable for explaining the price of the D4 RIN. The low R-squared values, especially for the years with a BTC in place at the beginning of the year, may be due to seasonal effects in the data. Once it becomes clear that the BTC is set to expire at the end of a given year, there tends to be a large run-up of quantities and prices for biodiesel [30]. Due to the timing of when it typically becomes apparent that the BTC will not be renewed for the next year, this run-up is typically concentrated in the last half of the year. Table 3.27 reports the results of a regression of nominal monthly D4 RIN prices on our predicted nominal blend gaps for years in which the BTC is in effect ex-ante, like Table 3.26. However, this time we included dummy variables for the first and third quarters of the year.

Table 3.27: OLS of monthly nominal wet D4 RIN prices on monthly predicted nominal blend gaps and two quarterly dummies if the BTC IS in place ex-ante

	Wet D4 RIN price, \$/gal
Blend gap, \$/gal	0.835*** (0.149)
Quarter 1	-0.439*** (0.141)
Quarter 3	0.326** (0.137)
Constant	0.253 (0.230)
Observations	36
R-squared	0.574

Standard errors in parentheses
 *** p<0.01, ** p<0.05, * p<0.1

The model performs much better with these dummy variables for seasonal effects included. Even so, our goal with these monthly models is to identify variables that have significant relationships with D4 RIN prices and can be included in regressions based on the annual data, which is not possible with quarterly dummies. Based on the results of the monthly regressions, we used the following variables for our annual modeling. First, we used the real soybean oil price

for predicting a real biodiesel breakeven price. Second, we converted that result to nominal terms and used the gap between the predicted nominal biodiesel breakeven price and the nominal diesel fuel price for predicting the nominal D4 RIN price. Finally, we converted that result back to real terms and used the predicted real D4 RIN price for predicting the real D5 RIN price. The results of following this procedure with annual data are presented in Tables 3.28 through 3.30.

Table 3.28: OLS of annual real biodiesel breakeven price on annual real soybean oil price

	Biodiesel breakeven price, 2017 \$/gal
Soybean oil price, 2017 \$/gal	0.999*** (0.0167)
Constant	0.660*** (0.0537)
Observations	8
R-squared	0.998
Standard errors in parentheses *** p<0.01, ** p<0.05, * p<0.1	

Table 3.29: OLS of annual nominal wet D4 RIN prices on annual predicted nominal blend gaps if the BTC is NOT in place ex-ante

	Wet D4 RIN price, \$/gal
Blend gap, \$/gal	0.939** (0.235)
Constant	0.142 (0.273)
Observations	5
R-squared	0.842
Standard errors in parentheses *** p<0.01, ** p<0.05, * p<0.1	

Table 3.30: OLS of annual nominal wet D4 RIN prices on annual predicted nominal blend gaps if the BTC IS in place ex-ante

	Wet D4 RIN price, \$/gal
Blend gap, \$/gal	0.885 (0.723)
Constant	0.150 (1.10)
Observations	3
R-squared	0.599

Standard errors in parentheses
 *** p<0.01, ** p<0.05, * p<0.1

The relationships indicated in the monthly data seem to hold up well in the annual data, as well. The coefficients in the above annual regressions are similar to their counterparts in the monthly regressions. This includes the coefficient on the predicted blend gap used to predict nominal D4 prices in years without a BTC in effect at the start of the year. In that case, the match is with the coefficient found in Table 3.27 once seasonal effects were controlled for. Those effects fall out in the annual data, so the fact that the annual regression finds a similar coefficient on the nominal blend gap is encouraging in regards to the consistency of our approach. The last remaining question, and by far the most important, is whether this multi-step prediction method actually appears to work or not. Figures 3.26 and 3.27 present line graphs of our method's annual predictions of D4 and D5 prices alongside historical D4 and D5 prices. Tables 3.31 and 3.32 present regressions of historical D4 and D5 prices on our predictions.

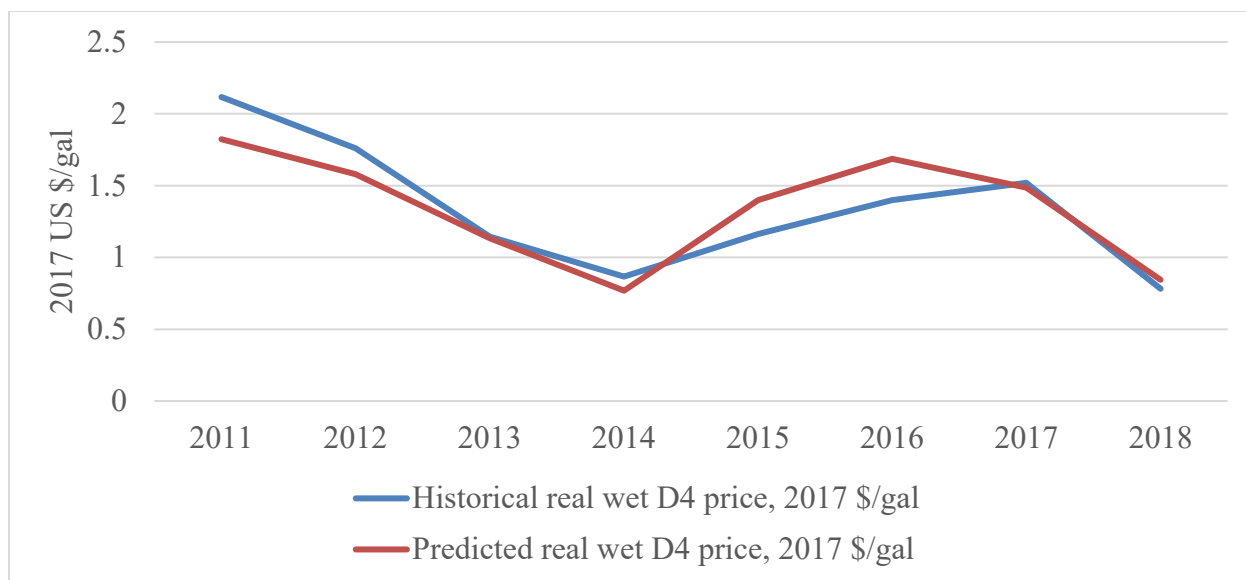


Figure 3.26: Historical vs predicted real wet D4 RIN prices

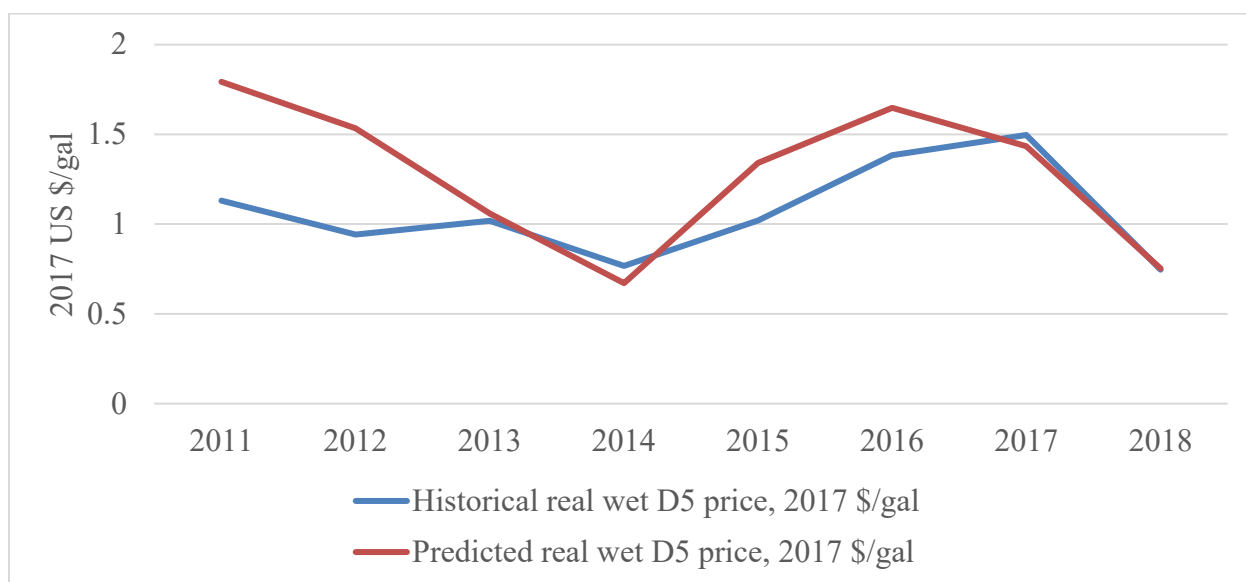


Figure 3.27: Historical vs predicted real wet D5 RIN prices

Table 3.31: Robust OLS of historical annual real wet D4 RIN prices on predicted annual real wet D4 RIN prices 2011-2018

	Historical real wet D4 RIN price, 2017 \$/gal
Predicted real wet D4 RIN price, 2017 \$/gal	1.05*** (0.206)
Constant	-0.059 (0.230)
Observations	8
R-squared	0.810
Robust standard errors in parentheses *** p<0.01, ** p<0.05, * p<0.1	

Table 3.32: OLS of historical annual real wet D5 RIN prices on predicted annual real wet D5 RIN prices 2013-2018

	Historical real wet D5 RIN price, 2017 \$/gal
Predicted real wet D5 RIN price, 2017 \$/gal	0.719** (0.172)
Constant	0.245 (0.207)
Observations	6
R-squared	0.814
Standard errors in parentheses *** p<0.01, ** p<0.05, * p<0.1	

For both D4 and D5 RINs, this method produces predictions that, on visual inspection, seem to follow the data reasonably well. The regression results confirm this. For our predictions to be taken as unbiased, the constants in these regressions should not be statistically different from zero, as neither are, and the coefficients should not be statistically different from one. Again, neither are. An F-test for the one restriction that the regression coefficient should be one yields a p-value of 0.828 for D4 RINs and a p-value of 0.176 for D5 RINs, greater than accepted thresholds for statistical significance in both cases. Our D5 predictions may perhaps suffer because they are

based on a sample beginning in 2013, whereas our D4 predictions are based on a sample beginning in 2011.

Producer Revenue from the Blender Tax Credit

The biodiesel Blender Tax Credit has been in existence since 2005 and allows those who purchase biodiesel or renewable diesel for blending into final transportation fuel products to claim a tax credit of \$1 for each gallon they buy. As has already been mentioned, the BTC is in nominal terms and has been “on-again, off-again” for much of its history. When the BTC is known to be in effect when a sale of biodiesel or renewable diesel is being negotiated, it increases the value of these alternative fuels relative to fossil-derived diesel fuel, thereby influencing the prices of biodiesel, renewable diesel, and D4 RINs. This effect is illustrated in Figure 3.28 below. In most of the years in which the BTC has initially been “off,” it has since been retroactively reinstated. Therefore, contracts for the sale of biodiesel and renewable diesel usually have a provision for sharing revenue from the BTC if it is not in effect at the time of sale, but is later reinstated retroactively [29]. A 50/50 split between the seller and the buyer is reported anecdotally as the most common such arrangement [29].

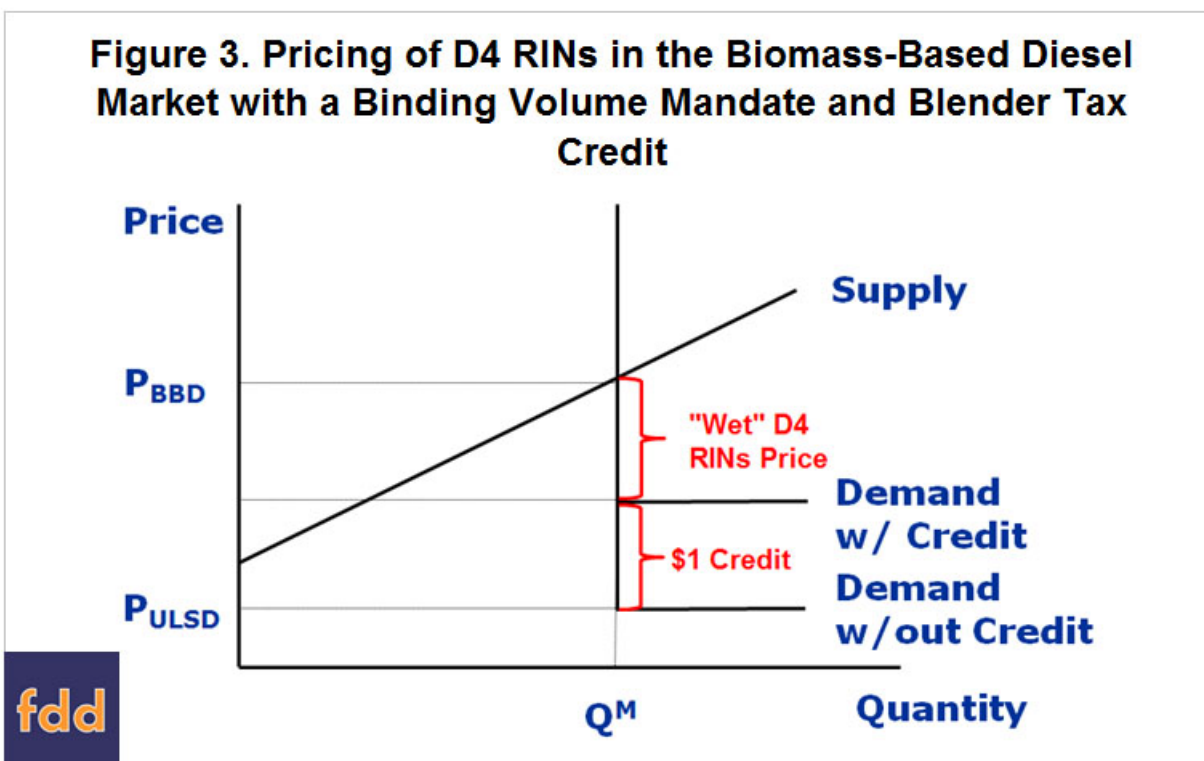


Figure 3.28: A theoretical model of wet D4 RINs pricing with a Blender Tax Credit, from Irwin, S. and Good, D., 2017

For our purposes, we needed to estimate the effects of the BTC on the market prices of renewable diesel and D4 RINs. This was necessary in order to test the validity of our decision to model the D4 RIN market differently based on the BTC's status, and also in order to assign a monetary value to the biofuel producer's share of the BTC's benefit. We accomplished this by regressing nominal biodiesel selling prices on the nominal prices of fossil diesel fuel, D4 RIN prices, and a dummy variable for the BTC's being "on" in advance for the year in question. The coefficient on D4 RIN prices was constrained to be equal to 1, since the full price of the D4 RIN is included as seller revenue in our model. This regression was performed twice, once with monthly data and once with yearly data. The date range in each case was January 2011 to December 2018, corresponding to the time period since the D4 mandate under the RFS began to function "normally," with compliance enforced at the end of each calendar year [35]. The results of these regressions are presented in Tables 3.33 and 3.34 below.

Table 3.33: Constrained OLS of monthly nominal biodiesel selling prices on monthly nominal wholesale US No. 2 diesel fuel prices, monthly nominal D4 RIN prices and a dummy variable for the BTC's being in effect ex-ante for the year in question

	Nominal biodiesel selling price, \$/gal
Nominal US No. 2 diesel fuel, \$/gal	0.830*** (0.0318)
Nominal wet D4 RINs, \$/gal	1 (constrained)
BTC	0.495*** (0.0461)
Constant	0.318*** (0.0779)
Observations	96
Standard errors in parentheses *** p<0.01, ** p<0.05, * p<0.1	

Table 3.34: Constrained OLS of annual nominal biodiesel selling prices on annual nominal wholesale US No. 2 diesel fuel prices, annual nominal D4 RIN prices and a dummy variable for the BTC's being in effect ex-ante for the year in question

	Nominal biodiesel selling price, \$/gal
Nominal US No. 2 diesel fuel, \$/gal	0.855*** (0.0779)
Nominal wet D4 RINs, \$/gal	1 (constrained)
BTC	0.490*** (0.109)
Constant	0.260 (0.190)
Observations	8
Standard errors in parentheses *** p<0.01, ** p<0.05, * p<0.1	

In the regression tables above, we see that the selling price of biodiesel tends to be roughly equal to the fossil diesel wholesale price plus the D4 RIN plus some value from the BTC, if it is in effect. These results support the theoretical model of RIN pricing presented in Figure 3.28, and thereby our BTC-dependent approach to modeling D4 RINs. The fact that biodiesel selling prices don't exhibit a 1:1 response to changes in the price of fossil diesel may be due to physical differences in the products which limit their interchangeability. Transesterified biodiesel, which comprises the largest share of the biodiesel / renewable diesel market, is not a perfect "drop-in" substitute for fossil-derived diesel fuel in most cases [105, 126, 127, 163]. Of more importance for our purposes is the fact that the BTC appears to contribute roughly \$0.50 per gallon to the selling price of biodiesel in years in which it is in effect ex-ante. This implies a roughly 50/50 split of the value of the tax credit between sellers and buyers, in line with anecdotal evidence about the splitting of retroactively reinstated BTC benefits [29].

In our analysis, therefore, we assign a nominal \$0.50 per gallon benefit to the producer in years in which the BTC is in effect, whether ex-post or ex-ante. This policy effect is simulated via a random variable that gives a 37.5% chance of the BTC's being in effect ex-ante for any given year, and an 80% chance of its being reinstated retroactively in any year for which it was NOT in place ex-ante. This sums to an 87.5% chance of the producer's receiving revenue from the BTC in any given year. These probabilities were based on the history of the BTC from 2011 through 2018, which represented the best available sample period for examining policymakers' attitudes toward the BTC now that the RFS is also in effect. In the scenarios in which we assume that the BTC will disappear going forward, we set both the probability of the BTC's being "on" in any year and its monetary value to zero.

Modeling the California Low Carbon Fuel Standard

For this analysis, we assume that the biofuel producer in question chooses to sell all of their fuel products in California. Indeed, more than 80% of the supply of renewable fuels in California currently comes from out-of-state [36]. In order to determine how much revenue our model plant would generate from LCFS credits, we need to approximate the number of credits our plant's products would generate based on their assumed CI scores, and we also need to develop reasonable expectations for the market prices of those credits.

In order to determine the number of credits (or deficits) that a given quantity of a given fuel sold in California generates under the LCFS, one compares the lifecycle CI score for that fuel product to that year's target CI level for the relevant reference fuel category. Fuels with CI scores higher than that year's target generate deficits, while fuel with CI scores lower than the target generate credits [49]. The target for each reference fuel category declines linearly until 2030, when the total CI of California's transportation fuel sector is supposed to reach 20% reduction from 2011 levels stipulated in the statute [36, 49]. By comparing our proposed biofuel production pathway to analogous pathways already certified under the LCFS, we arrived at an assumed CI score of 30 g CO₂ equivalent per MJ for all three of our biofuel products.

The publicly available CI scores for 18 pathways producing biomass-based diesel from soybean oil averaged to around 54 g CO₂ equivalent per MJ, with roughly 29 g CO₂ equivalent per MJ being due to induced land use change (iLUC) [164, 165]. Publicly available scores for five canola oil-to-biomass-based diesel pathways averaged to approximately 55, with around 19 g CO₂ equivalent per MJ of iLUC [164, 165]. Since a pennycress-fed pathway would have an iLUC score of zero [1, 14, 16], comparison to either of these analogous pathways would point to a CI score between 25 and 35 for the renewable diesel produced by the process modeled here. Another pathway was already certified to produce renewable naphtha from tallow, with a CI score of around 40 [164]. The tallow rendering process seems to add up to 14 points to a process's CI score [166], and since that process would be unnecessary for our facility, it seems reasonable to assume that our renewable naphtha product would also have a CI score between 25 and 35. There were no CI data scores available for approved renewable jet fuel pathways, but its closeness to renewable diesel made it reasonable to assume that its CI score would be in line with our renewable diesel CI score. Thus, we assumed a CI score of 30 for all three of our products. We combined this grounded assumption with information taken from the LCFS's credit price calculator tool [36] regarding the declining target CI for each reference fuel category (diesel fuel, jet fuel, and California reformulated gasoline) to estimate the number of LCFS credits would generate in each year of our plant's productive life.

LCFS is "technology-blind", meaning that, unlike under the RFS, all approved pathways generate a single type of credit, regardless of what technology they employ [49]. This prevents the identification of a single breakeven relationship defining the credit supply curve, like the one we were able to identify for D4 RINs. Even so, the ARB's publicly available credit price and

quantity data [167, 168] still reveal some trends and tendencies that can inform our modeling efforts. The target CI score for transportation fuels in California has decreased in a roughly linear fashion beginning in 2015 [36]. Over that same period, the ARB-reported average price of LCFS credits has increased exponentially, until appearing so stabilize between \$150 and \$200 per MT CO₂ equivalent in real 2017 terms (see Figure 3.29 below). This is to be expected, based on the economic principle of diminishing marginal returns to investment; the cheapest and easiest means of complying with the LCFS are exploited first, followed by progressively less and less cost-effective means as the policy gets more and more restrictive.

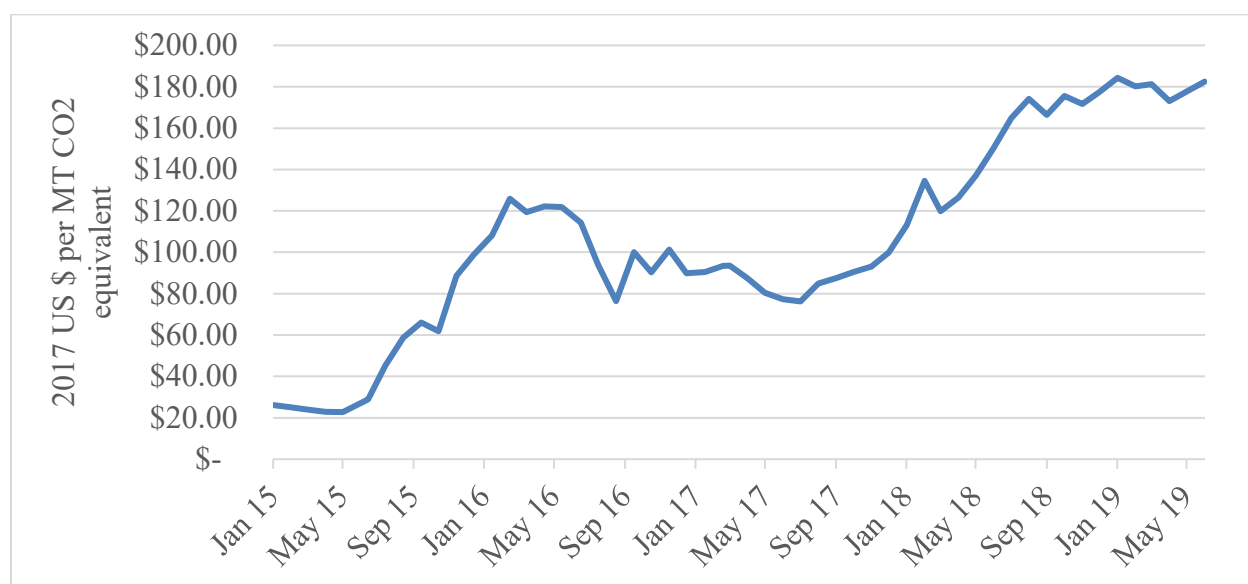


Figure 3.29: ARB LCFS Credit Price, real 2017 US \$ per MT CO₂ equivalent

This idea is further supported by the results of regression-based analysis, though the limited sample size prevents us from drawing firm conclusions. Table 3.35 below contains the results of regressing quarterly data for the real LCFS carbon price on the number of deficits generated by the policy's obligated parties in that quarter, and on the number of deficits squared. The results show that the squared term has a positive coefficient, and is more highly significant ($p=0.447$ vs. $p=0.641$) than the coefficient on the non-squared number of deficits generated. This would tend to point towards a greater-than-linear response of LCFS credit price to LCFS credit demand, represented here by the number of deficits generated under the policy. The results are not statistically significant, but they are consonant with basic economic reasoning and with the visual

evidence presented in Figure 3.29. The price of LCFS credits appears to be increasing exponentially.

Table 3.35: OLS of quarterly real LCFS credit prices on the number of deficits generated that quarter and the number of deficits generated in that quarter squared, beginning Q1 2015

	Real LCFS credit price, 2017 \$/MT CO2 equivalent
Deficits generated	0.0000146 (0.0000306)
(Deficits generated)^2	5.84e-12 (7.46e-12)
Constant	41.2 (27.2)
Observations	17
R-squared	0.709

Standard errors in parentheses
*** p<0.01, ** p<0.05, * p<0.1

To understand LCFS prices more fully, however, we must take into account the fact that the statute includes a price ceiling for its credits at \$200 per MT CO2 equivalent, in real 2016 dollars [49]. To defend this price cap, the ARB operates a “Credit Clearing Market” in which obligated parties with a year-end deficit can be considered to be in compliance if they purchase a pro-rated share of the credits available in the Clearing Market at year’s end [49]. The Credit Clearing Market will not post prices in excess of the statutory price cap. We discussed the price cap and the apparent exponential growth in credit prices with ARB personnel, and they indicated that they expected increased investment in production capacity for low-carbon alternative fuels to bring enough new supply into the market to allow them to continue to defend the \$200 price ceiling. They cited regulatory uncertainty due to a 2013 legal challenge to the LCFS and a 2015 re-adoption of the policy as one factor that had restrained such investments thus far.

We judged that the best way to reconcile the ARB’s expectations with the story that available data seemed to be telling was to set our model’s maximum LCFS price at the statutory price cap, and determine the minimum LCFS price from the most-recent monthly data, in which a

“levelling off” of LCFS prices can be discerned beginning in July 2018 (see Figure 3.29). Using the distribution fitting functionality in @Risk, a Pert distribution with the statutory cap (\$204.28 in real 2017 terms) as the upper bound and \$163.54 (2017 USD) as the lower bound was found to best approximate the sample data. The mode in each period was set as the previous period’s random draw multiplied by an annual growth factor determined by the data. This annual growth factor was identified using the semi-log method detailed above. The regression results indicated a significant ($p = 0.0624$) growth trend of 6.50% even in the recent “levelling off” period. This method also does some limited justice to the autocorrelated, persistent nature of the LCFS credit price series. This approach is, in essence, a stripped-down version of the approach detailed above for diesel fuel, soybean oil, and DDGS prices. We judged that implementing the full approach for LCFS prices would be overkill, due to the series’ limited sample size, relatively narrow sample price band, and lack of correlation to other key inputs in the model. The equation used for the LCFS price in any period is presented in full below. “Max” and “Min” expressions were used, as necessary, to prevent the mode’s being outside of the range between the stipulated maximum and minimum prices.

$$LCFS_t = RiskPert(\$163.54, Max(\$163.54, Min(LCFS_{t-1} * 1.065, \$204.28)), \$204.28) \quad \text{Equation 3.12}$$

Modeling Electricity and Natural Gas Prices

Electricity and natural gas prices were handled similarly to LCFS prices, with a stripped-down version of the weighted, bounded lag structure that we detail above for diesel, soybean oil, and DDGS prices. Our analysis was tasked with considering two potential plant sites, one in Indiana and one in Iowa. Yearly data on industrial electricity rates for those sates were obtained from the EIA website [169]. Natural gas monthly price data were also obtained from the EIA [170]. All price data were converted into real 2017 terms via the CPI. The electricity price data were found to fit best to a triangular distribution, while a Pert distribution was used for natural gas prices. Lower bounds were set at 75% of the minimum real price observed in the sample data. Upper bounds for the electricity price distributions were set at 150% of the maximum real price observed in the sample data. The upper bound on natural gas prices was set at 125% of the

maximum observed real price. Neither Iowa electricity prices nor US natural gas prices demonstrated a significant growth trend, while industrial electricity rates in Indiana did (1.22% annually, $p = 0.000$). Natural gas prices are in 2017 US \$ per thousand cubic feet. Electricity prices are in 2017 US \$ per kWh. The full equations are presented below. “Min” expressions were used, as necessary, to prevent the modes’ being greater than the stipulated maxima.

$$\text{Natural Gas}_t = \text{RiskPert}(\$2.67, \text{Natural Gas}_{t-1}, \$7.64) \quad \text{Equation 3.13}$$

$$\begin{aligned} \text{IN electricity}_t &= \text{RiskTriang}(\$0.0392, \text{Min}(\text{IN electricity}_{t-1} \\ &\quad * 1.0122, \$0.113), \$0.113) \end{aligned} \quad \text{Equation 3.14}$$

$$\text{IA electricity}_t = \text{RiskTriang}(\$0.0415, \text{IA electricity}_{t-1}, \$0.0941) \quad \text{Equation 3.15}$$

Modeling Fuel Yield

On the advice of ARA engineers, we follow McGarvey and Tyner in modeling both the total volumetric fuel yield (92% of feed oil volume) and the renewable naphtha yield (23% of feed oil volume) as deterministic, assigning the renewable jet fuel yield to a Pert distribution with a minimum of 30% by volume, a mode of 33% by volume, and a maximum of 36% by volume. The balance of the total fuel yield is assigned to renewable diesel. We also included a “max diesel” scenario for sake of comparison, in which the renewable jet fuel yield was fixed at zero, implying a renewable diesel yield of 69% of feed oil volume. All yields are on a dry volumetric basis, and a single random draw from the renewable jet fuel distribution is used for the entire life of the plan in each iteration of the model.

Modeling the Nth Plant

The cost and yield estimates that we rely upon in this analysis are based on initial test runs of a process that is still in the early stages of commercialization. An important question to address, then, is what impact future refinements to the process could be expected to have on its financial performance. In the TEA literature, this is referred to as the performance of the “nth plant”, as opposed to the “pioneer plant”. We follow McGarvey and Tyner, 2018, in taking the specifications of process performance received from ARA as representative of the pioneer plant, and then apply

“learning curves” to some of the cost data to approximate reasonable expectations for the performance of an n^{th} plant [2]. Where our approach differs from that taken by McGarvey and Tyner is in not applying a learning curve to feedstock costs. This is because we choose to model the cost of pennycress oil based on its opportunity cost rather than its cost of production. Pennycress seed oil may well become less expensive to produce in the near future; agronomic research to that end is ongoing. However, its marketplace value would only significantly diverge from the “going rate” for substitute vegetable oils like soybean oil if it were produced in very, very large quantities. Given that it is not currently produced commercially at any serious scale [45], that outcome seems unlikely in the near future.

Obtaining Breakeven Jet Fuel “Bonus”

One measure we use of the proposed plant’s financial attractiveness is what we call a “breakeven incentive” for renewable jet fuel. This is the amount of extra revenue per gallon of renewable jet fuel that would be necessary to make the NPV of the investment equal to zero, leaving all price projections unchanged. To generate this output metric, a cell to contain this incentive, and then referencing this cell in the discounted cash flow analysis, so that its contents are added to the per-gallon price of renewable jet fuel received by the plant operators in each period. After each iteration of the model, Excel’s Goal Seek tool changes the value of the incentive cell so that the NPV of the plant is equal to zero. @Risk then stores this result, and at the end of the 5000 iterations we run, a distribution of breakeven incentives is defined such that we can identify a level of additional price support for renewable jet fuel that would cause a facility such as the one modeled here to at least break even, with any specified degree of confidence (50%, 75%, 90%, etc.).

Obtaining Breakeven Constant and Growing Crude Oil Prices

Two other measures we generate of the proposed plant’s financial viability are variations on the idea: If all the other prices we model (except for RINs) remain unchanged, how much would the price of crude oil (and thereby the prices of fossil jet, diesel, and gasoline) have to increase in order for our plant to break even? To answer this question, we need to be able to vary all of our fossil fuel prices simultaneously by changing the value of a single cell, simulating simultaneous movements in these prices in response to changes in the price of crude oil. We do

this by making use of the regression relationships we already established between diesel fuel, jet fuel, and gasoline prices (see Tables 2.1 and 2.2) to define all of our fossil fuel prices based on the price of jet fuel, which we vary in each iteration to set the NPV for that iteration to zero. We allow RINs to vary based on the implied price for fossil diesel fuel, which, as we have seen, defines one endpoint for the “gap” that D4 and D5 RINs cover. All other price projections remain unchanged. The price of jet fuel is used to drive the price of diesel fuel, and the price of diesel fuel drives the price of gasoline. Thus all our fossil fuel prices move together in an “index” of sorts, driven by the jet fuel price. The price of diesel fuel, along with the forecasted price for soybean oil, drives RINs prices (see “Endogenous RIN Price Modeling” above). We could just as easily have used the diesel fuel or gasoline prices as the “driver”. The important point is that these prices move together as we change one of them in each iteration to find a breakeven price. We then use EIA data on the wholesale prices of crude oil [171] and jet fuel [172] to establish a regression relationship between these prices that allows us to report our breakeven price in terms of the price of crude oil. For details, see Table 3.36 below. We do not allow any of these linked prices to take negative values, even if implied by the regression relationships.

Table 3.36: Robust OLS of historical annual real wholesale crude oil prices (averages of Brent and West Texas Intermediate) on annual real wholesale jet fuel prices, 1990-2017

	Real wholesale crude oil prices, 2017 \$/barrel
Real wholesale jet fuel prices, 2017 \$/gal	34.1*** (0.569)
Constant	0.733 (0.750)
Observations	28
R-squared	0.993

Robust standard errors in parentheses

*** p<0.01, ** p<0.05, * p<0.1

We carry out two versions of this procedure. In one, we are finding a breakeven constant real price of crude oil, which is constant in real terms in every year of a given iteration. The same cell is referenced for the real jet fuel price in every year of the model. This approximates the EIA’s “Low Oil Price” projection scenarios [171]. In the other, we are finding a breakeven starting price

for crude oil, which then grows by 2.25% in real terms throughout the life of the plant. In this version, only the first year's jet fuel price directly references the cell whose value we are changing to find the breakeven point. The real jet fuel price in every subsequent year is equal to the previous year's real jet fuel price, multiplied by one plus the 2.25% growth rate. This procedure approximates the expectations of the EIA's "Reference Case" crude oil price projections [171]. These results are presented in the Results chapter below. As explained above, the prices of diesel fuel, gasoline, and D4 and D5 RINs are all defined based on the jet fuel price.

Obtaining Breakeven Prices of Pennycress Seed Oil

Our pennycress seed oil BEPs are used to investigate the feasibility of more-favorable pricing regimes for pennycress oil, given the cost structures of the rest of the supply chain, and to understand how far such cases diverge from our base pricing assumption. We calculate two such BEPs, a breakeven buying price for pennycress oil as an input, from the perspective of the biofuels producer, and a breakeven selling price from the perspective of a pennycress seed processor. Pennycress oil is not yet commercially produced or traded, and so we cannot yet know how it would be priced in a real market. Some link between its price and the price of soybean oil seems likely, however, due to significant co-movement between the prices of commodity vegetable oils and due to its substitutability with soybean oil for the purposes of fatty acid methyl ester (FAME) biodiesel production [53, 54, 124, 125, 128, 129]. For this reason, and in order to facilitate comparison to our base assumption, we measure our pennycress seed oil BEPs as a percent of the projected price of soybean oil.

The procedure for obtaining the buying price BEP from the perspective of the biofuels producer is simple. A single parameter is defined that is multiplied by the soybean oil price in every period to yield the buying price of pennycress oil at the biofuels facility. The price of soybean oil used to help determine RINs prices remains unchanged by this parameter. This factor is expressed in percentage terms, and its value is changed in each iteration of the model to drive that iteration's pioneer or n^{th} CH facility's NPV to zero. These values are stored after each iteration of the model, and then compiled into a distribution of breakeven pennycress oil buying prices, expressed as a percent of projected soybean oil prices.

To calculate the selling price BEP for pennycress oil from the perspective of the seed processor, we lean on TEAs of pennycress seed production and processing conducted by

researchers affiliated with the University of Tennessee, Knoxville, and led by Dr. Burton English [40, 41]. We combine parameters from their work with our price projections and financial assumptions to build a discounted cash flow model for a representative pennycress seed processor, using our projected DDGS prices as proxies for prices of pennycress meal sold as an animal feed additive. The processor's other source of revenue is selling pennycress oil. We then follow a procedure identical to that used for the CH facility's pennycress BEP. A single, constant factor is defined that is multiplied by the soybean oil price received by the seed processor in every period of each iteration. That parameter is expressed in percentage terms, used to drive the NPV of the seed processing facility to zero in each iteration of the model, with the resulting values from each iteration stored and compiled into a distribution of seed processor's pennycress oil selling BEPs.

DATA

Consumer Price Index

All conversion of data from nominal to real terms was done using the monthly, seasonally adjusted CPI, collected by the Organization for Economic Co-Operation and Development (OECD) and available from the Federal Reserve Economic Data online portal maintained by the Federal Reserve Bank of St. Louis [173]. The last update of that series available for use in this paper ended at the CPI number for June 2019. The series is currently maintained with 2015 as the base year. Every observation was divided by the average of 2017's monthly observations and then multiplied by 100 to re-scale it for constant 2017 US dollars.

CH Plant Technical and Financial Parameters

The technical parameters of the biofuels facility modeled here were obtained from ARA engineers under a non-disclosure agreement. These parameters included the total capital investment necessary to build the plant, fixed operating costs such as labor and royalties, the plant's total heat, electricity, and water requirements, the plant's nameplate capacity, and the plant's volumetric conversion rates for each element in the product slate. Due to ongoing refinements to the process, some of these parameters differed somewhat from those used for a similar process by McGarvey and Tyner (2018). We assumed a three-year construction period, with 35% of the total capital investment's occurring in the first year, 50% in the second year, and 15% in the third year. Production begins in the third year, at 50% of maximum output capacity. We assumed a 75-25 split between debt and equity financing and a ten-year loan repayment period at an 8% nominal interest rate. Working capital in each year was calculated as 40% of the difference between the next year's total operating costs and the present year's total operating costs, in real terms. We assumed a real discount rate of 10%, a nominal discount rate of 12%, and an inflation rate of 2%. The effective income tax rate was assumed to be 16.9%, with positive net tax flows allowed for years with negative net income under the assumption that the proprietors of the proposed biofuels facility would have a net tax liability from other pursuits in every year. The depreciation life of the capital investment for tax purposes was taken to be ten years, and a double declining balance method with a switch to straight line was used.

Learning Curves for Nth Plant Cost Reductions

We take our expectations for cost reductions for the nth plant from McGarvey and Tyner (2018). Based on analogy to the Brazilian sugarcane ethanol industry, they assumed a 12% reduction in the total capital investment necessary for the nth plant, and a 2.6% reduction in operating costs [2]. We apply the total capital investment learning curve as they do, and we apply the operating cost learning curve to all operating costs other than the cost of pennycress seed oil.

Feeding Model Nutritional Data

Nutritional data for maize, high-protein soybean meal, and DDGS were obtained from the routinely updated INRA, CIRAD, AFZ, and FAO information platform “Feedipedia” [140-142]. Pennycress meal crude protein and amino acid profile were obtained directly from the literature [38, 56, 57]. The energy contents of pennycress meal were approximated by the average of values given by Feedipedia for *Camelina sativa* meal and three kinds of rapeseed meal [143, 144]. Nutritional requirements for beef cattle published by the National Research Council were accessed via a University of Arkansas Cooperative Extension Service publication [136]. NRC nutritional requirements for dairy cows, swine, laying hens, and broilers were accessed via the online Merck Veterinary Manual [135, 137, 138]. The NRC guidelines for poultry were last updated in 1994, and so the listed lysine requirements for laying hens and broilers was adjusted upward based on values given in more-recent literature to more closely reflect the needs of modern commercial birds [139].

Feeding Model Price Data

Monthly cash prices in Decatur, Illinois for US No. 2 yellow corn, high-protein soybean meal, and DDGS from January 2001 to October 2018 were obtained from the USDA Agricultural Marketing Service custom report portal [133, 134, 145]. Central Illinois price data were used because the price series at that location were complete for all commodities of interest, and because Illinois is located in between Iowa and Indiana, where the two proposed biofuel plant sites are located. See Figures 4.1 through 4.3 below for graphical representations of these data (converted to real 2017 terms). Table 4.1 contains descriptive statistics (again, with the data converted to real 2017 terms). The yellow corn price was converted from dollars per bushel to dollars per ton for consistency with the other two prices.



Figure 4.1: US No. 2 yellow corn, 2017 US \$ per ton, Decatur, IL

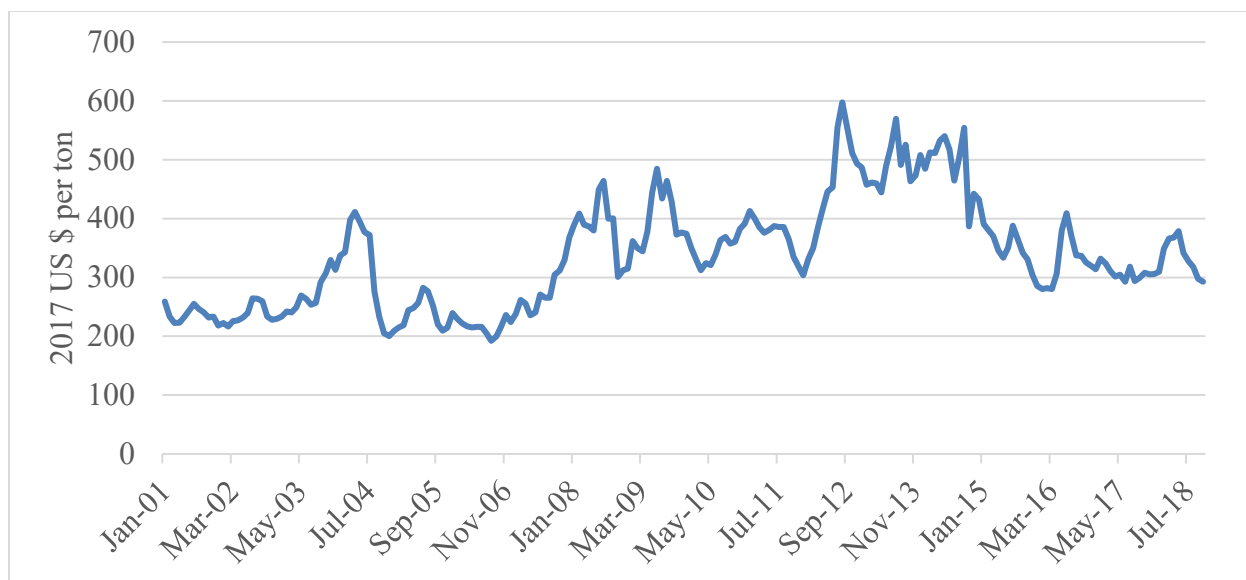


Figure 4.2: High-protein soybean meal, 2017 US \$ per ton, Decatur, IL



Figure 4.3: Dried distiller's grains with solubles, 2017 US \$ per ton, Central IL

Table 4.1: Descriptive statistics for price data used in simplified feed rationing model

VARIABLES (all in 2017 US \$ per ton)	N	mean	st. dev.	min	max
US yellow No. 2 corn	214	154.4	57.88	80.03	318.5
High-protein soybean meal	214	336.7	92.92	192.3	597.5
Dried distiller's grains with solubles	214	153.8	53.08	78.03	321.6

Fossil Transportation Fuel Price Data

Monthly wholesale prices for US No. 2 diesel fuel and motor gasoline from January 1983 to December 2017 and for jet fuel from April 1990 to December 2017 were obtained from the US Department of Energy's (DOE) Energy Information Administration (EIA) [172, 174, 175]. The monthly refiner's acquisition prices of Brent and West Texas Intermediate crude oil from May 1987 to December 2017 were also obtained from the EIA, and then averaged together to approximate a single "world price" for FOB crude oil [171]. All nominal price data were converted to real prices using the US Consumer Price Index (CPI), with 2017 at the base year [173]. Diesel, jet fuel, and gasoline prices were reported in dollars per gallon, while crude oil prices were reported in dollars per 42-US-gallon barrel. Figures 4.4 through 4.7 present these data graphically, and Table 4.2 contains descriptive statistics.



Figure 4.4: FOB crude oil price, 2017 US \$ per barrel

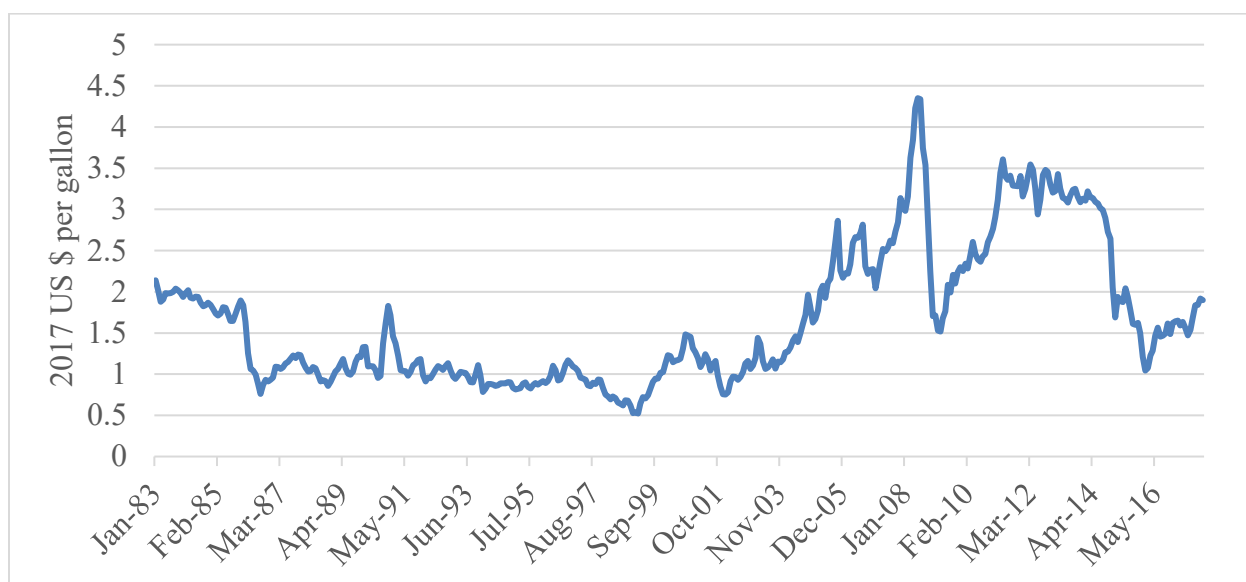


Figure 4.5: Wholesale US No. 2 diesel fuel price, 2017 US \$ per gallon



Figure 4.6: Wholesale kerosene-type jet fuel price, 2017 US \$ per gallon

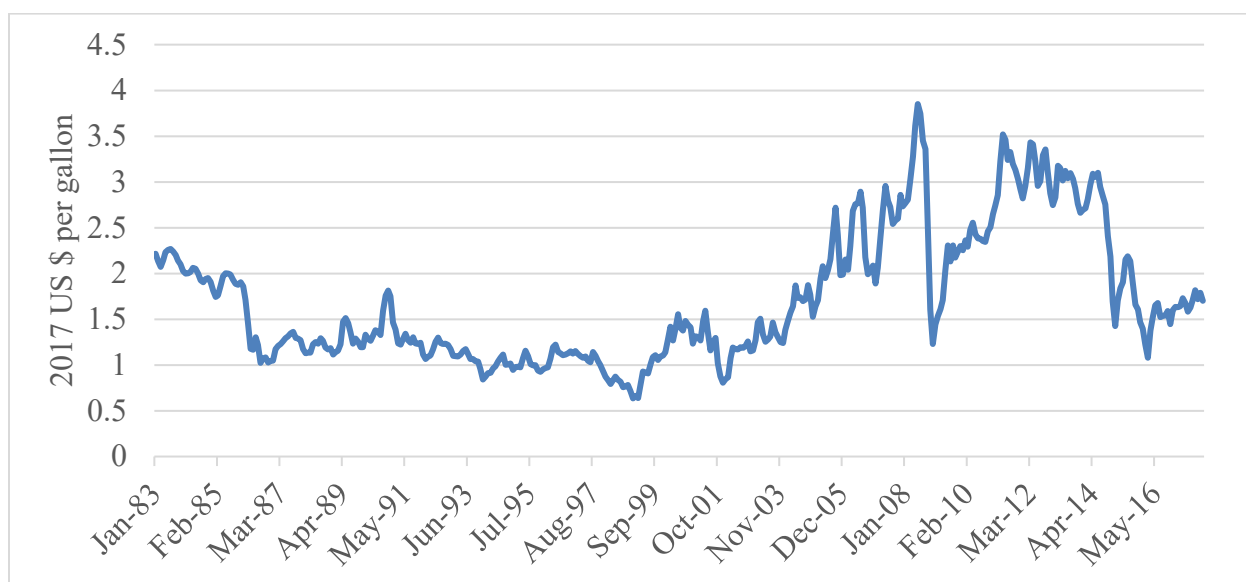


Figure 4.7: Wholesale motor gasoline price, 2017 US \$ per gallon

Table 4.2: Descriptive statistics for fossil-derived transportation fuel price data

VARIABLES	N	mean	st. dev.	min	max
Crude oil (2017 US \$ per barrel)	368	55.43	30.28	15.78	150.0
US No. 2 diesel fuel (2017 US \$ per gallon)	420	1.660	0.838	0.522	4.350
Motor gasoline (2017 US \$ per gallon)	420	1.710	0.718	0.635	3.851
Kerosene-type jet fuel (2017 US \$ per gallon)	333	1.658	0.907	0.453	4.372

Soybean Oil and Biodiesel Price Data

We obtained monthly January 2000 to October 2018 soybean oil price data for Decatur, Illinois from the USDA's Agricultural Marketing Service custom report portal [176]. Decatur price data were chosen for their completeness over the period of interest, and because Illinois served as a convenient midpoint between the two proposed sites for our plant, one of which was in Iowa and the other in Indiana. These price data were converted from dollars per hundred pounds into dollars per gallon using an assumed density of 7.68 pounds per gallon for soybean oil. They were then converted into real 2017 terms using the monthly, seasonally adjusted CPI [173]. For biodiesel selling prices, we depended on Don Hofstrand's compilation of the USDA Agricultural Marketing Service's Iowa FOB-at-plant biodiesel prices, which he includes in his publicly available biodiesel profitability model [34]. We also rely on Hofstrand's model for our estimates of biodiesel breakeven prices. Both these monthly series are reported in nominal dollars per gallon beginning April 2007, and they are updated regularly. We only used data from January 2011 to December 2018, because we were interested mostly in the period since RFS2 became fully functional. These data were also converted into real terms using the monthly, seasonally adjusted CPI with 2017 as the base year [173]. Figures 4.8 to 4.10 represent these data graphically, and Table 4.3 contains descriptive statistics.



Figure 4.8: Soybean oil prices in Decatur, IL, 2017 US \$ per gallon

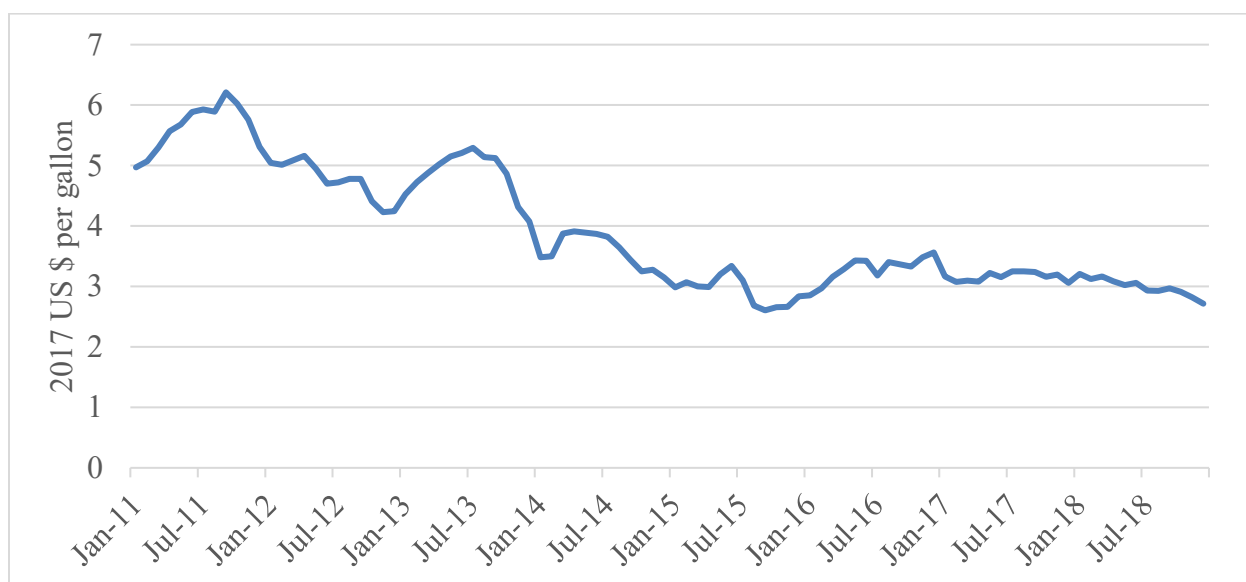


Figure 4.9: FOB-at-plant Iowa biodiesel prices, 2017 US \$ per gallon

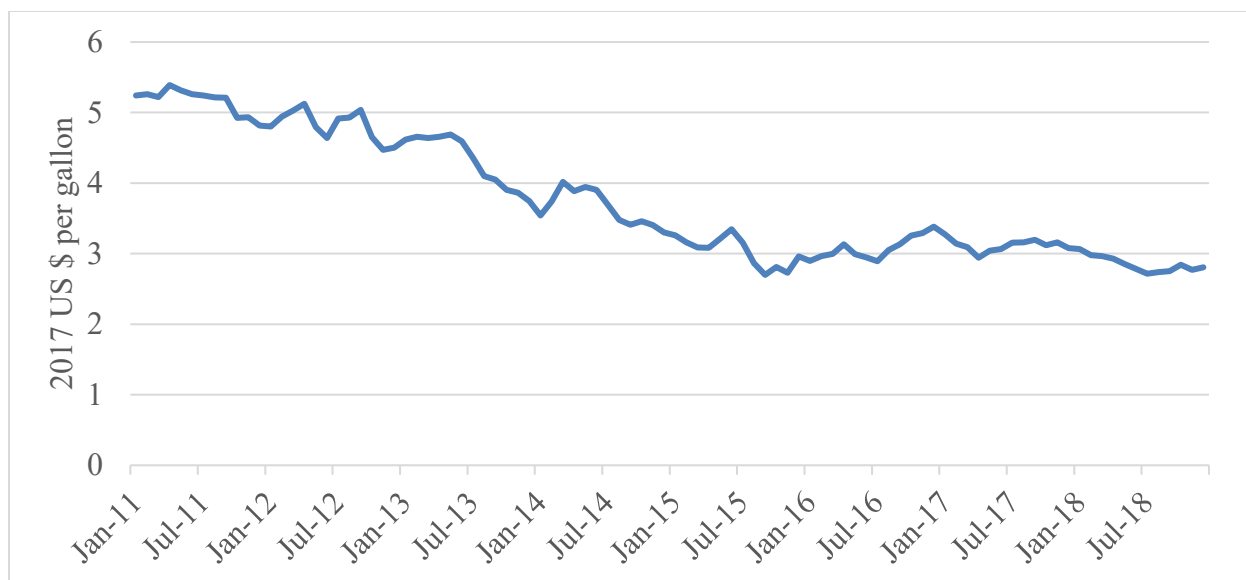


Figure 4.10: Modeled breakeven biodiesel price at “typical” Iowa biodiesel plant, 2017 US \$ per gallon

Table 4.3: Descriptive statistics for soybean oil and biodiesel price data

VARIABLES (all in 2017 US \$ per gallon)	N	mean	st. dev.	min	max
Soybean oil	226	2.816	0.917	1.324	5.405
FOB biodiesel price	96	3.903	1.005	2.605	6.211
Breakeven biodiesel price	96	3.755	0.871	2.699	5.390

Pennycress Supply and Seed Processing Data

Data about pennycress oil supply to our potential sites and about the costs of pennycress seed processing were taken from published and unpublished work by a team of researchers led by Dr. Burton English of the University of Tennessee, Knoxville [40, 41]. These data will not be reproduced here, but are available upon request.

D4 and D5 RINs Price Data

D4 and D5 RINs daily price data from 3 January 2011 to 31 December 2018 were obtained from Progressive Fuels Limited [120]. Prices of RINs generated in the current year were assembled into a series of “own year” RINs for both D4 and D5 RINs, and these daily data were then averaged by month to yield a monthly RIN price dataset. This was then converted to real 2017 terms using the monthly, seasonally adjusted CPI [173]. Since RINs are technically traded on an ethanol-equivalent basis, we further transformed the data by multiplying the posted RINs prices by 1.5, which is the “equivalence value” for fuels in the D4 and D5 group. These fuels (such as biodiesel) typically have 1.5 times the energy density of ethanol, and therefore generate 1.5 ethanol-equivalent RINs per physical gallon. By multiplying the ethanol-equivalent prices by 1.5, we get the “wet” RINs, or the RIN value per physical gallon of product, which is more intuitive and easier to work with. Figures 4.11 and 4.12 represent these data graphically. Descriptive statistics are contained in Table 4.4.

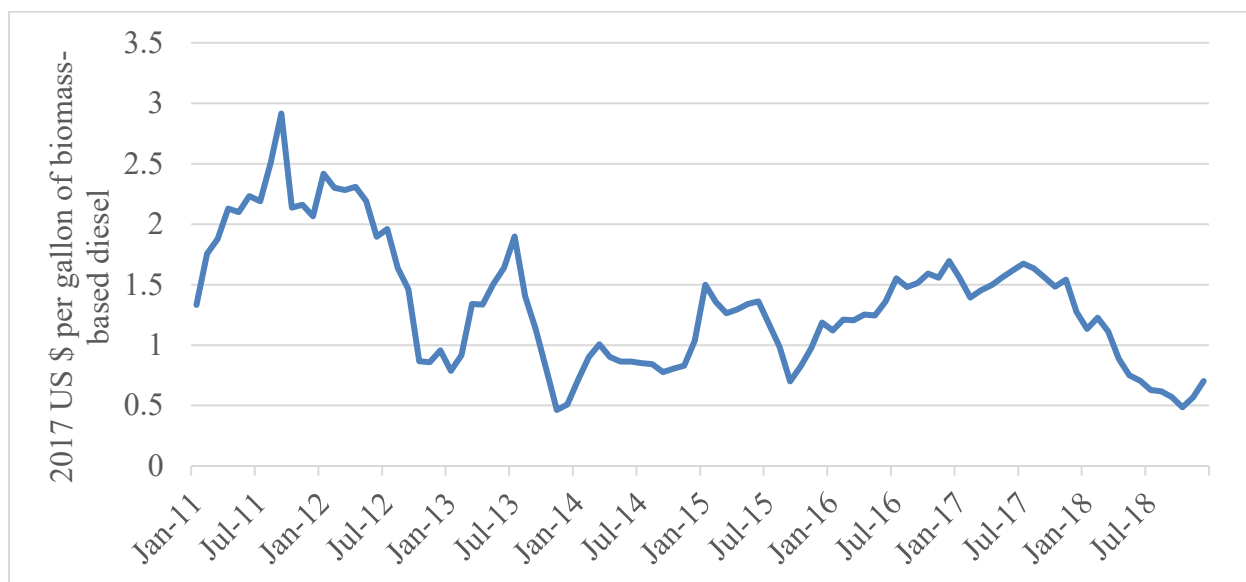


Figure 4.11: “Wet” D4 RINs price, 2017 US \$ per gallon of biomass-based diesel

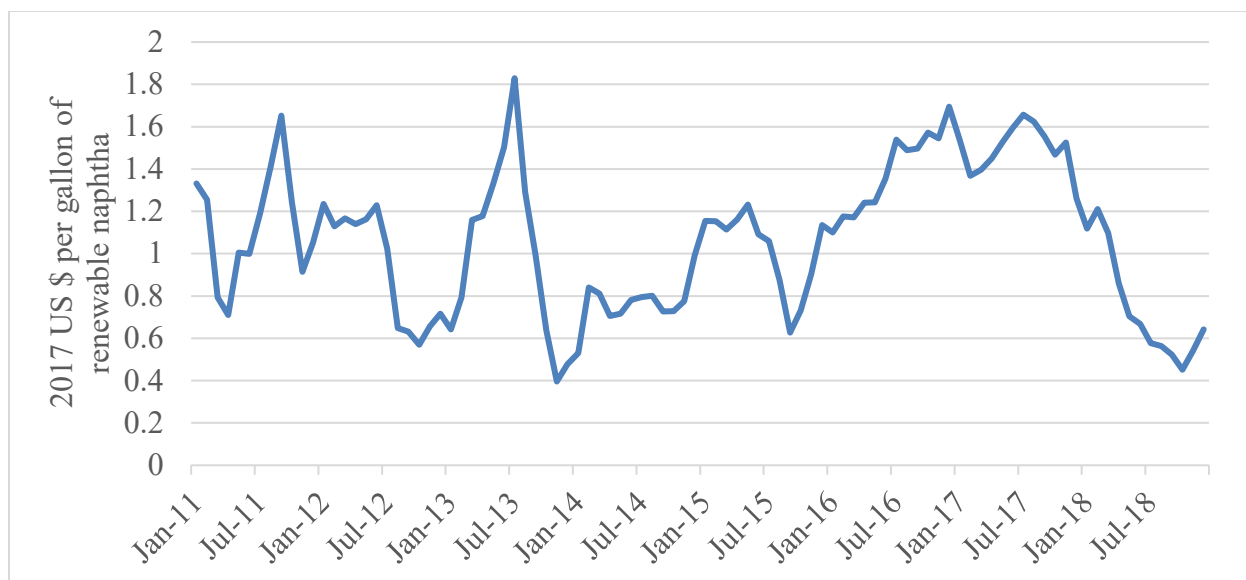


Figure 4.12: “Wet” D5 RINs price, 2017 US \$ per gallon of renewable naphtha

Table 4.4: Descriptive statistics for D4 and D5 RINs data

VARIABLES	N	mean	st. dev.	min	max
“Wet” D4 RINs price, 2017 US \$ per gallon biomass-based diesel	96	1.344	0.531	0.463	2.915
“Wet” D5 RINs price, 2017 US \$ per gallon renewable naphtha	96	1.063	0.349	0.396	1.829

LCFS Credit Price and Quantity Data

Publicly available price and quantity data for the LCFS credit market were obtained for the 2015-2019 period from the California ARB’s website [167, 168]. Average nominal prices are available from the ARB at a monthly frequency. Data on the number of credits and deficits generated, the number of credits traded, and the level of the overall “bank” of LCFS credits (which do not expire) are available at a quarterly frequency. The monthly data used begin in January 2015 and end in June 2019. The quarterly data run from the first quarter of 2015 through the first quarter

of 2019. The LCFS measures both deficits and credits in metric tons (MT) of CO₂ equivalent. Monthly price data were adjusted for inflation to real 2017 US \$ per MT CO₂ equivalent using the monthly, seasonally adjusted CPI [173]. For the quarterly data, the monthly CPI was averaged by quarter and used as a deflator. Figures 4.13 to 4.15 below represent these data graphically. Descriptive statistics may be found in Table 4.5.

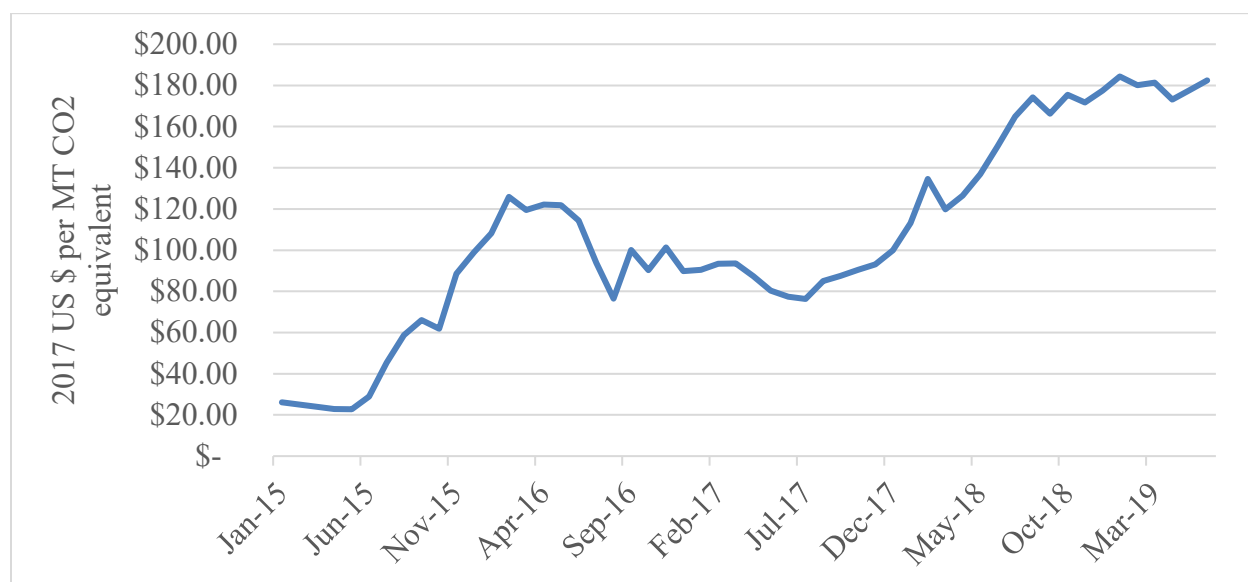


Figure 4.13: Monthly LCFS credit prices, 2017 US \$ per MT CO₂ equivalent

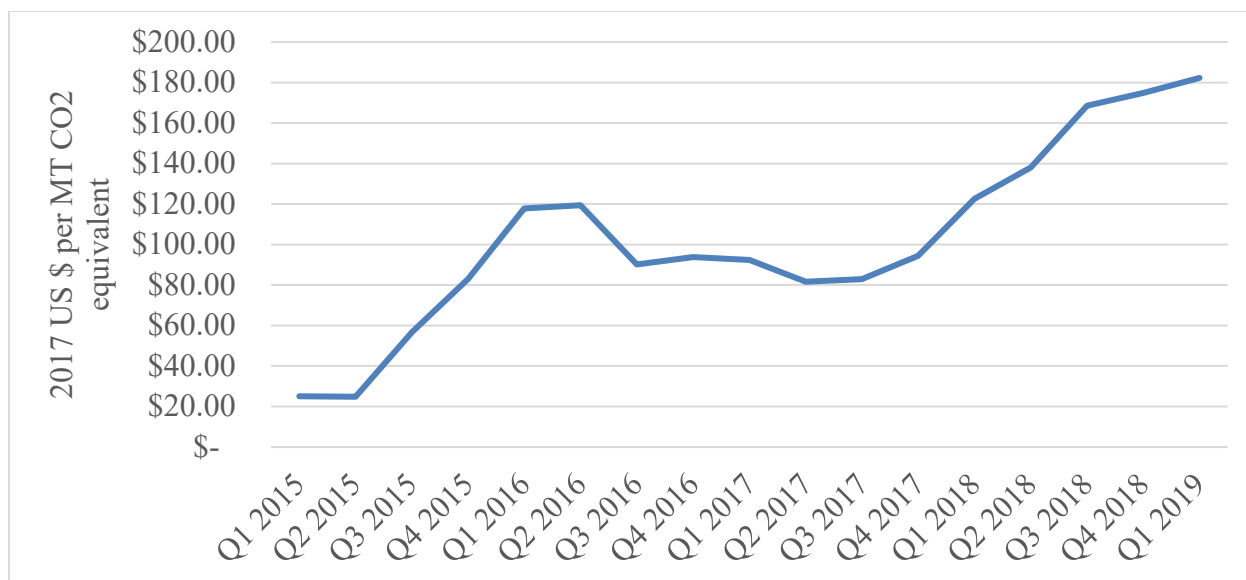


Figure 4.14: Quarterly LCFS credit prices, 2017 US \$ per MT CO2 equivalent

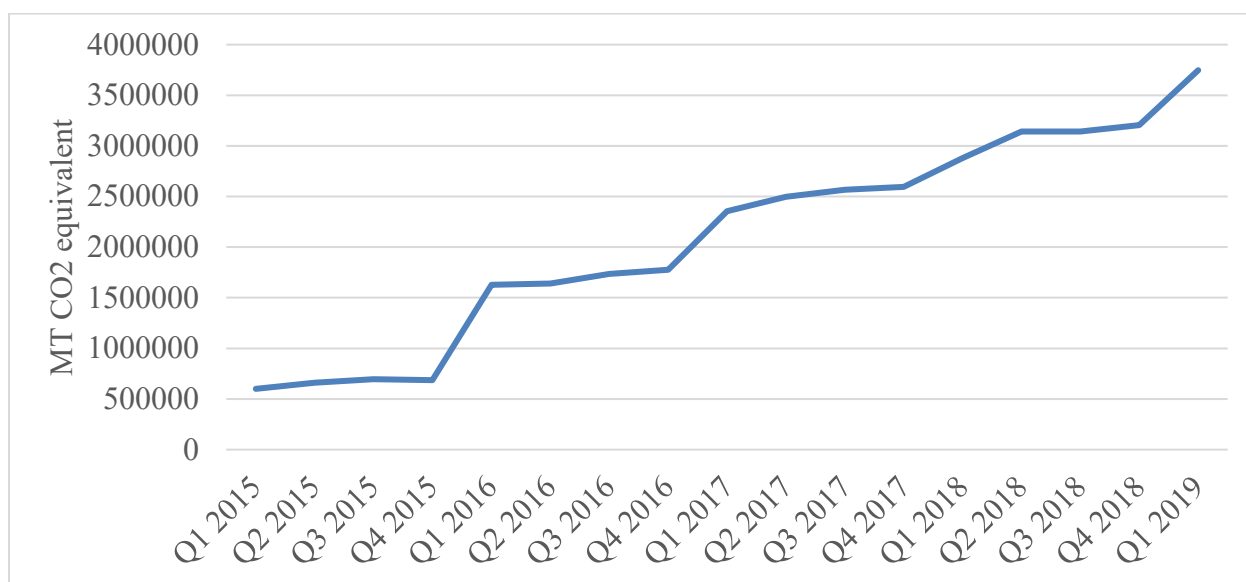


Figure 4.15: Quarterly deficits generated by obligated parties under the LCFS, MT CO2 equivalent

Table 4.5: Descriptive statistics for monthly LCFS prices and quarterly LCFS prices and deficits generated

VARIABLES	N	mean	st. dev.	min	max
Monthly LCFS credit price, 2017 US \$ per MT CO2 equivalent	54	107.0	47.53	22.76	184.3
Quarterly LCFS credit price, 2017 US \$ per MT CO2 equivalent	17	102.9	46.00	24.83	182.3
Quarterly deficits generated, MT CO2 equivalent	17	2.091e+06	1.011e+06	600,144	3.747e+06

Utilities Price Data

US monthly industrial natural gas prices for the period from January 2001 to December 2017 were obtained from the EIA [170]. These prices were reported in nominal US dollars per thousand cubic feet of natural gas, and were converted to real 2017 terms using the monthly, seasonally adjusted CPI [173]. Yearly industrial electricity rates from 1995 to 2017 for Iowa and Indiana were also obtained from the EIA [169]. These prices were reported in nominal US cents per kilowatt-hour, and were converted into real 2017 US dollars per kilowatt-hour by dividing by 100 and using the annual averages of the monthly CPI as a deflator [173]. These price data are represented graphically in Figures 4.16 and 4.17, and we present their summary statistics in Table 4.6.



Figure 4.16: Monthly industrial natural gas price data, 2017 US \$ per thousand cubic feet

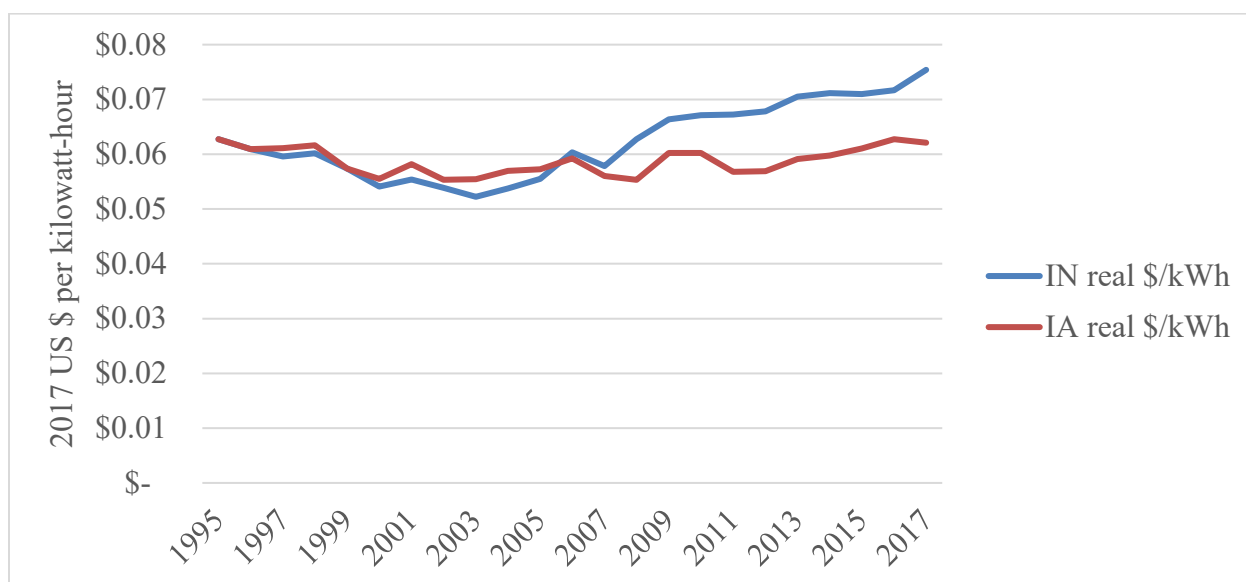


Figure 4.17: Yearly industrial electricity rates in Indiana and Iowa, 2017 US \$ per kilowatt-hour

Table 4.6: Descriptive statistics for monthly industrial gas price data and yearly industrial electricity rate data

VARIABLES	N	mean	st. dev.	min	max
Monthly industrial natural gas prices, 2017 US \$ per thousand cubic feet	204	6.671	2.608	2.951	14.99
Yearly Indiana industrial electricity rates, 2017 US \$ per kWh	23	0.0624	0.00689	0.0522	0.0754
Yearly Iowa industrial electricity rates, 2017 US \$ per kWh	23	0.0588	0.00252	0.0553	0.0627

RESULTS

On the following pages, we present tables summarizing the results of our stochastic analysis organized by metric and by site. Commentary on the results of each metric precedes the associated tables. Particular emphasis is given to the 90th percentile values for distributions of breakeven prices, as these are the values that would result in the modeled facility's at least breaking even in 90% of cases, and is therefore taken as a possible benchmark for interest from a risk-averse investor. We then discuss which scenarios produced the most favorable results, and which scenario variables appear to have the greatest impact on a plant's financial performance. Graphs of each output distribution not included here are located in the Appendix. Overall, our results show that a greenfield CH aviation biofuels production facility like the one modeled here is not financially viable under current economic conditions, even with existing policy supports. However, there are indications that a greenfield CH facility that maximizes its renewable diesel production at the expense of renewable jet fuel could be a highly attractive investment under certain conditions.

Summary

Net Present Value

Distributions of net present values (NPVs) demonstrated a similar degree of variability in returns across scenarios, with nearly identical standard deviations of roughly \$40 million and max-to-min ranges around \$200 to \$300 million in all cases. They differ from each other primarily when it comes to where they are centered. Distribution means ranged from roughly negative \$59 million to nearly \$89 million (2017 USD). Six of our sixteen scenarios (three for each site) resulted in NPV distributions with mean values greater than zero.

Table 5.1: Net present value results for Iowa site, 2017 US \$, negative values in parentheses

Scenarios			mean	st. dev.	min	max
Pioneer	BTC	Jet and Diesel	\$(15,955,946.29)	\$40,009,288.68	\$(151,525,347.66)	\$140,164,471.38
Pioneer	BTC	Max Diesel	\$61,155,823.82	\$40,008,849.57	\$(80,199,741.19)	\$202,598,687.95
Pioneer	NO BTC	Jet and Diesel	\$(56,886,816.97)	\$39,252,164.41	\$(186,568,091.83)	\$95,030,014.17
Pioneer	NO BTC	Max Diesel	\$(28,283,811.98)	\$38,540,613.53	\$(146,138,870.65)	\$112,577,019.45
Nth	BTC	Jet and Diesel	\$11,739,444.42	\$39,983,217.61	\$(123,549,768.45)	\$167,962,291.78
Nth	BTC	Max Diesel	\$88,849,736.63	\$39,984,748.25	\$(52,376,666.05)	\$230,635,240.14
Nth	NO BTC	Jet and Diesel	\$(29,191,426.26)	\$39,226,033.37	\$(158,828,396.83)	\$122,827,834.57
Nth	NO BTC	Max Diesel	\$(589,899.18)	\$38,515,581.70	\$(118,315,795.50)	\$140,613,571.64

Table 5.2: Net present value results for Indiana site, 2017 US \$, negative values in parentheses

Scenarios			mean	st. dev.	min	max
Pioneer	BTC	Jet and Diesel	\$(17,689,959.02)	\$40,040,433.91	\$(153,039,101.17)	\$138,071,928.85
Pioneer	BTC	Max Diesel	\$59,421,157.75	\$40,027,169.34	\$(81,372,082.14)	\$200,764,015.98
Pioneer	NO BTC	Jet and Diesel	\$(58,620,829.70)	\$39,282,214.68	\$(188,631,368.50)	\$92,937,471.64
Pioneer	NO BTC	Max Diesel	\$(30,018,478.06)	\$38,557,731.93	\$(147,311,211.60)	\$110,742,347.49
Nth	BTC	Jet and Diesel	\$10,050,516.02	\$40,013,127.16	\$(125,024,164.36)	\$165,924,155.35
Nth	BTC	Max Diesel	\$87,160,171.88	\$40,002,088.79	\$(53,518,526.14)	\$228,848,269.64
Nth	NO BTC	Jet and Diesel	\$(30,880,354.66)	\$39,254,867.52	\$(160,838,028.31)	\$120,789,698.14
Nth	NO BTC	Max Diesel	\$(2,279,463.93)	\$38,531,732.56	\$(119,457,655.59)	\$138,826,601.15

Breakeven Jet Fuel Incentive

Our breakeven jet fuel incentive metric is the amount of additional real, constant, per-gallon revenue over projected jet fuel prices that would be needed for the project to break even. This might take the form of a tax credit like the Biodiesel Blender Tax Credit (BTC), for example. The degree of variation in these estimates is high, as may be seen by comparing distribution means and standard deviations below. In all cases, the standard deviation is greater than half of the mean. Were our interest in using these mean values to predict the true level of the breakeven jet fuel bonus, then this would make our results statistically insignificant. Our interest, however, is in using these results to identify a cutoff level of support that would render an investment in a greenfield

aviation biofuels facility like the one modeled here relatively safe, despite the high degree of variability. Thus, we focus on the 90th percentile values of these distributions. Additional fuel producer revenue of \$0.40 to \$0.80 per gallon of jet fuel (in constant 2017 US dollars) would be sufficient to make a plant like the one modeled here into an attractive investment in any of the scenarios we considered, as can be seen below. Real wholesale jet fuel prices were at \$1.85 per gallon (2017 USD) in July 2019, which means that this level of support would represent an increase of roughly 20 to 40 percent in the base price received by producers of renewable jet fuel, in addition to payments for the values of California Low Carbon Fuel Standard (LCFS) credits and D4 Renewable Identification Numbers (RINs).

We can get an idea of the minimum percentage increase in jet fuel price required for aviation biofuels to break even, on average, by comparing the lowest mean incentive required (\$0.20 per gallon, 2017 USD) to the mean projected jet fuel price in the first year of our model, which is \$1.87 per gallon (2017 USD). This gives a low-end price increase estimate of roughly 11%. Repeating the same procedure for the worst-performing pathway gives an estimated required price increase of 26%.

Table 5.3: Breakeven jet fuel incentive results for Iowa site, 2017 US \$ per gallon

Scenarios			mean	st. dev.	min	max	90 th percentile
Pioneer	BTC	Jet and Diesel	\$0.28	\$0.19	\$0.00	\$1.11	\$0.55
Pioneer	NO BTC	Jet and Diesel	\$0.47	\$0.25	\$0.00	\$1.40	\$0.80
Nth	BTC	Jet and Diesel	\$0.20	\$0.15	\$0.00	\$0.90	\$0.41
Nth	NO BTC	Jet and Diesel	\$0.33	\$0.21	\$0.00	\$1.19	\$0.61

Table 5.4: Breakeven jet fuel incentive results for Indiana site, 2017 US \$ per gallon

Scenarios			mean	st. dev.	min	max	90 th percentile
Pioneer	BTC	Jet and Diesel	\$0.29	\$0.19	\$0.00	\$1.12	\$0.57
Pioneer	NO BTC	Jet and Diesel	\$0.48	\$0.25	\$0.00	\$1.42	\$0.81
Nth	BTC	Jet and Diesel	\$0.20	\$0.15	\$0.00	\$0.91	\$0.42
Nth	NO BTC	Jet and Diesel	\$0.34	\$0.21	\$0.00	\$1.21	\$0.63

Breakeven Crude Oil Price

Mean values and standard deviations for our crude oil breakeven prices are somewhat variable from one scenario to another. One interesting pattern that emerges from these results is that the standard deviations for scenarios in which the BTC continues its recent behavior are higher than “No BTC” scenarios, while their mean values are lower. At least some of this increase in variation is likely due to our stochastic implementation of the BTC. Another possibility may be that factors other than the price of crude oil exert more influence on financial outcomes in these scenarios.

Our 90th percentile results tell a clearer story than the mean and standard deviation results. They indicate that starting crude oil prices around \$100-\$130 real 2017 USD per barrel with 2.25% real annual price growth or constant crude oil prices between \$130 and \$170 real 2017 USD per barrel would make the modeled greenfield CH biofuels facility an attractive investment, assuming that input price levels remain as projected here. A real crude oil price of \$100 per barrel (2017 USD) would be in the 85th percentile of all historical crude oil prices from 1987 to 2017, while \$130 per barrel would be in the 99th percentile [171]. Any of these would imply diesel fuel prices greater than the highest value of our 2018 projections.

Looking at the mean results for the best-performing scenario that produces both renewable jet and renewable diesel can give us an idea of the minimum percentage increase in crude oil price that would be required to make aviation biofuels production profitable, on the mean. An nth plant in Iowa with the BTC in place has a mean breakeven starting crude oil price of \$84.87 per barrel (2017 USD). The mean first-year crude oil price implied by our stochastic forecast was \$64.67 per barrel (2017 USD). Refiner’s cost for a barrel of crude was roughly \$55.73 per barrel (2017 USD) in August 2019. In percentage terms, then, a price increase of at least 31% over projection or 52% over actual prices would be required for aviation biofuels production to break even, on average.

Our projections follow those of the EIA, and crude oil prices when the analysis was conducted were on the low end of their projections, and therefore on the low end of ours. This explains a curious feature of our results: The probability-of-loss and breakeven jet fuel incentive metrics paint a much more optimistic picture than do the starting and constant crude oil breakeven prices. Our implied projections of crude oil prices, while still substantially lower than these BEP

results, are nearer to the breakeven levels than actual prices have been since the projection model was built.

Table 5.5: Breakeven constant crude oil price results for Iowa site, 2017 US \$ per barrel

Scenarios			mean	st. dev.	min	max	90 th percentile
Pioneer	BTC	Jet and Diesel	\$123.02	\$35.07	\$0.89	\$199.38	\$160.90
Pioneer	BTC	Max Diesel	\$82.17	\$47.69	\$0.87	\$183.63	\$145.20
Pioneer	NO BTC	Jet and Diesel	\$140.95	\$23.21	\$19.45	\$207.16	\$169.85
Pioneer	NO BTC	Max Diesel	\$133.58	\$27.16	\$5.18	\$201.16	\$165.39
Nth	BTC	Jet and Diesel	\$110.55	\$41.86	\$0.85	\$194.85	\$155.39
Nth	BTC	Max Diesel	\$67.23	\$46.29	\$0.74	\$177.75	\$136.44
Nth	NO BTC	Jet and Diesel	\$135.34	\$25.41	\$2.45	\$203.60	\$165.81
Nth	NO BTC	Max Diesel	\$128.20	\$30.24	\$1.26	\$196.95	\$161.10

Table 5.6: Breakeven constant crude oil price results for Indiana site, 2017 US \$ per barrel

Scenarios			mean	st. dev.	min	max	90 th percentile
Pioneer	BTC	Jet and Diesel	\$123.83	\$34.53	\$1.26	\$199.69	\$161.29
Pioneer	BTC	Max Diesel	\$83.02	\$47.75	\$0.96	\$183.99	\$145.95
Pioneer	NO BTC	Jet and Diesel	\$141.10	\$23.74	\$2.96	\$207.40	\$170.07
Pioneer	NO BTC	Max Diesel	\$133.97	\$26.87	\$4.20	\$201.46	\$165.70
Nth	BTC	Jet and Diesel	\$111.33	\$41.54	\$0.79	\$195.19	\$155.61
Nth	BTC	Max Diesel	\$68.13	\$46.53	\$0.81	\$178.26	\$137.97
Nth	NO BTC	Jet and Diesel	\$135.68	\$25.24	\$1.30	\$203.86	\$166.05
Nth	NO BTC	Max Diesel	\$128.79	\$29.62	\$1.40	\$197.29	\$161.41

Table 5.7: Breakeven starting crude oil price results with 2.25% real annual price growth for Iowa site, 2017 US \$ per barrel

Scenarios			mean	st. dev.	min	max	90 th percentile
Pioneer	BTC	Jet and Diesel	\$95.30	\$26.46	\$0.86	\$154.42	\$123.35
Pioneer	BTC	Max Diesel	\$63.16	\$34.98	\$0.84	\$134.24	\$107.51
Pioneer	NO BTC	Jet and Diesel	\$110.39	\$17.48	\$15.91	\$161.18	\$132.04
Pioneer	NO BTC	Max Diesel	\$103.62	\$20.69	\$4.34	\$156.87	\$127.56
Nth	BTC	Jet and Diesel	\$84.87	\$31.29	\$0.83	\$150.09	\$118.32
Nth	BTC	Max Diesel	\$52.03	\$33.88	\$0.74	\$129.22	\$100.18
Nth	NO BTC	Jet and Diesel	\$105.02	\$19.35	\$2.13	\$157.19	\$127.96
Nth	NO BTC	Max Diesel	\$98.24	\$22.92	\$1.16	\$152.49	\$123.39

Table 5.8: Breakeven starting crude oil price results with 2.25% real annual price growth for Indiana site, 2017 US \$ per barrel

Scenarios			mean	st. dev.	min	max	90 th percentile
Pioneer	BTC	Jet and Diesel	\$95.97	\$26.07	\$1.17	\$154.65	\$123.75
Pioneer	BTC	Max Diesel	\$63.81	\$35.05	\$0.92	\$134.90	\$108.15
Pioneer	NO BTC	Jet and Diesel	\$110.56	\$17.90	\$2.54	\$161.39	\$132.36
Pioneer	NO BTC	Max Diesel	\$103.98	\$20.50	\$3.54	\$157.11	\$127.87
Nth	BTC	Jet and Diesel	\$85.50	\$31.08	\$0.78	\$150.35	\$118.61
Nth	BTC	Max Diesel	\$52.69	\$34.03	\$0.80	\$129.49	\$99.95
Nth	NO BTC	Jet and Diesel	\$105.33	\$19.26	\$1.19	\$157.50	\$128.21
Nth	NO BTC	Max Diesel	\$98.79	\$22.46	\$1.27	\$152.79	\$123.74

Breakeven Pennycress Seed Oil Prices

All of our BEPs for pennycress seed oil are measured as a percent of the price of soybean oil, for the sake of comparison, and to account for the fact that the prices of commodity oils tend to exhibit significant degrees of co-movement [128]. Six scenarios in total had 50th percentile scores over 100%. These were the same scenarios that had positive mean NPVs. From 10th percentile values of the other scenarios we see that discounts of 2-6% over soybean oil prices would make fuel conversion a very safe investment, indeed. From Figure 5.1 we see that the

crushers would be able to accommodate these discounts with a high degree of safety, themselves, as the 90th percentile of their minimum selling price distribution is roughly 94% of the soybean oil price.

Table 5.9: Biofuels producer's breakeven cost of pennycress oil at an Iowa site, as a percent of projected soybean oil prices

Scenarios			50 th percentile	st. dev.	min	max	10 th percentile
Pioneer	BTC	Jet and Diesel	99.01%	2.35%	93.24%	113.11%	96.59%
Pioneer	BTC	Max Diesel	103.45%	2.77%	96.31%	118.95%	100.59%
Pioneer	NO BTC	Jet and Diesel	96.66%	2.07%	91.74%	108.89%	94.52%
Pioneer	NO BTC	Max Diesel	98.31%	2.18%	93.28%	110.53%	96.06%
Nth	BTC	Jet and Diesel	100.59%	2.50%	94.49%	115.71%	98.02%
Nth	BTC	Max Diesel	105.03%	2.93%	97.59%	121.58%	102.01%
Nth	NO BTC	Jet and Diesel	98.23%	2.22%	92.99%	111.49%	95.94%
Nth	NO BTC	Max Diesel	99.89%	2.34%	94.56%	113.15%	97.49%

Table 5.10: Biofuels producer's breakeven cost of pennycress oil at an Indiana site, as a percent of projected soybean oil prices

Scenarios			50 th percentile	st. dev.	min	max	10 th percentile
Pioneer	BTC	Jet and Diesel	98.90%	2.34%	93.16%	112.92%	96.51%
Pioneer	BTC	Max Diesel	103.35%	2.76%	96.26%	118.78%	100.49%
Pioneer	NO BTC	Jet and Diesel	96.56%	2.06%	91.67%	108.69%	94.42%
Pioneer	NO BTC	Max Diesel	98.21%	2.18%	93.22%	110.36%	95.96%
Nth	BTC	Jet and Diesel	100.48%	2.49%	94.42%	115.52%	97.94%
Nth	BTC	Max Diesel	104.93%	2.92%	97.54%	121.41%	101.91%
Nth	NO BTC	Jet and Diesel	98.14%	2.22%	92.92%	111.30%	95.85%
Nth	NO BTC	Max Diesel	99.79%	2.33%	94.50%	112.99%	97.40%

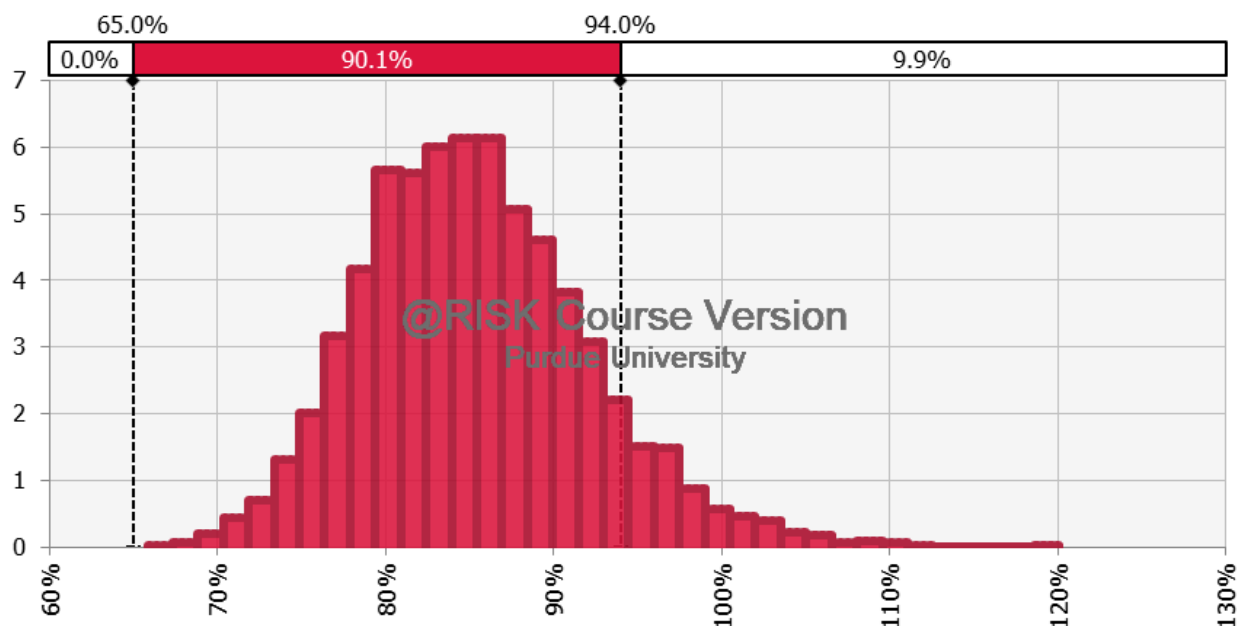


Figure 5.1: Seed processor's breakeven selling price of pennycress oil, as a percent of projected soybean oil prices

Ranking Scenarios and Identifying Key Variables

Including both the Iowa and Indiana siting options, we examined sixteen greenfield scenarios in our study, allowing us to compare the relative impacts of four binary variables on the project's financial performance. As previously stated, in none of these scenarios would a greenfield CH aviation biofuels facility represent a financially viable investment.

Many of the lessons to be drawn from our results are unsurprising: n^{th} plants performed marginally better than pioneer plants, and scenarios based on Iowa's relatively lower electricity prices yielded more favorable results than otherwise equivalent scenarios using Indiana's electricity prices. More interesting are the results pertaining to the impact of the BTC's status and the plant's choice of product mix. Table 5.11 below presents a snapshot of the results for all sixteen scenarios, ranked by increasing probability of loss (POL) from top to bottom. Other metrics are presented alongside POL, and the ranking of scenarios would have been similar if any of these other results had been used as criteria, as can be seen from the consistent "good-to-bad" green-to-red color coding in the table. The four binary variables that define each scenario are listed on the left-hand side of the table, arranged left to right from most influential to least, as will be explained below.

Table 5.11: Ranking of scenarios based on probability of loss (P.O.L.), with impacts on other metrics also shown. Color gradients show ranking of scenarios based on each metric. Green is good; red is bad.

Scenarios				Net Present Value, 2017 US \$	Breakeven Jet Fuel Incentive, 2017 US \$ per gallon			Breakeven Starting Crude Oil Price, 2017 US \$ per barrel		
				P.O.L. 50th percentile	50th percentile	75th percentile	90th percentile	50th percentile	75th percentile	90th percentile
BTC	Max Diesel	Nth	Iowa	1.0% \$ 87,972,409.55				\$ 49.27	\$ 80.64	\$100.18
BTC	Max Diesel	Nth	Indiana	1.2% \$ 86,014,381.63				\$ 50.26	\$ 82.04	\$ 99.95
BTC	Max Diesel	Pioneer	Iowa	5.8% \$ 60,302,921.46				\$ 66.74	\$ 92.28	\$107.51
BTC	Max Diesel	Pioneer	Indiana	6.4% \$ 63,039,803.84				\$ 68.42	\$ 93.05	\$108.15
BTC	Jet and Diesel	Nth	Iowa	39.6% \$ 10,276,312.50	\$ 0.17	\$ 0.28	\$ 0.41	\$ 92.15	\$107.57	\$118.32
BTC	Jet and Diesel	Nth	Indiana	41.6% \$ 8,296,522.08	\$ 0.17	\$ 0.29	\$ 0.42	\$ 92.87	\$108.12	\$118.61
NO BTC	Max Diesel	Nth	Iowa	51.8% \$ (2,093,978.06)				\$101.35	\$113.30	\$123.39
NO BTC	Max Diesel	Nth	Indiana	53.6% \$ (4,031,713.80)				\$101.74	\$113.68	\$123.74
BTC	Jet and Diesel	Pioneer	Iowa	66.4% \$ (17,362,862.55)	\$ 0.26	\$ 0.40	\$ 0.55	\$ 99.68	\$113.60	\$123.35
BTC	Jet and Diesel	Pioneer	Indiana	68.2% \$ (19,407,557.12)	\$ 0.26	\$ 0.41	\$ 0.57	\$100.28	\$113.99	\$123.75
NO BTC	Max Diesel	Pioneer	Iowa	76.5% \$ (29,769,587.15)				\$105.87	\$117.78	\$127.56
NO BTC	Jet and Diesel	Nth	Iowa	77.5% \$ (31,049,109.22)	\$ 0.31	\$ 0.47	\$ 0.61	\$106.62	\$118.31	\$127.96
NO BTC	Max Diesel	Pioneer	Indiana	77.9% \$ (31,838,671.90)				\$106.16	\$118.05	\$127.87
NO BTC	Jet and Diesel	Nth	Indiana	78.8% \$ (33,075,649.66)	\$ 0.32	\$ 0.49	\$ 0.63	\$107.00	\$118.59	\$128.21
NO BTC	Jet and Diesel	Pioneer	Iowa	91.9% \$ (58,717,748.33)	\$ 0.46	\$ 0.64	\$ 0.80	\$111.59	\$122.72	\$132.04
NO BTC	Jet and Diesel	Pioneer	Indiana	92.4% \$ (60,820,595.39)	\$ 0.48	\$ 0.66	\$ 0.81	\$111.94	\$123.06	\$132.36

With the results arranged in this way, we can see which scenario variables generally proved to be relatively more important. If a single scenario variable's impact always outweighed all the others', then the scenarios would be ranked by that variable first, and then by the other three. This would result in seeing all the scenarios in which that variable took its more-favorable value ranked above all the scenarios in which it took its less-favorable value, and the column for that variable would contain two solid blocks in Table 5.11 above. This is very nearly the case for the "BTC / NO BTC" variable. Its large impact on the project's financial success is to be expected. As modeled here, the default "BTC continues" scenario results in added nominal revenues of \$0.50 per gallon of renewable diesel in years for which it is reinstated retroactively, which occurs in 40% of all years. For a plant like this one rated to process 5000 barrels of feed oil per day, this equates to roughly \$13 million dollars of revenue per year in nominal terms. In years in which it is in effect ex-ante, at least some of that value gets absorbed by the model in the form of lower RINs prices, as indicated in Tables 3.29 and 3.30.

If a scenario variable were always less influential than all the other variables, then the scenarios would be ranked by that variable last, after the impacts of all the other variables had been accounted for. This would result in a simple one-by-one alternating pattern between the values of that scenario variable, as is very nearly the case for our "Iowa / Indiana" variable above. That this

variable should be relatively unimportant to our model is not surprising, since a slight difference in electricity prices (see Table 4.6) comprised the sole distinction between the two sites in this analysis. The product slate choice and Nth versus pioneer distinctions appear to have roughly equivalent impacts on the ranking of our scenarios. Still, the choice of product slate can be shown to be of greater practical importance to the “go – no go” decision for the proposed biofuel facility. Four scenarios had probabilities of loss lower than 10%, and the fifth-best scenario’s POL was 39.6%. These four scenarios included two pioneer plants and two nth plants, but all four of them had “max diesel” product slates. According to our analysis, then, a greenfield CH biofuels facility using a vegetable oil feedstock that is priced equivalently to soybean oil is a favorable investment under current policy only if it maximizes its output of renewable diesel fuel at the expense of renewable jet fuel.

DISCUSSION

Conclusions

Our results show that aviation biofuels production at a greenfield CH plant fed by pennycress seed oil is not economic under current market and policy conditions. Our breakeven metrics for a renewable jet fuel policy incentive, crude oil prices, and the input cost of pennycress oil indicate this could change if one of the following were to occur:

- A crude oil price increase of at least 31-52%
- A jet fuel price increase of at least 11-26%
- A pennycress oil price discount of 2-6% from soybean oil prices
- Some combination of the above

These findings are heavily influenced by current policy design.

Support for the conclusion that the pathway considered would not be economic under current conditions can be drawn from the results for NPVs, POLs, breakeven jet fuel incentives, and crude oil BEPs. Starting with the NPV results, we see in Tables 5.1 and 5.2 that no scenario in which jet fuel was produced resulted in a mean NPV that was significantly higher than zero. Moving to POL, we see that the best-performing scenario for a plant producing both jet fuel and diesel fuel would still be expected to earn less than the stipulated rate of return in 39.6% of all cases. The breakeven jet fuel incentive results contained in Tables 5.3 and 5.4 show that the mean level of policy support needed for a jet-fuel-producing plant was positive in all cases. Finally, the mean crude oil BEP results presented in Tables 5.5 to 5.8 for plants that produced renewable jet fuel are all greater than \$84 per barrel (2017 USD), which would be in the 78th percentile of historical prices from 1987 to 2017, and would imply a diesel fuel price in the 94th percentile of our projections for 2018. At the time of writing, the most recent available data had the composite refiner acquisition cost of crude oil at \$55.73 per barrel in August of 2019 (2017 USD) [171, 173].

Price Sensitivities

The relative sensitivities of our results to the factors listed above are somewhat counterintuitive. One would not expect for larger price changes to be required for crude oil than for jet fuel, since changes to the crude oil price impact the prices received for all three of the fuel

products that our plant would produce, and since renewable jet fuel makes up only 33-39% of our plant's total output volume. It is similarly surprising that our results would appear to be so much more sensitive to changes in input price than to changes in output price. This is but one example among many of the determinative impacts of policy on the economics of biofuels production, as all of these counterintuitive results can be traced back to the interactions between these prices and the markets for D4 and D5 RINs. In the model of RIN price discovery that we use in this analysis, the gap between the market prices of soybean oil and No. 2 diesel fuel is the driver of the D4 RIN price, which, in turn, drives the price of the D5 RIN. Thus, if the price of diesel fuel rises relative to the price of soybean oil, then RIN prices fall. This mechanism has the effect of buffering our biofuels producer's profitability from changes in the crude oil price, since those changes get passed on to the diesel fuel price, and then (in the opposite direction) to RINs prices. Changes to the price of jet fuel, however, are not assumed to generate countervailing movements in RINs markets, since renewable jet fuel comprises a small fraction of RFS compliance. This explains our finding that a producer of aviation biofuels would be more sensitive to a movement of the jet fuel price than to a movement of the crude oil price, if the jet fuel price movement were independent of the prices of other fossil fuels, especially diesel fuel. Such an "independent" movement of the jet fuel price might arise from the initiative of the large airlines that are responsible for the majority of jet fuel consumption, from a policy support targeted at renewable jet fuel, or from a decrease in the relative demand for road transport fuels resulting from the increased prevalence of electric cars.

Similarly, the aviation biofuels producer modeled here appears to be starkly more sensitive to changes in the input price than changes in the prices of outputs. This is also due to the current functioning of RINs markets, as modeled here. Our analysis considers the case of pennycress seed oil, a novel biofuel feedstock, which we assume would make up a relatively small portion of the total biofuel feedstock market. Based on this assumption, the aforementioned blend gap driving RINs prices would continue to be set by the price of soybean oil, the higher-volume "marginal" input to biofuels production in the US. Decreases in the price of pennycress oil, then, behave similarly to independent movements of the jet fuel price: they do not generate a countervailing movement in RINs values. The ratio between the volume of pennycress oil used by our plant and the volume of renewable jet fuel it produces is roughly 3:1, which accounts for most of the difference we see in sensitivity between the two prices.

As to a 2-6% “discount” for pennycress oil versus soybean oil, our crusher’s perspective pennycress oil output BEP results (See Figure 5.1.) indicate that, in a vacuum, a pennycress oil price that low would make the entire pennycress-fed, CH aviation biofuels pathway economic, as long as the RFS and LCFS continue. By “in a vacuum”, we mean to exclude the possibility that soybean oil biodiesel producers would bid up the market price of pennycress oil to match the price of soybean oil, in which case crushers would earn negative economic profits by selling the oil at a lower price. This “vacuum” might take the form of contracting between pennycress seed crushers and CH aviation biofuels producers, backwards vertical integration from the biofuels producers, or high transaction costs for biodiesel producers, perhaps due to a thin market for pennycress in the early stages of commercialization. Alternatively, a market price gap between pennycress oil and soybean oil might result from seasonal price effects, since pennycress harvest precedes soybean harvest by four to six months, or from the functional properties of the oils, themselves. This could be because of an as-yet unidentified functional deficiency in pennycress oil for the purposes of biodiesel production. A functionality-based price gap could also arise from pennycress oil’s inedible nature if enough of it were produced to significantly shift the aggregate supply of vegetable oil to the biofuels sector. In this case, edible oils such as soybean oil could face a higher effective demand than inedible oils, due to their use in food.

Diesel Fuel vs. Jet Fuel and the BTC

The BTC plays a significant role in the financial viability of the plant modeled here. The only scenarios to exhibit positive mean NPVs assumed that the operation of the BTC continued to reflect its recent behavior throughout the life of the plant. If we examine results for otherwise-equivalent pairs of “BTC” and “NO BTC” scenarios in Tables 5.1 and 5.2, we can see that the BTC’s continuation adds roughly \$41 million to the mean NPV of “Jet and Diesel” scenarios and roughly \$89 million to the NPVs of “Max Diesel” scenarios (2017 USD). A similar comparison of the POLs in Table 5.11 shows that the continuation of the BTC reduces the probability of earning less than the stipulated rate of return by roughly 20-40 percentage points for plants that produce renewable jet fuel and by 50-70 percentage points for “max diesel” plant configurations. This is noteworthy, since the presence of the RFS has called into question the usefulness of the BTC as a policy measure [29]. While the BTC might be a source of unnecessary windfall profits for fatty acid methyl esters (FAME) biodiesel producers [29], it appears important to the financial

health of producers of high-quality “drop-in” biofuels via the CH process modeled here, or via any such process that has relatively higher production costs than would a FAME process.

Finally, we can observe that if our model facility maximizes its output of renewable diesel fuel at the expense of renewable jet fuel, it performs markedly better. Most of this effect is due to renewable diesel’s qualifying for the BTC, whereas renewable jet fuel does not. Compare the mean NPVs in Tables 5.1 and 5.2 for otherwise-identical “Max Diesel” and “Jet and Diesel” scenarios that include the BTC. They reveal that maximizing renewable diesel production at the expense of renewable jet fuel production was worth about \$77 million (2017 USD) of mean NPV in such cases. To isolate the portion of that value that results from fossil diesel fuel’s higher market price, we can compare the mean NPVs for matched pairs of “NO BTC” scenarios in those same tables. The results indicate that, without the BTC, maximizing renewable diesel output added roughly \$28 million to mean NPV (2017 USD). This points to roughly \$49 million (2017 USD) of NPV that renewable jet fuel-producing plants would surrender, on average, due solely to the fact that jet fuel does not qualify for the benefits of the BTC. Even so, “leveling the playing field” between middle distillate fuels, in terms of policy, would still leave an average value of \$28 million (2017 USD) that biofuels plants would forfeit by choosing to produce renewable jet fuel. Both the policy environment and historic market conditions stack the deck in favor of maximizing renewable diesel output.

Evaluating Hypotheses

Our first hypothesis stated that production of aviation biofuels from pennycress seed oil at a greenfield CH facility would not be economically viable at projected prices, even with policy supports such as the RFS and LCFS in place. Our results support this hypothesis. No scenario involving the production of renewable jet fuel from pennycress oil resulted in a mean NPV that was statistically different from zero.

Our second hypothesis stated that the biodiesel BTC would have no significant impact on the economic viability of the modeled plant, now that policies such as the RFS and LCFS are in effect. Our results do not support this hypothesis. Only those scenarios in which the NPV continued throughout the life of the plant were projected to perform favorably, and the status of the BTC proved to be the single most important of our four scenario variables, as demonstrated in Table 5.11 and the following discussion.

Contributions of this Study

The literature contains only one TEA of aviation biofuels production via the CH process, a study by Elspeth McGarvey and Dr. Wally Tyner published in *Biofuels, Bioproducts, and Biorefining* in 2018 [2]. That paper, therefore, provides the most useful point of comparison for our study. Nevertheless, there is still some value in comparing our results to those from studies of other closely related hydroprocessed renewable jet fuel (HRJ) pathways, such as those that rely on the already-commercialized HEFA technology. So, we will begin with these more distantly-related studies in order to provide some broader context before focusing our attention on direct comparison with McGarvey and Tyner's article.

The literature on using HEFA and similar non-CH technologies to produce aviation biofuels from vegetable oils renders a split decision in regards to these pathways' financial viability. Some conclude that such pathways would be economic [24, 95, 113], while others appear to disagree [21, 25]. Still others find that these pathways are economic, but only if the feedstock price is relatively low, which for our purposes usually means lower than the price of soybean oil [22, 93]. Despite the diversity of these studies' verdicts, they are consistent in demonstrating that the economic feasibility of such pathways depends mightily on the cost of the seed oil feedstock and on the level of policy support received. Our study has contributions to make in our approach to both of these factors.

Among the literature's relevant TEAs, three classes of feedstock are considered: used cooking oil (UCO) [22, 25], soybean oil [21, 24, 113], and seed oil from novel oilseed crops, such as *Brassica carinata* [22] and *Camelina sativa* [22, 93, 95]. The studies that use UCO or soybean oil as feedstocks model their costs based on real price data. Modeling the costs of oil from novel oilseed crops is more difficult, as price data for these oils do not yet exist. Such is the case for pennycress oil. TEAs using a novel oilseed crop as a feedstock follow two approaches for modeling the price of seed oil: they either use a BEP or minimum selling price (MSP) based on production, processing, and transportation costs [22, 93], or they use the prices of other commodity oils as proxies [55].

Our study bridges the gap between these two approaches by comparing a breakeven cost of pennycress oil from the perspective of the biofuels producer to a breakeven selling price of pennycress oil from the perspective of the seed processor, with both of them measured as a percent of the projected soybean oil price. Like the simple MSP approach, this method explores whether

each step of the value chain has enough operating margin to cover its costs, but it does so in a way that allows explicit comparison to the proxy-based approach. So, we can estimate where the crossover point between profitability and unprofitability is located along the spectrum between the “lowball” MSP assumption and the “highball” soybean oil-as-proxy assumption. In the case of pennycress oil, that crossover point appears to be no more than 6 percentage points away from the unprofitable case of using the soybean oil price as a proxy. This finding may pave the way for future inquiries into the potential pricing of pennycress and similar crops.

Of the TEAs we reviewed that analyze the use of vegetable oil feedstocks and not-CH-but-similar conversion technologies to produce aviation biofuels, only three explicitly model the value of RIN credits under the RFS, and none of them include the value of LCFS credits [22, 24, 113]. All of the studies that include a RIN credit recognize the highly-variable nature of RINs prices, and typically account for that variability by defining a distribution of possible RINs prices based on historical data. Even so, these approaches clearly leave room for improvement. Only Bann et al. (2017) distinguish between D4 RINs earned by jet and diesel fuel analogs and the D5 RINs earned by renewable naphtha products [24], and only Blazy et al. (2016) appear to explicitly account for the correlations between the prices of RINs and their other inputs and outputs [113]. Our study improves on these approaches in two ways. First, we include LCFS credit prices, which we model based on the statutory price cap and recent historical data. Second, this study is the first to apply the theory that RINs prices follow the gap between FAME biodiesel unit costs and the unit prices of fossil diesel fuel. Though this theory is still unproven, it is backed by clear economic reasoning [31] and an impressive correspondence between its price predictions and real price data [32]. Relying on this model, RINs prices would be expected to vary systematically based on the gap between the (proxy) price of our key input, pennycress oil, and the prices of our fuel product outputs (indexed by diesel fuel prices). If this is how RINs prices truly behave, then modeling them this way has important ramifications for biofuels TEAs. Comparing our study to that of McGarvey and Tyner (2018) highlights this fact.

McGarvey and Tyner (2018) conduct stochastic TEAs of CH pathways converting one of three feedstocks (brown grease, yellow grease, or *B. carinata* oil) to renewable diesel, renewable jet, and renewable naphtha. They examine four scenarios for each feedstock, consisting of pioneer or ⁿth plants on either greenfield or brownfield sites [2]. The *B. carinata* case offers the most direct comparison to this analysis. There are many similarities between the two studies, as we rely on

McGarvey and Tyner (2018) for the learning curves we use for cost reductions in our n^{th} plant scenarios, we both use the price of soybean oil as a proxy for our feedstock cost, and we share many of the same financial assumptions. We differ in a number of modeling choices, in our exclusion of a generalized brownfield scenario, in our use of updated CH process technical parameters, and in our previously-discussed exploration of feedstock BEPs and what they can tell us. However, the most instructive comparisons to be drawn between their work and ours have to do with our approaches to RINs price modeling and the overall favorability of our results compared to theirs.

Whereas McGarvey and Tyner (2018) model RINs deterministically, using a single per-gallon dollar value for every period of their model, we use a dynamic model, resulting in RINs values that move in each period to more closely match the magnitude of the biggest shortfall facing a biofuels facility that uses vegetable oil as an input: the gap between its high input price and its low output price. One might expect, then, that our results would be more optimistic than theirs. Indeed, that is precisely what we find. For McGarvey and Tyner's greenfield *B. carinata* cases, only n^{th} plants ever stand any chance at all of having positive NPVs, and even then, the chances of losing money are greater than 90% [2]. In our study, six out of our eight scenarios that included production of renewable jet fuel performed significantly better, with probabilities of loss (POLs) less than 80%. Two of these had POLs less than 50% and positive mean NPVs (see Tables 4.1, 4.2, and 4.11). This difference in projected outcomes appears even starker when we take into account that our updated plant parameters included an 80% increase in the total capital investment for a plant of the same output capacity. That amounts to a difference of over \$100 million (2017 USD). Adding a credit that large to the NPV results in Tables 5.1 and 5.2 would be sufficient to make even the most pessimistic of our scenarios yield a positive mean NPV. Unfortunately, there are too many other differences between our analyses to isolate the role played here by our dynamic RINs modeling, but the magnitude of the difference in outcomes is certainly suggestive.

Practical Implications

This analysis shows that, even with other policies such as the RFS and LCFS in place, the biodiesel BTC remains an important factor for the economics of producing drop-in biofuels at greenfield sites. This may be because low-cost FAME biodiesel technology currently “sets the curve” when it comes to the values of D4 and D5 RINs. That is certainly how we model those

prices here, and if we are right to do so, then that presents a few practical implications for biofuel producers using CH or other similar technologies. First, it implies that it may be worthwhile for them to join in with the “biodiesel lobby” in their efforts to ensure the BTC’s survival. Second, it highlights the importance of identifying opportunities to market high-quality biofuels at a premium over their lower-quality analogs. The RFS doesn’t distinguish between FAME biodiesel and high-quality renewable diesel from CH or HEFA processes, even though the latter may be used at much higher percentages in final fuel blends [6]. The RVOs mandated by the RFS would need to be substantially higher than their current levels for that difference to become significant for compliance purposes. The 2018 biodiesel RVO, for example, was set at 2.1 billion gallons [105], which equated to roughly 3.5% of total sales of ultra-low-sulfur diesel fuel in that year [177]. Even so, some buyers may be interested in a fuel blend that contains a higher proportion of biofuels, and these buyers may be willing to pay a premium for higher quality products.

Our study indicates that, even if a pathway like the one modeled here were financially viable, a rational, profit-maximizing biofuels producer would probably choose not to produce any significant amount of renewable jet fuel. This may be the most significant hurdle to the commercial production of aviation biofuels, regardless of crude oil prices, feedstock prices, or policy: likely due at least in part to large airlines’ buying power in the market for jet fuel, the price of diesel fuel is consistently higher than the price of kerosene-type jet fuel [172, 174]. Further, they are chemically similar enough that production processes like CH allow for jet production to be foregone in favor of diesel production. Producing renewable jet fuel instead of renewable diesel fuel results in losing money. Unless the stable, long-running price relationship between these two fuels [172, 174] is disrupted by developments like the growing electrification of ground-based transport, only an actor with a firm vested interest in producing renewable jet fuel would be likely to do so.

This leaves those who have such a vested interest in using renewable jet fuel with three options for encouraging its production. They can push for additional policy incentives that specifically target aviation biofuels, perhaps along the lines of the biodiesel BTC, they can contract to buy renewable jet fuel from a biofuels producer at a significant premium over fossil jet fuel, or they can integrate backwards into biofuels production, and perhaps all the way to feedstock processing or growing. Our results support the idea that each step of such a vertically-integrated system could generate sufficient margin to pay its costs, thus showing an accounting profit, but

the system's economic profits would likely be negative as a result of foregoing one or more higher-value opportunities along the way.

Limitations

For all of our analysis, we rely heavily on the assumption that current and historical market behavior continues to be typical for the 23-year project life. The future is unpredictable, and so this assumption could lead us to conclusions that do not represent the reality of future events. For our stochastic price projections, we assume that the autocorrelations and real growth rates within each series and the correlations between series observed in the sample period remain constant for the 23-year project life. This implies two limitations to our research. First, if any of these observed characteristics were to undergo significant change in the next 23 years, then our projections would no longer reflect the behaviors of the real prices. Second, 2017 is the last year in which our model uses historical price data, which means that we rely on projected prices starting in 2018. Since real prices for crude oil and soybean oil in 2018 and 2019 have been on the low end of their historical ranges, our projections based on those historical ranges tend to “overshoot” those prices. This fact negatively impacts the usefulness of our crude oil BEP results, which are based on projections of the soybean oil price that are somewhat higher than current market prices for soybean oil. Comparing our crude oil BEP results to either the historical distribution of real crude oil prices or to the distribution of our projections of the crude oil price in 2018 is likely to be more instructive than a naïve comparison to current market prices.

The model of D4 RINs pricing we rely on for our projections is intuitively appealing, and appears to perform reasonably well, but it has not yet been rigorously proven. It is possible that RINs markets do not, in fact, function the way we assume that they do. This would undermine the validity of our results. Even if our model of RINs pricing does reflect the real operations of those markets, we make further assumptions that also must hold for our results to be reliable, namely, that soybean oil FAME biodiesel continues to act as the marginal gallon in the D4 and D5 “buckets” of the RFS and that the ratios of those RVOs to US biodiesel production capacity remains steady. If either of these fails to hold for the life of the project considered, our estimates of RINs prices may no longer reflect reality.

Our identification of DDGS as a proxy for pennycress seed meal prices is based on shadow prices drawn from a linear program, and not from real market data. This could hardly be avoided,

as there is no real market data for the price of pennycress seed meal. Even so, this approach at modeling the potential demand for this product is limited by several things which we do not take into account, such as international trade or general equilibrium effects of pennycress meal production. The fact that our pennycress meal shadow prices are mechanistically determined by the system of given prices in our model may also introduce issues with endogeneity that would call into question our use of OLS to identify DDGS as a predictor of pennycress prices. A more robust approach might have been able to avoid these issues, but would have been beyond the scope of this study.

Another important limitation of our analysis is that we assume that pennycress seed oil would be priced as a perfect substitute for soybean oil. This assumption might or might not be representative of how pennycress oil would actually be priced; it relies on an assumption that the market for pennycress oil as a biofuel feedstock would be reasonably competitive, and that pennycress supply would not be so large as to begin to significantly shift the supply-demand balance in the market for biofuels feedstocks. Further, by making this market-based assumption about the pricing of pennycress seed oil, we are explicitly not considering the case of a vertically-integrated system. Such a system could perhaps cover its costs while producing aviation biofuels under current conditions, and thus run an “accounting profit”, and investing in such a system might be a valid decision for reasons related to corporate social responsibility, public relations, or other strategic concerns, regardless of the market value of pennycress oil. It should be noted, however, that a vertically integrated system that undervalues one of its throughputs may show an accounting profit, but it ignores relevant opportunity costs, and thus cannot yield an economic profit. If our base assumption regarding the pricing of pennycress oil is correct, then it would always be more profitable to sell it at the market price than to “buy” it from yourself at a lower-than-market price in order to run an accounting profit on your own biofuels production activities.

Both of the above limitations rest on the fact that we assume that pennycress would be supplied and used in the marketplace in ways that are closely analogous to existing commercial oilseeds like soybeans and canola. In fact, the pennycress supply chain might prove to be quite different. Pennycress meal might be best used for purposes other than animal feed, and pennycress oil might be best used for purposes other than biofuel production. New markets could emerge, like the market for the ethanol byproduct DDGS in the early 2000s. The offseason nature of pennycress compared to soybeans might cause them to be priced and consumed in very different

ways. Existing commercial oilseed crops are the best model we have for how pennycress might behave if produced commercially, but we cannot guarantee that the analogy we rely on between those crops and pennycress will prove reliable.

Policy is inherently unpredictable, yet in analyses such as ours, it is often necessary to make assumption about the futures of relevant policies, and we certainly do so here. We assume that both the RFS and the LCFS continue for the life of the investment. Further, we assume that the current balance between the levels of those mandates and the relevant production capacities (whether production of biofuels in the case of the RFS or “production” of carbon reductions in the case of the LCFS) remains stable at current levels through the life of the plant. These two policies play a central role in our analysis, and so any change in either of them would have drastic implications for our results.

Finally, it is important to note that we diverge from McGarvey and Tyner (2018) in not considering a “brownfield” case, in which the plant modeled is located on a site which already possesses some industrial infrastructure. Capital requirements would be reduced in such a case compared to the ground-up greenfield case we consider. Estimates of the magnitude of these reductions exist in the literature [25], and they are large enough that they would likely have a significant impact on our results, if applied. However, the actual magnitude of any savings from a brownfield location is highly site-specific, making such generalizations of little practical value, and their impact on a project’s predicted financial performance, though large, is highly predictable. Any savings to the total capital investment necessary for a project simply shift its distribution of expected NPVs to the right by roughly the dollar amount of the savings. Thus, in our view, the fundamental economics are best represented by the greenfield setting, with any deviations from those assumptions handled on a case-by-case basis.

Suggestions for Further Research

Our analysis shows that the economic viability of producing aviation biofuels from pennycress seed oil using CH technology is highly sensitive to the cost of pennycress oil; a 2-6% decrease to our base price assumption is sufficient to radically improve projected financial outcomes. Further, we lean on the work of other researchers to find evidence that such price decreases would not be likely to threaten the financial viability of pennycress production and processing. At this stage, a more thorough, rigorous investigation of the likely market valuation

of inedible oilseed cash cover crops such as pennycress could make an important contribution to our understanding of biofuels pathways like the one modeled here. General equilibrium modeling using a framework like the Global Trade Analysis Project (GTAP) model might serve as a good jumping-off point.

Our analysis also shows that, even if a facility like the one modeled here were economically viable, a rational, profit-maximizing owner of such a facility would choose to forego production of renewable jet fuel in order to maximize output of renewable diesel. This clarifies the options facing actors in the civil aviation industry for using biofuels to reduce their carbon footprints: in the absence of additional policy supports, they may either pay high enough prices for renewable jet fuel to match the price of renewable diesel fuel, plus the expected value of the BTC, or they may integrate backwards into biofuel production. A relevant line of research, then, would compare the costs and benefits of these options with those of other mitigation strategies, such as purchasing carbon offsets or investing in advances in airplane and engine design.

Our analysis is based on an assumption that conversion to liquid transport fuels would represent the “highest and best” use of pennycress seed oil, but this assumption may not be valid. Further research by chemical engineers into potential higher-value co-products is therefore warranted. For example, pennycress oil contains high levels of erucic acid [53], which may have a higher value in other industrial applications than in fuel production [178]. The possibility of isolating some or all of the erucic acid from pennycress oil prior to converting it into biofuels was discussed with ARA engineers, but the details of such a process were not worked out at the time this study was conducted. Further research into biofuel co-products from novel oilseed feedstocks may completely change the picture presented in studies like ours of such pathways’ economic viability.

APPENDIX

Pioneer Plant

BTC continues

Product slate contains both jet and diesel fuel

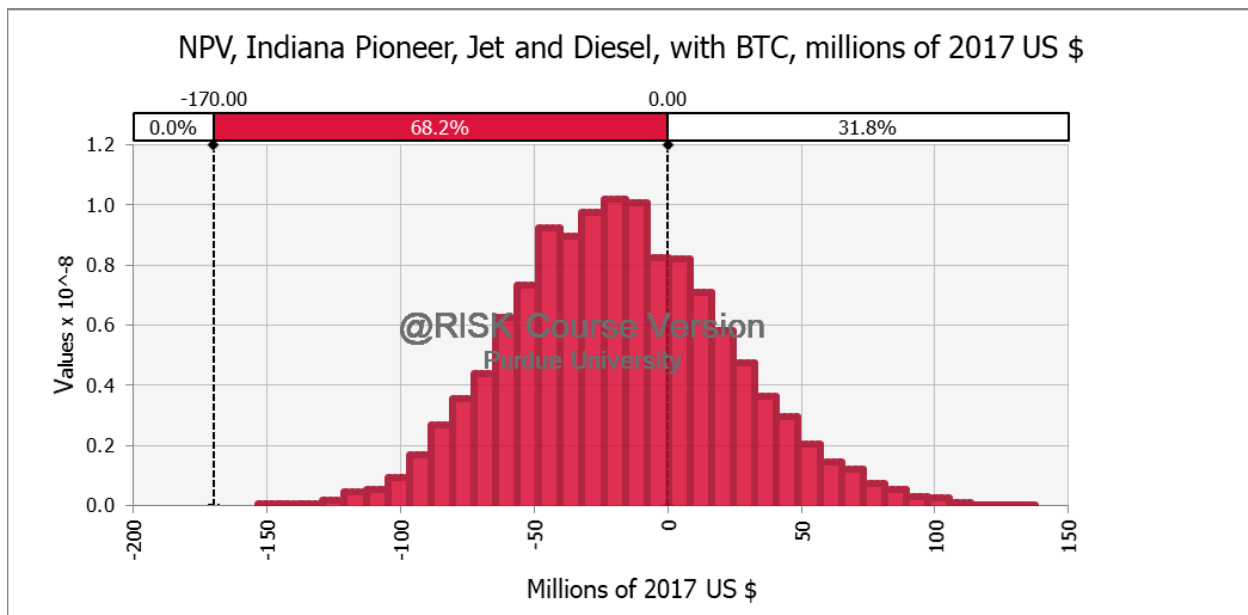


Figure A.1: Distribution of NPVs at pioneer Indiana site with the default product slate and a BTC

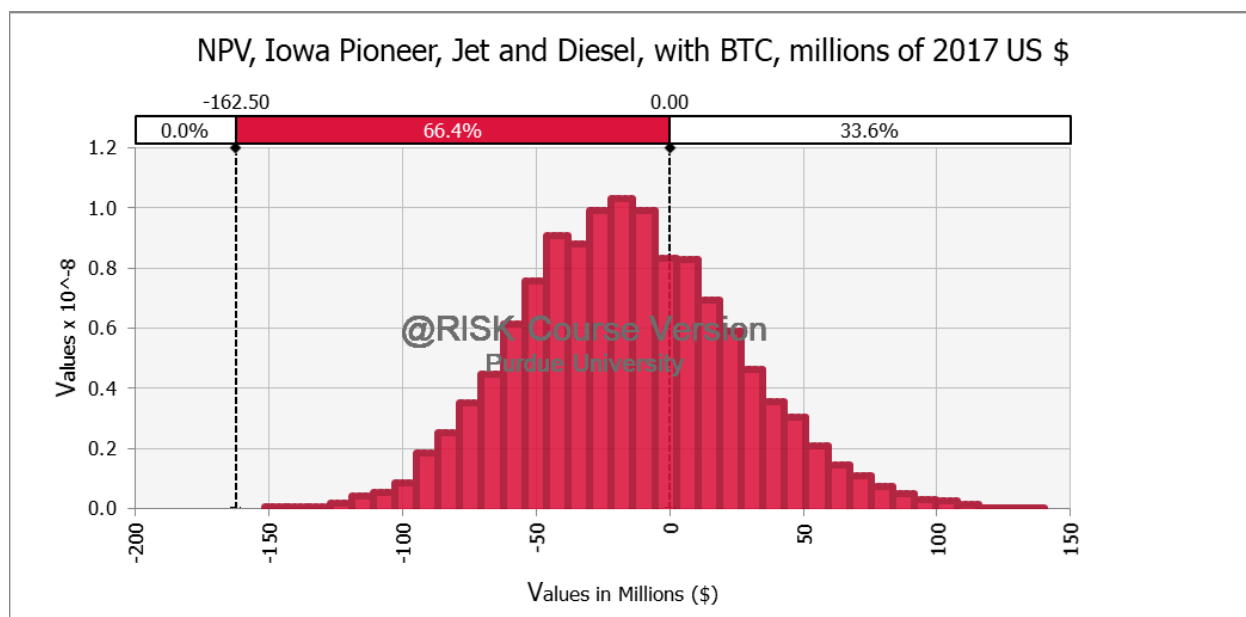


Figure A.2: Distribution of NPVs at pioneer Iowa site with the default product slate and a BTC

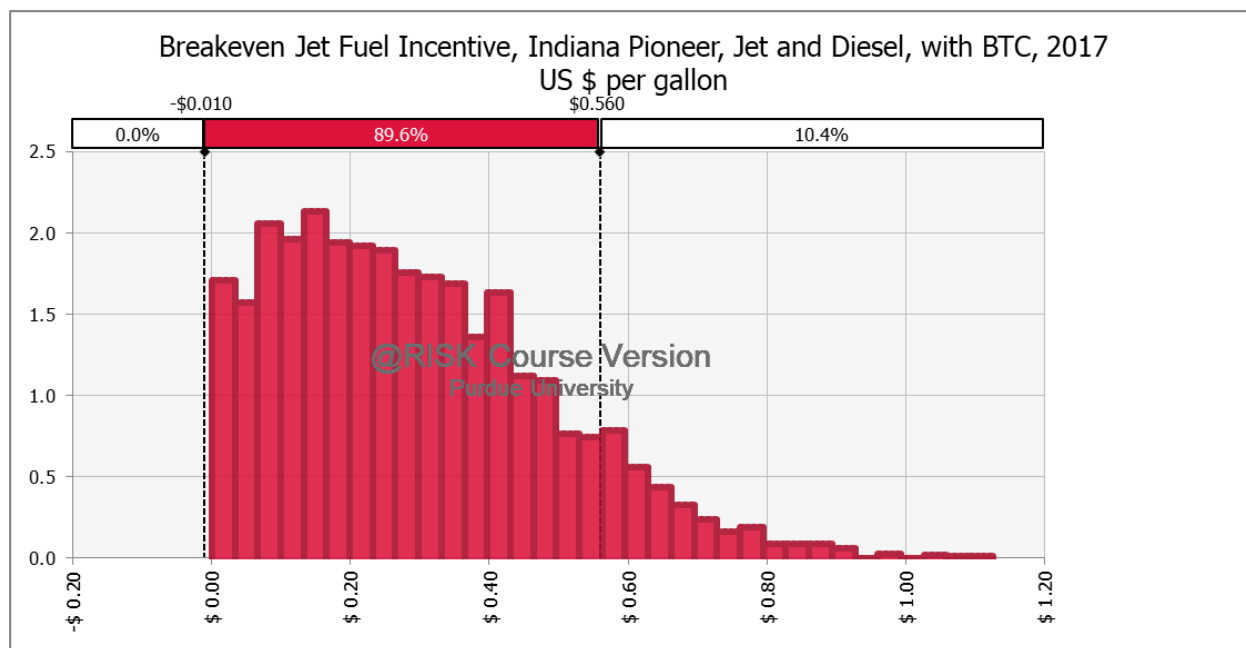


Figure A.3: Distribution of breakeven jet fuel incentives at pioneer Indiana site with the default product slate and a BTC

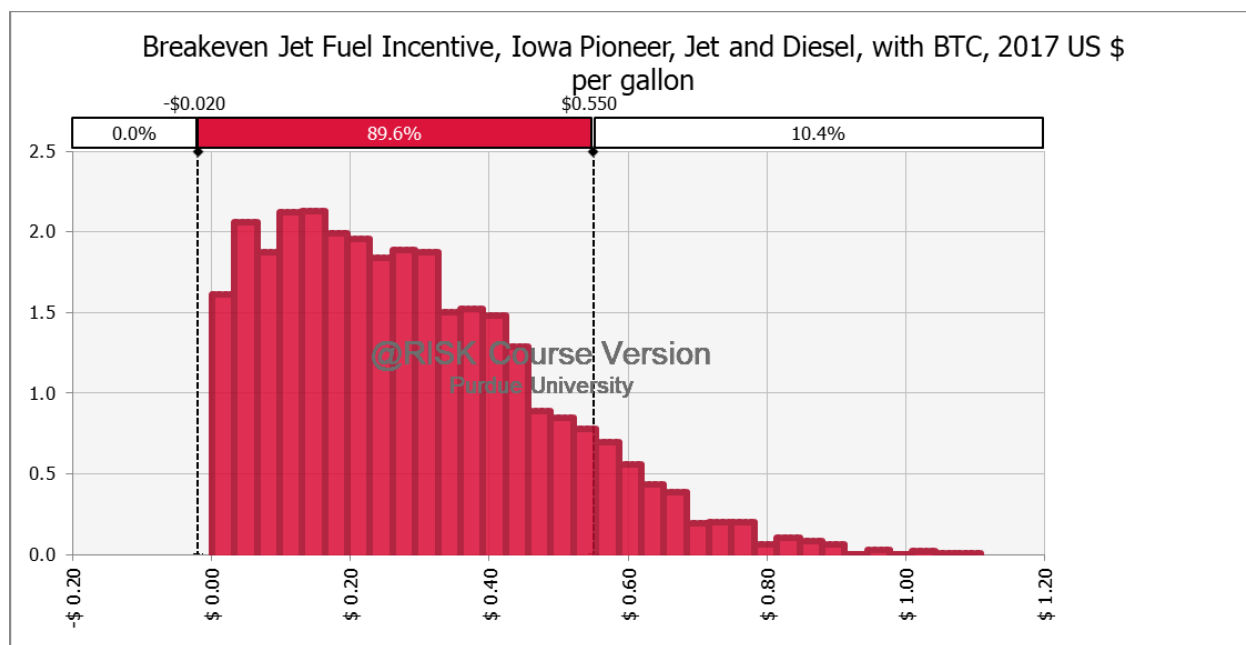


Figure A.4: Distribution of breakeven jet fuel incentives at pioneer Iowa site with the default product slate and a BTC

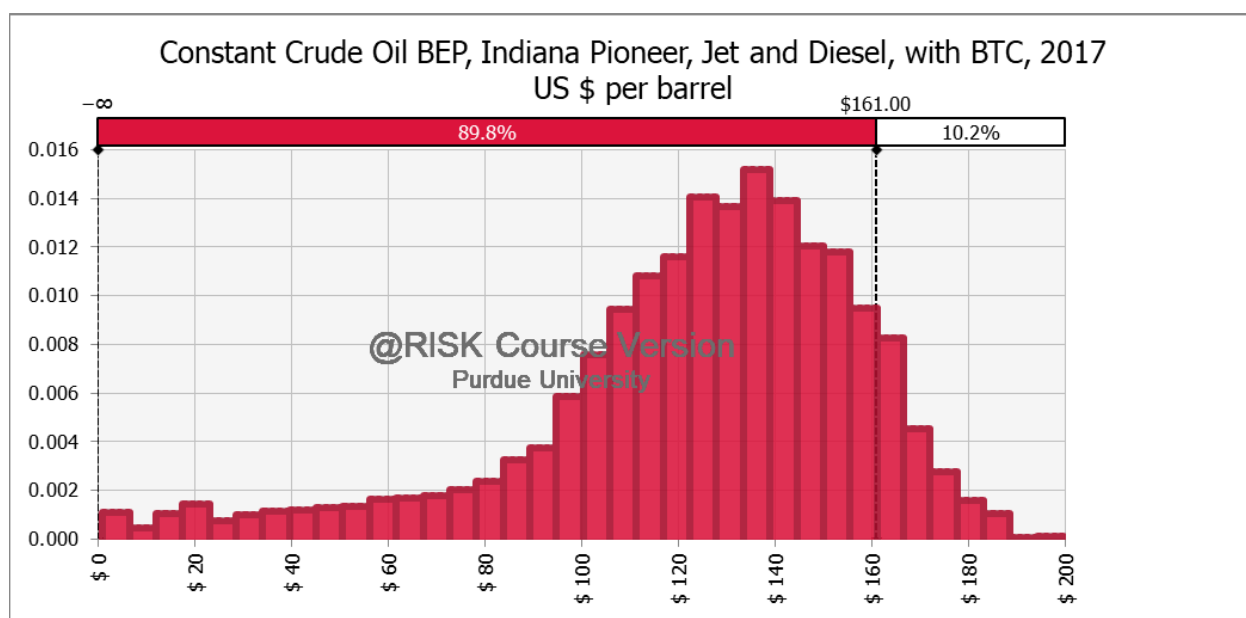


Figure A.5: Distribution of breakeven constant crude oil prices at pioneer Indiana site with the default product slate and a BTC

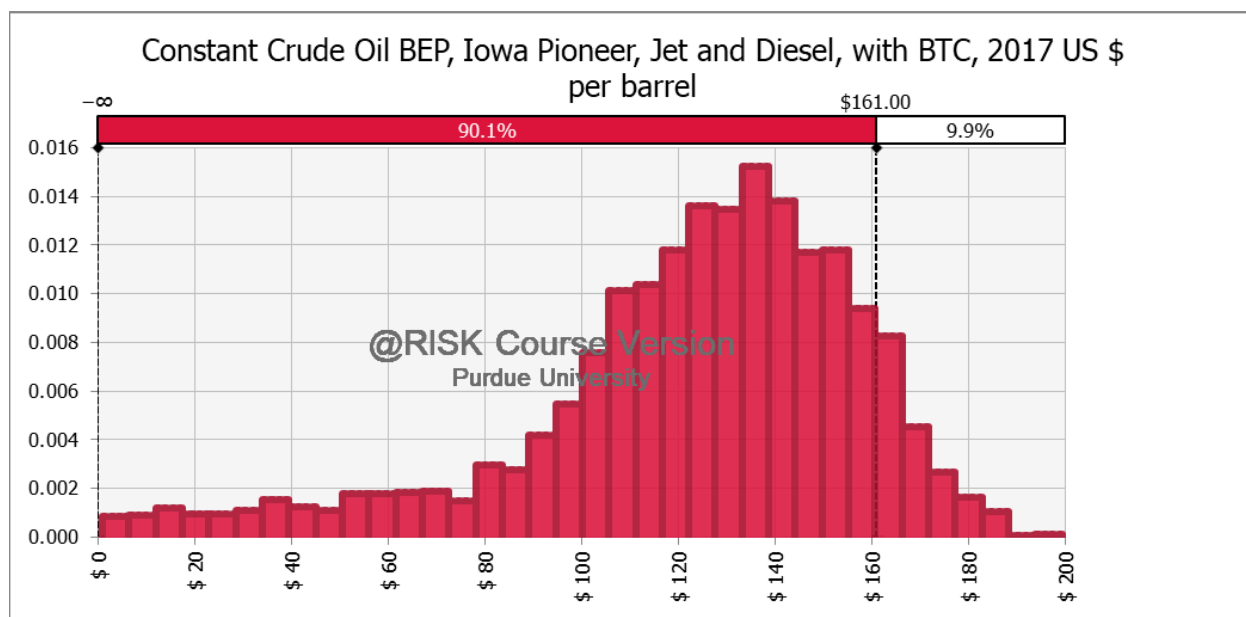


Figure A.6: Distribution of breakeven constant crude oil prices at pioneer Iowa site with the default product slate and a BTC

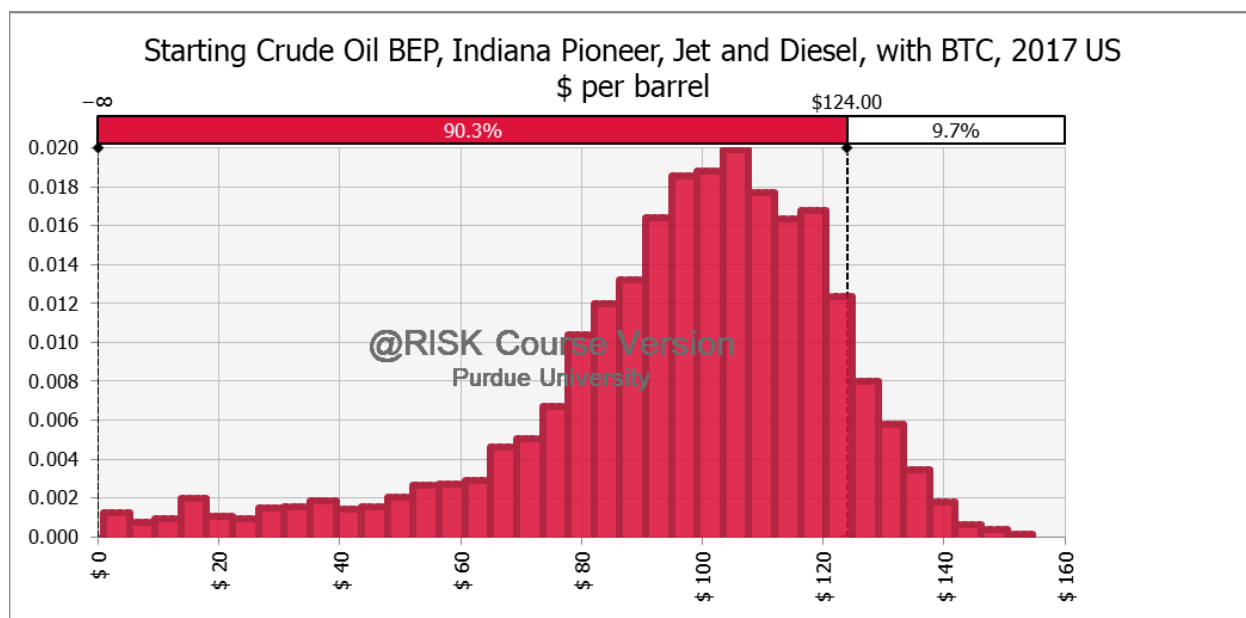


Figure A.7: Distribution of breakeven starting crude oil prices at pioneer Indiana site with 2.25% real annual price growth, the default product slate, and a BTC

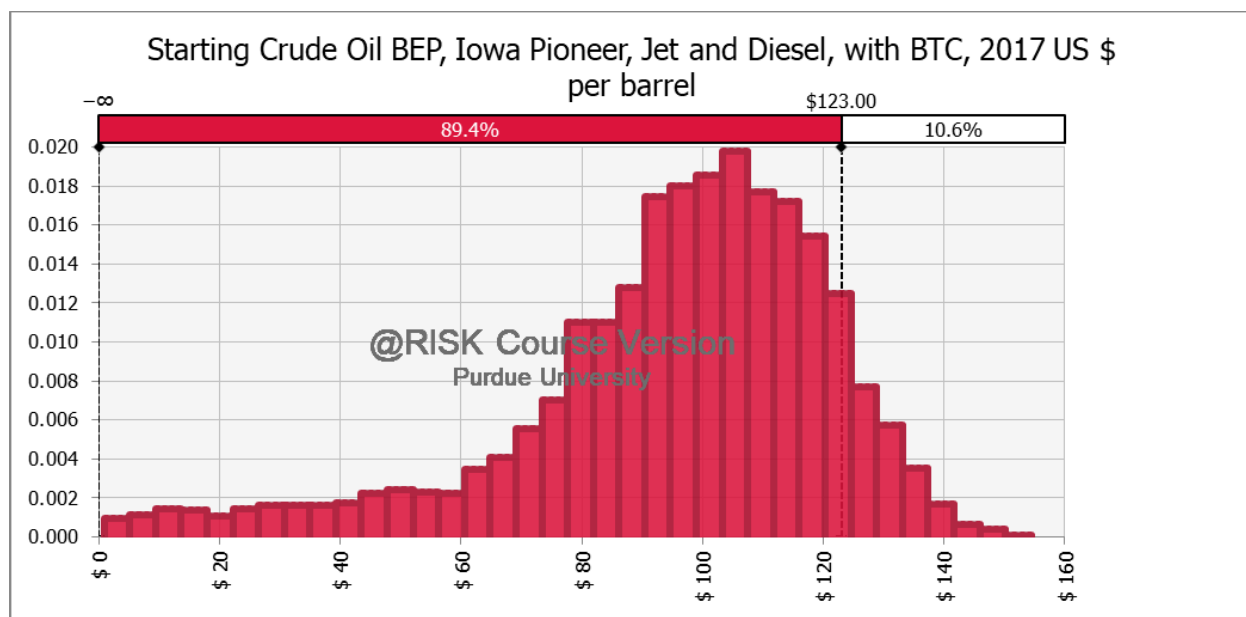


Figure A.8: Distribution of breakeven starting crude oil prices at pioneer Iowa site with 2.25% real annual price growth, the default product slate, and a BTC

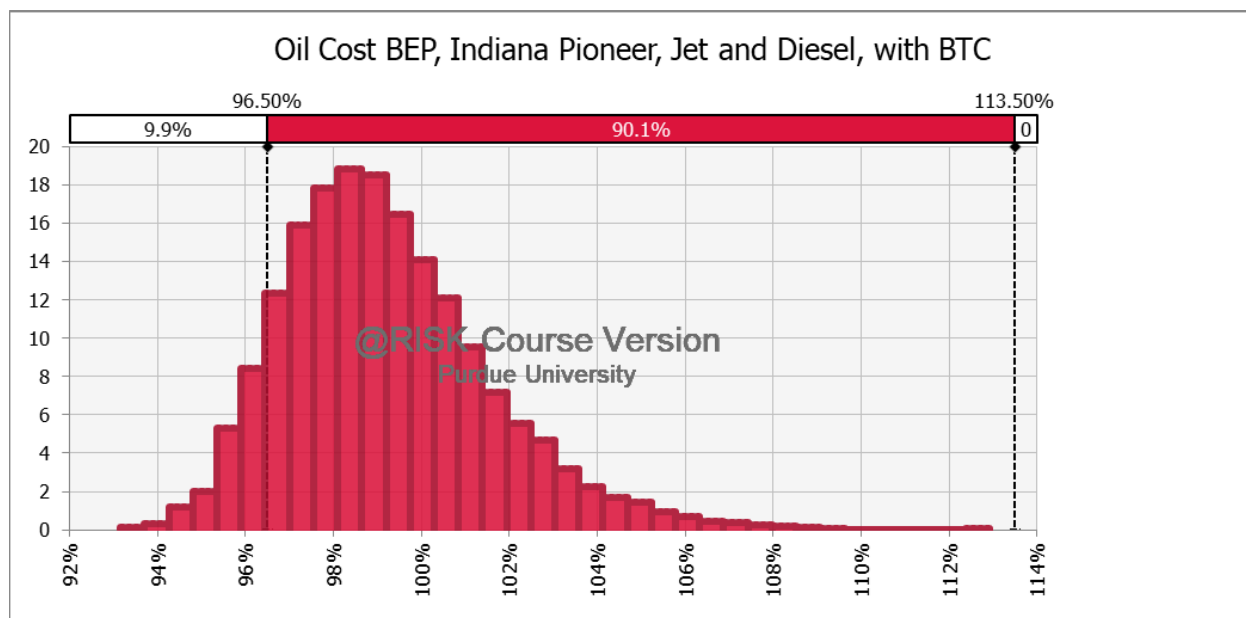


Figure A.9: Distribution of breakeven pennycress oil costs at pioneer Indiana site with the default product slate and a BTC, as a percent of soybean oil prices

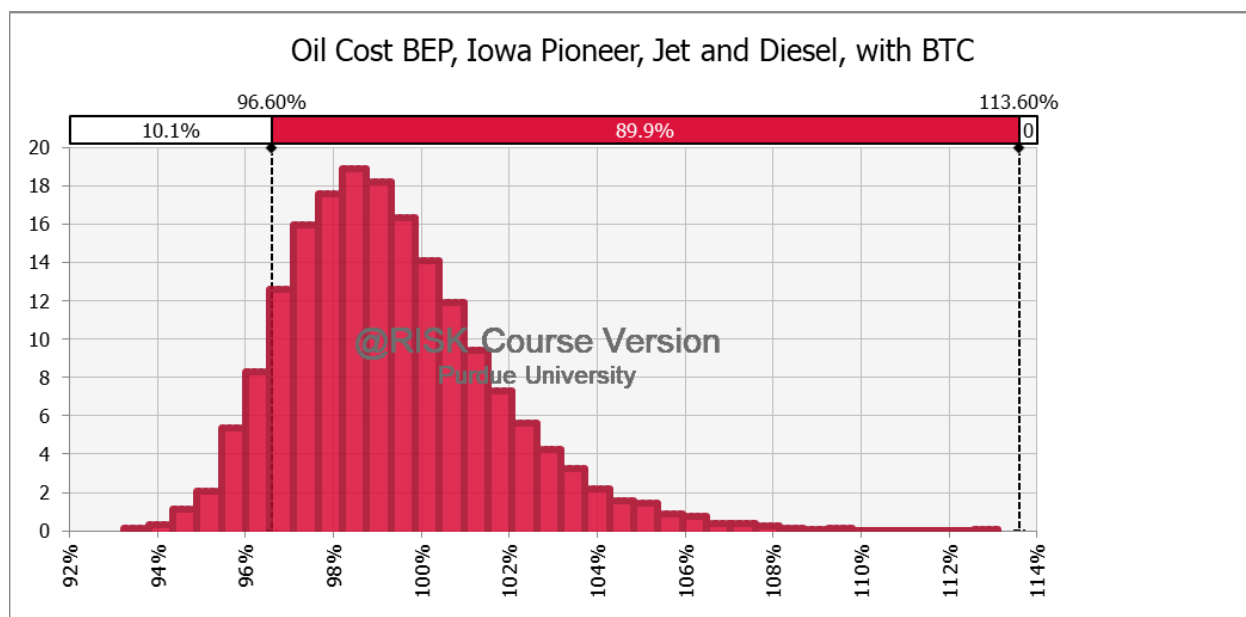


Figure A.10: Distribution of breakeven pennycress oil costs at pioneer Iowa site with the default product slate and a BTC, as a percent of soybean oil prices

Maximum diesel fuel product slate

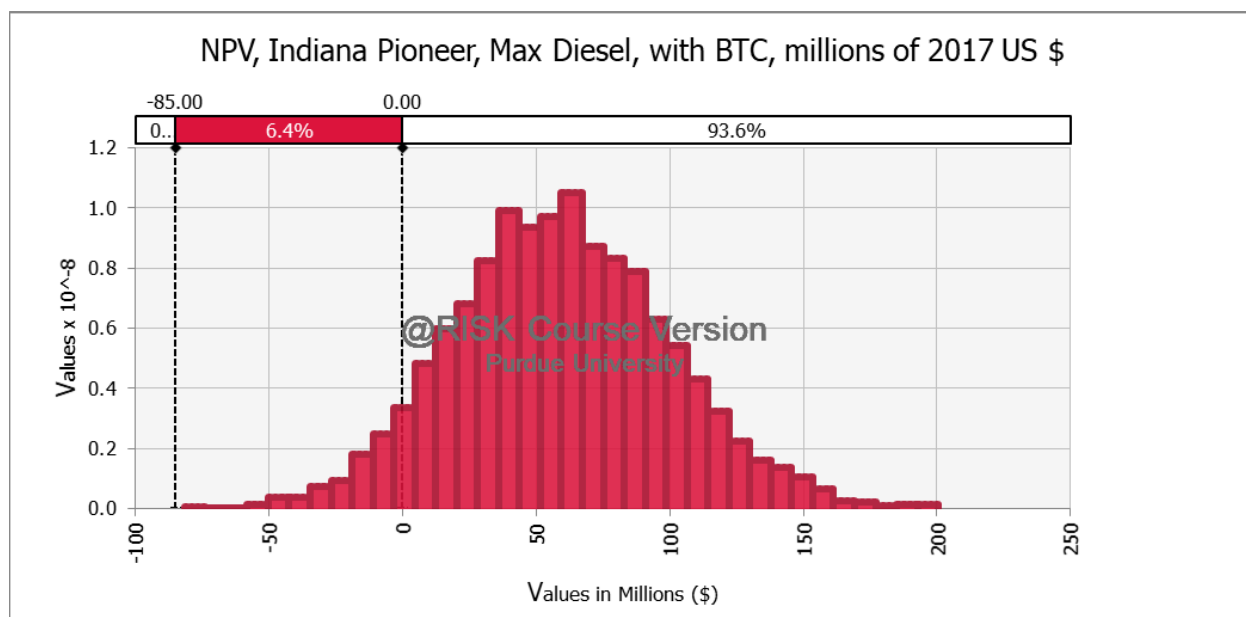


Figure A.11: Distribution of NPVs at pioneer Indiana site with a maximum diesel product slate and a BTC

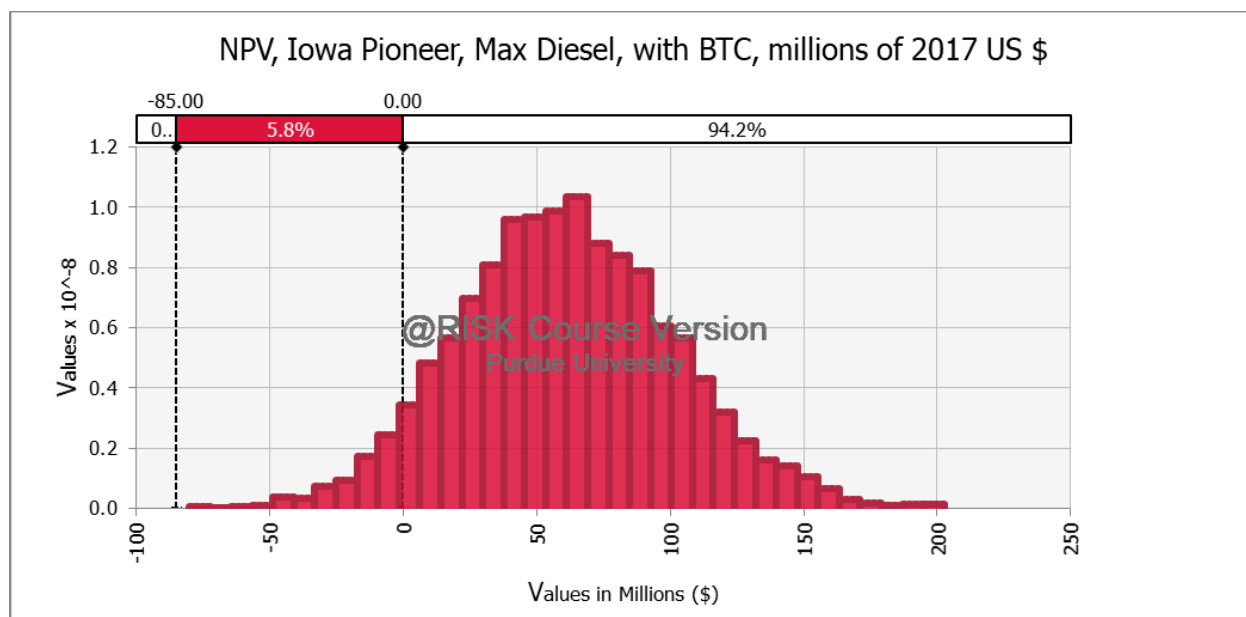


Figure A.12: Distribution of NPVs at pioneer Iowa site with a maximum diesel product slate and a BTC

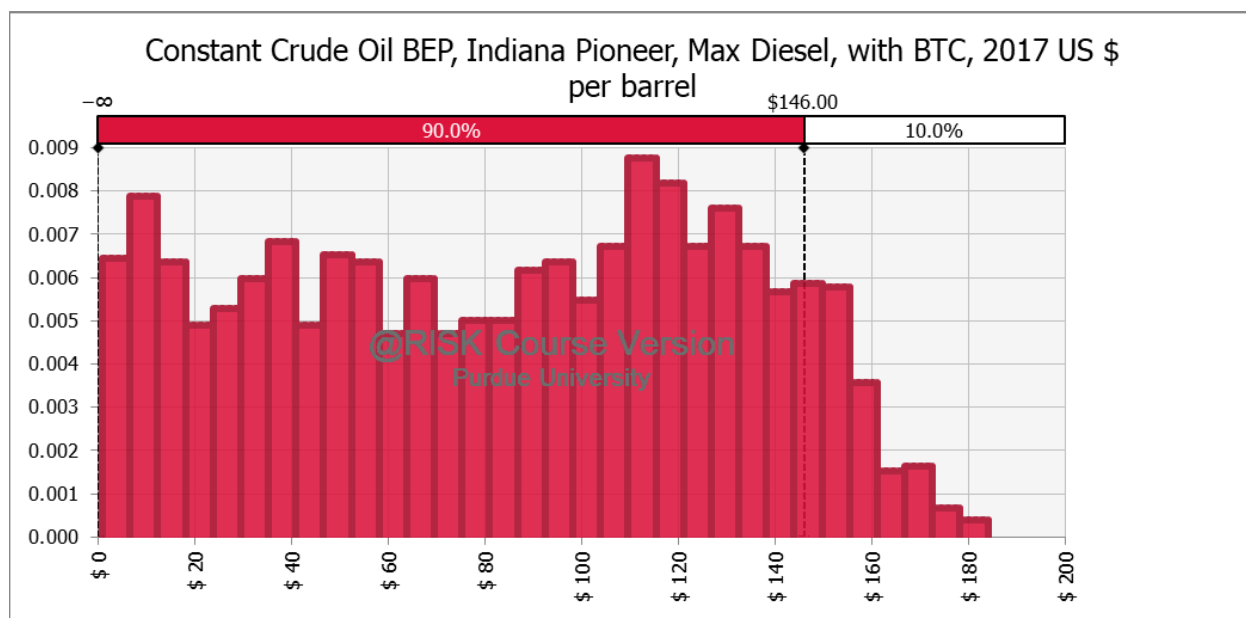


Figure A.13: Distribution of breakeven constant crude oil prices at pioneer Indiana site with a maximum diesel product slate and a BTC

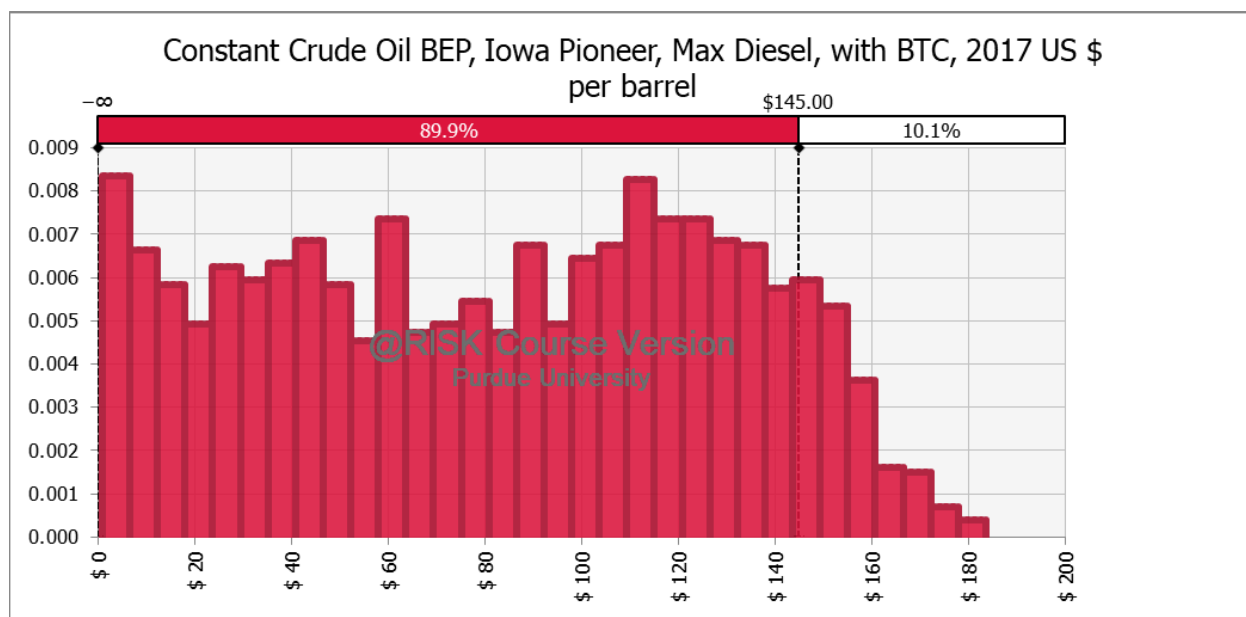


Figure A.14: Distribution of breakeven constant crude oil prices at pioneer Iowa site with a maximum diesel product slate and a BTC

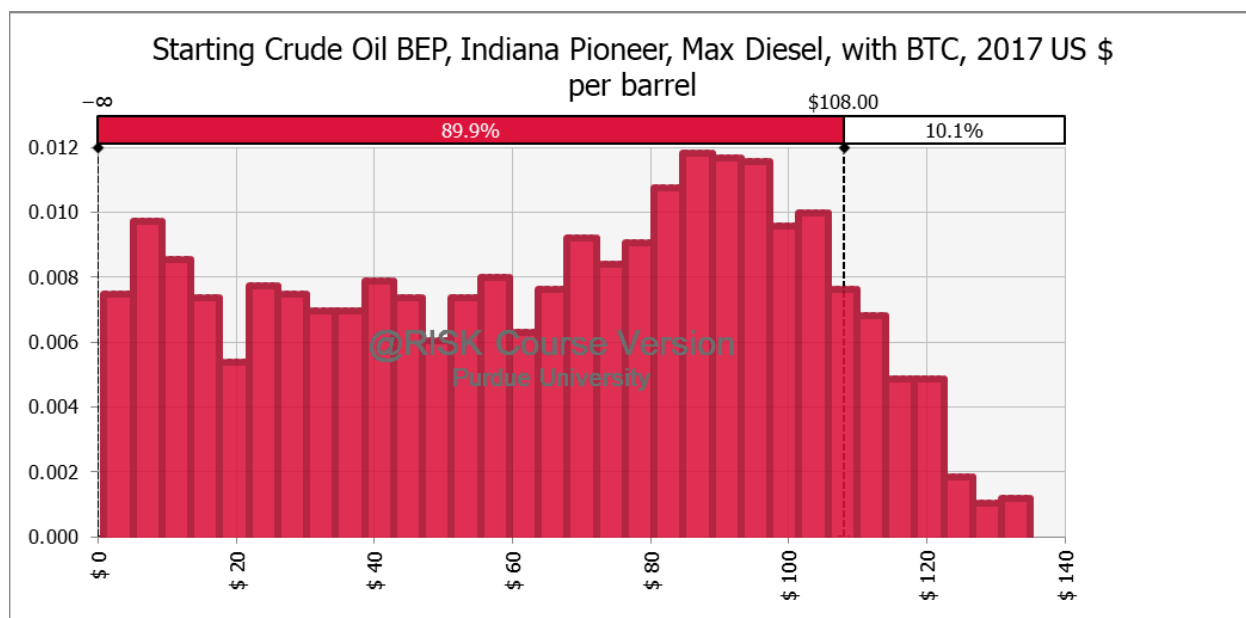


Figure A.15: Distribution of breakeven starting crude oil prices at pioneer Indiana site with 2.25% real annual price growth, a maximum diesel product slate, and a BTC

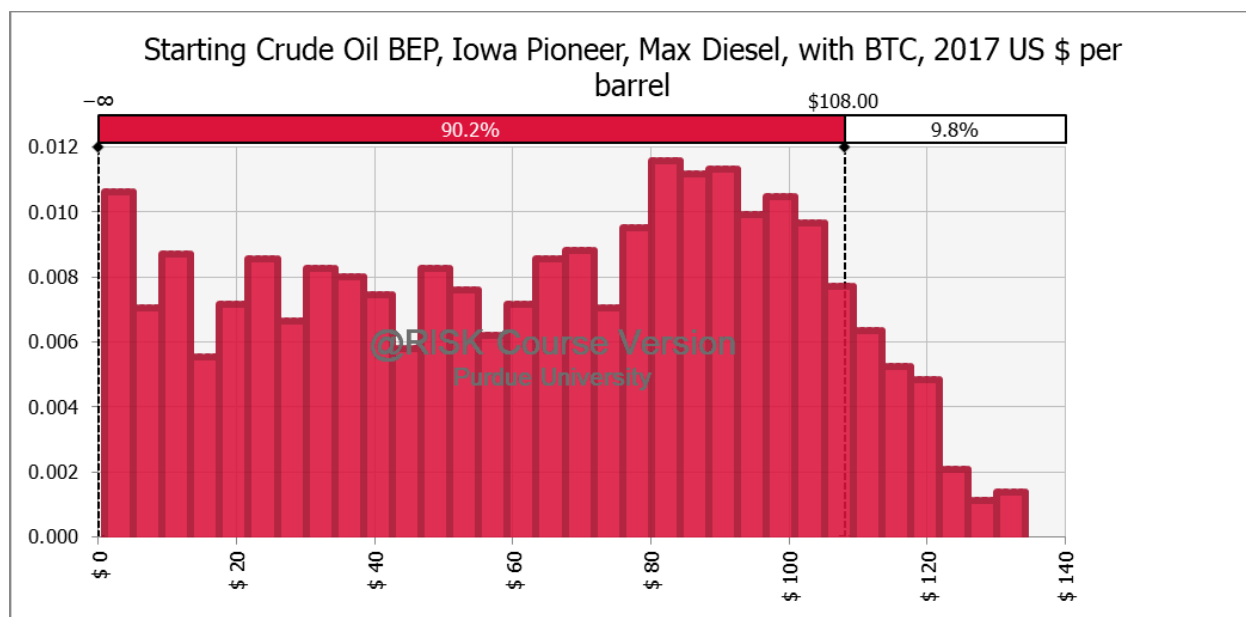


Figure A.16: Distribution of breakeven starting crude oil prices at pioneer Iowa site with 2.25% real annual price growth, a maximum diesel product slate, and a BTC

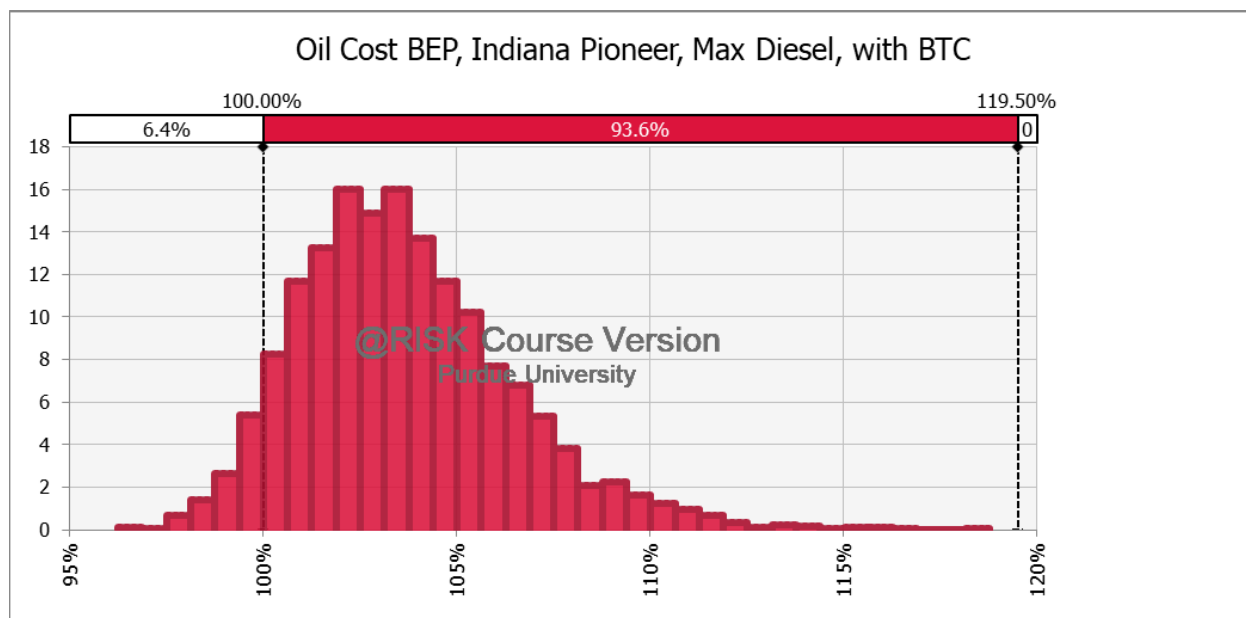


Figure A.17: Distribution of breakeven pennycress oil costs at pioneer Indiana site with a maximum diesel product slate and a BTC, as a percent of soybean oil prices

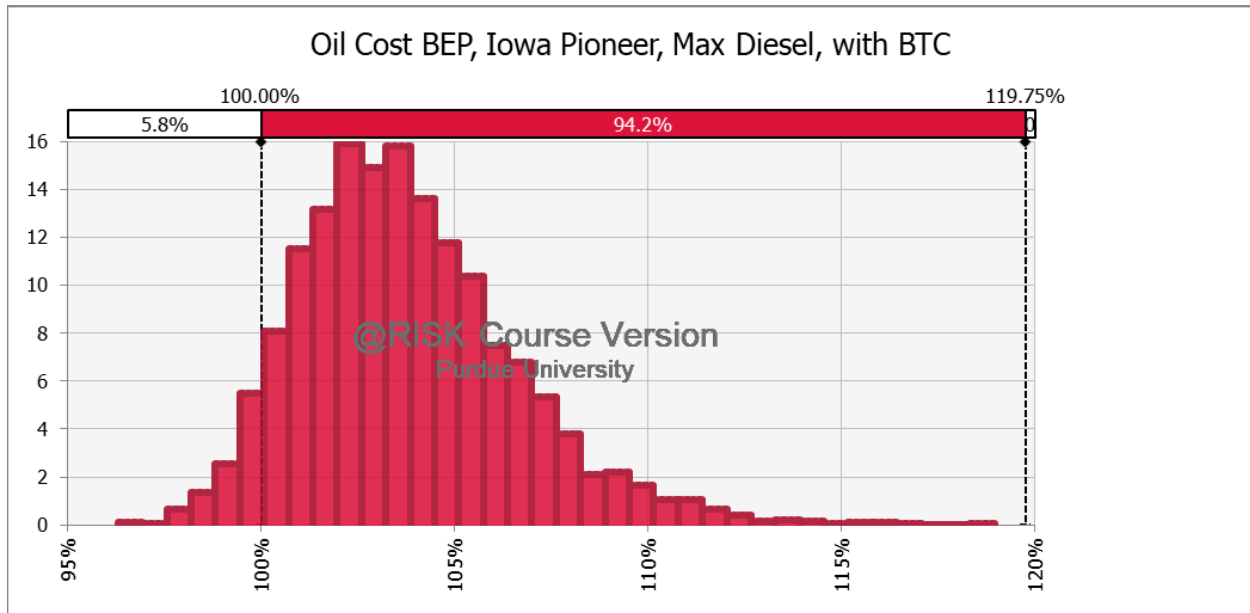


Figure A.18: Distribution of breakeven pennycress oil costs at pioneer Iowa site with a maximum diesel product slate and a BTC, as a percent of soybean oil prices

BTC is discontinued

Product slate contains both jet and diesel fuel

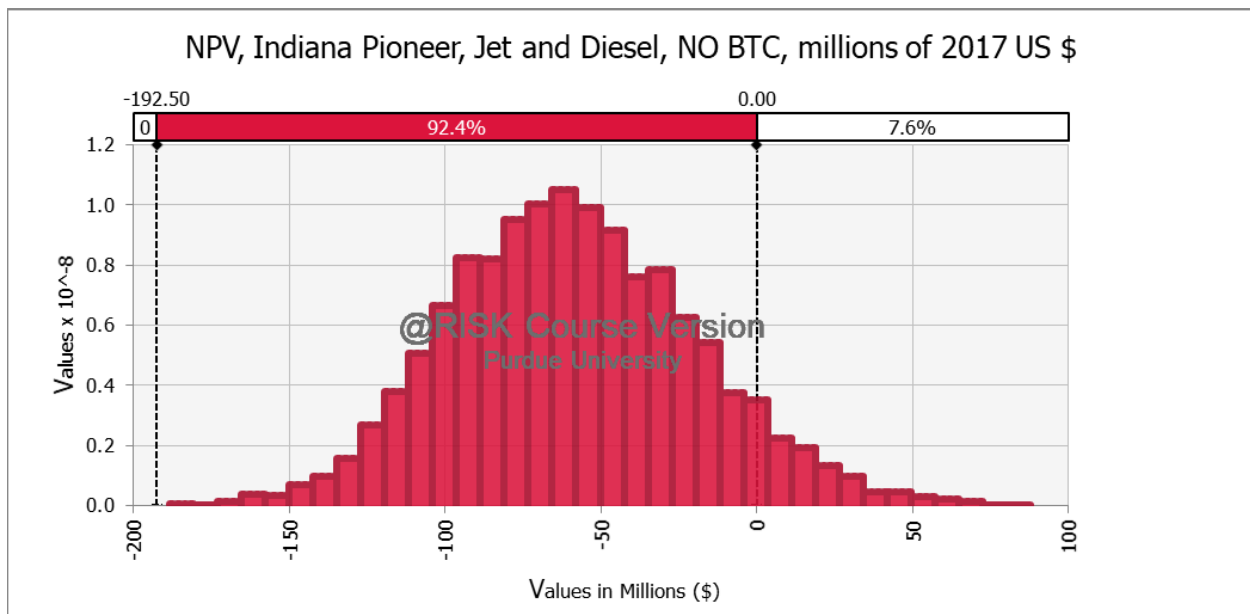


Figure A.19: Distribution of NPVs at pioneer Indiana site with the default product slate and NO BTC

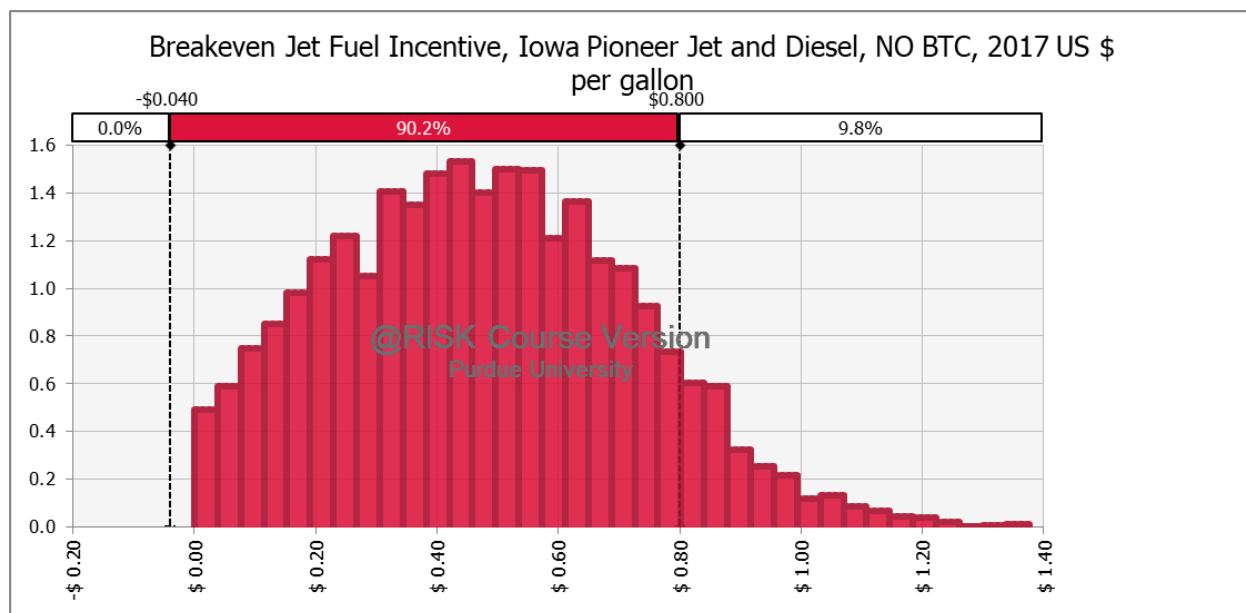


Figure A.22: Distribution of breakeven jet fuel incentives at pioneer Iowa site with the default product slate and NO BTC

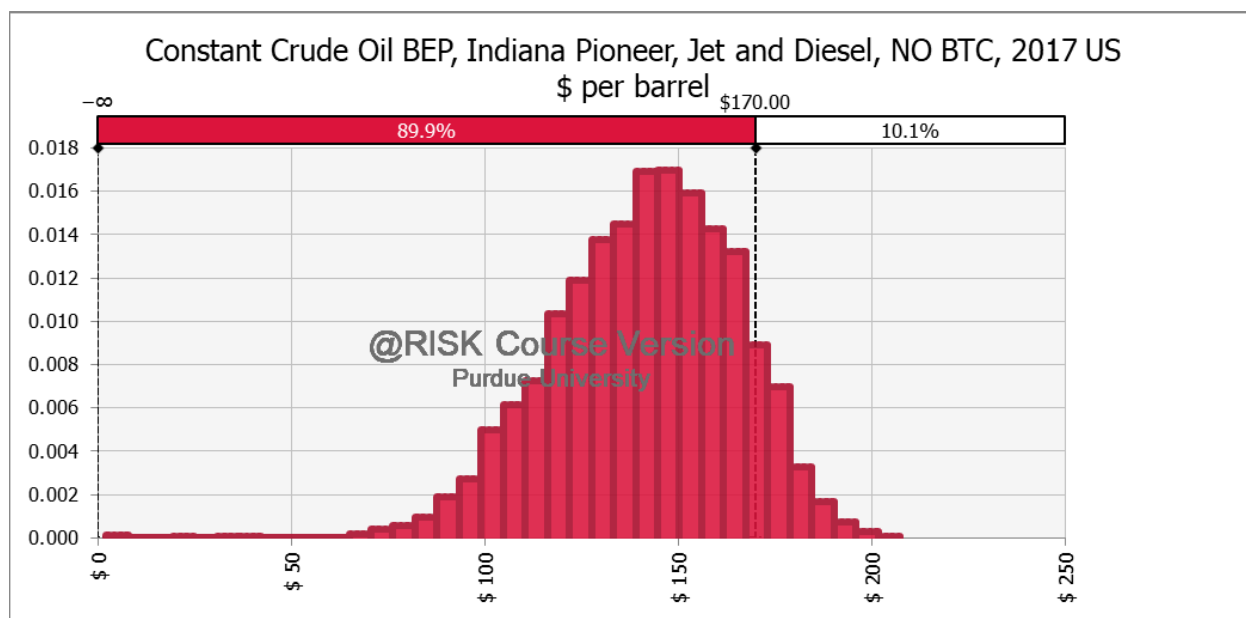


Figure A.23: Distribution of breakeven constant crude oil prices at pioneer Indiana site with the default product slate and NO BTC

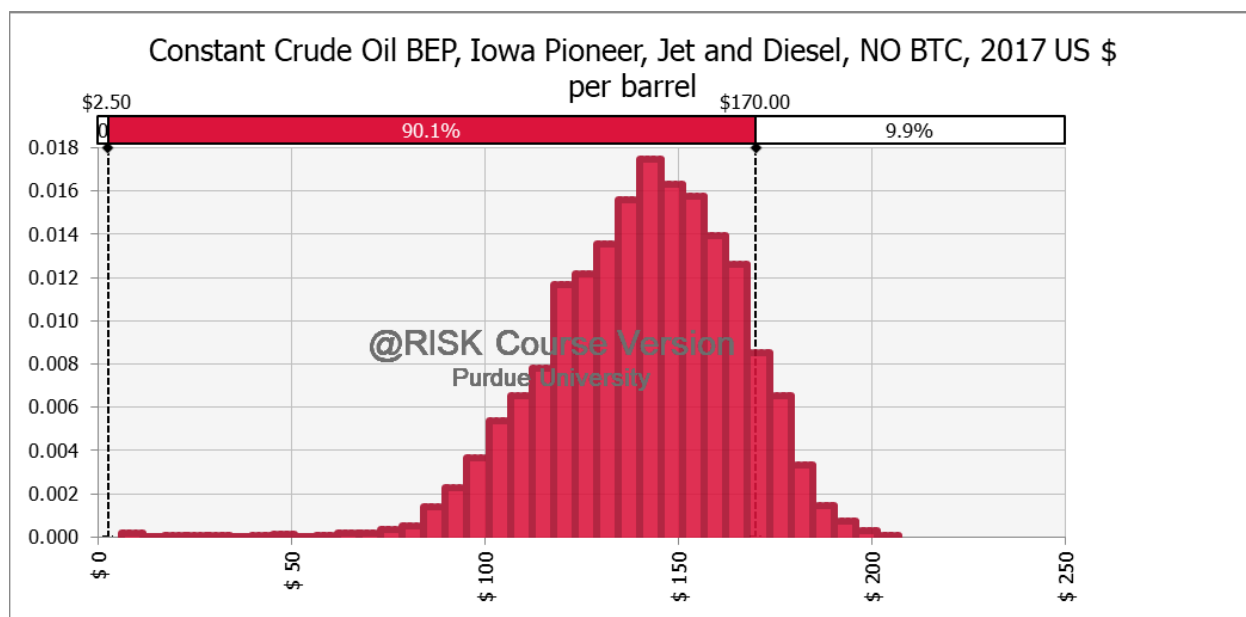


Figure A.24: Distribution of breakeven constant crude oil prices at pioneer Iowa site with the default product slate and NO BTC

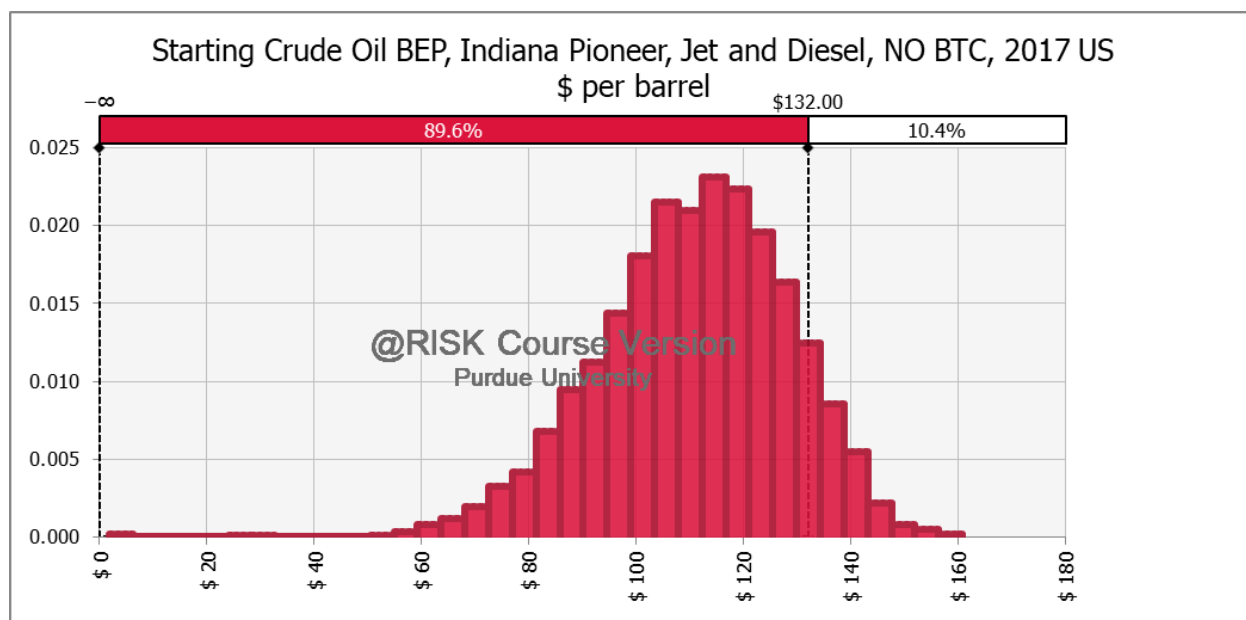


Figure A.25: Distribution of breakeven starting crude oil prices at pioneer Indiana site with 2.25% real annual price growth, the default product slate, and NO BTC

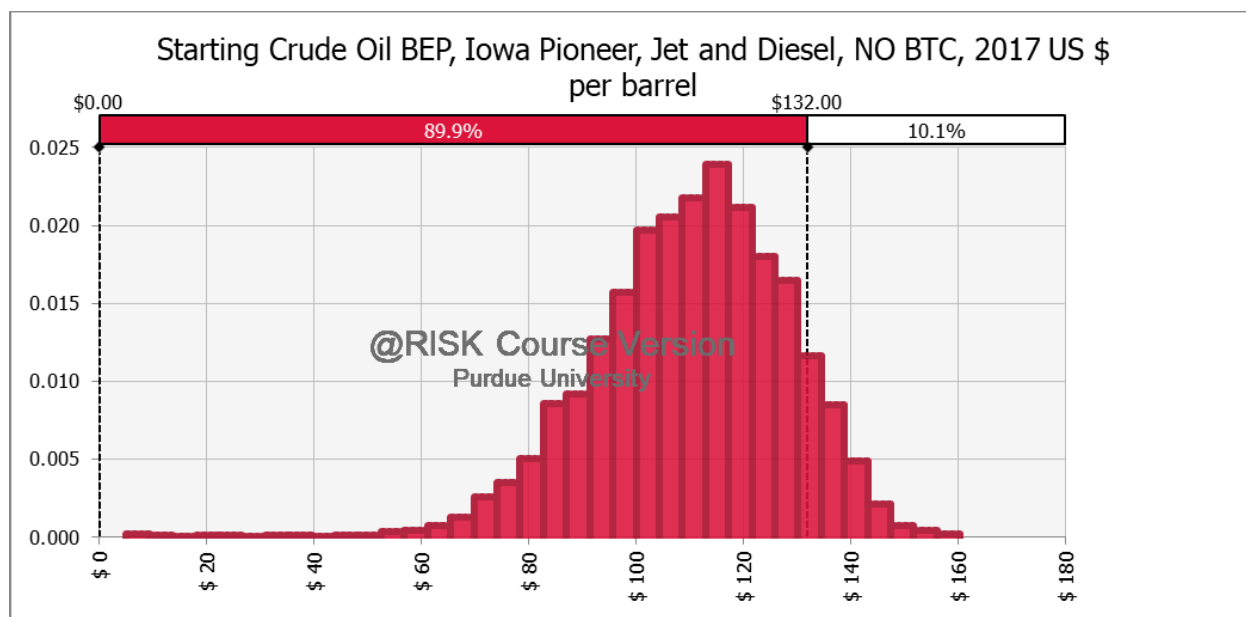


Figure A.26: Distribution of breakeven starting crude oil prices at pioneer Iowa site with 2.25% real annual price growth, the default product slate, and NO BTC

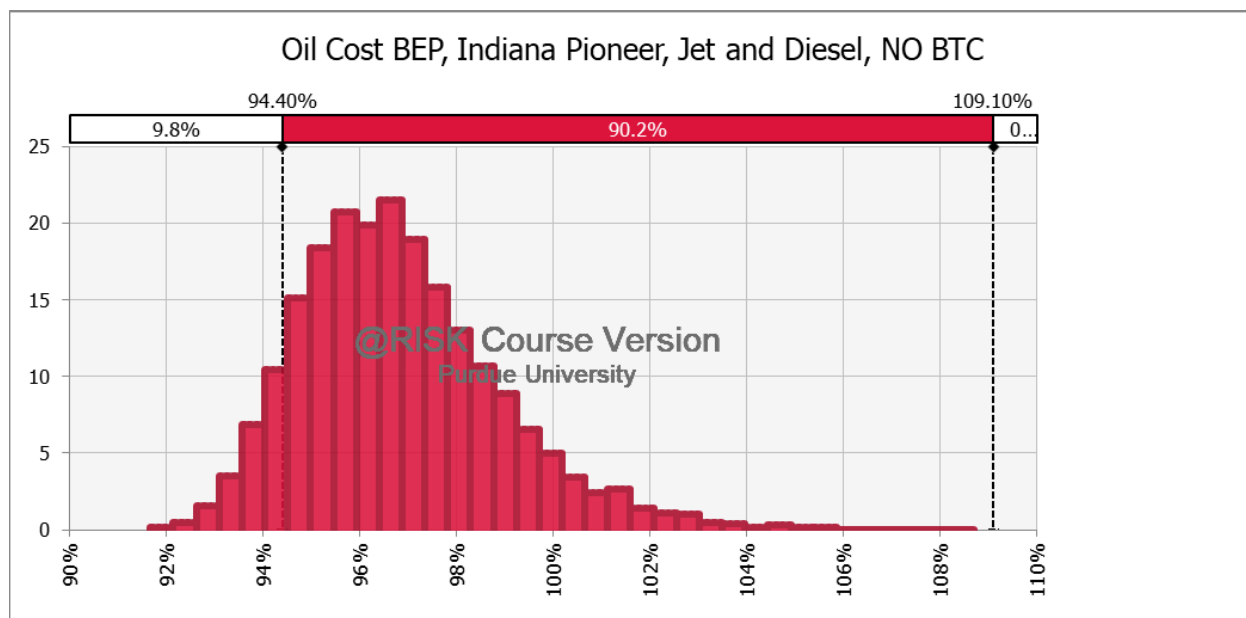


Figure A.27: Distribution of breakeven pennycress oil costs at pioneer Indiana site with the default product slate and NO BTC, as a percent of soybean oil prices

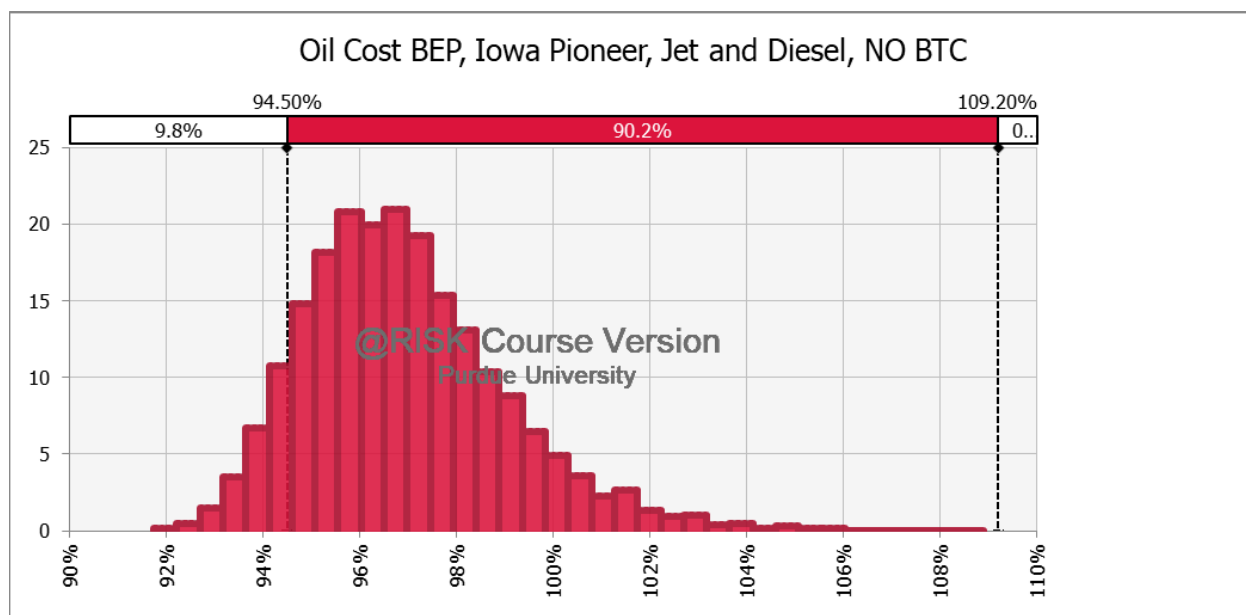


Figure A.28: Distribution of breakeven pennycress oil costs at pioneer Iowa site with the default product slate and NO BTC, as a percent of soybean oil prices

Maximum diesel fuel product slate

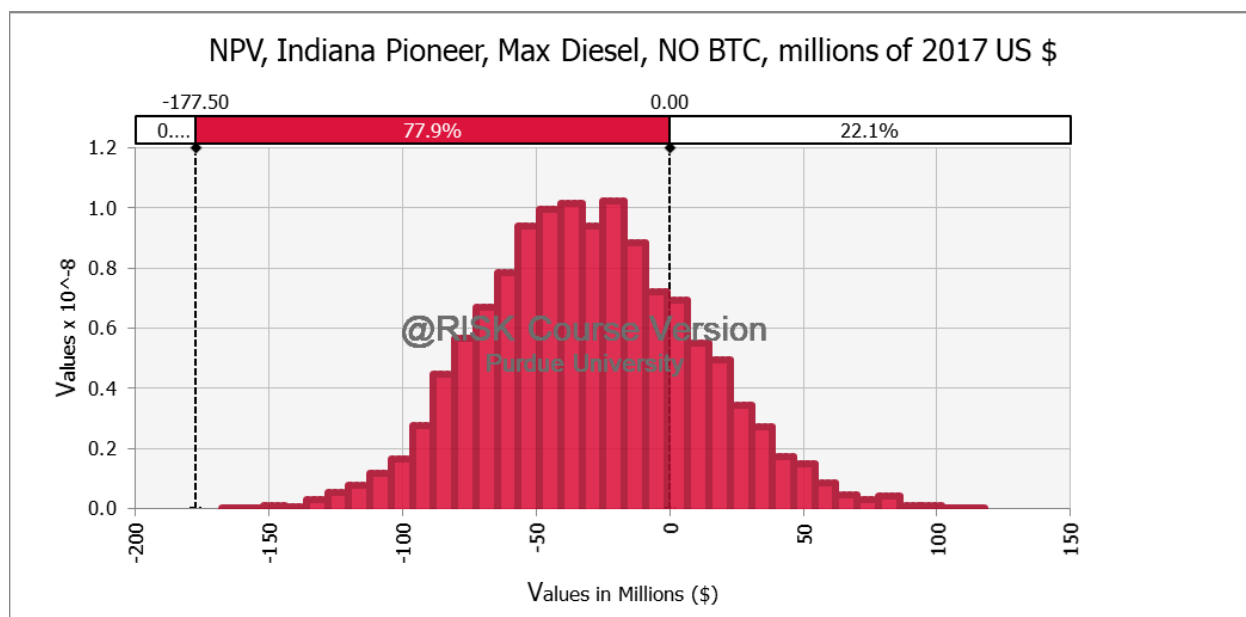


Figure A.29: Distribution of NPVs at pioneer Indiana site with a maximum diesel product slate and NO BTC

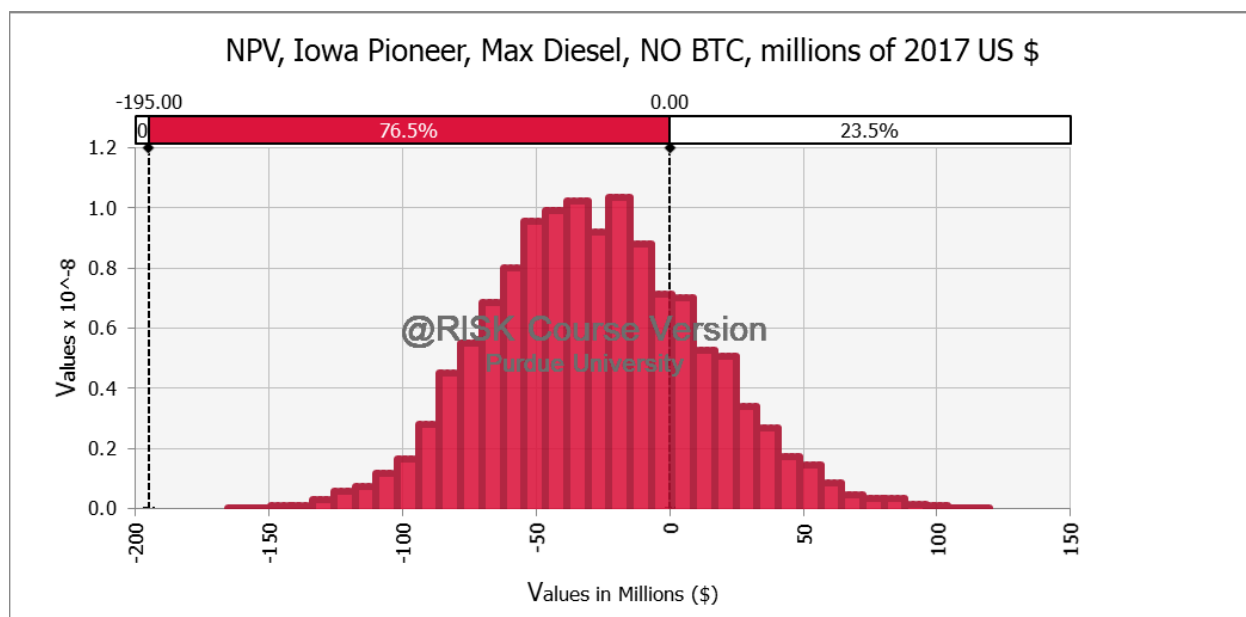


Figure A.30: Distribution of NPVs at pioneer Iowa site with a maximum diesel product slate and NO BTC

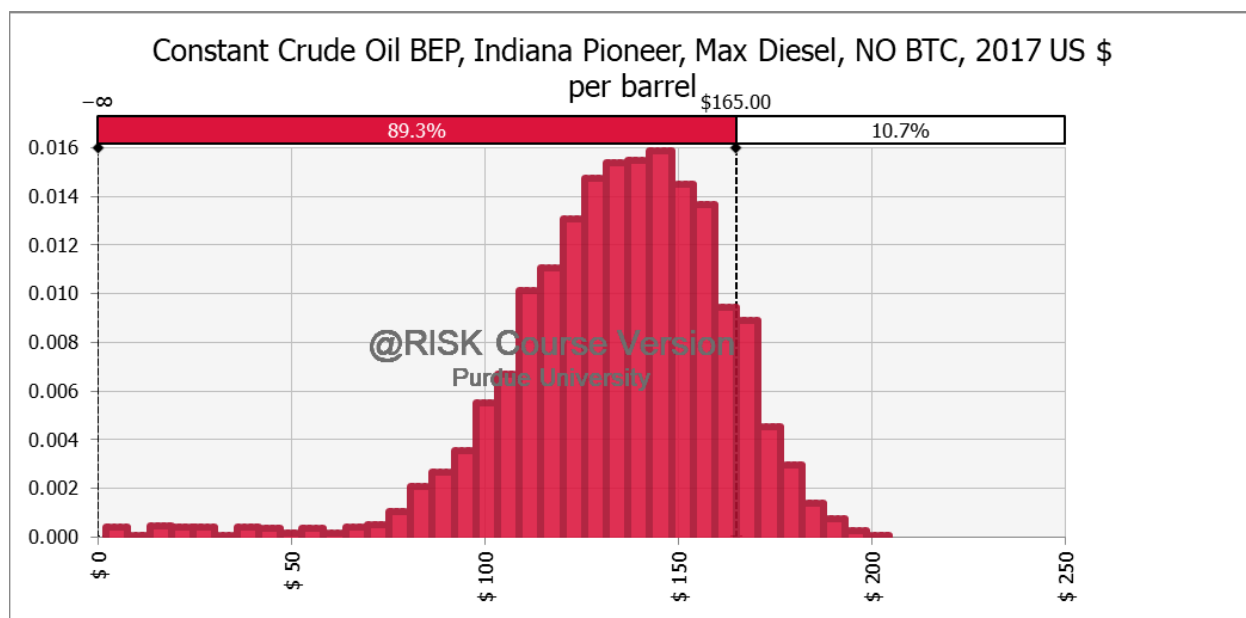


Figure A.31: Distribution of breakeven constant crude oil prices at pioneer Indiana site with a maximum diesel product slate and NO BTC

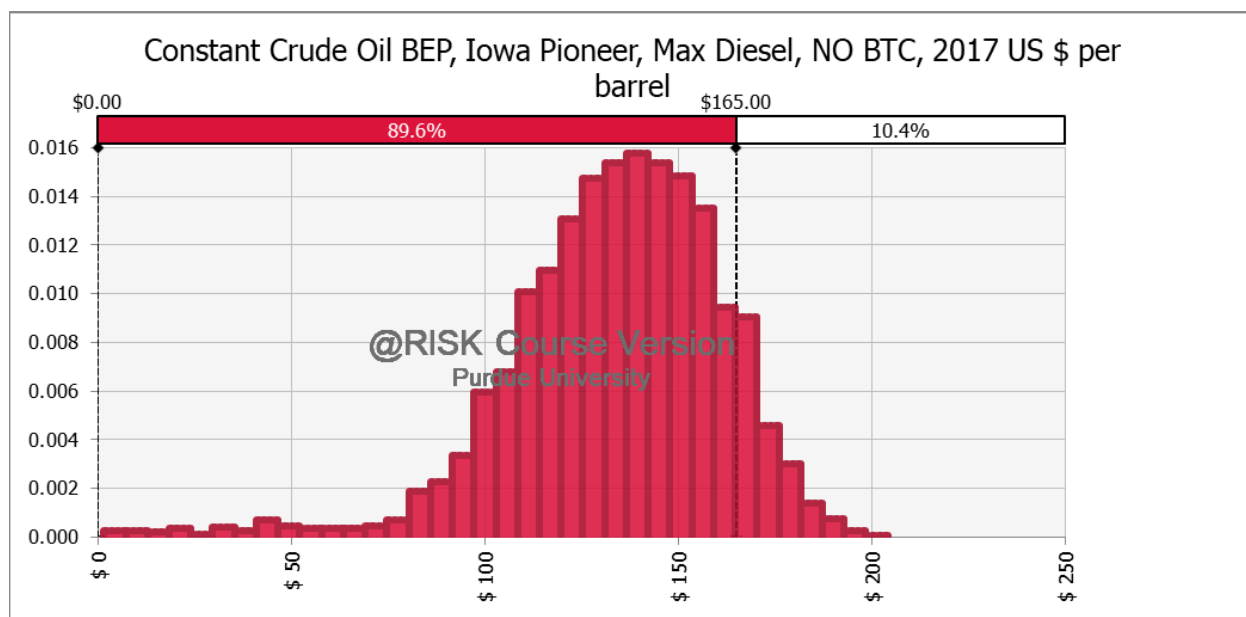


Figure A.32: Distribution of breakeven constant crude oil prices at pioneer Iowa site with a maximum diesel product slate and NO BTC

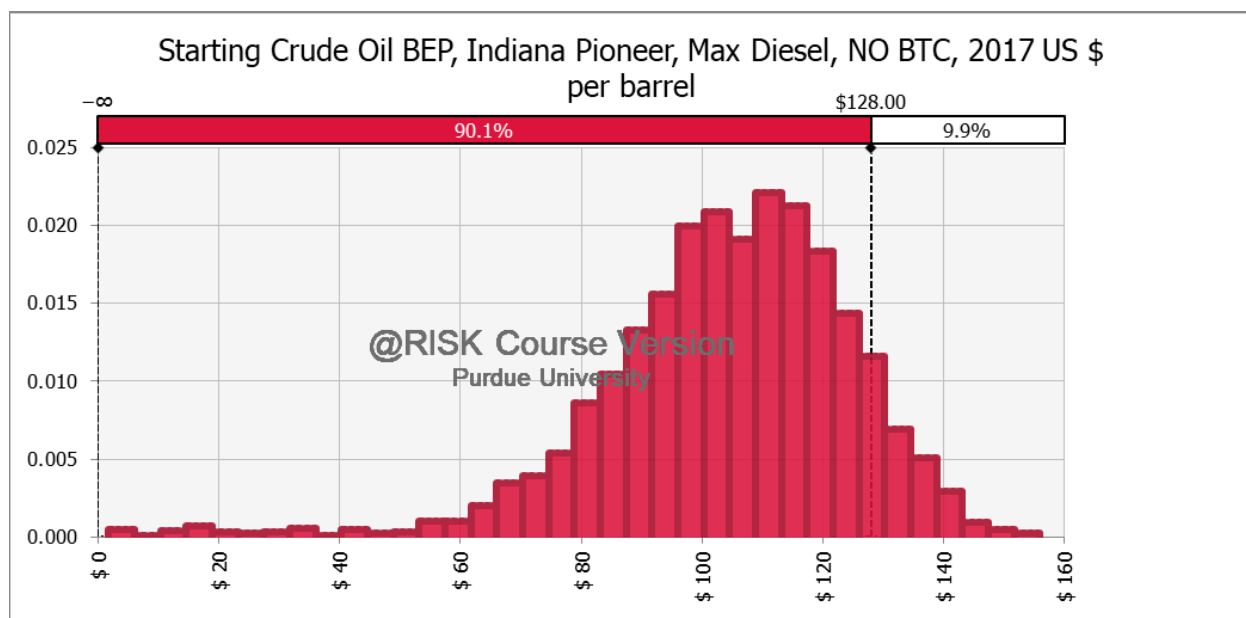


Figure A.33: Distribution of breakeven starting crude oil prices at pioneer Indiana site with 2.25% real annual price growth, a maximum diesel product slate, and NO BTC

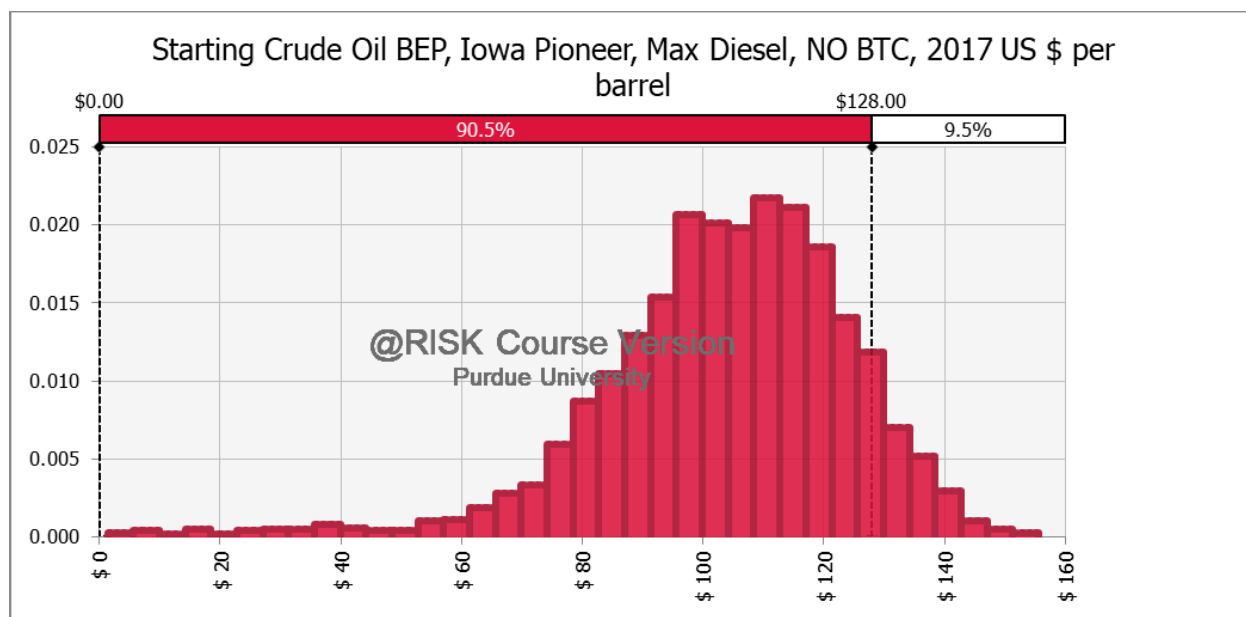


Figure A.34: Distribution of breakeven starting crude oil prices at pioneer Iowa site with 2.25% real annual price growth, a maximum diesel product slate, and NO BTC

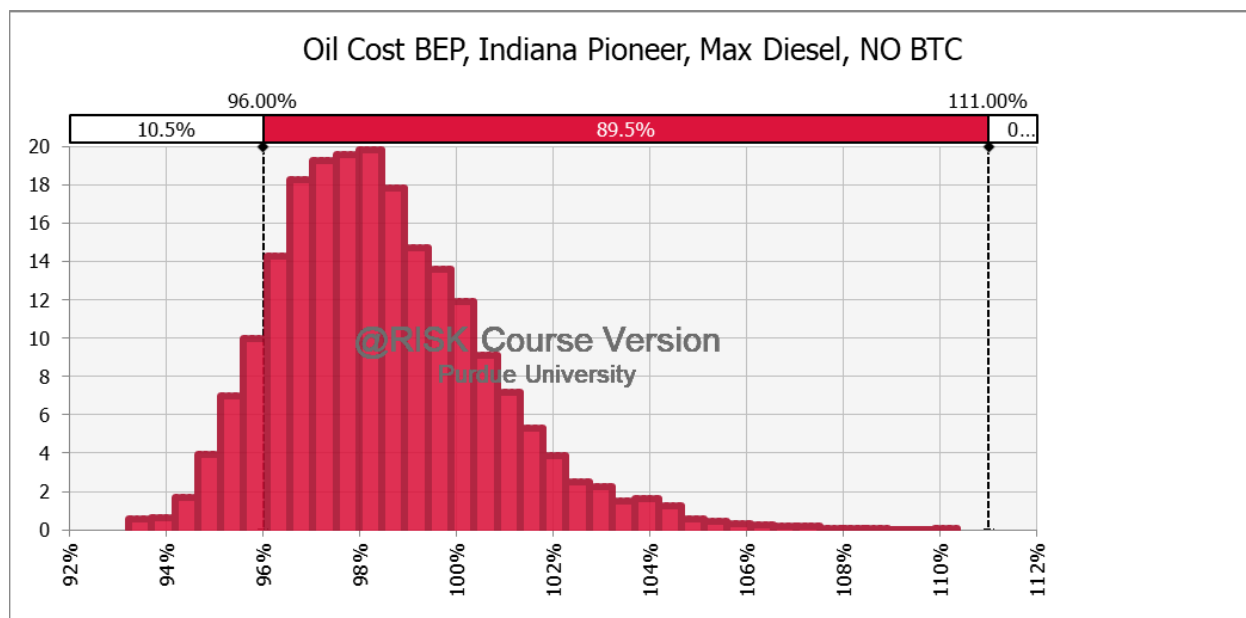


Figure A.35: Distribution of breakeven pennycress oil costs at pioneer Indiana site a maximum diesel product slate and NO BTC, as a percent of soybean oil prices

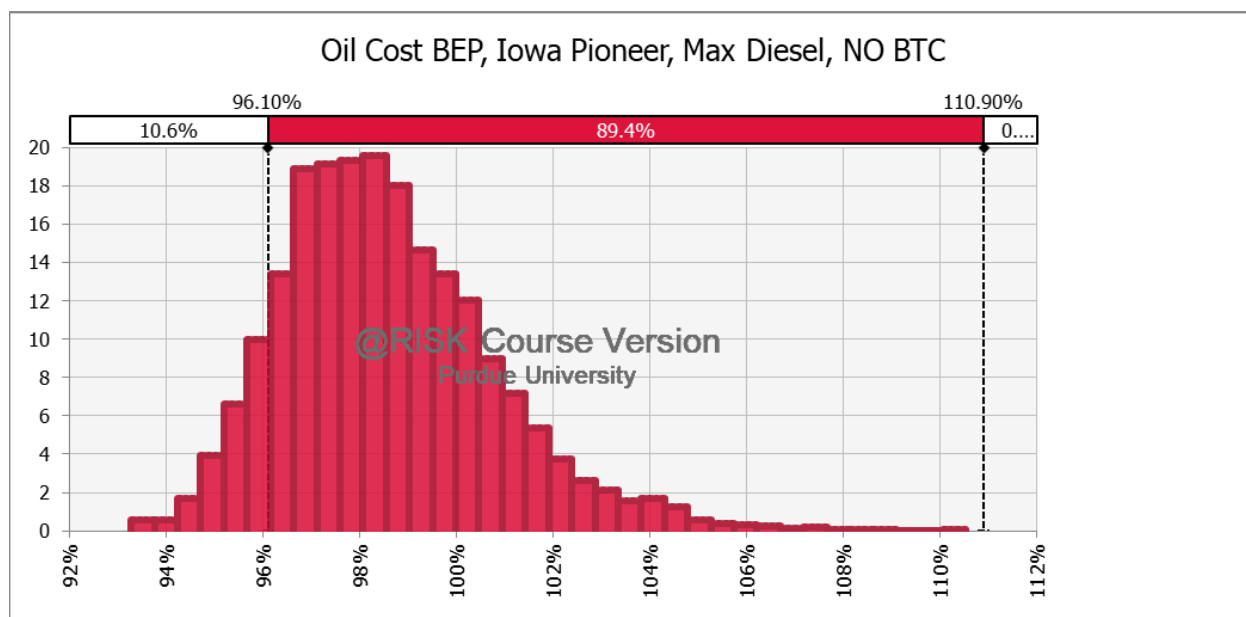


Figure A.36: Distribution of breakeven pennycress oil costs at pioneer Iowa site a maximum diesel product slate and NO BTC, as a percent of soybean oil prices

Nth Plant

BTC continues

Product slate contains both jet and diesel fuel

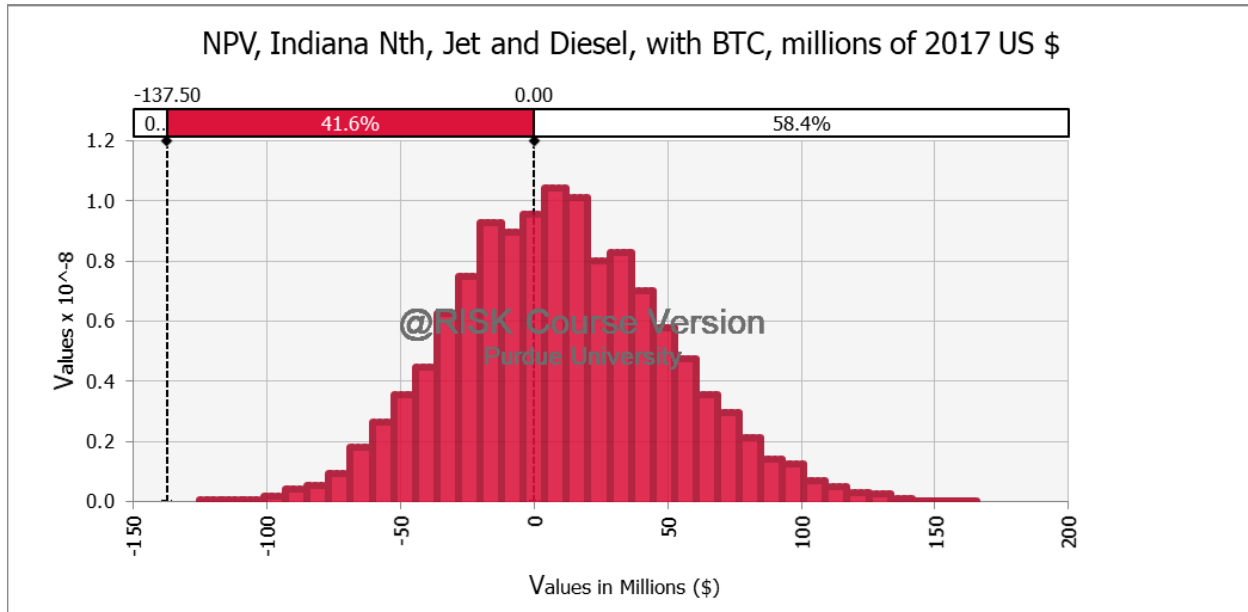


Figure A.37: Distribution of NPVs at Nth Indiana site with the default product slate and a BTC

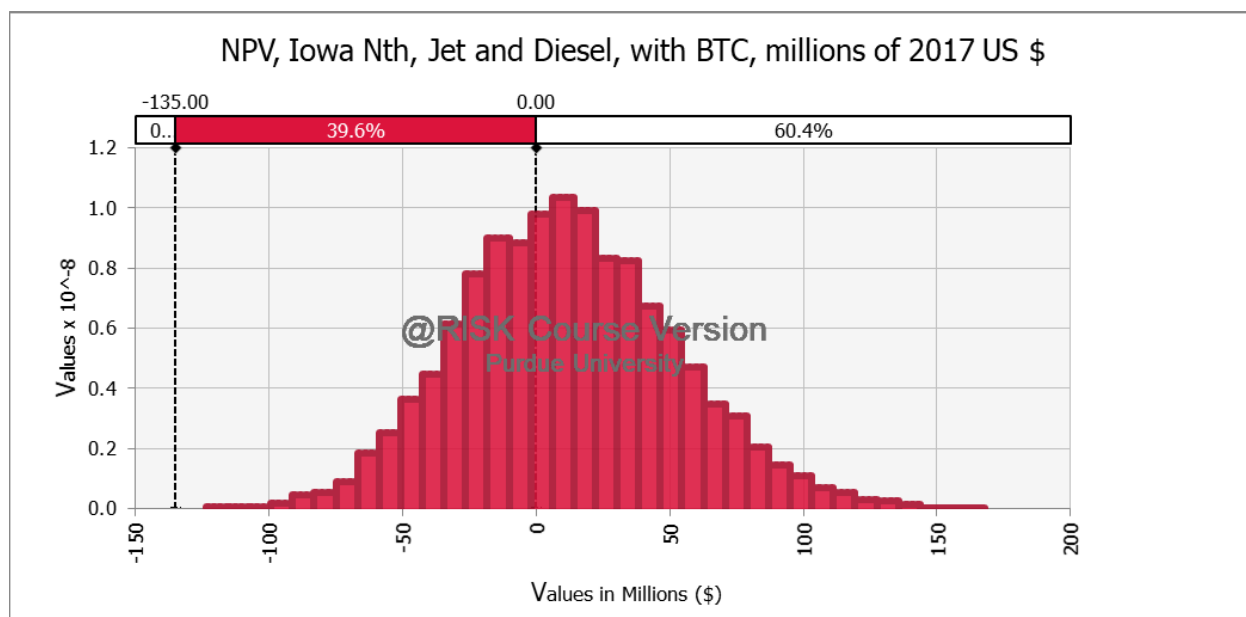


Figure A.38: Distribution of NPVs at Nth Iowa site with the default product slate and a BTC

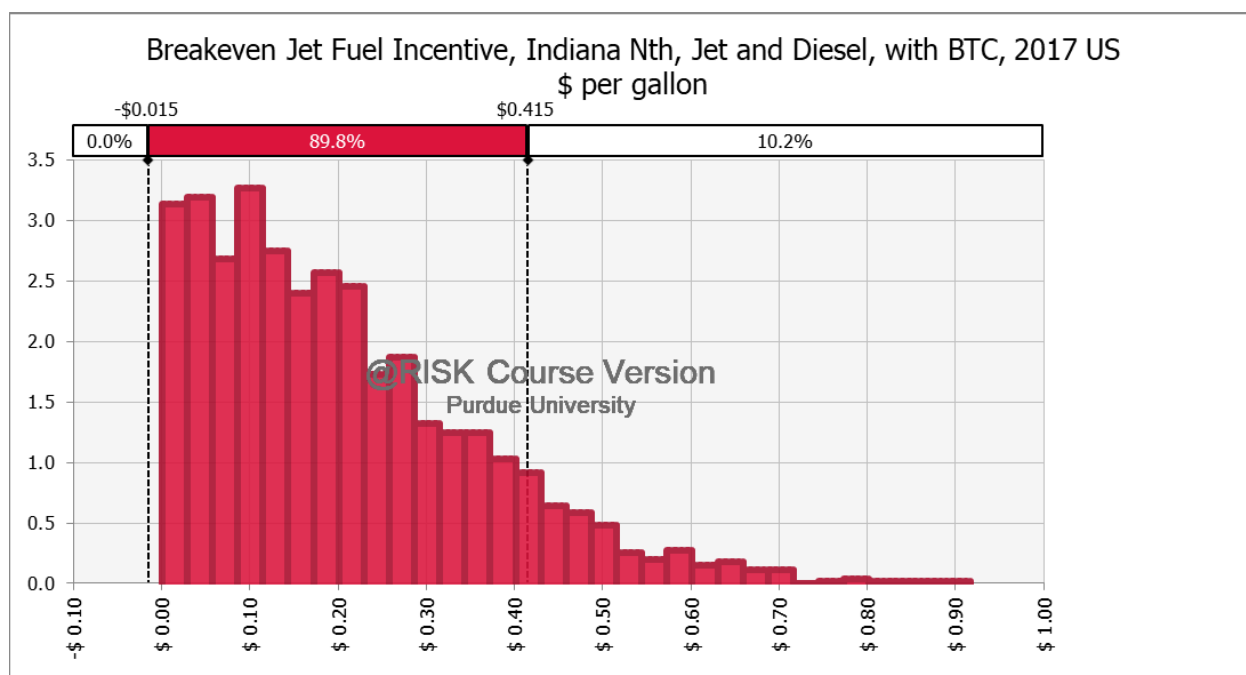


Figure A.39: Distribution of breakeven jet fuel incentives at Nth Indiana site with the default product slate and a BTC

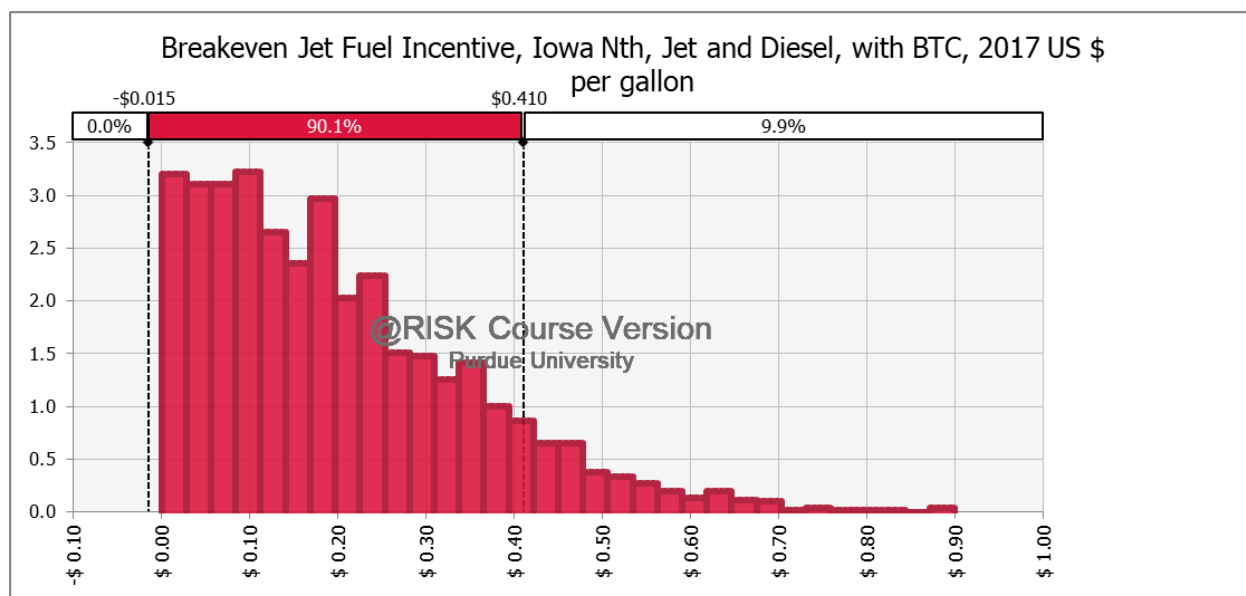


Figure A.40: Distribution of breakeven jet fuel incentives at Nth Iowa site with the default product slate and a BTC

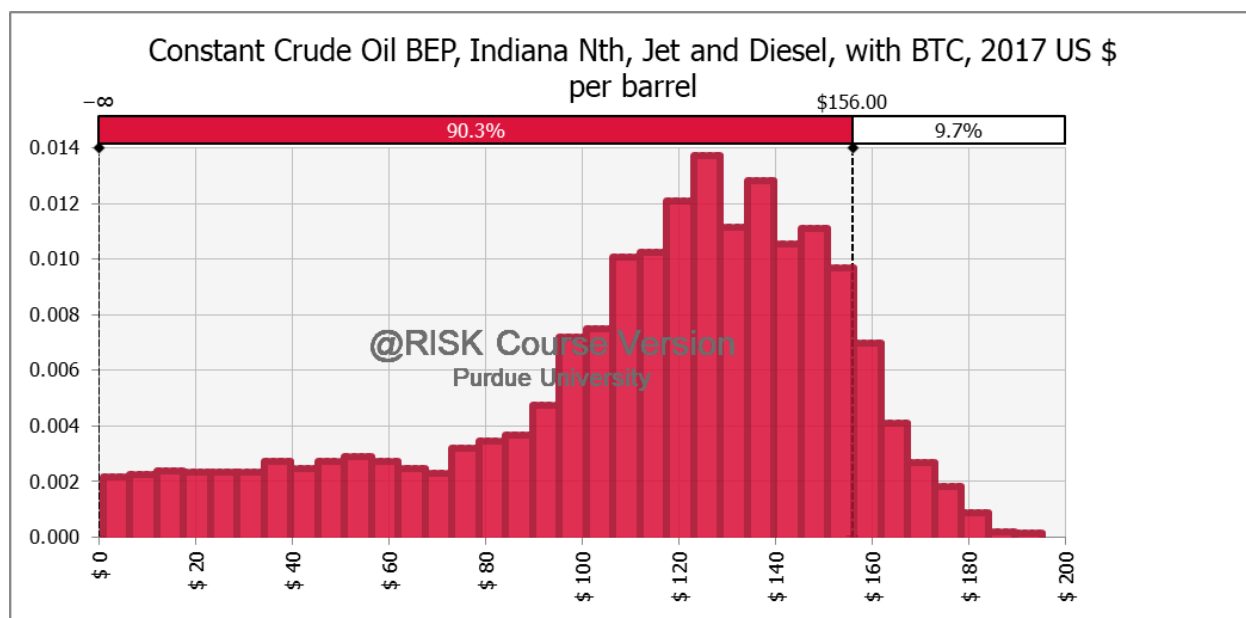


Figure A.41: Distribution of breakeven constant crude oil prices at Nth Indiana site with the default product slate and a BTC

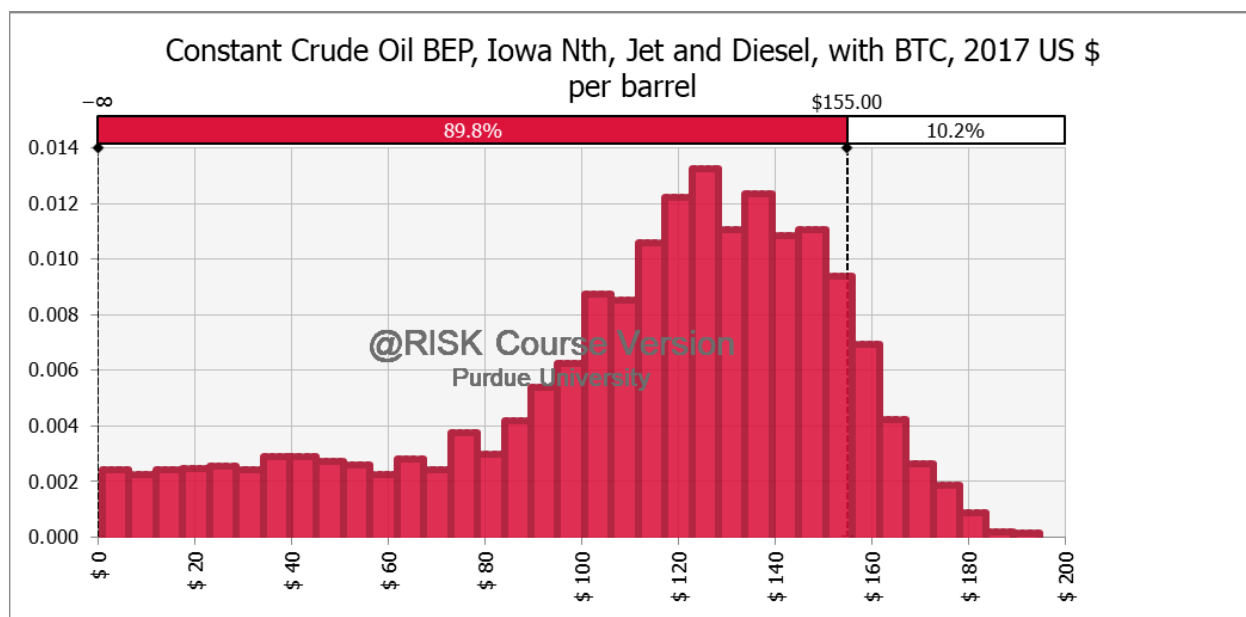


Figure A.42: Distribution of breakeven constant crude oil prices at Nth Iowa site with the default product slate and a BTC

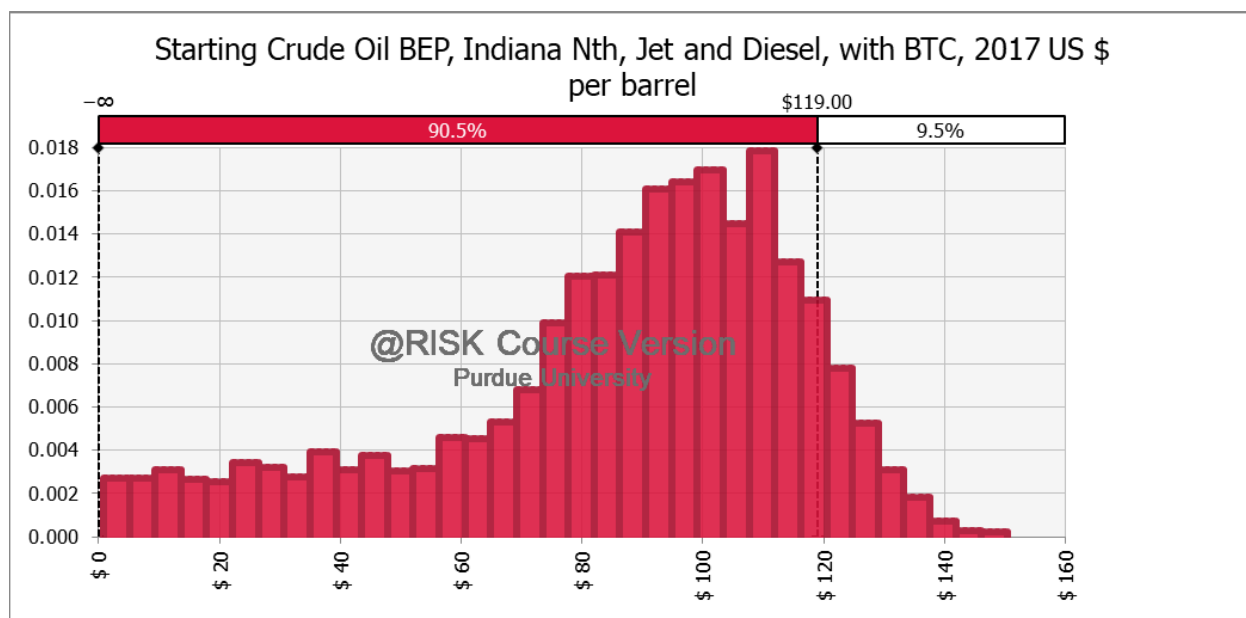


Figure A.43: Distribution of breakeven starting crude oil prices at Nth Indiana site with 2.25% real annual price growth, the default product slate, and a BTC

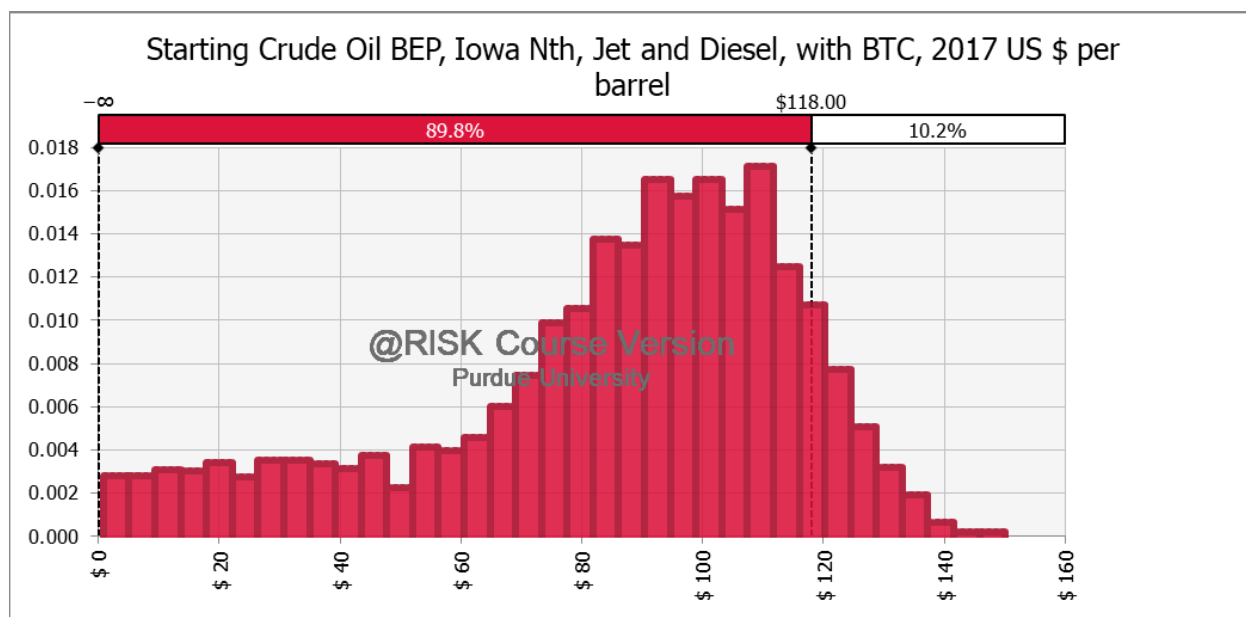


Figure A.44: Distribution of breakeven starting crude oil prices at Nth Iowa site with 2.25% real annual price growth, the default product slate, and a BTC

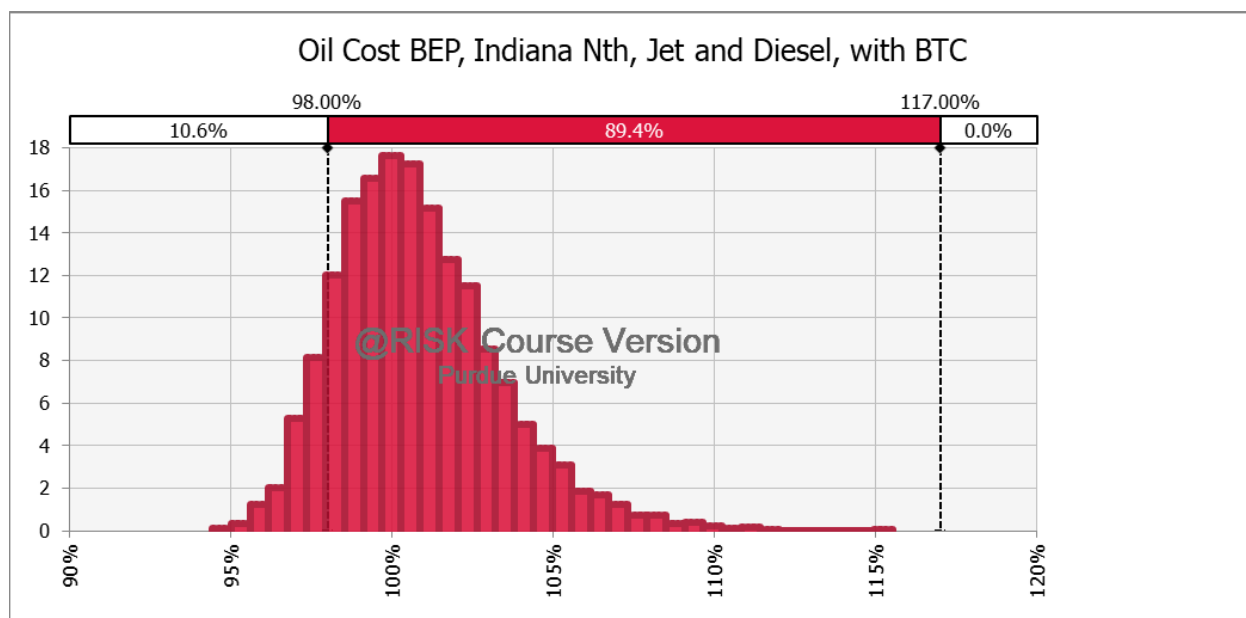


Figure A.45: Distribution of breakeven pennycress oil costs at Nth Indiana site with the default product slate and a BTC, as a percent of soybean oil prices

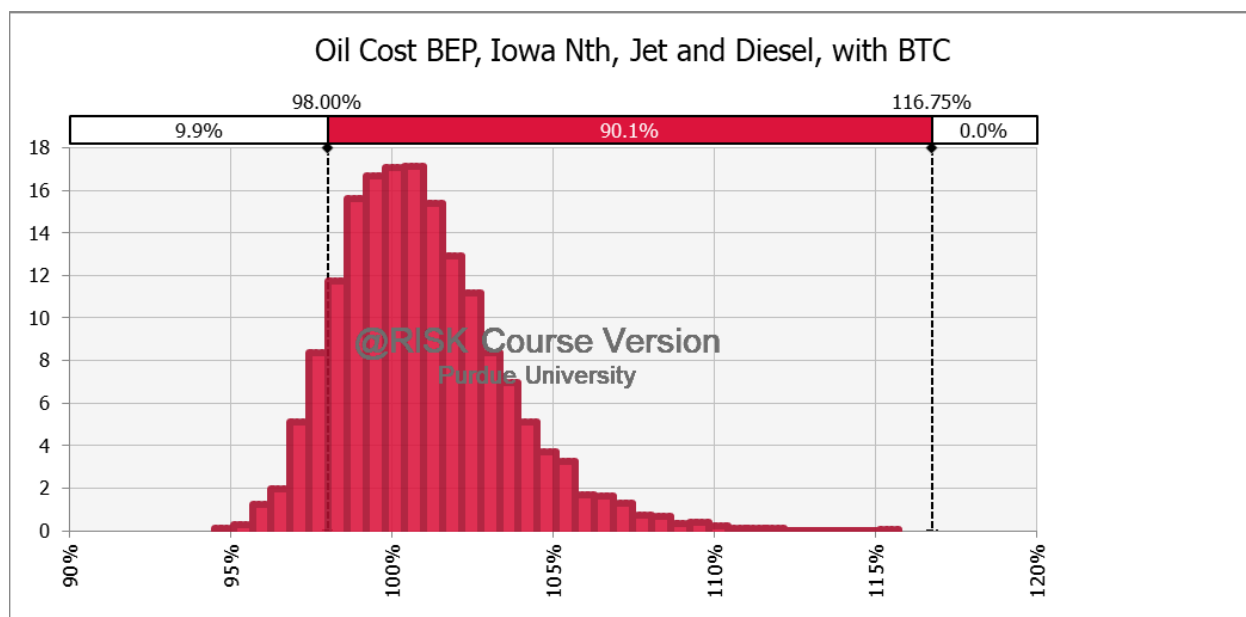


Figure A.46: Distribution of breakeven pennycress oil costs at Nth Iowa site with the default product slate and a BTC, as a percent of soybean oil prices

Maximum diesel fuel product slate

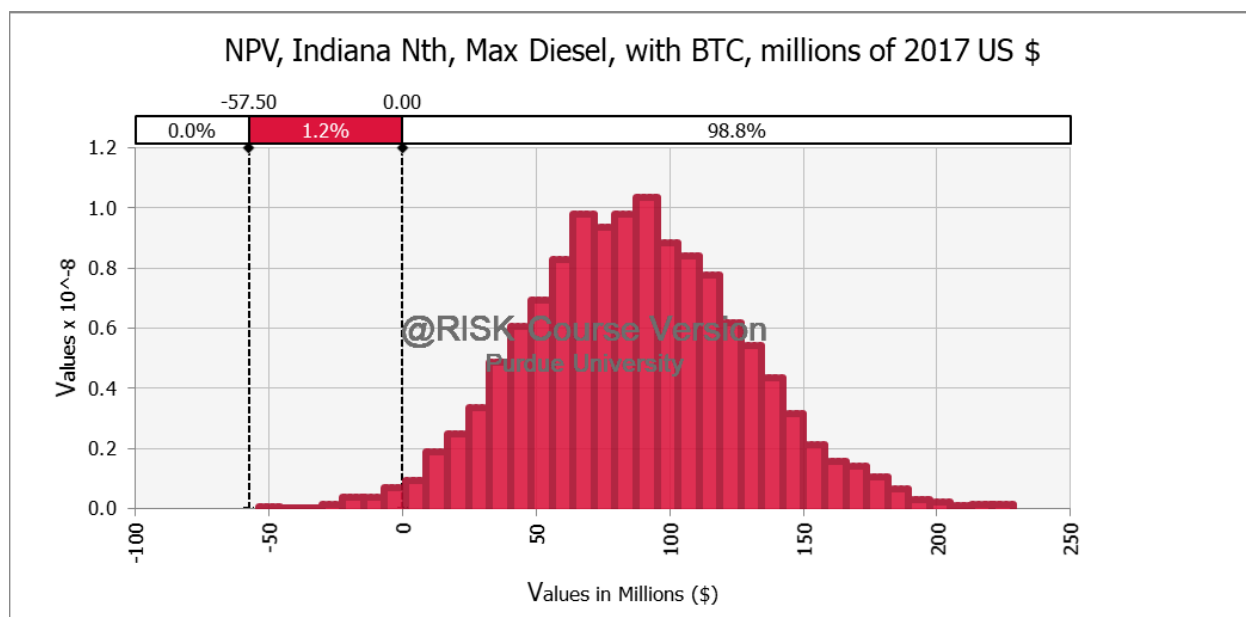


Figure A.47: Distribution of NPVs at Nth Indiana site with a maximum diesel product slate and a BTC

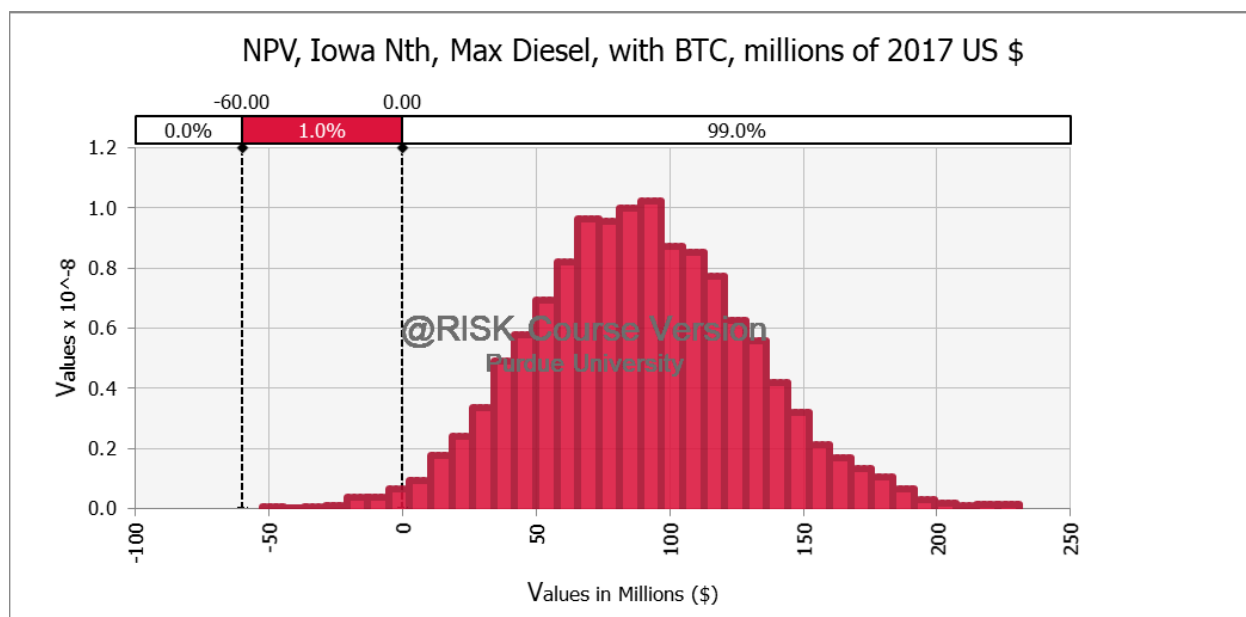


Figure A.48: Distribution of NPVs at Nth Iowa site with a maximum diesel product slate and a BTC

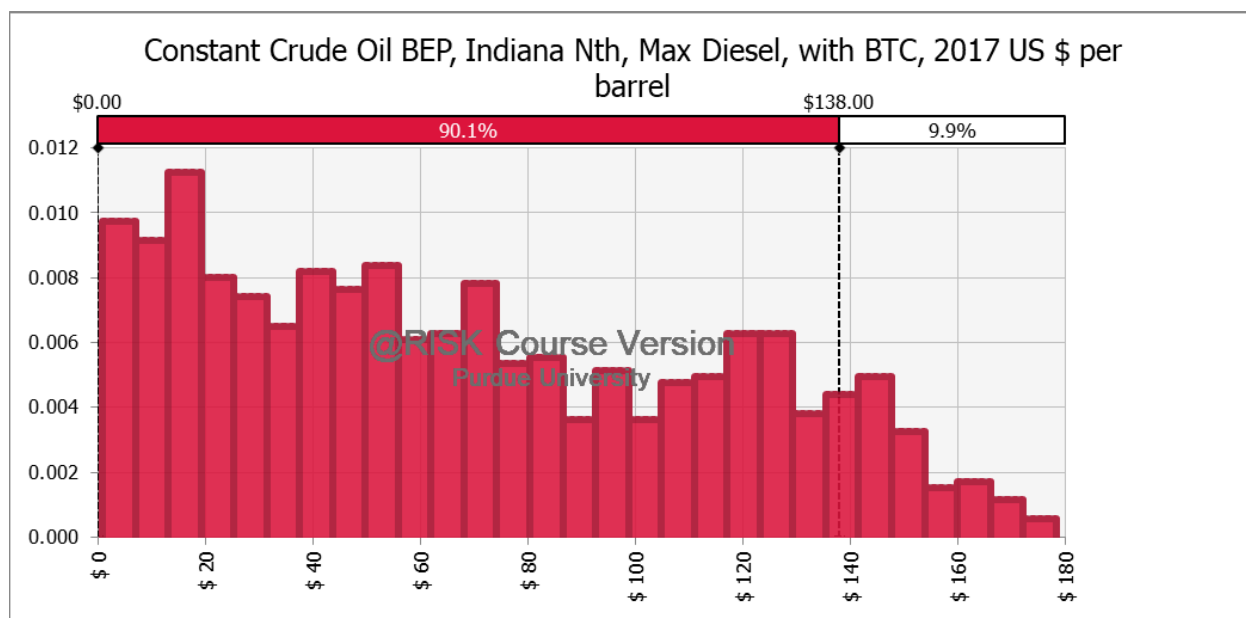


Figure A.49: Distribution of breakeven constant crude oil prices at Nth Indiana site with a maximum diesel product slate and a BTC

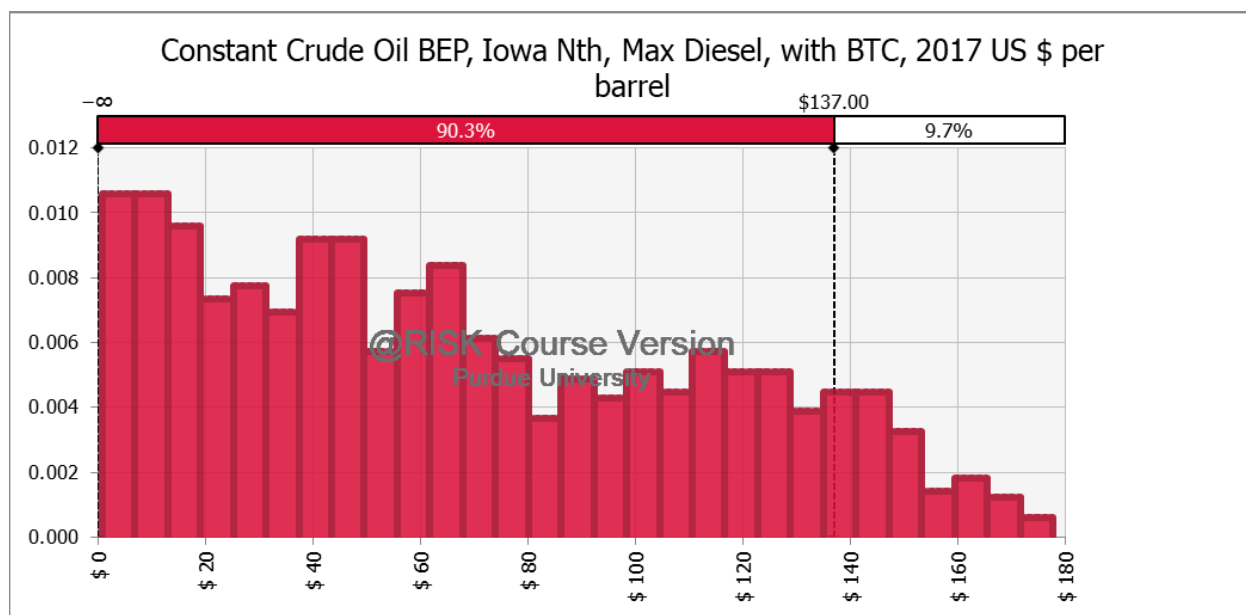


Figure A.50: Distribution of breakeven constant crude oil prices at Nth Iowa site with a maximum diesel product slate and a BTC

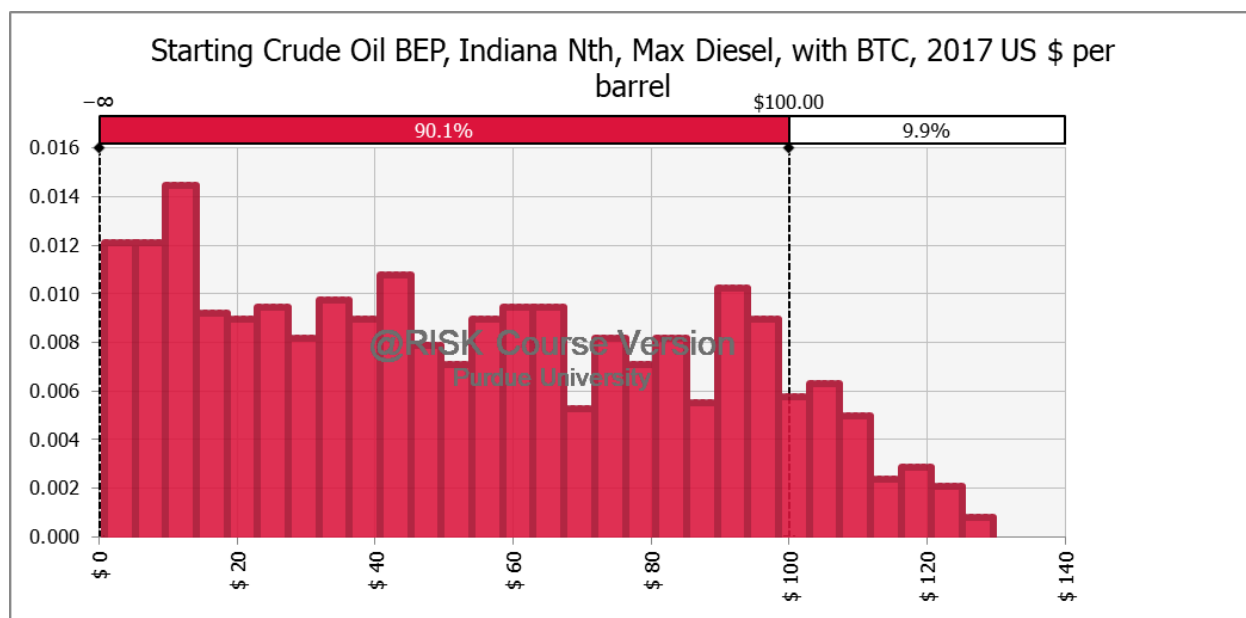


Figure A.51: Distribution of breakeven starting crude oil prices at Nth Indiana site with 2.25% real annual price growth, a maximum diesel product slate, and a BTC

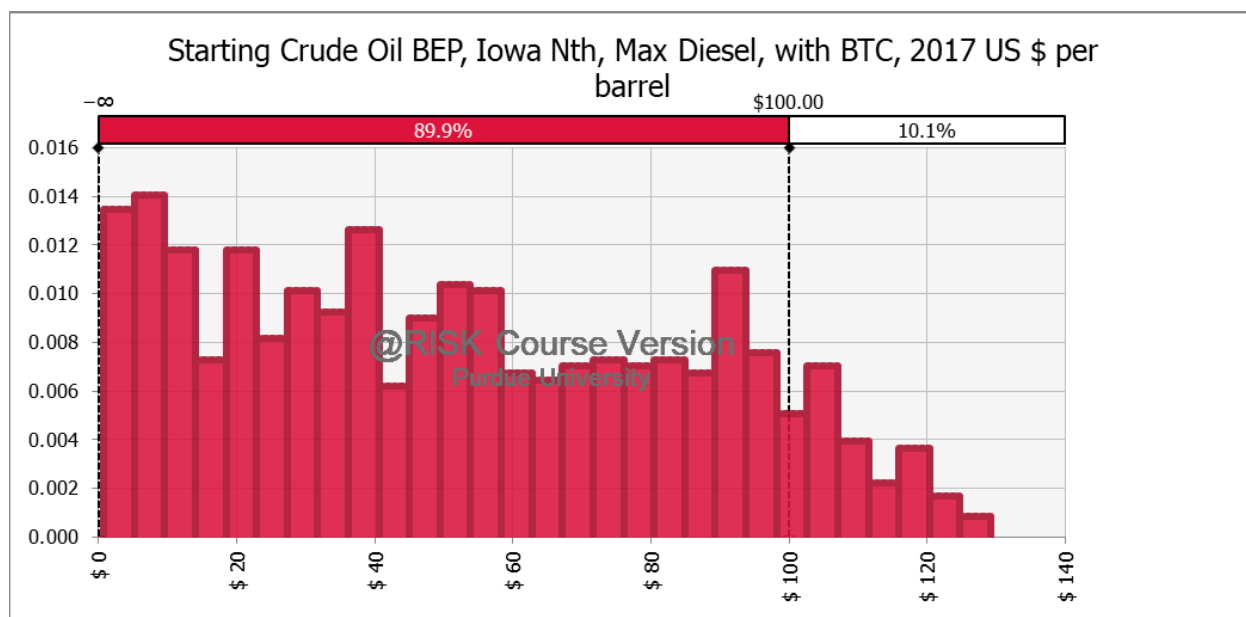


Figure A.52: Distribution of breakeven starting crude oil prices at Nth Iowa site with 2.25% real annual price growth, a maximum diesel product slate, and a BTC

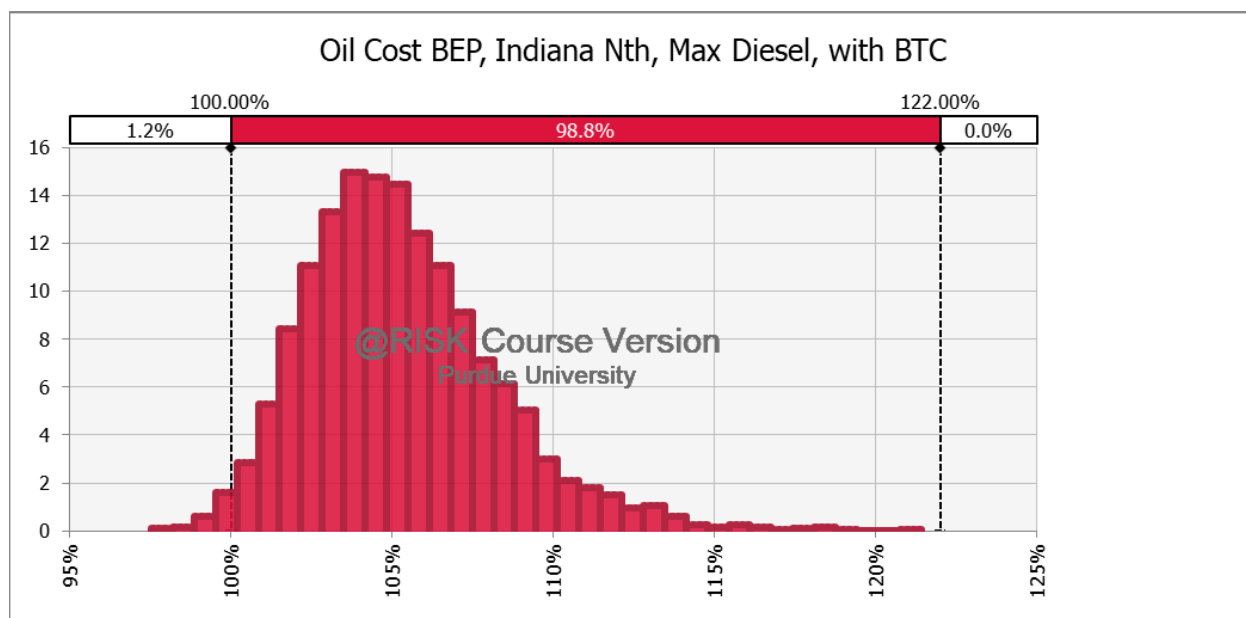


Figure A.53: Distribution of breakeven pennycress oil costs at Nth Indiana site with a maximum diesel product slate and a BTC, as a percent of soybean oil prices

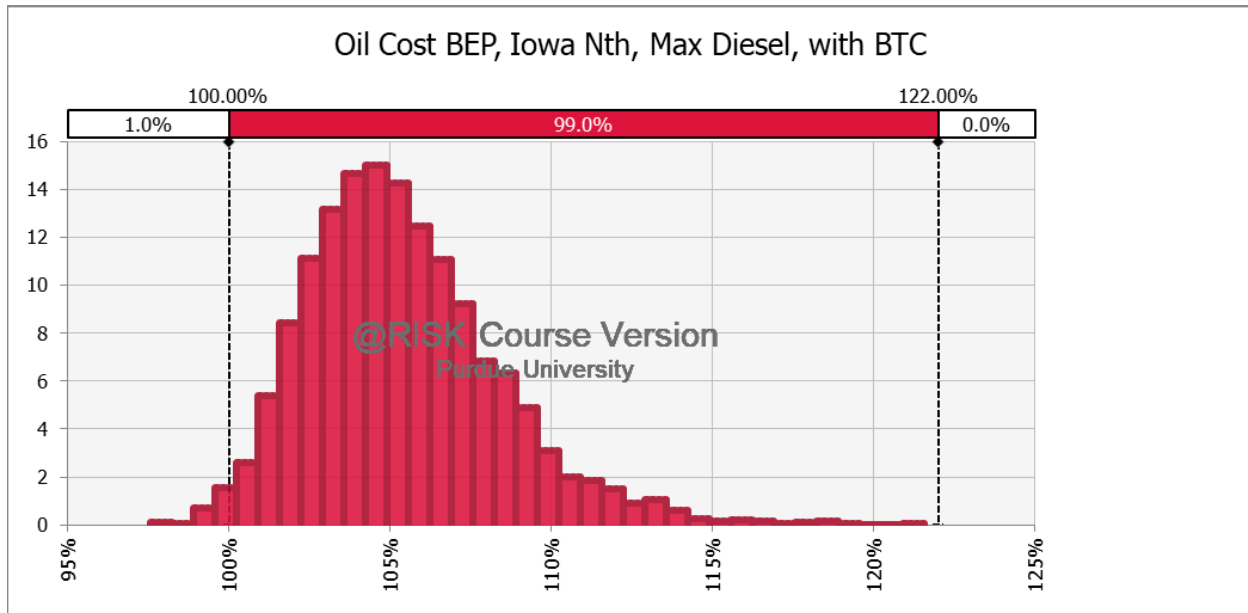


Figure A.54: Distribution of breakeven pennycress oil costs at Nth Iowa site with a maximum diesel product slate and a BTC, as a percent of soybean oil prices

BTC is discontinued

Product slate contains both jet and diesel fuel

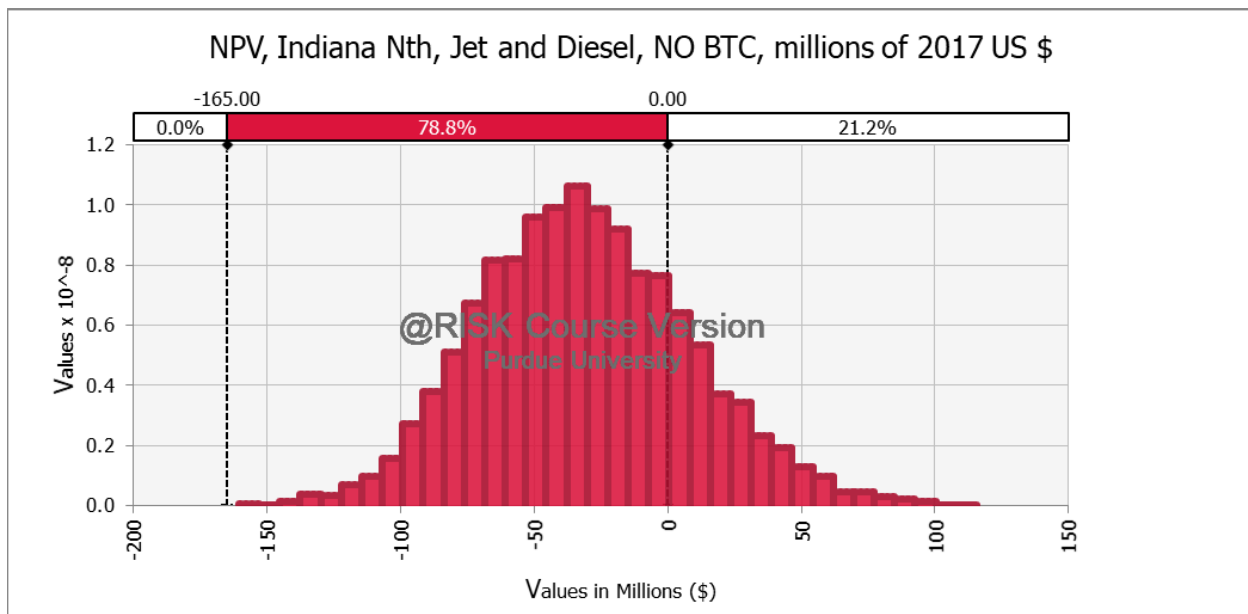


Figure A.55: Distribution of NPVs at Nth Indiana site with the default product slate and NO BTC

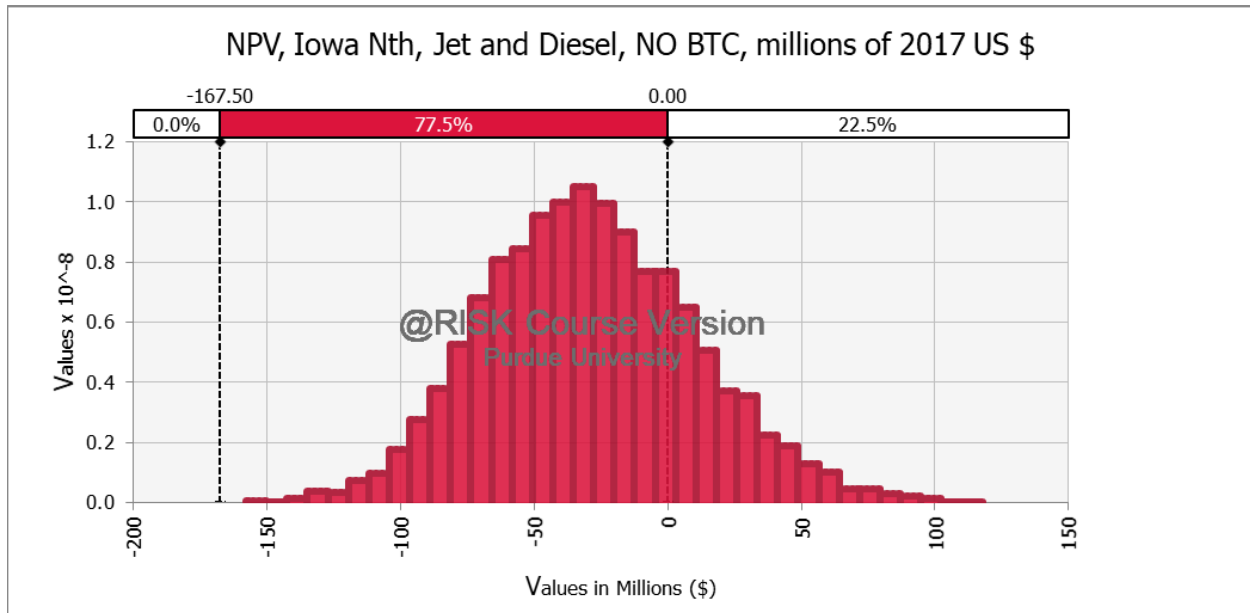


Figure A.56: Distribution of NPVs at Nth Iowa site with the default product slate and NO BTC

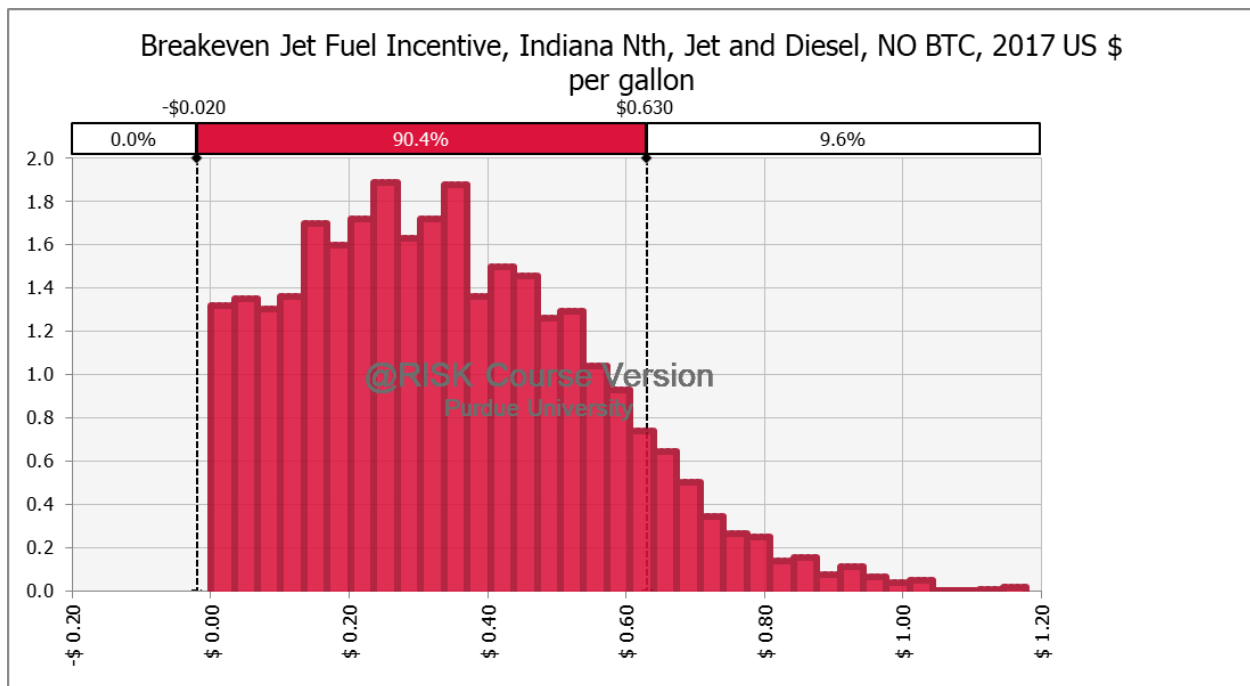


Figure A.57: Distribution of breakeven jet fuel incentives at Nth Indiana site with the default product slate and NO BTC

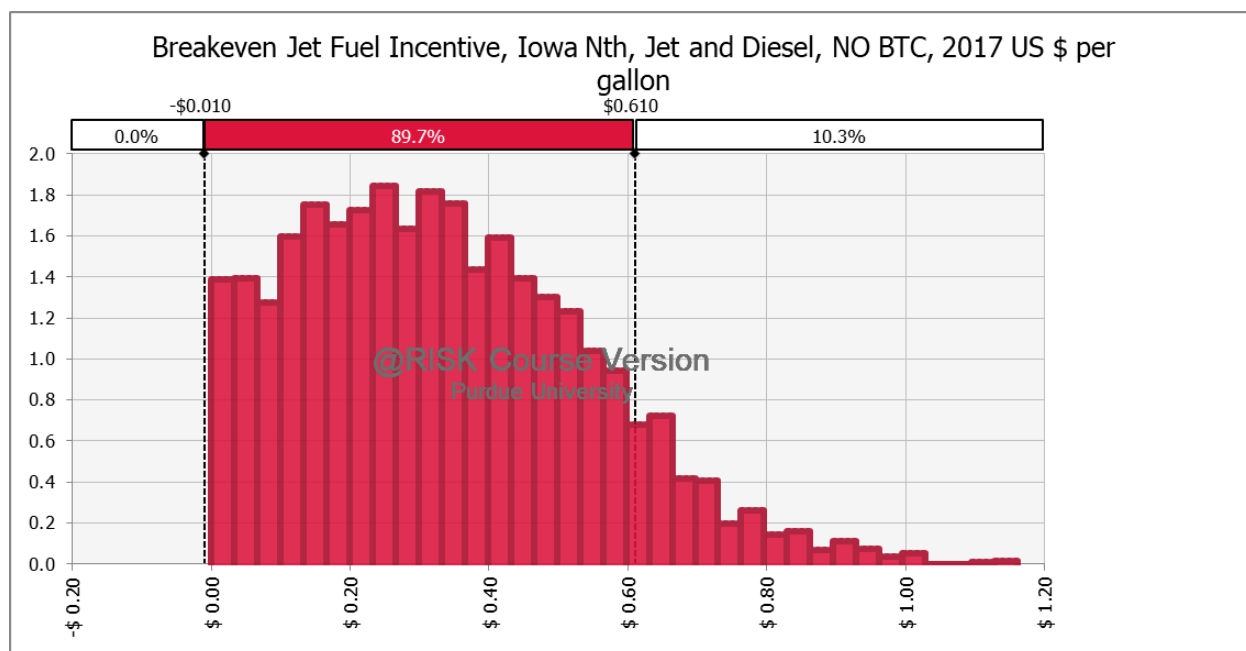


Figure A.58: Distribution of breakeven jet fuel incentives at Nth Iowa site with the default product slate and NO BTC

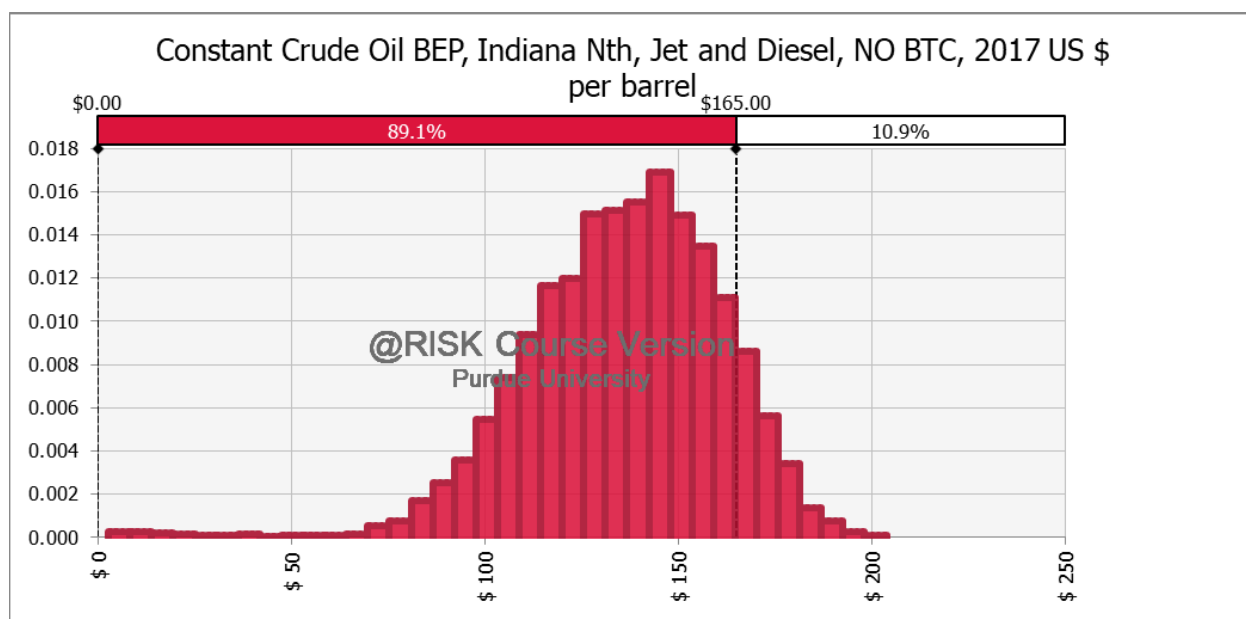


Figure A.59: Distribution of breakeven constant crude oil prices at Nth Indiana site with the default product slate and NO BTC

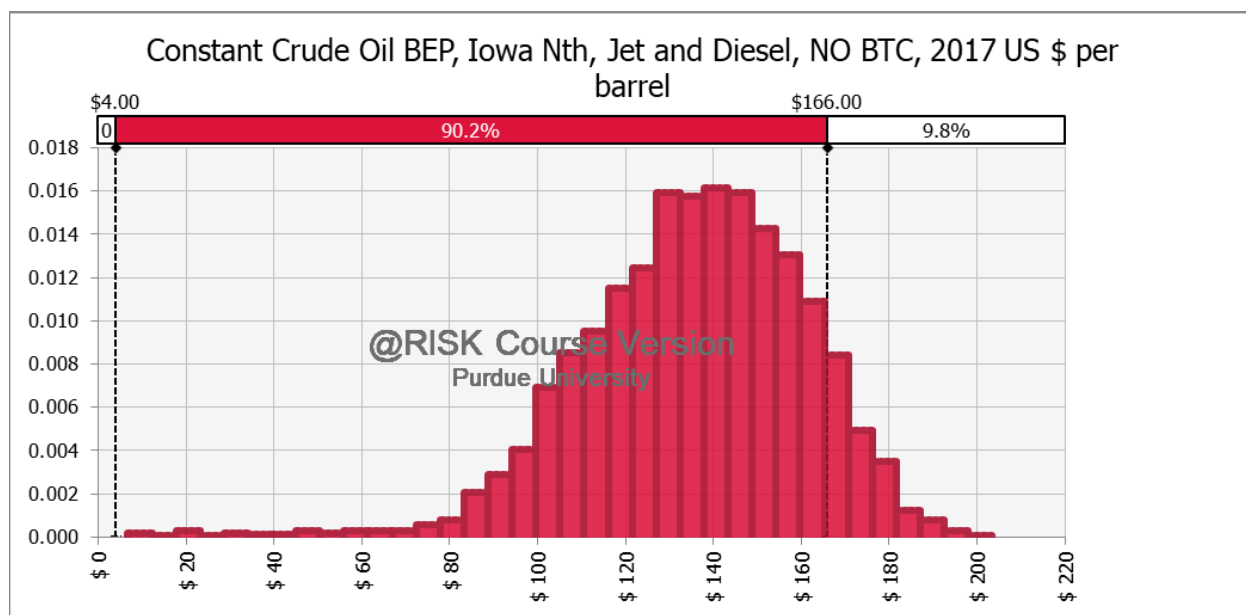


Figure A.60: Distribution of breakeven constant crude oil prices at Nth Iowa site with the default product slate and NO BTC

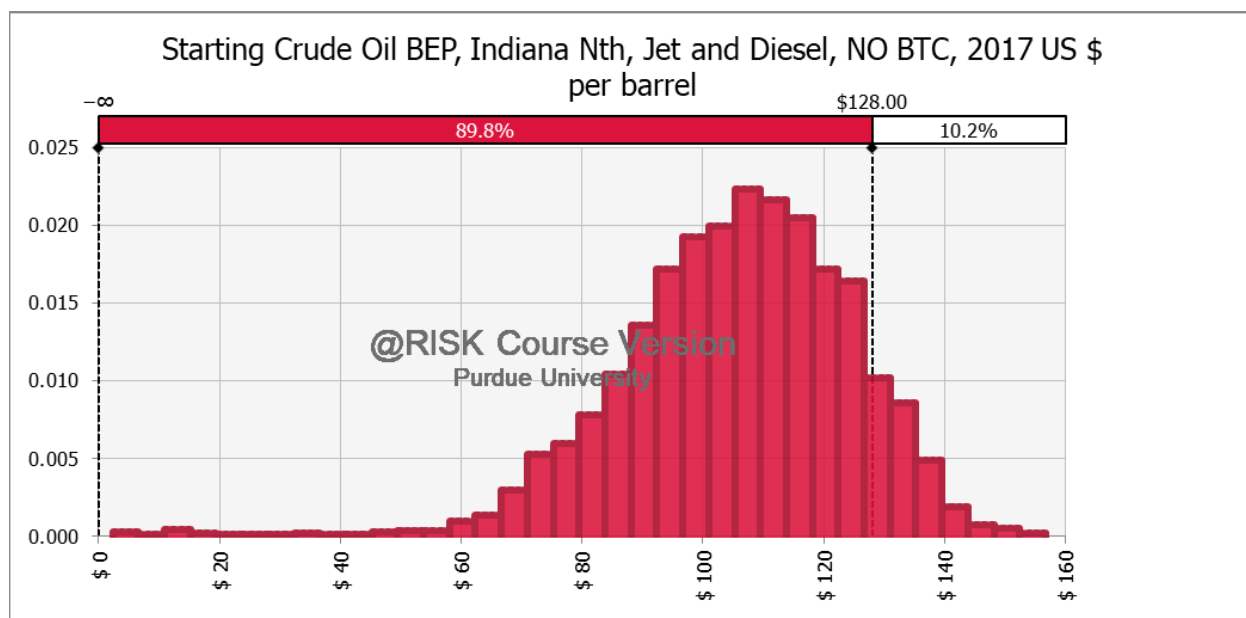


Figure A.61: Distribution of breakeven starting crude oil prices at Nth Indiana site with 2.25% real annual price growth, the default product slate, and NO BTC

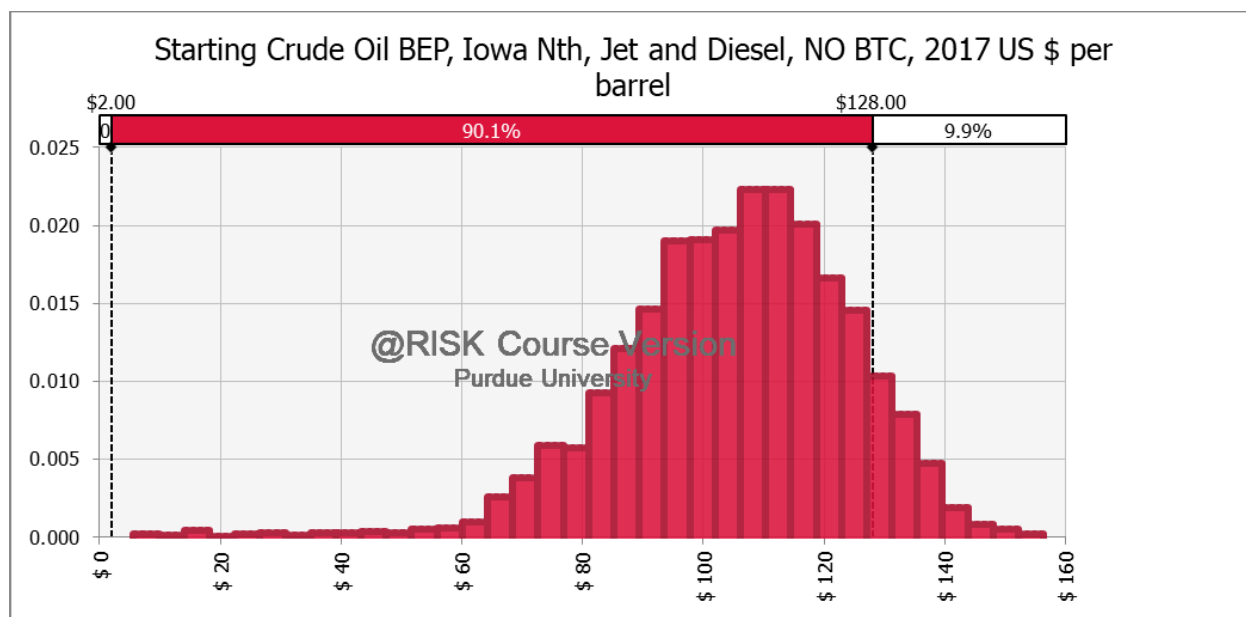


Figure A.62: Distribution of breakeven starting crude oil prices at Nth Iowa site with 2.25% real annual price growth, the default product slate, and NO BTC

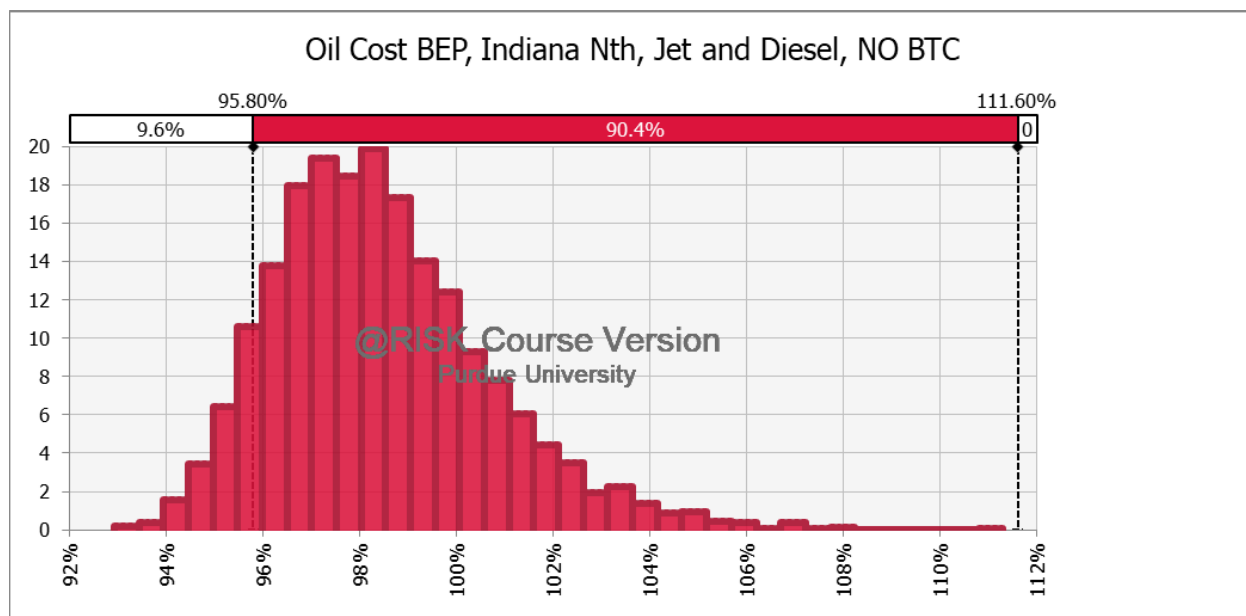


Figure A.63: Distribution of breakeven pennycress oil costs at Nth Indiana site with the default product slate and NO BTC, as a percent of soybean oil prices

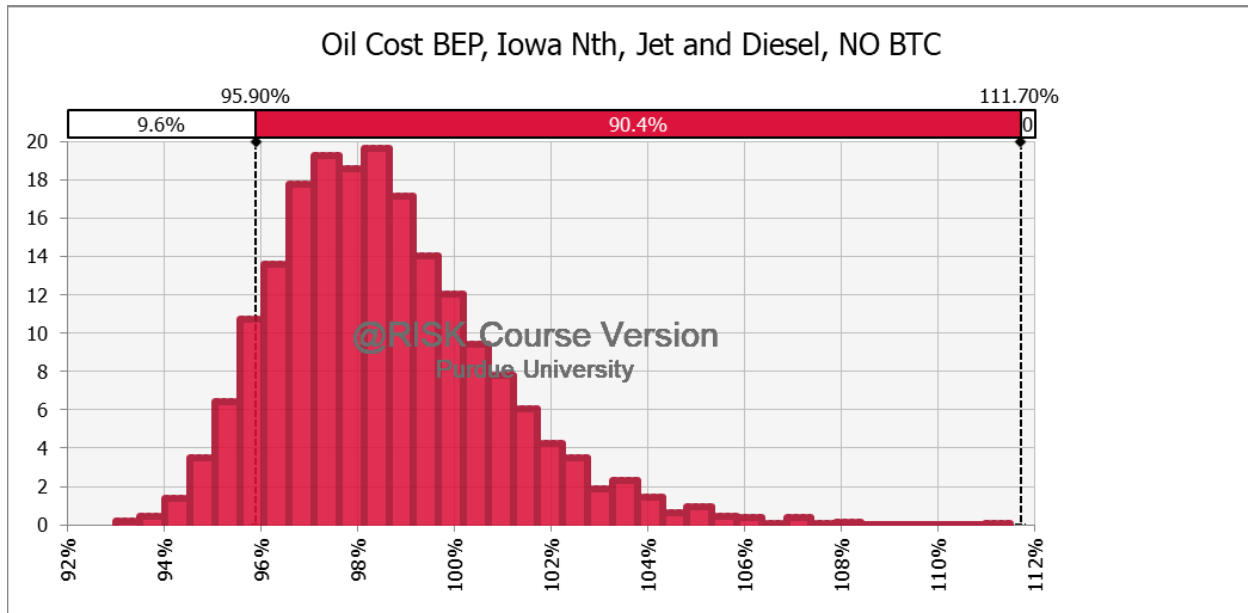


Figure A.64: Distribution of breakeven pennycress oil costs at Nth Iowa site with the default product slate and NO BTC, as a percent of soybean oil prices

Maximum diesel fuel product slate

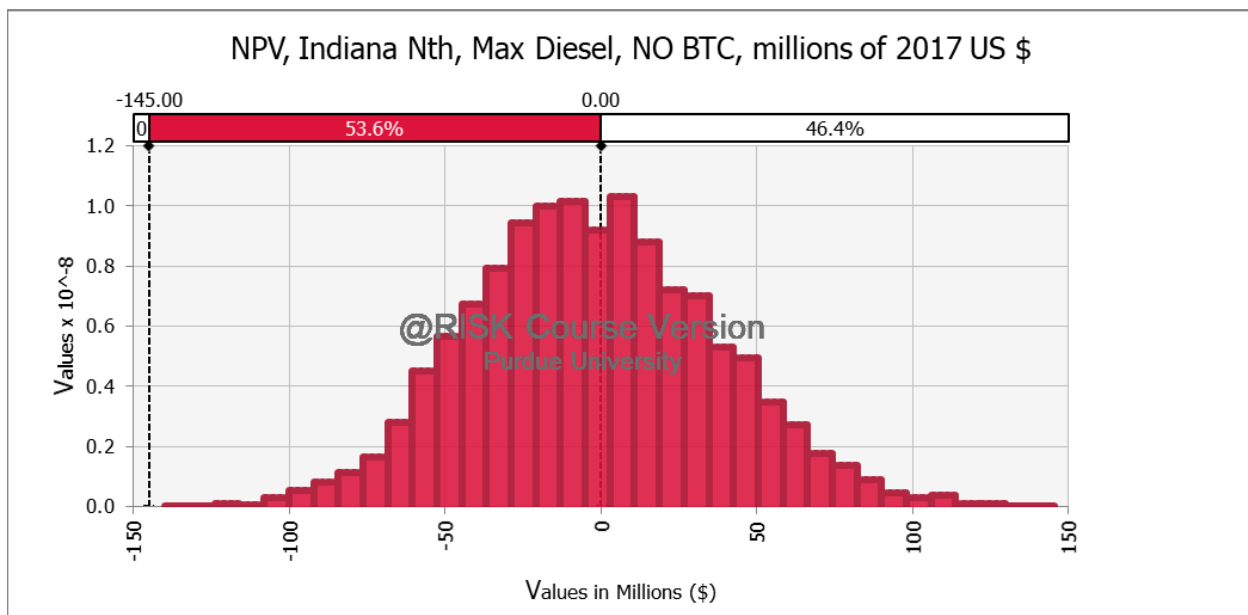


Figure A.65: Distribution of NPVs at Nth Indiana site with a maximum diesel product slate and NO BTC

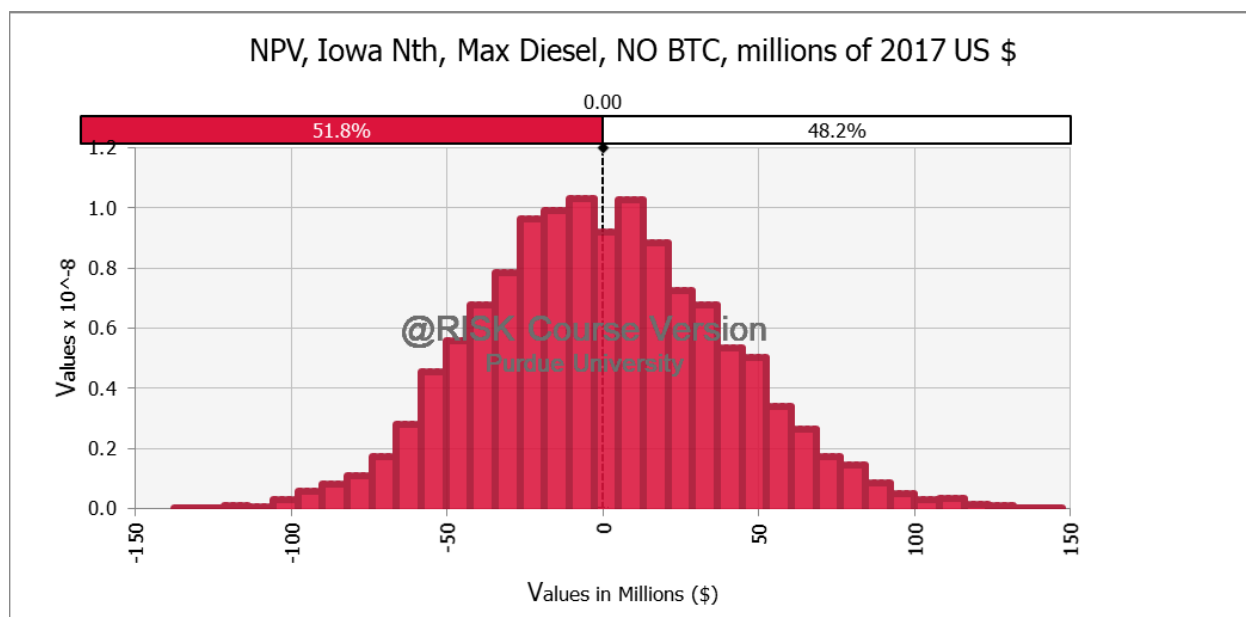


Figure A.66: Distribution of NPVs at Nth Iowa site with a maximum diesel product slate and NO BTC

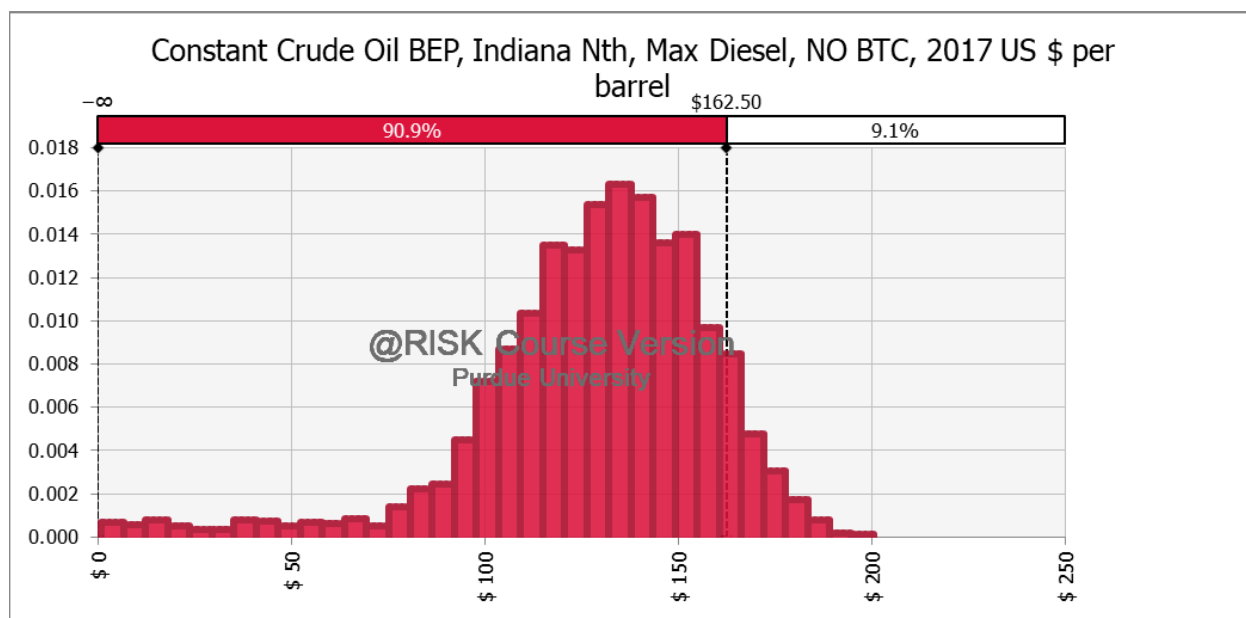


Figure A.67: Distribution of breakeven constant crude oil prices at Nth Indiana site with a maximum diesel product slate and NO BTC

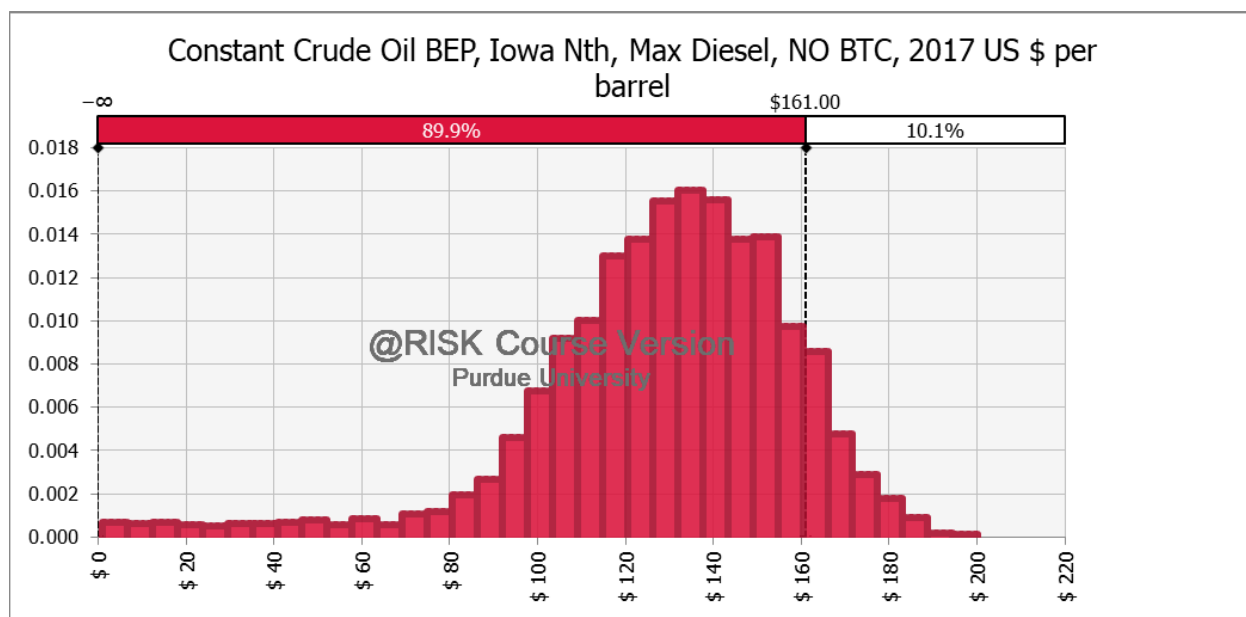


Figure A.68: Distribution of breakeven constant crude oil prices at Nth Iowa site with a maximum diesel product slate and NO BTC

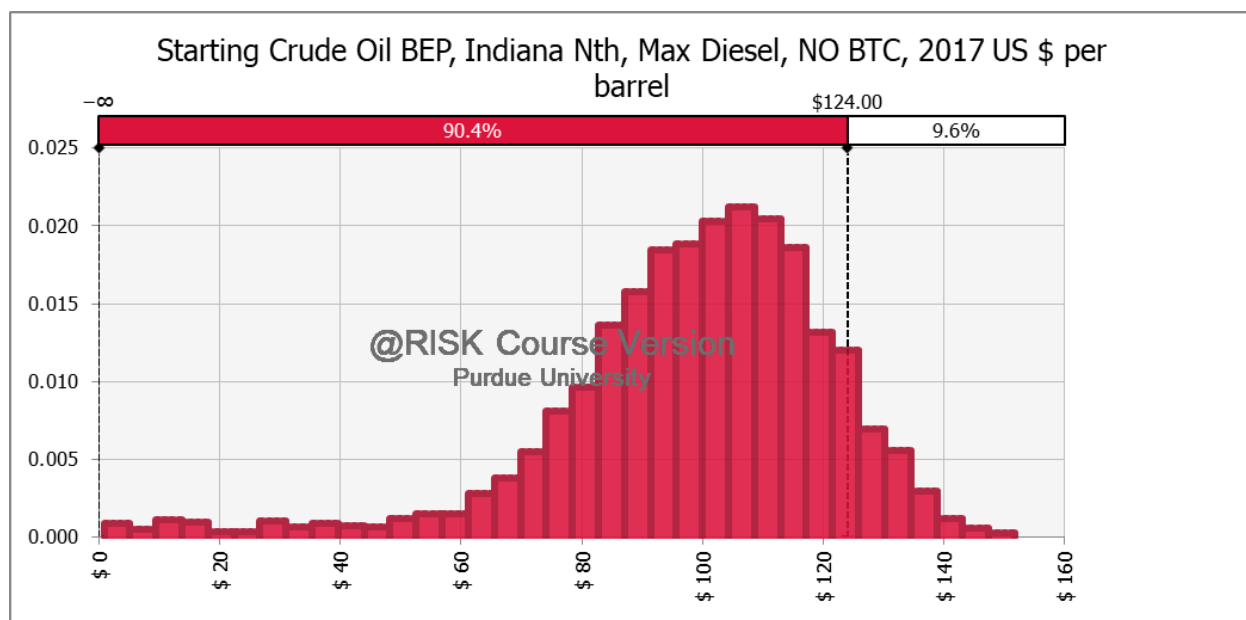


Figure A.69: Distribution of breakeven starting crude oil prices at Nth Indiana site with 2.25% real annual price growth, a maximum diesel product slate, and NO BTC

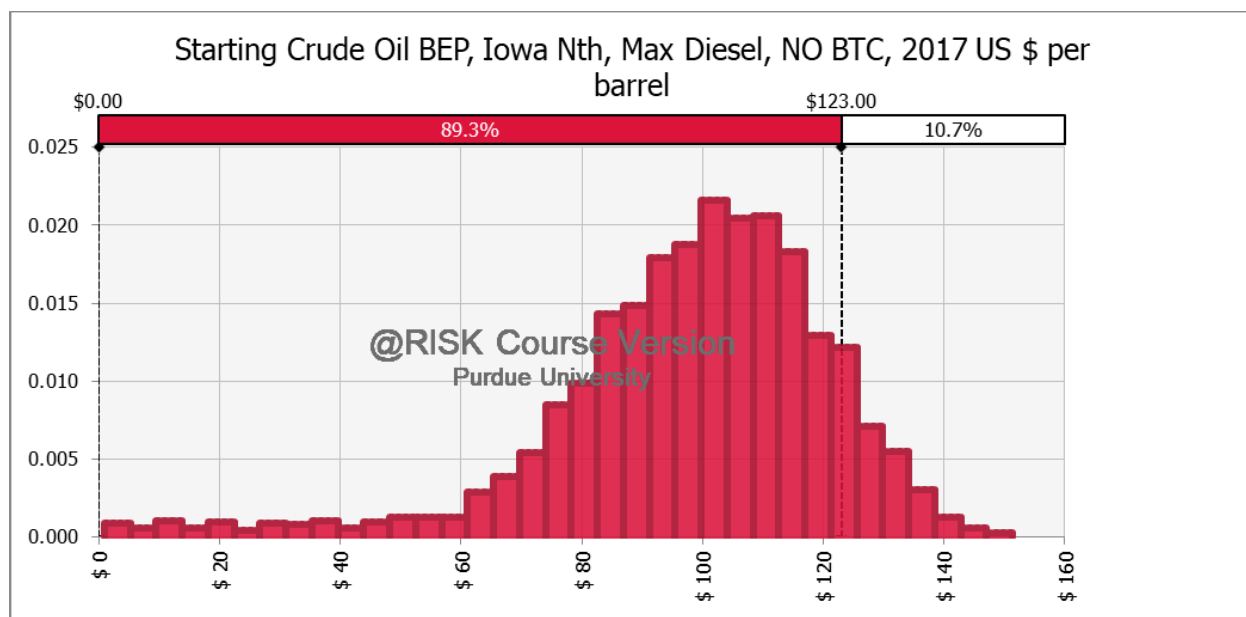


Figure A.70: Distribution of breakeven starting crude oil prices at Nth Indiana site with 2.25% real annual price growth, a maximum diesel product slate, and NO BTC

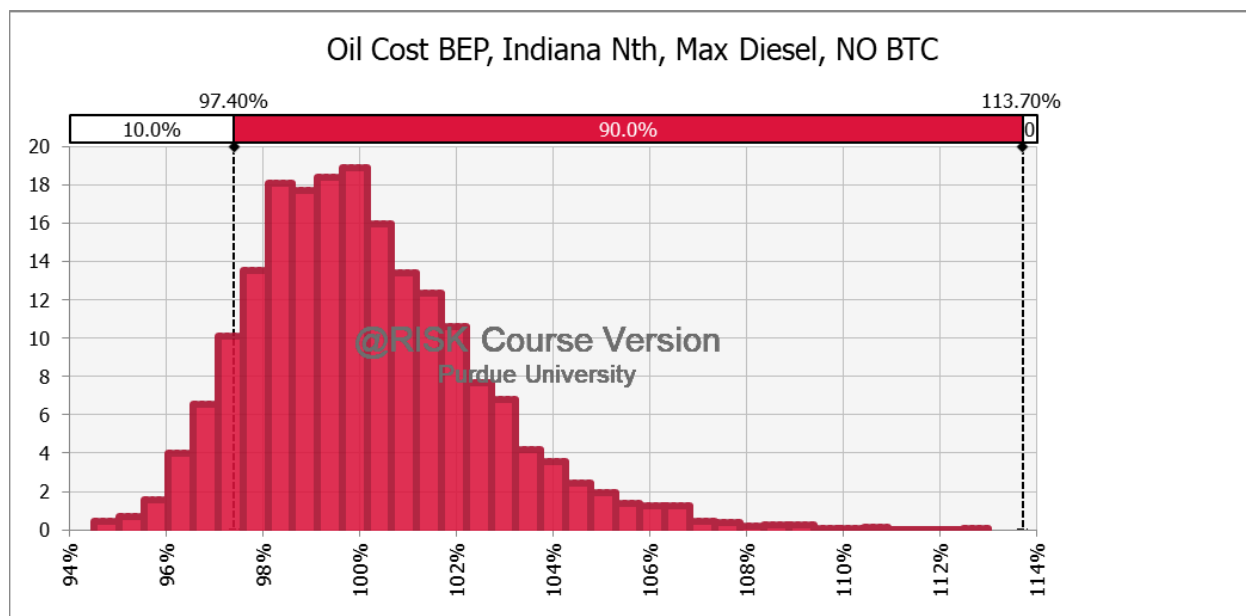


Figure A.71: Distribution of breakeven pennycress oil costs at Nth Indiana site with a maximum diesel product slate and NO BTC, as a percent of soybean oil prices

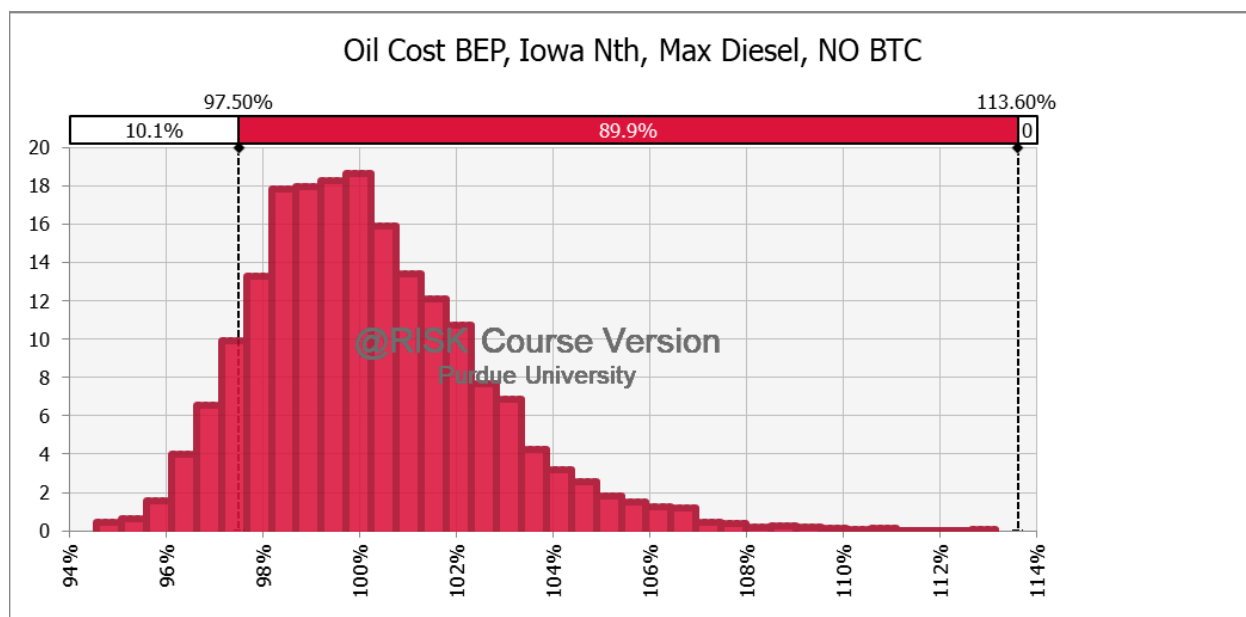


Figure A.72: Distribution of breakeven pennycress oil costs at Nth Iowa site with a maximum diesel product slate and NO BTC, as a percent of soybean oil prices

REFERENCES

1. Lüdeke-Freund, F., et al., *Sustainable plant oil production for aviation fuels: Assessment challenges and consequences for new feedstock concepts*. Sustainability Accounting, Management and Policy Journal, 2012. **3**(2): p. 186-217.
2. McGarvey, E. and W.E. Tyner, *A stochastic techno-economic analysis of the catalytic hydrothermolysis aviation biofuel technology*. Biofuels, Bioproducts and Biorefining, 2018. **0**(0).
3. Boeing, *Current Market Outlook 2017-2036*. 2017.
4. EPA, *EPA Finalizes First Steps to Address Greenhouse Gas Emissions from Aircraft Engines*, O.o.T.a.A.Q. US Environmental Protection Agency, Editor. 2016.
5. Sgouridis, S., P.A. Bonnefoy, and R.J. Hansman, *Air transportation in a carbon constrained world: Long-term dynamics of policies and strategies for mitigating the carbon footprint of commercial aviation*. Transportation Research Part A: Policy and Practice, 2011. **45**(10): p. 1077-1091.
6. Mawhood, R., et al., *Production pathways for renewable jet fuel: a review of commercialization status and future prospects*. Biofuels, Bioproducts and Biorefining, 2016. **10**(4): p. 462-484.
7. FAA, *United States Aviation Greenhouse Gas Emissions Reduction Plan*, U.S.F.A. Administration, Editor. 2012.
8. ICAO. *ICAO Global Framework for Aviation Alternative Fuels*. 2017 19 December 2017]; Available from: <https://www.icao.int/environmental-protection/GFAAF/Pages/default.aspx>.
9. ICAO. *What are Alternative Fuels in Aviation?* 2017 19 December 2017]; Available from: <https://www.icao.int/environmental-protection/GFAAF/Pages/FAQs.aspx>.
10. ICAO. *What is ICAO Doing in the Field of Aviation Alternative Fuels?* 2017 19 December 2017]; Available from: <https://www.icao.int/environmental-protection/GFAAF/Pages/FAQs.aspx>.
11. ICAO. *What is CORSIA and How Does it Work?* 2017 19 December 2017]; Available from: https://www.icao.int/environmental-protection/Pages/A39_CORSIA_FAQ2.aspx.
12. ICAO. *Carbon Offsetting and Reduction Scheme for International Aviation (CORSIA)*. 2017 19 December 2017]; Available from: <https://www.icao.int/environmental-protection/Pages/market-based-measures.aspx>.

13. Han, J., et al., *Life-cycle analysis of bio-based aviation fuels*. Bioresource Technology, 2013. **150**(Supplement C): p. 447-456.
14. Stratton, R.W., H.M. Wong, and J.I. Hileman, *Quantifying Variability in Life Cycle Greenhouse Gas Inventories of Alternative Middle Distillate Transportation Fuels*. Environmental Science & Technology, 2011. **45**(10): p. 4637-4644.
15. Hileman, J.I. and R.W. Stratton, *Alternative jet fuel feasibility*. Transport Policy, 2014. **34**(Supplement C): p. 52-62.
16. Fan, J.Q., et al., *A life cycle assessment of pennycress (Thlaspi aruense L.) -derived jet fuel and diesel*. Biomass & Bioenergy, 2013. **55**: p. 87-100.
17. Phippen, W.B. and M.E. Phippen, *Soybean Seed Yield and Quality as a Response to Field Pennycress Residue*. Crop Science, 2012. **52**(6): p. 2767-2773.
18. Sindelar, A.J., et al., *Winter oilseed production for biofuel in the US Corn Belt: opportunities and limitations*. Global Change Biology Bioenergy, 2017. **9**(3): p. 508-524.
19. Carvalho Carli, T. and W.B. Phippen, *EFFECTS OF NITROGEN ON FIELD PENNYCRESS (Thlaspi arvense L.) SEED PRODUCTION*, in *Association for the Advancement of Industrial Crops, 27th annual meeting "Industrial Crops: Research to Commerical Application"*. 2015: Overton Hotel and Conference Center, Lubbock, Texas, USA.
20. Applied Research Associates, I. *ARA and Blue Sun Performing on Navy Certification Contract for 100% Drop-in Fuels*. 2015 17 December 2017]; Available from: <https://www.ara.com/news/ara-and-blue-sun-performing-navy-certification-contract-100-drop-fuels>.
21. Pearlson, M., C. Wollersheim, and J. Hileman, *A techno-economic review of hydroprocessed renewable esters and fatty acids for jet fuel production*. Biofuels, Bioproducts and Biorefining, 2013. **7**(1): p. 89-96.
22. Chu, P.L., et al., *Financial analysis and risk assessment of hydroprocessed renewable jet fuel production from camelina, carinata and used cooking oil*. Applied Energy, 2017. **198**(Supplement C): p. 401-409.
23. Wang, W.-C., *Techno-economic analysis of a bio-refinery process for producing Hydro-processed Renewable Jet fuel from Jatropha*. Renewable Energy, 2016. **95**(Supplement C): p. 63-73.
24. Bann, S.J., et al., *The costs of production of alternative jet fuel: A harmonized stochastic assessment*. Bioresource Technology, 2017. **227**(Supplement C): p. 179-187.

25. de Jong, S., et al., *The feasibility of short-term production strategies for renewable jet fuels – a comprehensive techno-economic comparison*. Biofuels, Bioproducts and Biorefining, 2015. **9**(6): p. 778-800.
26. Liu, G., B. Yan, and G. Chen, *Technical review on jet fuel production*. Renewable and Sustainable Energy Reviews, 2013. **25**(Supplement C): p. 59-70.
27. Li, L., et al., *Catalytic Hydrothermal Conversion of Triglycerides to Non-ester Biofuels*. Energy & Fuels, 2010. **24**(2): p. 1305-1315.
28. Li, L., *Method of converting triglycerides to biofuels*. 2010, Google Patents.
29. Irwin, S., *Blender and Producer Sharing of Retroactively Reinstated Biodiesel Tax Credits: Time for a Change?*, in *farmdoc daily*. 2017: Department of Agricultural and Consumer Economics, University of Illinois at Urbana-Champaign.
30. Irwin, S., *Understanding the Behavior of Biodiesel RINs Prices*, in *farmdoc daily*. 2014: Department of Agricultural and Consumer Economics, University of Illinois at Urbana-Champaign.
31. Irwin, S., *Biodiesel Supply, Demand, and RINs Pricing*, in *farmdoc daily*. 2013: Department of Agricultural and Consumer Economics, University of Illinois at Urbana-Champaign.
32. Irwin, S. and D. Good, *How to Think About Biodiesel RINs Prices under Different Policies*, in *farmdoc daily*. 2017: Department of Agricultural and Consumer Economics, University of Illinois at Urbana-Champaign.
33. Irwin, S. and D. Good, *Projecting Biodiesel RINs Prices under Different Policies*, in *farmdoc daily*. 2017: Department of Agricultural and Consumer Economics, University of Illinois at Urbana-Champaign.
34. Hofstrand, D., *Biodiesel Profitability*. 2018, Iowa State University Ag Marketing Resource Center.
35. *Small Entity Compliance Guide for “Changes to Renewable Fuel Standard Program (RFS2)”*, O.o.T.a.A.Q. Assessment and Standards Division, U.S. Environmental Protection Agency, Editor. 2010.
36. ARB. *Data Dashboard*. 2018 15 February 2018 20 February 2018]; Available from: <https://www.arb.ca.gov/fuels/lcfs/dashboard/dashboard.htm>.
37. Hubbs, T., et al., *Valuing Dried Distillers Grains with Solubles for Use in Swine Diets*. Journal of the ASFMRA, 2009. **2009**: p. 1-13.

38. Alhotan, R.A., et al., *Nutritive value and the maximum inclusion level of pennycress meal for broiler chickens*. Poultry Science, 2017. **96**(7): p. 2281-2293.
39. Tretsven, J.O. and J.A. Nelson, *Wild yellow mustard seed and fanweed seed as concentrate feeds for milking cows*. Bull. Mont. agric. Exp. Stn., 1946(435).
40. Trejo-Pech, C.O., et al., *Return and Risk Profile of a Potential Pennycress Processing Facility for the Aviation Industry*, in *Southern Agricultural Economics Association (SAEA) Annual Meeting*. 2019: Birmingham, AL.
41. Markel, E., et al., *Potential for Pennycress to Support a Renewable Jet Fuel Industry*. SciEnvironm, 2018. **1**(121).
42. Kousoulidou, M. and L. Lonza, *Biofuels in aviation: Fuel demand and CO2 emissions evolution in Europe toward 2030*. Transportation Research Part D: Transport and Environment, 2016. **46**(Supplement C): p. 166-181.
43. Fiorentino, G., et al., *Life cycle assessment of Brassica carinata biomass conversion to bioenergy and platform chemicals*. Journal of Cleaner Production, 2014. **66**(Supplement C): p. 174-187.
44. D'Avino, L., et al., *The role of co-products in biorefinery sustainability: energy allocation versus substitution method in rapeseed and carinata biodiesel chains*. Journal of Cleaner Production, 2015. **94**(Supplement C): p. 108-115.
45. Sedbrook, J.C., W.B. Phippen, and M.D. Marks, *New approaches to facilitate rapid domestication of a wild plant to an oilseed crop: example pennycress (Thlaspi arvense L.)*. Plant Sci, 2014. **227**: p. 122-32.
46. Holm, L.D., Jerry; Holm, Eric; Pancho, Juan; Herberger, James, *World Weeds: Natural Histories and Distributions*. 1997, New York: John Wiley & Sons, Inc.
47. Warwick, S.I., A. Francis, and D.J. Susko, *The biology of Canadian weeds. 9. Thlaspi arvense L. (updated)*. Canadian Journal of Plant Science, 2002. **82**(4): p. 803-823.
48. Best, K.F. and G.I. McIntyre, *THE BIOLOGY OF CANADIAN WEEDS: 9. Thlaspi arvense L.* Canadian Journal of Plant Science, 1975. **55**(1): p. 279-292.
49. ARB. *LCFS Basics*. 2016 10 May 2016 20 February 2018]; Available from: <https://www.arb.ca.gov/fuels/lcfs/background/basics.htm>.
50. Moser, B.R., et al., *Composition and physical properties of cress (Lepidium sativum L.) and field pennycress (Thlaspi arvense L.) oils*. Industrial Crops and Products, 2009. **30**(2): p. 199-205.

51. Evangelista, R.L., T.A. Isbell, and S.C. Cermak, *Extraction of pennycress (Thlaspi arvense L.) seed oil by full pressing*. Industrial Crops and Products, 2012. **37**(1): p. 76-81.
52. Dose, H.L., et al., *Early planting dates maximize winter annual field pennycress (Thlaspi arvense L.) yield and oil content*. Industrial Crops and Products, 2017. **97**: p. 477-483.
53. Moser, B.R., et al., *Production and Evaluation of Biodiesel from Field Pennycress (Thlaspi arvense L.) Oil*. Energy & Fuels, 2009. **23**(8): p. 4149-4155.
54. Moser, B.R., *Biodiesel from alternative oilseed feedstocks: camelina and field pennycress*. Biofuels, 2012. **3**(2): p. 193-209.
55. Mupondwa, E., et al., *Technoeconomic analysis of camelina oil extraction as feedstock for biojet fuel in the Canadian Prairies*. Biomass and Bioenergy, 2016. **95**(Supplement C): p. 221-234.
56. Selling, G.W., et al., *Extraction of proteins from pennycress seeds and press cake*. Industrial Crops and Products, 2013. **41**: p. 113-119.
57. Hojilla-Evangelista, M.P., et al., *Effects of cold-pressing and seed cooking on functional properties of protein in pennycress (Thlaspi arvense L.) seed and press cakes*. Industrial Crops and Products, 2013. **45**: p. 223-229.
58. Hojilla-Evangelista, M.P., et al., *Extraction, Composition and Functional Properties of Pennycress (Thlaspi arvense L.) Press Cake Protein*. Journal of the American Oil Chemists Society, 2015. **92**(6): p. 905-914.
59. Rajapakse, B., *Nutritive Value of Mechanically-Pressed Camelina (Camelina sativa), Carinata (Brassica Carinata) and Soybean (Glycine max) Meals for Broiler Chickens, in Faculty of Agriculture*. 2015, Dalhousie University: Halifax, Nova Scotia. p. 221.
60. Tyagi, A.K., *Influence of water soaking of mustard cake on glucosinolate hydrolysis*. Animal Feed Science and Technology, 2002. **99**(1): p. 215-219.
61. Payvastegan, S., P. Farhoomand, and N. Delfani, *Growth Performance, Organ Weights and, Blood Parameters of Broilers Fed Diets Containing Graded Levels of Dietary Canola Meal and Supplemental Copper*. The Journal of Poultry Science, 2013. **50**(4): p. 354-363.
62. Johnson, G.A., et al., *Field pennycress production and weed control in a double crop system with soybean in Minnesota*. Agronomy Journal, 2015. **107**(2): p. 532-540.
63. Gesch, R.W., D.W. Archer, and M.T. Berti, *Dual Cropping Winter Camelina with Soybean in the Northern Corn Belt*. Agronomy Journal, 2014. **106**(5): p. 1735-1745.
64. Clopton, J.R. and H.O. Triebold, *FANWEED SEED OIL: Potential Substitute for Rapeseed Oil*. Industrial and Engineering Chemistry, 1944. **36**(3): p. 218-219.

65. Carr, P.M., *Potential of fanweed and other weeds as novel industrial oilseed crops*. New Crops, 1993: p. 384-388.
66. *Field Pennycress*. 2017 14 December 2017]; Available from: <https://www.agmrc.org/commodities-products/grains-oilseeds/pennycress/>.
67. Kladivko, E.J., et al., *Cover crops in the upper midwestern United States: Potential adoption and reduction of nitrate leaching in the Mississippi River Basin*. Journal of Soil and Water Conservation, 2014. **69**(4): p. 279-291.
68. Mitich, L.W., *Field pennycress (Thlaspi arvense L.) - the stinkweed*. Weed Technology, 1996. **10**(3): p. 675-678.
69. Moyer, J.R. and R. Hironaka, *Digestible energy and protein content of some annual weeds, alfalfa, bromegrass, and tame oats*. Canadian Journal of Plant Science, 1993. **73**(4): p. 1305-1308.
70. Isbell, T.A., S.C. Cermak, and L.F. Marek, *Registration of Elizabeth Thlaspi arvense L. (Pennycress) with Improved Nondormant Traits*. Journal of Plant Registrations, 2017. **11**(3): p. 311-314.
71. Isbell, T.A., et al., *Registration of Katelyn Thlaspi arvense L. (pennycress) with improved nondormant traits*. Journal of Plant Registrations, 2015. **9**(2): p. 212-215.
72. Venkatesh, R., S.K. Harrison, and R.M. Riedel, *Weed hosts of soybean cyst nematode (Heterodera glycines) in Ohio*. Weed Technology, 2000. **14**(1): p. 156-160.
73. Riga, E., *The effects of Brassica green manures on plant parasitic and free living nematodes used in combination with reduced rates of synthetic nematicides*. Journal of Nematology, 2011. **43**(2): p. 119-121.
74. Odland, T.E.K., H.C., *Value of cover crops in continuous corn culture*. Journal of the American Society of Agronomy, 1938.
75. Moschler, W.W., et al., *Winter Cover Crops for Sod-Planted Corn: Their Selection and Management I*. Agronomy Journal, 1967. **59**(6): p. 547-551.
76. Teasdale, J.R., *Contribution of Cover Crops to Weed Management in Sustainable Agricultural Systems*. Journal of Production Agriculture, 1996. **9**(4): p. 475-479.
77. Kaspar, T.C., J.K. Radke, and J.M. Laflen, *Small grain cover crops and wheel traffic effects on infiltration, runoff, and erosion*. Journal of Soil and Water Conservation, 2001. **56**(2): p. 160-164.

78. Ding, G., et al., *Effect of cover crop management on soil organic matter*. Geoderma, 2006. **130**(3): p. 229-239.
79. Blanco-Canqui, H., et al., *Can Cover Crop and Manure Maintain Soil Properties After Stover Removal from Irrigated No-Till Corn?* Soil Science Society of America Journal, 2014. **78**(4): p. 1368-1377.
80. Osborne, S.L., et al., *The Impact of Corn Residue Removal on Soil Aggregates and Particulate Organic Matter*. BioEnergy Research, 2014. **7**(2): p. 559-567.
81. Beale, O.W., G.B. Nutt, and T.C. Peele, *The Effects of Mulch Tillage on Runoff, Erosion, Soil Properties, and Crop Yields I*. Soil Science Society of America Journal, 1955. **19**(2): p. 244-247.
82. Mitchell, W.H. and M.R. Tell, *Winter-Annual Cover Crops for No-Tillage Corn Production I*. Agronomy Journal, 1977. **69**(4): p. 569-573.
83. Vaughn, S.F., et al., *Herbicidal activity of glucosinolate-containing seedmeals*. Weed Science, 2006. **54**(4): p. 743-748.
84. Norsworthy, J.K., et al., *Suppression of Digitaria sanguinalis and Amaranthus palmeri using autumn-sown glucosinolate-producing cover crops in organically grown bell pepper*. Weed Research, 2007. **47**(5): p. 425-432.
85. Boydston, R.A. and A. Hang, *Rapeseed (Brassica napus) Green Manure Crop Suppresses Weeds in Potato (Solanum tuberosum)*. Weed Technology, 2017. **9**(4): p. 669-675.
86. Boydston, R.A., et al., *Evaluating Mustard Seed Meal for Weed Suppression in Potato (Solanum tuberosum)*. Journal of Agricultural Science, 2018. **10**(2): p. 48.
87. *Pollinator Research Action Plan*, U.S.E.P.A. United States Department of Agriculture, Editor. 2015.
88. Westphal, C., I. Steffan-Dewenter, and T. Tscharntke, *Mass flowering crops enhance pollinator densities at a landscape scale*. Ecology Letters, 2003. **6**(11): p. 961-965.
89. Riedinger, V., et al., *Early mass-flowering crops mitigate pollinator dilution in late-flowering crops*. Landscape Ecology, 2014. **29**(3): p. 425-435.
90. Schmidt, M.H., et al., *Relative importance of predators and parasitoids for cereal aphid control*. Proceedings of the Royal Society of London. Series B: Biological Sciences, 2003. **270**(1527): p. 1905.
91. Groeneveld, J.H. and A.-M. Klein, *Pollination of two oil-producing plant species: Camelina (Camelina sativa L. Crantz) and pennycress (Thlaspi arvense L.) double-cropping in Germany*. GCB Bioenergy, 2014. **6**(3): p. 242-251.

92. Haenke, S., et al., *Landscape configuration of crops and hedgerows drives local syrphid fly abundance*. Journal of Applied Ecology, 2014. **51**(2): p. 505-513.
93. Natelson, R.H., et al., *Technoeconomic analysis of jet fuel production from hydrolysis, decarboxylation, and reforming of camelina oil*. Biomass and Bioenergy, 2015. **75**: p. 23-34.
94. Wang, W.-C. and L. Tao, *Bio-jet fuel conversion technologies*. Renewable and Sustainable Energy Reviews, 2016. **53**: p. 801-822.
95. Li, X., E. Mupondwa, and L. Tabil, *Technoeconomic analysis of biojet fuel production from camelina at commercial scale: Case of Canadian Prairies*. Bioresource Technology, 2018. **249**(Supplement C): p. 196-205.
96. Seber, G., et al., *Environmental and economic assessment of producing hydroprocessed jet and diesel fuel from waste oils and tallow*. Biomass and Bioenergy, 2014. **67**(Supplement C): p. 108-118.
97. de Jong, S., et al., *Cost optimization of biofuel production – The impact of scale, integration, transport and supply chain configurations*. Applied Energy, 2017. **195**(Supplement C): p. 1055-1070.
98. Chiamonti, D., et al., *Sustainable bio kerosene: Process routes and industrial demonstration activities in aviation biofuels*. Applied Energy, 2014. **136**(Supplement C): p. 767-774.
99. Coppola, E., *CHJ Pathway: Readijet™ Renewable Jet Fuel Produced by Catalytic Hydrothermolysis (CH)*. ASTM.
100. Toor, S.S., L. Rosendahl, and A. Rudolf, *Hydrothermal liquefaction of biomass: A review of subcritical water technologies*. Energy, 2011. **36**(5): p. 2328-2342.
101. ARB. *Guidance Documents and FAQs*. 2017 22 November 2017 20 February 2018]; Available from: <https://www.arb.ca.gov/fuels/lcfs/guidance/guidance.htm#faqs>.
102. EPA. *Overview for Renewable Fuel Standard*. 2017 7 June 2017 19 February 2018]; Available from: <https://www.epa.gov/renewable-fuel-standard-program/overview-renewable-fuel-standard>.
103. in *United States Code*. 2014, Cornell Law School Legal Information Institute: United States.

104. EPA. *Renewable Identification Numbers (RINs) under the Renewable Fuel Standard Program*. 2017 20 March 2017 19 February 2018]; Available from: <https://www.epa.gov/renewable-fuel-standard-program/renewable-identification-numbers-rins-under-renewable-fuel-standard>.
105. EPA. *Renewable Fuel Annual Standards*. 2017 8 June 2017 19 February 2018]; Available from: <https://www.epa.gov/renewable-fuel-standard-program/renewable-fuel-annual-standards>.
106. EPA. *Lifecycle Analysis of Greenhouse Gas Emissions under the Renewable Fuel Standard*. 2016 16 August 2016 19 February 2018]; Available from: <https://www.epa.gov/renewable-fuel-standard-program/lifecycle-analysis-greenhouse-gas-emissions-under-renewable-fuel>.
107. EPA. *Approved Pathways for Renewable Fuel*. 2018 2 January 2018 19 February 2018]; Available from: <https://www.epa.gov/renewable-fuel-standard-program/approved-pathways-renewable-fuel>.
108. in *United States Code*. 2014, Cornell Law School Legal Information Institute: United States.
109. ARB. *Low Carbon Fuel Standard*. 2017 13 December 2017 20 February 2018]; Available from: <https://www.arb.ca.gov/fuels/lcfs/lcfs.htm>.
110. ARB, *Low Carbon Fuel Standard: evaluation of alternative jet fuel inclusion*. 2017.
111. Bittner, A., W.E. Tyner, and X. Zhao, *Field to flight: A techno-economic analysis of the corn stover to aviation biofuels supply chain*. Biofuels Bioproducts & Biorefining-Biofpr, 2015. **9**(2): p. 201-210.
112. Zhao, X., T.R. Brown, and W.E. Tyner, *Stochastic techno-economic evaluation of cellulosic biofuel pathways*. Bioresource Technology, 2015. **198**: p. 755-763.
113. Blazy, D., et al., *Chapter 15 A Monte Carlo-based Methodology for Valuing Refineries Producing Aviation Biofuel*, in *Commercializing Biobased Products: Opportunities, Challenges, Benefits, and Risks*. 2016, The Royal Society of Chemistry. p. 336-351.
114. Getinet, A., G. Rakow, and R.K. Downey, *Agronomic performance and seed quality of Ethiopian mustard in Saskatchewan*. Canadian Journal of Plant Science, 1996. **76**(3): p. 387-392.
115. Barro, F., et al., *Doubled haploid lines of Brassica carinata with modified erucic acid content through mutagenesis by EMS treatment of isolated microspores*. Plant Breeding, 2001. **120**(3): p. 262-264.

116. Pan, X., et al., *The effect of cultivar, seeding rate and applied nitrogen on Brassica carinata seed yield and quality in contrasting environments*. Canadian Journal of Plant Science, 2012. **92**(5): p. 961-971.
117. Marillia, E.-F., et al., *Palliser's promise: Brassica carinata, An emerging western Canadian crop for delivery of new bio-industrial oil feedstocks*. Biocatalysis and Agricultural Biotechnology, 2014. **3**(1): p. 65-74.
118. Li, Q., Y. Zhang, and G. Hu, *Techno-economic analysis of advanced biofuel production based on bio-oil gasification*. Bioresource Technology, 2015. **191**(Supplement C): p. 88-96.
119. Wright, T.P., *Factors Affecting the Cost of Airplanes*. Journal of the Aeronautical Sciences, 1936. **3**(4): p. 122-128.
120. *Complete RIN History*, P.F. Limited, Editor. 2019: Naples, FL.
121. Irwin, S., *Biodiesel Supply Response to Production Profits*, in *farmdoc daily*. 2013: Department of Agricultural and Consumer Economics, University of Illinois at Urbana-Champaign.
122. Irwin, S. and D. Good, *Revisiting the Estimation of Biomass-Based Diesel Supply Curves*, in *farmdoc daily*. 2017: Department of Agricultural and Consumer Economics, University of Illinois at Urbana-Champaign.
123. Abbott, P.C., *Biofuels, Binding Constraints, and Agricultural Commodity Price Volatility*, in *The Economics of Food Price Volatility*, J.-P. Chavas, D. Hummels, and B.D. Wright, Editors. 2014, University of Chicago Press: Chicago, IL. p. 91-131.
124. Drenth, A.C., et al., *Compression ignition engine performance and emission evaluation of industrial oilseed biofuel feedstocks camelina, carinata, and pennycress across three fuel pathways*. Fuel, 2014. **136**: p. 143-155.
125. Moser, B.R., *Fuel property enhancement of biodiesel fuels from common and alternative feedstocks via complementary blending*. Renewable Energy, 2016. **85**: p. 819-825.
126. Irwin, S., *Estimating the Biodiesel Supply Curve*, in *farmdoc daily*. 2013: Department of Agricultural and Consumer Economics, University of Illinois at Urbana-Champaign.
127. *U.S. monthly biodiesel production 2017-2019*. 2019.
128. Yu, T.-H., D.A. Bessler, and S.W. Fuller, *Cointegration and Causality Analysis of World Vegetable Oil and Crude Oil Prices*. 2006.

129. Moser, B.R., R.L. Evangelista, and T.A. Isbell, *Preparation and Fuel Properties of Field Pennycress (Thlaspi arvense) Seed Oil Ethyl Esters and Blends with Ultralow-Sulfur Diesel Fuel*. Energy & Fuels, 2016. **30**(1): p. 473-479.
130. Diniz, A.P.M.M., R. Sargeant, and G.J. Millar, *Stochastic techno-economic analysis of the production of aviation biofuel from oilseeds*. Biotechnology for Biofuels, 2018. **11**(1): p. 161.
131. *CAKE & MEAL, SOYBEAN, ANIMAL FEED - PRODUCTION, MEASURED IN TONS*, N.A.S. Service, Editor. 2017.
132. *ALCOHOL COPRODUCTS, DISTILLERS GRAINS, DRIED, INCL SOLUBLES - PRODUCTION, MEASURED IN TONS*, N.A.S. Service, Editor. 2017.
133. *High Protein Soybean Meal, \$/ton*, A.M. Service, Editor. 2018.
134. *Corn Distiller's Dried Grain, \$/ton*, A.M. Service, Editor. 2018.
135. Herdt, T.H. *Nutritional Requirements of Dairy Cattle*. 15 November 2018]; Available from: <https://www.merckvetmanual.com/management-and-nutrition/nutrition-dairy-cattle/nutritional-requirements-of-dairy-cattle>.
136. Gadberry, S., *Part 3: Nutrient Requirement Tables*, in *Beef Cattle Nutrition*. University of Arkansas Cooperative Extension Service: Little Rock, AR.
137. Cromwell, G.L. *Nutritional Requirements of Pigs*. 15 November 2018]; Available from: <https://www.merckvetmanual.com/management-and-nutrition/nutrition-pigs/nutritional-requirements-of-pigs>.
138. Klasing, K.C. *Nutritional Requirements of Poultry*. 15 November 2018]; Available from: <https://www.merckvetmanual.com/poultry/nutrition-and-management-poultry/nutritional-requirements-of-poultry>.
139. Wecke, C., A. Pastor, and F. Liebert, *Validation of the Lysine Requirement as Reference Amino Acid for Ideal In-Feed Amino Acid Ratios in Modern Fast Growing Meat-Type Chickens*. Vol. 06. 2016. 185-194.
140. Heuzé, V., G. Tran, and S. Kaushik. *Feedipedia: Soybean meal*. 2017 13 January 2017 15 November 2018]; Available from: <https://www.feedipedia.org/node/674>.
141. Heuzé, V., G. Tran, and F. Lebas. *Feedipedia: Maize grain*. 2017 7 September 2017 15 November 2018]; Available from: <https://www.feedipedia.org/node/556>.
142. Heuzé, V., et al. *Feedipedia: Corn distillers grain*. 2015 11 May 2015 15 November 2018]; Available from: <https://www.feedipedia.org/node/71>.

143. Heuzé, V., G. Tran, and F. Lebas. *Feedipedia: Camelina (Camelina sativa) seeds and oil meal*. 2017 11 September 2017 15 November 2018]; Available from: <https://www.feedipedia.org/node/4254>.
144. Heuzé, V., et al. *Feedipedia: Rapeseed meal*. 2018 15 June 2018 15 November 2018]; Available from: <https://www.feedipedia.org/node/52>.
145. *US No. 2 Yellow Corn, \$/bushel*, A.M. Service, Editor. 2018.
146. Campiche, J.L., et al., *Examining the Evolving Correspondence Between Petroleum Prices and Agricultural Commodity Prices*. 2007.
147. Abbott, P.C., C. Hurt, and W.E. Tyner, *What's Driving Food Prices?* 2008.
148. Harri, A., L. Nalley, and D. Hudson, *The Relationship between Oil, Exchange Rates, and Commodity Prices*. Journal of Agricultural and Applied Economics, 2009. **41**(2): p. 501-510.
149. Ciaian, P. and d.A. Kancs, *Interdependencies in the energy–bioenergy–food price systems: A cointegration analysis*. Resource and Energy Economics, 2011. **33**(1): p. 326-348.
150. Nazlioglu, S. and U. Soytas, *Oil price, agricultural commodity prices, and the dollar: A panel cointegration and causality analysis*. Energy Economics, 2012. **34**(4): p. 1098-1104.
151. Cheng, I.-H. and W. Xiong, *Financialization of Commodity Markets*. Annual Review of Financial Economics, 2014. **6**(1): p. 419-441.
152. Adams, Z. and T. Glück, *Financialization in commodity markets: A passing trend or the new normal?* Journal of Banking & Finance, 2015. **60**: p. 93-111.
153. Zhang, Q. and M. Reed, *Examining the Impact of the World Crude Oil Price on China's Agricultural Commodity Prices: The Case of Corn, Soybean, and Pork*. 2008, Southern Agricultural Economics Association.
154. Chari, V.V. and L. Christiano, *Financialization in Commodity Markets*. National Bureau of Economic Research Working Paper Series, 2017. **No. 23766**.
155. Good, D. and S. Irwin, *The Relationship between Biodiesel and Soybean Oil Prices*, in *farmdoc daily*. 2017: Department of Agricultural and Consumer Economics, University of Illinois at Urbana-Champaign.
156. Natanelov, V., et al., *Is there co-movement of agricultural commodities futures prices and crude oil?* Energy Policy, 2011. **39**(9): p. 4971-4984.
157. Henderson, B.J., N.D. Pearson, and L. Wang, *New Evidence on the Financialization of Commodity Markets*. The Review of Financial Studies, 2015. **28**(5): p. 1285-1311.

158. Irwin, S.H. and D.R. Sanders, *Index Funds, Financialization, and Commodity Futures Markets*. Applied Economic Perspectives and Policy, 2011. **33**(1): p. 1-31.
159. Hatzenbuehler, P.L., P.C. Abbott, and K.A. Foster, *Agricultural Commodity Prices and Exchange Rates under Structural Change*. Journal of Agricultural and Resource Economics, 2016. **41**(2): p. 204-224.
160. Taheripour, F. and W.E. Tyner, *Impacts of Possible Chinese 25% Tariff on U.S. Soybeans and Other Agricultural Commodities*. Choices, 2018. **33**(2): p. 1-7.
161. *Biodiesel producers and production capacity by state, March 2019* 2019.
162. EPA. *Cellulosic Waiver Credits under the Renewable Fuel Standard Program*. 2017 12 June 2017 20 June 2019]; Available from: <https://www.epa.gov/renewable-fuel-standard-program/cellulosic-waiver-credits-under-renewable-fuel-standard-program>.
163. Lahane, S. and K.A. Subramanian, *Effect of different percentages of biodiesel–diesel blends on injection, spray, combustion, performance, and emission characteristics of a diesel engine*. Fuel, 2015. **139**: p. 537-545.
164. ARB. *LCFS Pathway Certified Carbon Intensities*. 2019 30 August 2019 [cited 2019; Available from: <https://ww3.arb.ca.gov/fuels/lcfs/fuelpathways/pathwaytable.htm>.
165. ARB, *Detailed Analysis for Indirect Land Use Change*. 2015.
166. *CARB LCFS TIER 2 FUEL PATHWAY REPORT TALLOW RENEWABLE DIESEL* 2016, (S&T)² Consultants, Inc.: Delta, British Columbia.
167. *Monthly LCFS Credit Transfer Activity Report*, ARB, Editor. 2019.
168. *LCFS Quarterly Data Spreadsheet*, ARB, Editor. 2019.
169. *Form EIA-861M, Monthly Electric Power Industry Report*, EIA, Editor. 2019.
170. *United States Natural Gas Industrial Price Monthly*, EIA, Editor. 2019.
171. *Refiner Acquisition Cost of Crude Oil*, E.I. Administration, Editor. 2018.
172. *U.S. Kerosene-Type Jet Fuel Wholesale/Resale Price by Refiners, Monthly*, E.I. Administration, Editor. 2018.
173. *Consumer Price Index: Total All Items for the United States [CPALTT01USM661S]*, O.f.E.C.-O.a. Development, Editor. 2018: FRED, Federal Reserve Bank of St. Louis.
174. *U.S. No 2 Diesel Wholesale/Resale Price by Refiners*, E.I. Administration, Editor. 2018.

175. *U.S. Total Gasoline Wholesale/Resale Price by Refiners, Monthly*, E.I. Administration, Editor. 2018.
176. *Soybean Oil, \$/cwt.*, A.M. Service, Editor. 2018.
177. *Prime Suppliers Sales Volumes*, EIA, Editor. 2019.
178. Van Dyne, D.L. and M.G. Blase, *Process Design, Economic Feasibility, and Market Potential for Nylon 1313 Produced from Erucic Acid*. Biotechnology Progress, 1990. **6**(4): p. 273-276.